Titre: Title:	Freeze-Dried Chitosan Platelet-Rich Plasma Mixtures for Knee Meniscus Repair
Auteur: Author:	Leili Ghazi Zadeh
Date:	2018
Type:	Mémoire ou thèse / Dissertation or Thesis
Référence: Citation:	Ghazi Zadeh, L. (2018). Freeze-Dried Chitosan Platelet-Rich Plasma Mixtures for Knee Meniscus Repair [Thèse de doctorat, École Polytechnique de Montréal]. PolyPublie. https://publications.polymtl.ca/3779/

UNIVERSITÉ DE MONTRÉAL

FREEZE-DRIED CHITOSAN PLATELET-RICH PLASMA MIXTURES FOR KNEE MENISCUS REPAIR

LEILI GHAZI ZADEH

INSTITUT DE GÉNIE BIOMÉDICAL

ÉCOLE POLYTECHNIQUE DE MONTRÉAL

THÈSE PRÉSENTÉE EN VUE DE L'OBTENTION

DU DIPLÔME DE PHILOSOPHIAE DOCTOR

(GÉNIE BIOMÉDICAL)

DÉCEMBRE 2018

UNIVERSITÉ DE MONTRÉAL

ÉCOLE POLYTECHNIQUE DE MONTRÉAL

Cette thèse intitulée :

FREEZE-DRIED CHITOSAN PLATELET-RICH PLASMA MIXTURES FOR KNEE MENISCUS REPAIR

présentée par : GHAZI ZADEH Leili

en vue de l'obtention du diplôme de : Philosophiae Doctor

a été dûment acceptée par le jury d'examen constitué de :

M. GERVAIS Thomas, Ph. D, président

M. LAVERTU Marc, Ph. D, membre et directeur de recherche

M. BUSCHMANN Michael, Ph. D, membre et codirecteur de recherche

Mme HOEMANN Caroline, Ph. D, membre et codirectrice de recherche

M. LI Jianyu, Ph. D, membre

M. NAZHAT Showan N., Ph. D, membre externe

DEDICATION

TO THE MEMORY OF MY FATHER, WHO ALWAYS SUPPORTED ME, MY MOTHER, AND MY BROTHER: I OWE IT ALL TO YOU.

ACKNOWLEDGEMENTS

It all started in winter 2015 when I received an offer to pursue my Ph.D. in Biomaterials and Cartilage Lab (BCL), Department of Chemical Engineering, Biomedical Engineering Institute, Polytechnique Montreal, Quebec, Canada. At that time, I was a master student in the Netherlands studying Regenerative Medicine and Technology at Utrecht University with my interest in cartilage repair. I was genuinely excited and happy to start my Ph.D. on a project I really wanted. I was so passionate and determined to be accepted and work on meniscus repair with using biomaterials in large animal models in another country, Canada. My Ph.D. journey was a great experience and opportunity not only I grow up in science and academic life, but also, I learned how to turn the challenges into a solution and success, how to deal with turning points in my personal life, and how to be resilient in everyday life.

There are many people that have earned my gratitude for their contribution to my Ph.D. More specifically, I would like to thank groups of people, without whom this thesis would not have been possible: my advisor, co-advisor, my thesis committee members, my lab mates, my industrial collaborators, funding agencies, and my family.

First and foremost, I would like to thank my director Dr. Buschmann who gave me the chance to work in his laboratory in Canada. His practical guidance and management in our team helped me all the time of my research. I could not have imagined having a better advisor and mentor for my Ph.D. study. Under his supervision, I learned how to define a research problem, find a solution to it, and finally publish the results. On a personal level, Dr. Buschmann inspired me by his hardworking and passionate attitude. I am thankful for him to give me the opportunity to present my project at international and national conferences which leads to my professional growth and expanding my networking in the same scientific area.

Special thanks go to my enthusiastic supervisor, Dr. Lavertu, for his tremendous academic support during my journey especially toward the end of my Ph.D. Dr. Lavertu who provided me with another opportunity to join his team and have access to the laboratory and research facilities. Without his precious support, it would not be possible to conduct this research and finish it. To summarize, I would give Dr. Buschmann and Dr. Lavertu, most of the credit for becoming the kind of scientist I am today.

I am also thankful to my co-supervisor professor Caroline Hoemann, for her valuable contribution to the progress of my research especially for her constructive comments in my publications. Her motivation has made the journey of Ph.D. more interesting.

I would like to express my special appreciation and thanks to my amazing supervisor, Dr Anik Chevrier. Anik has been a tremendous mentor for me. I truly acknowledge her enthusiasm and passion in each step of my project. I remember my feeling and excitement the first day when Dr. Buschmann introduced me to Anik, almost 4 years ago. Her positive outlook, support, encouragement, and credible ideas have been great contributors to the completion of the thesis. I learned from Anik how to initiate a project and how to terminate it within the deadline.

Special thanks go to professors Showan Nazhat, Jianyu Li, David Menard, and Thomas Gervais, for being members of my thesis committee. I'm really thankful for all your assistance.

I acknowledge the technical contributions of the funding sources: Canadian Institutes of Health Research, Canada Foundation for Innovation, Groupe de Recherche en Sciences et Technologies Biomédicales, Natural Sciences, Engineering Research Council of Canada, and Ortho Regenerative Technologies Inc, Prima Quebec.

Thanks to my friends and my colleagues for listening, offering me advice, and supporting me through this entire process. Thank you: Nikrooz, Abbas, Colleen, Ashkan, Gabrielle, Mohamad, Daniel, Rasheh, David, Genevieve, Ousama, Nazanin, Parikshat, Ruilong, Emily, Fazl, and Chi-Yuan. I must also appreciate the contributions of my colleagues, Mark Hurtig, Julie Tremblay, Genevieve Picard, Vincent Darras, Nicolas Tran-Khanh, Sochdeadt Sim, Insaf Hadjab, and Chi-Yuan Chang. I would like to highley appreciate Dr. Morsey inspiration toward the end of my PhD. I look forward to continuing our relationships and further collaboraiton with you.

Last but not the least, I would like to thank my family: to the memory of my father, Hossien Ghazi zadeh, and my mother, Mina Moshrefi, for giving birth to me at the first place and supporting me spiritually throughout my life. This work would also have been impossible without their help. A special thank to my amazing brother, Reza Ghazi zadeh, being a source of my inspiration for his patience during my years of study abroad. Reza was always with me when I had challenges and difficulties. I love you with all my heart. You were terrific to me and still are. I dedicate this thesis to them.

RÉSUMÉ

Les maladies musculo-squelettiques constituent un problème important dans la pratique orthopédique. Les pathologies méniscales font partie des blessures les plus fréquentes au genou de l'articulation fémorotibiale, ce qui pose un défi unique aux chirurgiens orthopédistes et constitue une source majeure d'invalidité dans le monde. Le ménisque est un tissu complexe fibrocartilagineux qui absorbe les chocs lorsque les forces sont transmises au compartiment articulaire. Le taux et la réussite de guérison sont limités par les caractéristiques des déchirures, l'état chronique ou aigu, le profil du patient et la stabilité des articulations. Les techniques et traitements actuels de guérison ne sont efficaces que pour les lésions des zones vasculaires externes du ménisque, tandis que la guérison des lésions dans les zones avasculaires internes du ménisque demeure difficile, en particulier dans les cas de déchirures complexes ou traumatiques et dégénératives. La méniscectomie arthroscopique est la chirurgie du genou là couramment effectuée. Elle génère souvent une instabilité fonctionnelle à long terme et finit par évoluer vers une arthrose précoce du genou. La guérison du ménisque et les allogreffes constituent un traitement alternatif à la méniscectomie. Le fardeau clinique et financier important de l'arthrose pousse les scientifiques à étudier des stratégies d'augmentation et de régénération pour stimuler la réponse tissulaire du ménisque. Tout le processus de développement du produit, l'innocuité et l'efficacité des implants médicaux doivent être testés sur des modèles animaux précliniques avant l'application en clinique. Déterminer le modèle animal le plus approprié pour étudier les mécanismes et les processus de guérison du ménisque est essentiel. Ainsi, les grands modèles animaux qui reproduisent la fonction biomécanique, l'anatomie et la composition du ménisque humain sont intéressants et pertinents. Les ovins sont l'un des modèles bien établis d'évaluation préclinique des outils de remplacement et de guérison du ménisque. Mon objectif initial était d'effectuer une revue de la littérature portant sur les traitements actuels pour les lésions du ménisque, ainsi que les stratégies d'augmentation les plus courantes pour augmenter le taux de guérison du ménisque telles que la tréphination, l'abrasion synoviale, l'injection de plasma-riche en plaquettes (PRP) et l'enrobage à l'aide de matériaux de matrice extracellulaire. J'ai également discuté pourquoi des implants de chitosane et de composés sanguins autologues seraient en mesure d'améliorer la guérison du ménisque. Cette revue couvrant les algorithmes de traitement des lésions du ménisque m'a guidée vers une meilleure conception de mes recherches expérimentales au cours de mon doctorat. L'utilisation de PRP autologue a été proposée pour des applications cliniques potentielles,

en raison de sa simplicité d'isolation et de sa disponibilité. Le chitosane possède des effets thérapeutiques bénéfiques dans le contexte de pathologies orthopédiques. Des essais comparatifs randomisés et contrôlés sont nécessaires dans le domaine de la guérison du ménisque pour améliorer les symptômes chez les patients, la fonction articulaire et la qualité de vie. Il a été démontré que les formulations lyophilisées de chitosane (CS) pouvant être solubilisées dans du PRP améliorent la guérison du cartilage et de la coiffe des rotateurs dans des modèles animaux précliniques. Ces études m'ont motivé et m'ont amené à évaluer les mécanismes d'action et le processus de guérison induits par le chitosane-PRP dans un contexte de guérison des ménisques. Nos études *in vivo* nous ont permis d'affiner le modèle de mouton afin de se rapprocher de l'état pathologique de la maladie articulaire chez l'homme. Nous avons découvert qu'augmenter la guérison du ménisque en utilisant des implants hybrides chitosan-PRP en combinaison avec des sutures, la tréphination et l'abrasion est bénéfique et sans danger pour les traitements des anomalies méniscales complexes, ce qui pourrait prévenir l'apparition précoce de l'arthrose à long terme. Cependant, des travaux futurs sont nécessaires pour améliorer davantage les propriétés régénératrices, comprendre les mécanismes en jeu et évaluer l'effet des implants à long terme. Nous avons effectué une observation clinique, évalué la rétention des implants, une évaluation microscopique et macroscopique du ménisque, de la membrane synoviale et du cartilage et avons effectué une cartographie électromécanique des surfaces du cartilage articulaire, à 3 semaines, 6 semaines et 3 mois après la chirurgie. Nos hypothèses de départ pour ces études pilotes de faisabilité étaient les suivantes : 1) La réparation du ménisque serait améliorée par l'application de CS-PRP aux lésions, mais pas par l'application de PRP uniquement ; 2) Que la guérison seraient améliorés en utilisant des implants CS-PRP en conjonction avec la technique d'enrobage par rapport aux implants CS-PRP injectés dans le site de la lésion ou en enrobant seulement. Nous avons constaté que le modèle de lésion unilatérale permettait aux animaux de protéger le genou traité contre la mise en charge postopératoire et d'améliorer le taux de réussite de 25 à 50% par rapport au modèle bilatéral. Les brebis boitaient de façon intermittente quelques semaines après le traitement, peu importe lequel. Les implants de chitosane-PRP résidaient en partie dans les lésions et les canaux de tréphination un jour après la chirurgie. Les lésions étaient visibles macroscopiquement au moment de la nécropsie à 1 jour, 3, 6 semaines et 3 mois et les bords des lésions étaient généralement bien apposés. Un tissu de guérison rougeâtre et des signes de néovascularisation étaient visibles dans les genoux traités au chitosane-PRP à 6 semaines et à 3

mois et les hybrides induisaient le recrutement cellulaire de la périphérie vascularisée du ménisque vers les canaux de tréphination. Une intégration partielle et totale entre le tissu de guérison et le tissu méniscal d'origine a été réalisée dans ces genoux traités. De plus, les implants CS-PRP ont été bien tolérés dans l'environnement du genou et aucune preuve d'effet indésirable n'a été observée pendant la période de suivi. L'ajout d'une technique d'enrobage utilisant la matrice de membrane de collagène Chondro-Gide en conjonction avec des implants CS-PRP ou avec du PRP seul n'a pas amélioré la guérison. En résumé, nos données suggèrent que les implants de chitosane-PRP pourraient à eux seuls résoudre efficacement les limitations actuelles de la guérison du ménisque et posséderaient un potentiel plus grand que le PRP seul pour améliorer les résultats de la guérison et restaurer la fonction du ménisque. Notre troisième objectif était d'évaluer 1) La compatibilité des formulations de chitosane lyophilisées avec différents types de systèmes PRP commercialisés, et 2) De définir une gamme de degrés de désacétylation du chitosan (DDA) et le poids moléculaire moyen en nombre (Mn) qui produiraient des formulations lyophilisées avec des caractéristiques de performance satisfaisantes pour applications orthopédiques. Nos hypothèses de départ étaient les suivantes : 1) Les formulations de chitosan devraient être facilement solubles dans les PRPs du commerce, présenter des propriétés visqueuses et coaguler en temps voulu pour produire des caillots de chitosan-PRP hybrides homogènes qui résistent à la rétraction et sont forts mécaniquement, et 2). Bien que les différents systèmes de préparation de PRP produiraient des PRP ayant des propriétés variables, toutes les préparations de PRP seraient compatibles avec cette technologie. Des formulations contenant 1% m/v de CS, 1% m/v de tréhalose (lyoprotecteur), 42,2 mM de $CaCl_2$ (activateur de la coagulation) ont été préparées avec cinq chitosanes différents. Sept préparations différentes de PRP ont été utilisées pour solubiliser les formulations, notamment : 1) Arthrex Angel fixé à 2% d'hématocrite, 2) Arthrex Angel fixé à 7% d'hématocrite, 3) Harvest SmartPrep 2, 4) RegenLab RegenKit-BCT, 5) RegenLab RegenKit- THT, 6) système de double seringue Arthrex ACP, et 7) système ACE EZ-PRP. La performance des formulations de chitosane-PRP ont été évaluées via la solubilité, le pH et l'osmolalité, les propriétés de coagulation avec la thromboélastographie, les propriétés de coagulation avec une méthode Lee-White modifiée, la viscosité, l'expression des liquides, la résistance mécanique du caillot et l'homogénéité du caillot. L’évaluation macroscopique des formulations lyophilisées a montré qu’elles étaient toutes blanches, homogènes et légèrement rétractées des parois de la fiole après la lyophilisation. Les formulations lyophilisées ont facilement pû être solubilisées avec toutes les préparations de PRP.

Les formulations de CS-PRP étaient plus visqueuses que leurs contrôles de PRP, ce qui est attrayant pour une une injection *in vivo*. Dans le test de coagulation statique, tous les contrôles PRP coagulaient, exprimaient du sérum, se rétractaient et perdaient leur masse de manière significative, tandis que les caillots CS-PRP résistaient à la rétraction du caillot induite par les plaquettes. Les résultats histologiques ont révélé que la dispersion de CS était homogène dans les caillots de CS-PRP. Notre quatrième objectif était d'optimiser et de réduire de 3 à 1 ou 2 jours le cycle de lyophilisation (FD) traditionnellement utilisé dans notre laboratoire, et d'évaluer les performances du produit avec du PRP humain et du plasma commercial. Nos hypothèses de départ étaient les suivantes : 1) Le cycle de lyophilisation des formulations CS peut être optimisé pour minimiser le temps de lyophilisation global de 3 à 1-2 jours afin de produire des formulations lyophilisées stables, 2) Les formulations lyophilisées préparés avec le cycle de lyophylisation plus court seraient solubles dans le PRP humain, seraient visqueuses et coaguleraient rapidement pour produire des caillots hybrides homogènes forts mécaniquement. 3) Du plasma citraté commercial peut être utilisé pour évaluer les performances de la formulation. Des formulations contenant 1% m/v de chitosane DDA 82-84% Mn 45-55 kDa avec 1% m/v de tréhalose et 42,2 mM de $CaCl_2$ ont été préparées pour lyophilisation. La même méthodologie que celle décrite ci-dessus a été utilisée pour évaluer la performance des formulstions lyophilisés. Les formulations lyophilisées ont été solubilisés soit dans du PRP humain citraté soit dans du plasma commercial pour évaluer différentes caractéristiques. Les formulations de CS-PRP étaient plus visqueuses que leurs contrôles de PRP et de plasma. La thromboélastographie a révélé que le temps de réaction du caillot était plus court pour les formulations de chitosane-PRP. De plus, les formulations de chitosane-PRP ont résisté à la rétraction du caillot induite par les plaquettes, tandis que les contrôles PRP ont perdu jusqu'à 80% de leur masse d'origine après coagulation. Les résultats histologiques ont montré que le chitosane était dispersé de manière homogène dans les caillots de CS-PRP. En résumé, nos études pilotes de faisabilité chez le mouton ont montré des résultats prometteurs pour la guérison des lésions complexes par injection de chitosan-PRP, qui pourraient potentiellement être utilisé chez l'homme dans l'avenir. Nous avons raffiné le modèle animal et montré que les animaux pouvaient supporter les implants pendant toute la durée de l'étude sans effet délétère sur le compartiment articulaire, ce qui suggère une innocuité. De plus, les formulations lyophilisées de chitosane se sont révélées compatibles avec plusieurs PRP isolés avec des systèmes commerciaux. Enfin, l'optimisation du cycle de lyophilisation de 3 à 1 jour a été réalisée avec succès et les

formulations se sont comportées comme prévu lorsqu'elles étaient solubilisées dans du PRP ou du plasma.

ABSTRACT

Musculoskeletal diseases are a significant problem in orthopedic practice. Meniscal pathologies conditions are among the most frequent knee injuries of the femorotibial joint posing a unique set of challenges for orthopedic surgeons and are a leading source of disability worldwide. The meniscus is a fibrocartilage complex tissue that acts as shock absorbent for forces transmitted over the joint compartment. The rate of healing and success of current surgical meniscus repair are limited by the tear properties, chronic or acute state, patient profile, and joint stability. Current repair techniques and treatments are only effective for defects in outer vascular zones of meniscus while healing of the lesion in the inner avascular zones of menisci remains a significant and present challenge, especially in cases of complex or traumatic and degenerative tears. Arthroscopic meniscectomy is the most common knee surgery which often leads to long-term functional instability and eventually progresses to early knee osteoarthritis (OA). Meniscus repair and allografts have been gaining attention as alternatives to meniscectomy. The significant clinical and financial burden of OA drives scientists to investigate augmentation and regenerative strategies for stimulation of menisci tissue response.

All the product development process, safety, and efficacy of medical implants need to be tested in preclinical animal models before the application for clinical translation. Determining of the most suitable animal proxy for investigation of mechanisms and process of meniscus healing to the human joint is a necessity. Thereby, large animal models which duplicate human meniscus biomechanical function, anatomy, and composition are more translatable to clinical practice. Ovine is one of the well-established models for preclinical assessment of meniscus replacement and repair tools.

My initial objective was to review the literature and discuss the current clinical management guidelines for primary meniscus repair techniques as well as the most current augmentation strategies to enhance the rate of meniscus healing by using trephination, synovial rasping, abrasion, blood clot placement, platelet-rich plasma (PRP) injections, and wrapping with extracellular matrix materials. I also discussed the rationale for using chitosan polymer and autologous blood component implants to improve meniscus repair. Performing such a review covering treatment algorithms of meniscus lesions guided me to better design my experimental research using polymer-autologous blood component implants to improve meniscus repair during my Ph.D.

Autologous PRP is widely used as a source of growth factors in different medical fields. Chitosan (CS) has documented beneficial therapeutic effects in context of orthopedics pathologies. Further randomized and controlled comparative trials are necessary in the field of meniscus and cartilage repair for improving symptoms in patients, joint function, and quality of life. Freeze-dried formulations of CS that can be solubilized in PRP have been shown to improve repair of cartilage and rotator cuff in preclinical small and large animal models. This motivated and drove me to assess mechanisms of action and repair process by using of chitosan-PRP in the context of fibrocartilage menisci repair in sheep as a relevant large animal model.

Our *in vivo* studies allowed us to refine the sheep model in order to be relevant to the pathological condition of joint disease found in the humans. We discovered that augmenting meniscus repair by using chitosan-PRP hybrid implants in combination with sutures, trephination, and rasping is beneficial and safe for treatments of complex menisci defects which could have the potential to prevent early onset of OA in the long-term. However, future work is necessary to further enhance regenerative properties, understand the mechanisms involved, and evaluate the effect of the implants in the long-term. We performed clinical observation, assessed implant retention, microscopic and macroscopic evaluation of meniscus, synovium and cartilage and electromechanical mapping of articular cartilage surfaces, at 3 weeks, 6 weeks, and 3 months post-surgery. Our original hypotheses for these feasibility pilot studies were that I. Meniscus repair would be improved by the application of CS-PRP to the tears, but not by application of PRP alone, and II. That repair outcomes would be improved by using CS-PRP implants in conjunction with the wrapping technique over CS-PRP implants injected in the tear site alone or wrapping alone. We found that the unilateral tear model allowed the animals to protect the treated knee from weight-bearing post-operative and improved success rate from 25 to 50% compared to the bilateral model. The sheep had some intermittent lameness for the a few weeks post- treatment which was not specific to any treatment. The chitosan-PRP implants were partly resident in the tears and trephination channels at 1-day post-surgery. The tears were macroscopically visible at the time of necropsy at 1 day, 3, 6 weeks and 3 months and the edges of the tears were usually well apposed. A reddish repair tissue and signs of neo-vascularization were visible in chitosan-PRP treated knee at 6 weeks and 3 months and hybrids induced cell recruitment from the vascularized periphery of the menisci towards the trephination channels. Partial and total integration between the repair tissue and the original meniscal tissue was achieved in these treated knees. In addition, CS-PRP implants

were well-tolerated in the knee environment and evidences of adverse effect did not observe during the follow-up period. Addition of wrapping technique by using of collagen membrane matrix of Chondro-Gide in conjunction with CS-PRP implants or PRP alone did not improve repair. In summary, our data suggest that chitosan-PRP implants by themselves could be efficient in overcoming the current limitations of meniscus repair and have several regenerative features that reveal a greater potential than PRP alone to improve repair outcomes and restore meniscus function.

Our third aim was to assess I. The compatibility of freeze-dried chitosan formulations with different types of commercially marketed PRP systems, and II. Define a range of chitosan degree of deacetylation (DDA) and the number average molecular weight (Mn) that would yield freeze-dried formulations with satisfactory performance characteristics for clinical orthopedic conditions. Our starting hypothesis was that I. Chitosan formulations should be soluble and easily reconstituted in commercial PRPs, have paste-like properties and coagulate in a timely fashion to produce homogenous hybrid chitosan-PRP clots that resist retraction and are mechanically strong, and II. Although the different PRP preparation systems would yield PRPs with varying properties, all PRP preparations would be compatible with this technology. Formulations containing 1% w/v CS, 1% w/v trehalose as lyoprotectant, and 42.2 mM $CaCl_2$ as a clot activator were prepared with five different chitosan, encompassing the low, mid, and high range of DDA and Mn product specifications were freeze-dried. Seven different PRP preparations were used to solubilize the formulations *in vitro*. Performance characteristics of chitosan-PRP formulations for clotting properties, runniness, liquid expression, paste-like properties, clot mechanical strength, and clot homogeneity were assessed. Also, solubility, pH, and osmolality of all the formulations were measured. Macroscopic assessment of cakes showed all the cakes were white, homogenous, and were slightly retracted from the vial walls following lyophilization. We found that freeze-dried formulations were solubilized with all PRP preparations. CS-PRP formulations were less runny than their corresponding PRP controls demonstrating its paste-like properties for *in vivo* injection. Assessment by thromboelastography revealed that all CS-PRP formulations had a clot reaction time below 9 minutes. In the static clotting assay, all PRP controls clotted, expressed serum, retracted, and lost their mass significantly, while the CS-PRP clots resisted platelet-mediated clot retraction. Histological results revealed that CS dispersion was homogeneous within CS-PRP clots.

Our fourth objective was to optimize and reduce the freeze-drying (FD) cycle which has been historically used in our lab from 3 days to 1 or 2 days and to assess performance of the product with benchtop human PRP and human commercial plasma. Our starting hypotheses were that I. Freeze-drying cycle of CS formulations can be optimized to minimize overall freeze-drying time from 3 days to 1-2 days to produce cakes that will not collapse, II. FD cakes prepared with the shorter freeze-drying cycles would be soluble in benchtop human PRP to yield chitosan-PRP formulations which are paste-like, coagulate rapidly, and produce mechanically strong homogenous hybrid clots, and III. Commercial citrated plasma can be used instead of PRP to assess formulation performance. Formulations containing 1% w/v chitosan DDA 82-84% Mn 45-55 kDa with 1% w/v trehalose and 42.2 mM $CaCl_2$ were prepared for freeze-drying. The same methodology was used as described above to assess performance characteristics of the freeze-dried cakes. The cakes that were non-collapsed were solubilized either in citrated pooled normal plasma or benchtop human PRP to assess different performance characteristics. CS-PRP formulations were less runny than their PRP controls and citrated pooled normal plasma. Data from thromboelastography machine revealed clot reaction time was shorter for chitosan-PRP formulation. Also, chitosan-PRP formulations resisted platelet-mediated clot retraction while PRP controls lost up to 80 % of their original mass in the glass tubes. Histological findings showed that chitosan was homogeneously dispersed within CS-PRP clots.

In summary, our feasibility pilot studies in sheep showed promising results in terms of repair of complex defects by injection of chitosan-PRP that could be potentially translated to humans in the future. We refined the animal model and showed that animals could withstand implants for the duration of study with no deleterious effect to the other joint compartment, which suggests high safety. In addition, the chitosan formulations were shown to be compatible with several PRPs isolated with commercial systems. Lastly, optimization of freeze-drying cycles from 3 day to 1 day was successfully performed and formulations behaved as expected when solubilised in PRP or plasma.

TABLE OF CONTENTS

LIST OF TABLES

LIST OF FIGURES

LIST OF SYMBOLS AND ABBREVIATIONS

APM	Arthroscopic Partial Peniscectomy
α	Alpha
ACL	Anterior Cruciate Ligament
AAOS	American Association of Orthopaedic Surgeons
AC	Articuler Cartilage
β	Beta
b-FGF	Basic-Fibroblast Growth Factor
BM	Bone Marrow
BMAC	Bone MarrowAspirate Concenearte
BMS	Bone Marrow Stimulation
CS	Chitosan
CBC	Complete Blood Count
CMI	Collagen Meniscus Implants
CM	Chondrogenic Medium
CaCl2	Calcium Chloride
cm	Centimeter
CD	Cluster of Differentiation
DP	Deproteinization
DM	Demineralization
DC	Decolorization
DDA	Degree of Deacetylation
D	Dimensional
EGF	Epidermal Growth Factor

FU	Follow-Up
F	Femur
FD	Freeze-Dried
FBGC	Foreign Body Giant Cell
GF	Growth Factor
GP	Glycerol Phosphate
GPSIII	Gravitational platelet sepration system III
GAG	Glycosaminoglycan
H_2O	Water
HA	Hyaluronic Acid
HCl	Hydrochloric Acid
HGF	Hepatocyte Growth Factor
H&E	Hematoxylin and Eosin
IGF	Vascular Endothelial Growth Factor
IL	Interleukin
KOOS	Knee Injury and Osteoarthritis Score
IKDC	International Knee Documentation Committee
L-PRF	Leukocyte-Rich Platelet-Rich Fibrin
MRI	Magnetic Resonance Imaging
MRA	Magnetic Resonance Arthrography
MOON	Multicenter Orthopaedic Outcomes Network
MFC	Medial Femoral Condyle
MTP	Medial Tibial Plateau
mm	Millimeter

mL	Millilitre
MW	Molecular Weight
Mn	Number Average Molar Mass
MA	Maximal Amplitude
MSC	Mesenchimal Stem Cells
MCL	Medial Collateral Ligament
MLS	Meniscus-Like strucutre
MA	Maximal Amplitude
MPa	Megapascal
mTorr	Millitorr
μ	Micro
μL	Microlitre
NMR	Nuclear Magnetic Resonnace
N/S	Not-Specified
N/A	Non-Applicable
NH_3	Amino
NBF	Neutral Buffered Formalin
NaOH	Sodium Hydroxide
OA	Ostheoarthtics
PCNA	Proliferating Cell Nuclear Antigen
PDI	Polydispersity Index
PCL	Posterior Cruciate Ligament
PCP	Perimeneiscal Capaliary Plexux
PU	Polyurethane

PCL	Polycaprolacone
PLGA	Polylactic-co-Glycolic Acid
PLLA	Poly-L-lactic Acid
PGA	Polyglycolic Acid
PLGA	Polylactic-co-Glycolic Acid
PM	Partial Meniscectomy
PRP	Platelet-Rich Plasma
PPP	Platelet-Poor Plasma
PDGF-AB	Platelet Derived Growth Fcator-AB
P-PRF	Leukocyte-Poor Platelet-Rich Fibrin
PG	Proteoglycan
PS	Polysaccharide
P-PRP	Leukocyte-Poor Platelet-Rich Plasma
QofL	Quality of Life
QP	Quantitative Parameter
RBC	Red Blood Cell
R-R	Red-Red
R-PRP	Leukocyte-Rich Platelet-Rich Plasma
rhFVIIa	Recombinant Human Factor -rhFVIIa
RA	Rheumatoid Arthritis
ROM	Range of Motion
Saf-O	Safranin-O
SC	Stem Cell
SMSC	Synovium-Derived Mesenchymal Stem Cells

SEM	Scan Electron Microscpy
TGF-B	Transforming Growth Factor-Beta
Tp	Product Temperature
Tg	Glass Transition Temperature
Tg	Eutectic Temperature
TM	Total Meniscectomy
TE	Tissue Engineering
TEG	Thromboelastography
T	Tibia
TNF-α	Tumor Necrosis Factor
UK-ACL	University of Kentucky Anterior Cruciate Ligament Test
V/v	Volume/volume
VEGF	Vascular Endothelial Growth Factor
WOMET	Western Ontario Meniscal Evaluation Tool
WORMS	Whole Organ MRI Score
W-W	White-White
W-R	White-Red
WOMAC	Western Ontario and McMaster Universities Osteoarthritis Index

LIST OF APPENDICES

CHAPTER 1 INTRODUCTION

More than 1.7 billion people in the world are suffering from musculoskeletal conditions which cost an estimated $213 billion either directly or indirectly. Orthopedic disorders involving tissues such as cartilage, bone, intraarticular ligaments, and meniscus have significant socioeconomic impact (1, 2). Osteoarthritis (OA) is a slowly progressive joint disorder and the primary cause of musculoskeletal disability worldwide. Osteoarthritis is a multifactorial disease affecting the whole joint rather than only articular cartilage (AC). The meniscus is a fibrocartilaginous tissue located between the femur and tibia. The menisci are the crucial structures of knee joint acting as shock absorbent and protecting the articular cartilage. Inner zones of menisci lack blood supply and healing capacity, therefore, the potential for regeneration is very poor (3).

Meniscal tears are among the most common pathologies of the knee joint. Based on past reports, the incidence of meniscus tears are estimated to be as high as 70 per 100,000 knee injuries with even higher rate in the elderly, men, medial meniscus, and active populations (4). There is evidence suggesting that asymptomatic meniscal lesions are common incidental findings on knee magnetic resonance imaging (MRI) of at least one-third of the knees of middle or elderly individuals. Such tears limit the range of motion causing clinical symptoms such as sharp pain, swelling, effusion, locking, and catching in the knee (2, 5, 6). Arthroscopic partial meniscectomyis the most common orthopedic surgical procedure that is performed for small radial and complex meniscus tears (7-9). Although partial meniscectomy relieves pain, it is associated with a high risk of developing knee OA. Loss of meniscal function due to trauma, injury, or partial meniscectomy may lead to increased biomechanical stress and relative overloading on the joint which further progress to OA and pain over time. Knee OA is clinically associated with meniscal tear and degeneration (2, 10).

Surgical repair of meniscus tears can be performed by using suture-based devices. Complex or degenerative tears located in the avascular segments of the meniscus affect the fibrocartilage structures and surrounding tendons (4, 11). Complex tears which develop mostly in middle or older-aged patients involve a progressive horizontal cleavage of the meniscus usually in the multiplane direction without history of significant acute trauma. Patient- and clinical-reported outcomes of meniscus repair and meniscectomy have demonstrated significant failures involving re-tear or reoperation at long-term follow-up (9). Therefore, selection of appropriate management strategy depends on multiple factors for patients and needs carefull consideration (12).

Recent technologies are attempting to repair the tissue while paying more attention to preserve the structural integrity of the knee joint to lower the risk of OA. Therefore, the combination of sutures and biological augmentation strategies such as meniscus wrapping with extracellular matrix materials, trephination, synovial and meniscus rasping, fibrin/blood clot placement, and platelet-rich plasma (PRP) injections have been introduced to improve healing rate of the meniscus repair (4, 7, 13). For a tissue-engineered meniscus, selection of an optimal cell type, appropriate growth factors, and the type of scaffold are crucial. Tissue engineering approaches are still at the early development stage (14, 15). Safety and efficacy of ortho biological products need to be assessed more thoroughly in prospective and randomized clinical studies (16). The general aim of meniscus repair would be to restore the tissue structure and biomechanical function to minimize pain and OA in the long-term.

Platelet-rich plasma is an autologous biological agent with a raised platelet concentration above the physiological level and has been used predominantly in the musculoskeletal field for sports injuries. Activation of the platelets leads to the local liberation of several growth factors and cytokines from granules which play a pivotal role in the coordination of inflammation, cell proliferation, differentiation, angiogenesis, and tissue remodeling. Also, PRP contains the full complement of clotting factors which contribute to hemostasis and aggregation (17, 18). These anabolic platelet-derived growth factors have been shown to affect meniscal cell function positively and induce soft-tissue repair augmentation. Different commercial PRP preparation systems and medical devices are available, which generate PRPs that contain varying concentrations of platelets and blood components. The presence or absence of leukocytes and the structure of fibrin determine the different families of PRP (16). Potential anabolic or catabolic effecst of leukocytes and platelets in PRP is an intensive ongoing debate. Upon delivery of platelet-rich plasma to the desired site, PRP is activated which causes the fast release of growth factors from platelets. The short half-life of growth factors in PRP, the significant dilution of PRP by residual arthroscopic fluid at the time of injection, and variability in the content pose methodological challenges to investigators. To overcome theese limitations, clot activators and modified natural biopolymers can be added to PRP which resul in the formation of a dense matrix and prolongs the release of growth factors (GF). Further randomized controlled clinical trial studies with a large number of patients and a long-term follow-up remains a necessity (16, 19).

Chitosan (CS), a biocompatible and biodegradable cationic polysaccharide family derived from the alkaline deacetylation of chitin, has been used extensively for soft and hard tissue engineering (20). Chitosan accelerates healing of the wound and has some similarity to hyaluronan which is found in extracellular matrices of cartilage (23). Chitin is degraded by lysozymes and produce oligomers of *N*-acetylglucosamine. Theses oligomers act as templates for hyaluronan synthesis to promote cell adhesion and proliferation which lead to massive cell movement and tissue re-organization. Chitosan shows immunopotentiating activity by macrophages stimulation. This naturally-derived polysaccharide is well-tolerated at the articular synovial level and favors repair process in meniscus tissue through promotion of angiogenesis (21). Freeze-drying (FD) is a method for preservation of pharmaceutical products and drugs. FD is a three-step process that can provide increased long-term stability and minimize degradation of chitosan-based scaffold for manufacturing (22).

In the context of cartilage repair, our lab has shown that chitosan-glycerol phosphate solutions can be mixed with whole blood and implanted over cartilage defects to augment repair by increasing cell recruitment, transient vascularization, as well as a polarization of the macrophage phenotype towards the alternatively-activated pro-wound healing lineage, and stimulated secretion of anabolic wound repair factors, all of which are also expected to be beneficial in the context of meniscus repair (23, 24). We have developed freeze-dried formulations of chitosan that can be solubilized in PRP to form injectable CS-PRP implants for orthopedic tissue repair. Previous studies showed that CS-PRP implants resist platelet-mediated retraction post-clotting, release increased amounts of platelet-derived growth factors, and have prolonged residency *in vivo* compared to PRP alone. CS-PRP implants have also shown potential to improve repair of rotator cuff and cartilage in small and large animal models. Hence, the starting hypothesis for this project was that the biological effects of CS-PRP hybrid implants would also be beneficial for meniscus repair (19, 25).

CHAPTER 2 OBJECTIVES AND HYPOTHESIS

2.1 General objective and hypothesis

The overall objective of this thesis was to make an outstanding contribution to improve current surgical treatment repair strategies for meniscus tears. In this context, the research presented here is to enhance current surgical treatment of meniscus tears by assessing the effect of freeze-dried chitosan-PRP implants in ovine models.

Chitosan-blood hybrids have previously been shown to improve pre-clinical cartilage repair outcomes in small and large animal models through mechanisms involving increased cell recruitment, angiogenesis, cell migration, repair tissue synthesis, and tissue remodeling/integration. Since current surgical techniques for meniscus repair also rely on cell recruitment from adjacent tissues through trephination and rasping, chitosan-PRP hybrids are expected to enhance the success of meniscus repair through similar mechanisms of cell recruitment and angiogenesis. Here, platelet-rich plasma rather than whole blood will be mixed with the polymer. PRP is obtained through centrifugation of anti-coagulated blood to produce an increase in platelet concentration over baseline. Hybrid clots composed of chitosan and PRP are expected to have significant bioactivity through the release of platelet-derived growth factors in order to improve meniscus repair.

In the first study, feasibility of using CS-PRP implants to improve meniscus repair in ovine models was investigated. In the second study, compatibility of freeze-dried chitosan formulations with PRPs prepared with different commercial automated systems was assessed. Finally, in the third study, freeze-dried cycle of chitosan formulations was optimized and reduced from 3 days to 1 day and performance characteristics of the freeze-dried formulastions were evaluated.

2.2 Study 1: Freeze-dried chitosan-PRP injectable surgical implants for meniscus repair: pilot feasibility studies in ovine models

2.2.1 Objective for Study 1

The overall purpose of this study was to assess whether ovine meniscus repair would be improved by application of freeze-dried chitosan PRP to the tears over PRP alone or/and a meniscus wrapping technique.

The first pilot study used a bilateral longitudinal surgical laceration model where tears were treated with suturing along with the CS-PRP implant or with PRP alone for 3 weeks or 3 months.

The second pilot study used a unilateral complex laceration model where tears were treated with suturing along with the CS-PRP implant, or the tears were treated with a wrapping technique using a Chondro-Gide collagen membrane, or the tears were treated with both CS-PRP and the wrapping technique for 6 weeks.

The purpose of conducting sheep studies of meniscus repair is to approximate as closely as possible the clinical pattern and pathology of meniscus tears and repair. In this context, it is worth noting that the surgical model was significantly improved from the first to the second study.

2.2.2 Hypotheses for Study 1

Our original hypotheses were that:

First pilot study: Freeze-dried chitosan formulations can be reconstituted in autologous PRP and injected into meniscus defects, where they coagulate and form stable hybrid chitosan-PRP implants. Repair outcomes would be improved by using CS-PRP implants injected in the tear site through trephination channels, due to long-term residency over PRP alone. Suturing and application of CS-PRP via trephination was expected to augment repair of meniscus tears.

Second pilot study: Repair outcomes would be improved by using CS-PRP implants in conjunction with the wrapping technique over CS-PRP implants injected in the tear site alone or wrapping alone, due to increased implant retention and resulting bioactivity. Suturing, wrapping by membrane matrix, and application of CS-PRP via trephination was expected to augment repair of meniscus tears.

2.2.3 Methods for Study 1

Lyophilized formulations of chitosan were solubilized in autologous PRP and applied to surgically induced meniscus lacerations. In the first study, bilateral tears in 7 sheep were treated by suturing, trephination and injecting either CS-PRP or PRP into the tears. In the second study, unilateral tears in 6 sheep were treated by suturing, trephination and injecting CS-PRP in tears, wrapping the meniscus with a collagen membrane and injecting CS-PRP in tears and under the wrap or wrapping only. CS-PRP implants residency, recruitment of host cells, repair tissue integration, and vascularization were investigated by macroscopic, microscopic and histological procedures. Chondroprotective effects of the meniscus on the adjacent joints including articular cartilage of tibial plateau and the distal femurs were assessed by electromechanical mapping using the hand-held Arthro-BST device. Quality of adjacent articular cartilage and synovium was investigated by histology.

2.3 Study 2: Multiple platelet-rich plasma preparations can solubilize freeze-dried chitosan formulations to form injectable implants for orthopedic indications

2.3.1 Objective for Study 2

The purpose of this study was to determine whether the *in vitro* performance of the formulations depends on the type of PRP preparation used to solubilize chitosan. Our specific objectives were: I. Assess compatibility of this freeze-dried technology with the various types of PRP preparations that can be isolated with commercially available systems and II. Define a range of chitosan degree of deacetylation (DDA) and number average molecular weight (M_n) that would yield freeze-dried formulations with acceptable performance characteristics.

2.3.2 Hypotheses for Study 2

Our starting hypothesis was that although the different PRP preparation systems would yield PRPs with varying properties, all PRP preparations would be compatible with our freeze-dried chitosan technology.

PRP is a cost-effective source of platelet-derived growth factors and autologous cells and, ideally, this thesis will show that the freeze-dried chitosan technology is compatible with several autologous blood products, which would broaden its use clinically. We believe that applying these novel polymer-blood product formulations in conjunction with suture-based meniscus repair approaches to a large animal model, together with an assessment of *in vitro* performance, and checking of quality control will add a potential value and bring us one step closer to a new clinical option for meniscus repair. There are several commercial systems available on the market, and each system has a particular protocol for the isolation and administration of the PRP solution to the tissues. Variations include the initial volume of blood drawn, presence and type of anticoagulant, the spinning time, the speed of the centrifuge, addition or absence of activator, and whether the resultant PRP solution will include leukocytes or not.

2.3.3 Methods for Study 2

Blood was collected and PRP was isolated by using 1) Arthrex Angel set at 2% hematocrit, 2) Arthrex Angel set at 7% hematocrit, 3) Harvest SmartPrep 2, 4) RegenLab RegenKit-BCT, 5) RegenLab RegenKit-THT, 6) Arthrex ACP double syringe, and the 7) ACE EZ-PRP systems. Formulations containing chitosan, trehalose, and calcium chloride were freeze-dried. Freeze-dried formulations were mixed with PRPs and performance characteristics of CS-PRPs hybrids were assessed and tested *in vitro*. Solubility, pH, and osmolality of chitosan formulations were measured after and before reconstitution with different PRPs. Other properties of CS-PRPs hybrids such as paste-like properties, coagulation, clot retraction, and clot homogeneity were analyzed by runniness test, thromboelastography, liquid expression, and histology.

2.4 Study 3: Optimizing the freeze-drying cycle of FD-CS for orthopedic conditions: Assessing performance with human platelet rich plasma (PRP) and human commercial plasma

2.4.1 Objective for Study 3

The goal of the third study was to optimize and reduce the freeze-drying cycle of the chitosan formulations from 3 days to 1 day and to assess the performance of the product with benchtop

human PRP and human commercial plasma.

2.4.2 Hypotheses for Study 3

Our starting hypotheses were that: I. The freeze-dried cycle of the cakes can be optimized to decrease freeze-drying time from 3 days to 1 days and produce cakes that will not collapse, II. The freeze-dried cakes prepared with the shorter freeze-drying cycles should be soluble in benchtop human PRP to yield chitosan-PRP formulations which are paste-like, coagulate rapidly, and produce mechanically robust homogenous hybrid clots, and III. Commercial citrated plasma can be used instead of PRP to assess formulation performance.

2.4.3 Methods for Study 3

A series of freeze-drying cycles were designed based on a paper by Tang and Pikal. Formulations containing 1% (w/v) chitosan (DDA 82-84% and M_n 45-55 kDa) with 1% (w/v) trehalose and 42.2 mM calcium chloride were freeze-dried using different cycles. The cycles that produced non-collapsed cakes were selected for the second phase of the study where performance characteristics were assessed. Blood was collected and PRP was isolated by using ACE EZ-PRP system. Human commercial plasma was also used during the study. FD-CS formulations were mixed with PRP or human commercial plasma and tested *in vitro* by runniness test, thromboelastography, liquid expression, and histology.

CHAPTER 3 LITERATURE REVIEW

Menisci are vital for the normal functioning and longevity of the knee joint. It is essential to understand the ultrastructure and function of the meniscus to be able to design a meniscus implant which withstands the *in vivo* joint environment. The following sections will discuss the structure of the meniscus and how it relates to its function. The pathophysiology of the meniscus, as well as fundamentals to tissue engineering (TE) of the meniscus will then be discussed. A better understanding of the sheep and human meniscus composition and biomechanics advance not only therapies for repair of meniscus defects but also substantiate sheep as a suitable translational preclinical animal model for the human meniscus.

3.1 Structure and function of the knee meniscus

3.1.1 Anatomy of meniscus

The menisci (medial and lateral meniscus) of the knee are described as semilunar intraarticular fibrocartilagenous tissues located between the femoral condyles and the tibial plateau (26). Menisci are part of the surrounding ligamentous structures and bony attachments (7). The outer segment of the meniscus is convex, thick, and fixed to the fibrous capsule while the inner segment is concave, thin and free (26, 27). Both menisci are anchored to the underlying subchondral bone of the tibial plateau via meniscus horns. There is an array of ligamentous structures that help the stabilization of meniscus by transmitting of sheer and tensile load from the soft tissue to the bone (26, 28). Meniscofemoral ligaments (Humphrey and Wrisberg ligament) and transverse ligament keep the meniscus inside the joint compartment. Two ligaments attach the posterior horn of the lateral meniscus to the lateral insertion site of medial femoral condyle: Humphrey and Wrisberg ligament (Figure 3.1)**.** The lateral meniscus is more uniform, C-shaped, mobile, and larger than the medial meniscus (27, 28). From the posterior side, it is attached to the posterior cruciate ligament (PCL), and medial femoral condyle (MFC) via Weisberg and Humphrey ligaments and its anterior horn attaches to the anterior cruciate ligament (ACL). The medial meniscus is less uniform and wider at the posterior dimension connected to the PCL (24, 27) (Figure 3.1). Lateral meniscus covers 75-93%, and medial meniscus covers 51-74% of the proportion of tibial plateau. Gross examination of healthy meniscus reveals a smooth and lubricated tissue. With aging,

microanatomy and morphology of meniscus alter, and it becomes stiffer and more yellowish while losing its elasticity. The elastic properties of the meniscus are gradually replaced with fibrous tissue and cellular content decreases thus leading to initiation of the tears (26).

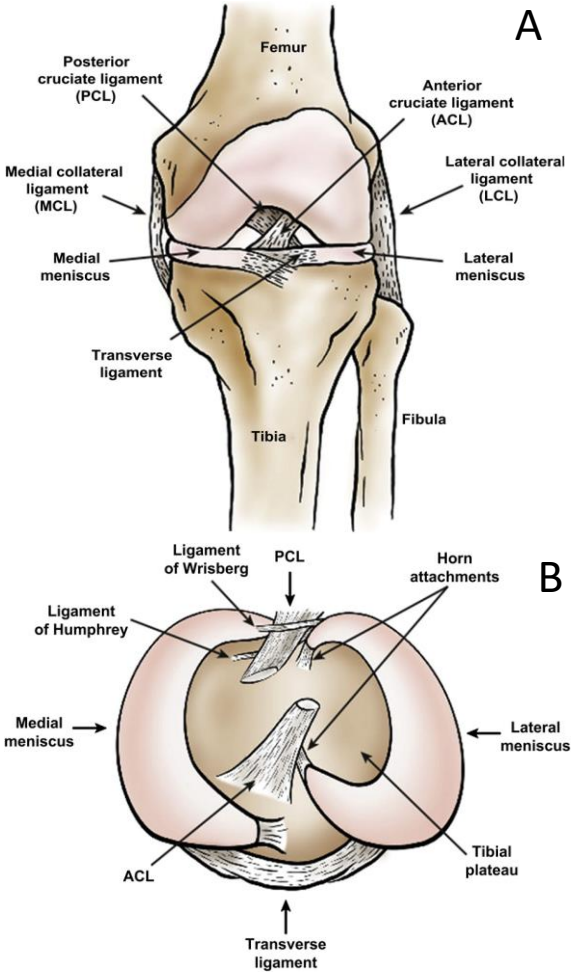

Figure 3.1 Gross anatomy of the knee joint. The menisci are two pads of fibrocartilage situated within the knee joint between the tibia and femur. Ligaments stabilize menisci within the joint. An anterior view (A) superior view (B), and the ligaments of the knee joint (28).

After 8-10 weeks of gestation, meniscus undergoes histological changes to adulthood. Cellular elements decrease as the fetus continues to develop and collagen fibers in the circumferential orientation increase. At maturity, the vasculature is limited to the outer portion of the meniscus. (26). The adult meniscus is a relatively avascular structure in which limited peripheral blood supply originates markedly from lateral and medial geniculate popliteal arteries which provide vascularization to the inferior and posterior of the meniscus. Branches from these arteries rise to a capillary plexus network within the synovial and capsular tissues of the knee joint along the periphery of the meniscus (26, 27). Radial branches from the perimeniscal capillary plexus (PCP) dive into the menisci with a higher supply to the anterior and posterior horn attachments. Endo-ligamentous vessels from the anterior and posterior horns process a short distance to the menisci body providing the potential for vascularization and nourishment. The tissue also receives nutrients and oxygen through synovial diffusion and mechanical pumping of the joint (26, 27). Anatomical studies showed that vascularization is limited to the periphery of the meniscus, estimated at 10-30% for the lateral meniscus and 10-25% for the medial meniscus, which determines its healing

properties and guides treatment options (27) (Figure 3.2). In menisci, the nerve fibers are associated with vascularity. Like blood vessels, the third inner region lacks neural innervation (29). The peripheral two-thirds of the body of the human meniscus is innervated by free nerve endings and three different mechano-sensors: ruffini corpuscles, pacinian corpuscles, and golgi tendon organ. Theses neural elements are rich in the posterior horns of the meniscus. It is hypothesized that the distribution of innervation and capability of generation of neurosensory signals in the meniscus depends on the feedback at the extreme of flexion and extension. The amount of blood vessels present in the meniscus depends on the individual's age as well as anatomical location (26, 27, 30).

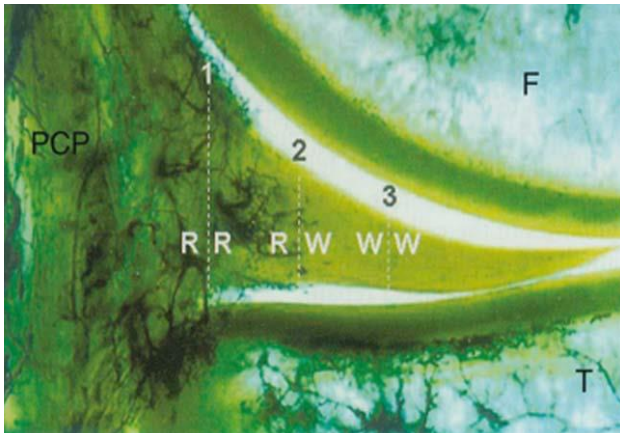

Figure 3.2 A frontal section of the vascularity of meniscus. Radial vessels from the perimeniscal capillary plexus (PCP) are penetrating the peripheral border of the medial meniscus via 3 zones: I. Red-red (R-R) zone is fully vascularized, II. White-red (R-W), and III. White-white (W-W) is within the avascular area of the meniscus. F: femur; T: tibia (27).

3.1.2 Biochemical composition of the meniscus

The meniscus is a structurally complex and inhomogeneous tissue. The meniscus has a dense extracellular matrix (ECM) which is primarily composed of a high quantity of water (72 %), fibrillar components, proteoglycans (PG), and cell binding glycoproteins interposed with cells (the remaining 28 %) (26, 28). It is critical to mention that the composition, vascularity, cellularity, shape, and size varies in all species based on age and gender (31). Human meniscus contains (dry weight) 60-70 % collagen, 17 % proteoglycans, and the remaining 1 % non-collagenous proteins, and adhesion molecules such as elastin. The role of the other fibrillar component of the meniscus, i.e., elastin, is not fully understood yet (28). Type I collagen is the predominant type of collagen in the vascular zone (80 % dry weight), with smaller quantities of variants such as type II, III, IV,

VI, and XVIII (<1 %). In the central avascular zone, collagen comprises up to 70 % dry weight, being 60 % type II collagen, and 40 % type I collagen (32). The structural orientation of collagen fibers is highly organized to provide the biomechanical properties of the tissue. The meniscus can be divided into three regions considering collagen orientation. The surfaces of the meniscus consist of randomly oriented collagen fibers. Just beneath this superficial network, there is layer of collagen fibrils. Towards the periphery, the collagen fibrils are organized in a radial perpendicular direction. In all other parts, the collagen mesh bundles intersect at various angles. The predominant portion of the meniscus collagen fibrils is localized in the central and internal region, where the bundles of collagen fibrils are arranged in a circular manner. Predominant collagen fibers lie along the circumferential axis enhancing structural integrity by the distribution of compressive forces from the femur while radially oriented collagen "tie" fibers resist longitudinal tears. The superficial fibers have no preferred configuration and participate in distribution of the shear stress (24). Proteoglycans are highly glycosylated hydrophilic proteins composed of core protein and glycosaminoglycans (GAG) that function as water absorption units. In a healthy human meniscus, main GAGs are chondroitin-6-sulfate (~60 %), dermatan sulfate (~30 %), chondroitin-4-sulfate (~20 %), and keratan sulfate (~15 %) (28). Aggrecan, biglycan, and decorin are the main PGs. A higher percentage of PGs are found within the white-red (W-R) and red-red (R-R) zones of the meniscus which could be the result of the compressive forces on the meniscus. The principal adhesion PG acting as anchor sites between ECM and cells are fibronectin, thrombospondin, and type VI collagen. Further research is necessary to evaluate the exact role of these GPs in the context of meniscus repair (33, 34).

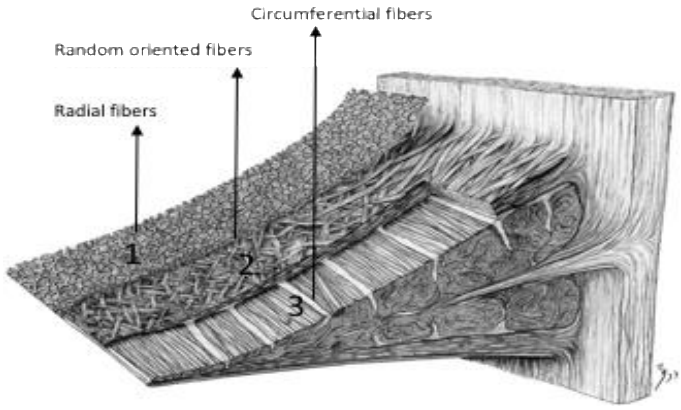

Figure 3.3 Schematic pattern of orientation of collagen fibers of the meniscus which can be categorized into 3 layers: I. Superficial network, II. Lamellar layer, and III. Circumferential fibers (27).

3.1.3 Cells of the meniscus

In the different regions of the meniscus cells are heterogeneous. Based on the morphology and phenotype, several types of cells are found in the meniscus including chondrocyte-like, fibroblast-like, and fibrochondrocytes. However, there is no consensus regarding the classification of meniscus cells. Various names such as fibrocytes, fibroblasts, meniscus cells, fibrochondrocytes, and chondrocytes are used in the literature (35). Histomorphometric studies demonstrated that in the periphery of the tissue, cellularity is the highest while it dramatically decreases radially inward (35). The peripheral vascularized zone of the meniscus is populated by oval and fusiform cells resembling fibroblasts in appearance and performance with known cluster of differentiation (CD) e.g., CD-34 positive and CD-31 negative markers (36). These cells exhibit long cellular extensions and are entrapped within a matrix extensively composed of type I collagen, to a lesser extent, types III and V collagen. These populations are in contact with cells from other zones of the tissue and tend to be closer together (37). The second population of cells which are found in the inner avascular portion of the tissue have a round morphology and are thus referred to as fibrochondrocytes or chondrocyte-like cells. These cell types do not present gap junctions and have been found to be CD-34 negative (38). They are embedded in an ECM consisting of primarily type II collagen associated with type I collagen and a higher concentration of GAGs. It has been shown that the cells can secrete a fibrocartilage matrix. Cells in the outer meniscus region have higher potential for migration when compared to inner cells and also seem to exhibit lower adhesion capacities (38, 39). A third population of cells found to reside within the superficial region of the meniscus has a flattened and fusiform morphology. Studies have shown that these cells might be progenitor cells involved in homeostasis, repair, and regeneration. Fusiform-shaped cells do not have cell extensions and are CD-34 positive and CD-31 negative (36).

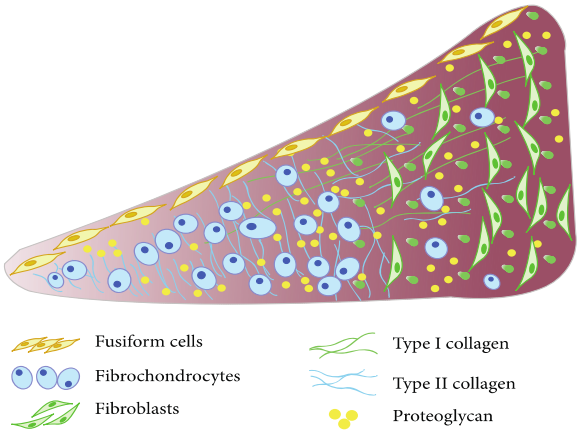

Figure 3.4 Schematic diagram of cell types in the meniscus. Cells of the superficial zone are fusiform; the cells in the outer periphery are mainly elongated fibroblasts with the process; moving toward the inner portion of the meniscus, the cells rounded and chondrocyte-like (40).

3.1.4 Biomechanics and related behaviour of the meniscus

To advance strategies for replacing and augmentating repair of menisci, understanding the biomechanics of the meniscus is important. The complex functionality of the meniscus is highly associated with its morphology and microstructure (27). The menisci play a primary role in transferring of load via increasing congruency and contact area and decreasing the contact stress in femorotibial joint. As a secondary role, it absorbs shock, provides stability, proprioception, lubrication, and the nutrient to the knee joint (27). The meniscus experiences different forces during loading such as compression, shear, and tensile load (41). When axial loading is applied on the knee joint, the meniscus is compressed and extrudes peripherally. The horn attachments and PCL act as anchors to the meniscus, converting axial loading to circumferential hoop stresses creating shear forces between the arrangements of collagen fibrils (27). Meniscal tissue is viewed as a biphasic medium due to its fluid phase and solid phase which have viscoelastic properties. Under compression, water is extruded into the joint space leading to lubrication of articular surfaces of the knee joint. Fluid transport aids to dissipate force as well as circulate nutrients in the avascular region of the meniscus (42).

Cadaveric biomechanical and animal model studies on menisci have shown that anterior-posterior laxity and lateral rotations are likely to be uninfluenced in medial meniscectomied knees when the ACL is intact demonstrating that the medial meniscus has a significant role as the stabilizer (41). Other studies showed that around 50% of the compressive load is transmitted by the meniscus during extension and 85% of load conveyed via flexion. In the knee joint, load sharing is transmitted through the menisci for up to 70% in the lateral compartment and 50% in

the medial side. Also, resection of 10-34% of the meniscus increases contact pressure as far as 350% (41, 42). The latter event causes gradual degeneration of articular cartilage (AC). Microstructural arrangement of collagens and PGs have an important role in applying load tensile strength giving evidence of the anisotropic nature of the tissue. The stresses and strains within the tissue are correlated with both the applied load and the rate of loading (27). More recently, suture- and anchor-based repair devices have been developed for the management of tears located at the body and posterior horn of both menisci which are challenging to approach. Several biomechanical tests analyze the strength of sutured-repaired tissue tears as well as mechanical effects of TE-scaffolds at different time points and during the healing process. Specimen of the meniscus which is mounted on the testing machine would be loaded-to-failure. Time-zero studies mostly used the tensile fixation strength by plotting the slope which is an indication of the stiffness of meniscus repair. At the early-to-mid healing phase, compressive forces or cycling loading would be applied (43).

Biomechanical characteristic of scar tissue and remodeling of meniscus would be defined at the late healing phase. Sutures showed a higher stiffness and higher load-to-failure than other devices. Also, top three sutures were PDS-0, Ethioband-0, and Orhocord-00. Vertically orientated configuration of repaired meniscus mimics the radial collagen fibers, captures more circumferential networks and remains the gold standard on biomechanical testing. Type of tear and selection of suture influence the repair tissue (44). Studies showed that the tensile modulus of the human meniscus measures between 100-300 megapascal (MPa) in the circumferential direction. Unconfined compression testing demonstrated that human menisci have an aggregate modulus between 0.09 and 0.15 MPa that compares to that of AC. In the future, a new generation of sutures or devices will be focusing on holding both the radial and circumferential fiber networks of the meniscus in the 3-dimensional (D) plane. Improvements in suture retention strength will be needed to further develop the mechanical strength of repairs of different meniscal tears (43) (25) (50).

3.2 Synovium

The major pathophysiologic changes seen in osteoarthritis (OA) joints are not only limited to degradation of the AC, thickening of the subchondral bone, osteophytes formation, degeneration

of ligaments, and the menisci but also affect inflammation of the synovium and hypertrophy of the joint capsule (52). Therefore, osteoarthritis should be considered as a disease of the whole joint as an organ (45). The histological patterns of synovium are changed by several inflammatory joint diseases including rheumatoid arthritis (RA) and OA (45, 46). The term synovium refers to the specialized connective tissue lining the spaces of diarthrodial joints, tendon sheaths, and fat pads. In synovial joints, the synovium seals the synovial cavity and aiding for pumping of fluid from surrounding tissues. The normal synovium has two layers of cells named intima and subintima (47). The inner layer, or intima, lies next to the joint cavity and consists of a layer of 1-4 cells mainly macrophages, fibroblasts, and synoviocytes with 20-40 μm thickness. Synoviocytes are the dominant cell population in healthy synovium. The outer layer, or subintima, is up to 5-mm thick and consists of blood vessels and lymphatic vessels. This layer is rich in type I collagen with less quantity of cells (45, 46). Two types of cells have been identified within the synovium: type A and type B. Type A synoviocytes which are derived from blood mononuclear cells and could be considered as macrophage-like cells and type B synoviocytes are synovial fibroblasts whichare responsible for eliminating pathogens from the joint and producing chemokines that contribute to inflammation, in order (48). The synovium has viscoelastic properties continuously produces lubricin and hyaluronic acid (HA) to maintain the synovial fluid (46). In OA patients, the histological pattern of synovium is characterized by synovial inflammation (synovitis), synovial lining hyperplasia, and stromal vascularization (45). Synovial inflammation results from the secretion of different cytokines and proinflammatory mediators which would be followed by macrophage activation and clusters of synoviocytes and chondrocytes observed in the synovium (17, 46). The underlying mechanisms are complex. In brief, molecules from degraded hyaline cartilage are released into the synovial cavity and initiate synovial inflammation in osteoarthritis. In early OA, damage to the meniscus and subchondral bone may release tissue debris. These molecules contribute to cartilage degeneration and osteophyte formation. Synoviocytes produce pro-inflammatory mediators and attract more immune cells (46, 49).

3.3 Meniscus injuries

Meniscal lesions represent the most frequent pathologies of the knee causing pain and disability. In the USA, the incidence of the number of meniscus-related injuries continued to rise and was

estimated to be 66 per 100,000 people annually, with 61 of those resulting in meniscectomies (50). Injury to the medial meniscus (stable knee) are more common (81%) than lateral ones. The peak incidence of injuries is three times higher for men versus women and occurs between 20 to 29 years of age in both sexes (27). Symptoms produced by meniscus tears include pain and swelling, accompanied by mechanical symptoms such as clicking, catching, and locking of the knee joint (27). Sports-related and traumatic injuries are the most frequent among young patients and are accompanied with ACL tears in more than 80% of the cases, while degenerative injuries occur in the older population and are caused by accumulative stress (>40 years) (28). Combination of rotation and axial loading cause tears leading to abnormal load (27, 41).

Tear damages can be classified based on the morphology, tear pattern, location, full or partial thickness, depth of tear, and meniscus zone. Main categories of tears include vertical longitudinal, bucket-handle, radial (transverse), horizontal (cleavage), and complex (degenerative flap) tears. Patient history, symptoms, description of the injury, and imaging results by magnetic resonance imaging (MRI) determines diagnostic consensus for surgery. Complex tears are usually correlated with two or more tear patterns in different planes. Traumatic degenerative tears in young patients of 20 years of age were characterized by MRI and arthroscopy. It was shown that complex tears could negatively affect the knee and may or may not be associated with a history of trauma. Complex degenerative tears have a poor healing potential and are not amenable to repair (59) (25) (51).

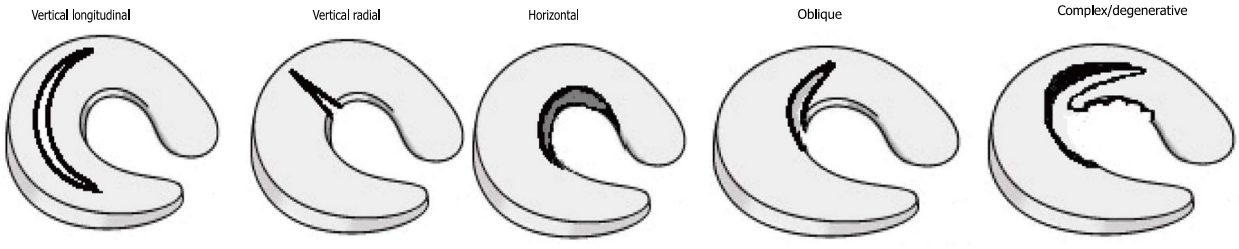

Figure 3.5 Drawing of common types of menisci tears (52).

3.3.1 Meniscus healing, regeneration, and remodelling

In the normal tissue repair process, access to nutrients, cells, and inflammatory mediators to initiate healing at the site of injury is a necessity. The inflammatory-reparative response in the connective tissue includes exudation, organization, vascularization, cell proliferation, and remodeling (53).

The 70 to 80% of the central meniscus is avascular and lacks hematoma formation following injury. Therefore, it has an inferior potential for healing and regeneration. The mechanisms of meniscal repair occur through two pathways. The extrinsic pathway is highly stimulated in R-R tears located at the outer zone, where functional blood capillaries exist which supply undifferentiated mesenchymal stem cells (MSCs) with nutrients and demonstrate the best prognosis for healing. Moderate vascularity in the W-R zone provides adequate healing. However, tears in the white-white (W-W) zone have minimal potential for repair due to the absence of blood vessels. The intrinsic pathway relies on the self-healing capacity of the meniscal cells and the synovial fluid (44, 54).

Initially, upon injury within the vascular zone of the meniscus, a blood clot forms providing a scaffold substrate that is rich in inflammatory and migratory cells. Hereafter, the defect is filled with a fibrovascular scar tissue which acts as glue. Vessels from the PCP as well as synovial fringe penetrate the fibrous scar guiding the healing response (53). Investigations and experimental studies in animals have shown the contribution of the synovial and vascular meniscus in the generation of fibrocartilage connective tissue or meniscus-like structure (MLS) in the total resected meniscus. Meniscus regeneration can happen in total meniscectomized knees by formation and regrowth of MLS and fibrocartilage metaplasia (53). However, remodeling responses were only observed in subtotal meniscectomized cases which had a blood supply. Following partial removal of meniscus tissue, a blood clot forms which is populated by mononuclear cells which are later modulated to become fibrochondrocytes that produce the ECM (53). However, in an attempt to get these tears to heal, external stimuli such as fibrin clot, fibrin glue, synovial grafts, periosteum, platelet-rich plasma (PRP), MSC, and growth factors (GF) have been sought to guide the intrinsic meniscus response to heal. Further studies are needed to investigate the impact of maintaining the blood supply on meniscus healing (40) (59).

3.3.2 Current surgical treatments and management strategies for meniscus lesions

In 1883, Annandale for the first time repaired the menisci by using sutures, 50 years later, King showed that removal of the meniscus in the canine generates some degenerative changes in the knee joint. In 1950 and 1960, any meniscus tears suspected by clinical examination was surgically removed (44). Due to the mechanical functionality of meniscus, degenerative changes to the

resected meniscus tissue, and technical challenges in surgery, the goal of meniscus injury treatment has now shifted toward salvaging of the meniscal tissue, if possible. Current treatment options for meniscus tears are classified into three categories: meniscus repair, total meniscectomy (TM) or partial meniscectomy (PM), and transplantation (7, 52). Since TM leads to progression of osteoarthritic changes in the joint, most of the meniscus tears are removed partially. Repair of the tears located at the vascular zone or some tears at the avascular zones is performed by sutures and arthroscopy. The other repair strategies such as staples, anchors, and arrows also maintain the tissue quality, minimize pain, and improve function (27).

Indications for meniscus repair are associated with several parameters such as tear properties and patient profile and include vascularity, tear morphology, length, depth, size, ligament stability, tear location, chronic or acute, age, health, symptoms, activity level, and expectations (7, 13). However, successful meniscus healing is more likely achieved in tears occurring in the vascular outer circumferences of the meniscus, making repair strategies less suitable for degenerative tears originating from the horizontal direction that tend to start at the inner avascular zones (7). Meniscus repair is limited to vertical, unstable, and peripheral tears. Longitudinal-vertical tears 1-2 cm in the R-R vascular zone and those located at the meniscocapsular zone are amenable for repair with sutures (55). Most of the tears occur at the medial and posterior horns of the meniscus (7). Recent results showed partial meniscectomy are performed more than repairs to preserve tissue and biomechanical function. Considering all the parameters mentioned above, longer longitudinal tears and bucket handles tears are repaired in some cases. Young active patients (> 40) with fresh tears less than two months old are good candidates for repair by sutures. ACL-reconstruction is highly recommended during the meniscus repair surgery (7, 55). However, irreparable unstable meniscus lesions or degenerative tears require PM or TM. Meniscus allografts or synthetic meniscus substitutes are indicated for severely damaged meniscus (14). The biomechanical effect of meniscectomy correlated with radiographic signs of osteoarthritis and patient-related outcome scores. However, the answer to the question as to whether knee OA could start with meniscus degenerating or whether degenerative lesions cause loss of meniscus function and trigger osteoarthritis is still unclear (2, 56).

Many augmentation approaches have been used for meniscus repair including mechanical stimulation (abrasion therapy, rasping, and trephination), synovial flap, gluing (fibrin glue), exogenous fibrin clot, facial sheath coverage, meniscus wrap technique, platelet lysates, GFs, gene

therapy, marrow venting procedure, and enhancement with PRP (7, 8). All biological enhancement techniques attempt to promote cellular proliferation, matrix production, and chemotaxis at the repair site in order to overcome limitations. Some of these techniques are used for enhancing vascularity, and others for improving cellularity in meniscus repair. Combination of all these strategies has been suggested in the literature together with suture reinforcement techniques (55, 57). Refreshing the tear edge before suture placement opens blood supply from the vascular zone to the avascular zone, thus recruiting fibrin, GFs, and thrombocytes to the defect site which is a necessity for wound healing. In the cases of isolated tears, fibrin clot placement inside the tear accelerates the rate of healing. Meniscal repair procedures are categorized into two types: open and arthroscopically-assisted. Arthroscopically-assisted meniscal repair techniques are more common and have mostly replaced open procedures (58, 65).

Meniscal repair techniques include inside-out, outside-in, and all inside repairs. Each has its advantages and complications (7, 55). Inside-out repair involves passing sutures from inside of the meniscus to the capsule and is used for tears in the meniscus body. Inside-out meniscus repair remains the gold standard to date (59, 60). Outside-in involves passing the suture from the capsule into the meniscus and is used for defects at the anterior horn side. All inside repair consists of placing stitches from the inside the meniscus to the capsule by leaving an anchor positioned behind the capsule. Inside-out and outside-in meniscal repair techniques have been reported to increase the risk of injury and neurovascular complications. In contrast, the all-inside technique is an arthroscopic procedure with the benefits of a reduced risk of neurovascular injury, particularly when peripheral tears within the meniscal R-R zone are repaired. They are frequently combined with augmentation strategies to improve the healing rate of the meniscus to overcome some of the limitations such as hypovascularity, high inflammation, hypocellularity of the meniscus environment. Both resorbable and non-resorbable sutures materials can be used for wound closures (58, 65).

3.4 Ovine animal models of meniscus repair

To restore the function of the meniscus and develop treatments for the human knee joint, investigators require appropriate preclinical animal models to test the safety and efficacy of new engineered technologies and functional aspects of the human knee (61). Animal models are

valuable tools proposed for studying not only the tissue pathophysiology and mechanisms leading to meniscus tear formation but also allow testing of new surgical devices and engineered implants for tissue regeneration (62). Mice, rat, rabbit, pig, cat, dog, horse, goat, and sheep are the different animal species that have been used so far for studying meniscus (69). However, there is no gold standard surrogate for the human menisci, and each of the animal models has its pros and cons (61, 63). The relevance of the models allows researchers to understand the structural and functional impairment that results from orthopedic pathologic conditions such as meniscal injury (70). However, selection of the most appropriate animal model and injury pattern is necessary to the translational relevance of a project.

Several parameters should be considered for selection or rejection of an animal model for orthopedics area such as: I. Anatomy similarities, II. Composition and biomechanics, III. Availability and cost, IV. Translation of information to humans, V. Ease of handling and housing. VI. The existing body of biological knowledge on the animal model. VII. Ethical implications. VIII. Ecological environment. IX. Adaptability to the experimental conditions, and X. Society acceptation of the model (79, 64). For instance, the biosynthetic activities of MFC change with joint instability and biochemical content of menisci is altered with exercise in rabbit (lapine) and rat (murine) models, respectively. Also, menisci size, the thickness of cartilage, and greater endogenous healing can limit a model's potential to evaluate the performance of repair meniscus devices and implants. An advantage of porcine (minipig) and swine is low cost, weight, similar size, and mechanical properties to humans. However, the strength of tendons and ligaments are half that of the humans which limit ACL-reconstruction associated with meniscus repair studies. The minipig has been used as a feasibility model for proof-of-concept studies and early stages of therapy evaluation. The canine (dog) model is well-established in terms of intraarticular knee surgeries approaches, vascularity, primary and secondary clinical outcome evaluation with arthroscopy (62). The dog has been a dominant model of musculoskeletal conditions for a long time; however emotional and ethical considerations limit its translation potential (65, 79). Primate and horses (equine) meet some biomechanical requirements for joint models, but they are too expensive for large-scale studies. The caprine (goat) is another animal model that has cartilage thickness close to human, but it is not readily available and hard to handle as compared with counterpart sheep (62).

Ovine (sheep stifle joint) is a well-accepted experimental large animal model for *in vivo* and translational orthopedic field (66). The ovine model was selected for this project for multiple reasons. Regardless of the differences between human knee joint and sheep stifle joint, ovine meniscus represents a scaled-down version of the human meniscus regarding the anatomical, biological, physiologic, and biochemical characteristic due to its size, the weight, the joint structure, meniscus remodeling, and healing process (67). Other advantages of using sheep include ease of handling and availability. In pursuit of investigating the biological aspects of healing and injury, this project seeks to investigate the effect of freeze-dried chitosan platelet rich plasma (FD-CS PPR) implants for augmentation of meniscus repair in ovine stifle joints for eventual application to the human knee joint. Reconstruction, replacement of the cranial and caudal cruciate ligaments, collateral ligaments, meniscus, treatment of the chondral and osteochondral lesions, treatment of osteoarthrosis and arthroplasty have also been performed and assessed in sheep. The primary structural characteristics such as the organization of ECM, water content, collage type distribution, vascularity, and cellularity are remarkably similar between sheep and human meniscus. Although composition and biochemical profile of human and sheep meniscus are identical, content, as well as regional variation of GAG, is notably different as evidenced by histology of the inner half of meniscus (63, 67). Therefore, it is essential to consider contralateral menisci in our study design. Vascular penetration is 11.2% in sheep while being around 14.4% in human (68). The ovine and human joint shares some characteristics such as gross anatomy, morphology, kinematics, and functional biomechanics. Load distribution, tensile, and compressive properties of menisci have been measured and show a close approximation in both sheep and human (63). Femur of both species has a rochlear groove permitting the joint articulation of femur and patellae. Articular cartilage of the medial tibial plateau (MTP) is two times thicker than lateral and presence of a massive bone stock below the tibial plateau lead to some differences in loading patterns which eventually could influence the treatments. Regarding kinematics, human knee joint archives a straight orientation at heel strike while sheep flex near 40^{o} in the same position (69).

There are some apparent differences between sheep and human which should be considered when we extrapolate the data (75). The presence of the tendon of the extensor digitorum longus muscle on the craniolateral aspect of the stifle joint, the absence of cranial meniscofemoral ligament (Humphrey) in the caudal joint space, attachment of the patellar tendon to the cranial pole of the patella, presence of four distinct articulations, asymmetrical shape of meniscus, and

proximity of MCL and tibial cortex are some of the differences in the anatomy of sheep stifle joint and human (83, 75). Arthroscopic-assisted visualization procedures are still a challenge for evaluation of safety and efficacy of implant and grafts in sheep (63). The rate of bone healing, and remodeling activity are similar (65). Length, width, and proportion to the tibia plateau are approximate between sheep and human. All of these should be addressed during design of scaffolds and device implantation. In the current study, we focus on the medial menisci since in both species the large quantity of force is transmitted through the medial compartment and medial menisci are clinically more relevant (63). However, with any animal model, there are limitations while interpreting the results of study and findings in a quadruped model should not be directly correlated to the human knee joint lesion. To study meniscus tear and healing response, we created a complex tear similar to clinically significant human lesions (63). In order to easily inject the implant and to visualize the medial compartment and central posterior zone of menisci, a bone block surgical approach was employed in sheep. In spite of the advantages of *in vitro* studies and to fill the gap between the *in vitro* and human clinical studies, biological behavior of menisci response needs to be evaluated in large animal model, especially in the avascular zone (63, 66). Recent studies are emphasizing on sheep as the gold standard animal model for meniscus implantation and evaluation of devices (63, 66) (Table 3.1).

Table 3.1 A brief description of physiological aspects of sheep as model for biomedical engineering.

Animal model	**Purpose of the study**	**Strength of the model**	**Weakness of the model**	**Cell morphology**	**GAG content**	**Collagen type I**	**Collagen type II**	**Vascularity penetration**
Sheep 71, 74, 76, 79, 80	Effect of synovial implantation Transplantation of meniscus allografts Effects of abrasion therapy Autologous perichondrial tissue	Meniscus size close to human	Tenotomy required (Achilles) Difficult access to posterior area	Round in deep layer and fusiform at superficial	Present in inner zone	Detected throughout the matrix	Detected in matrix and inner regions of meniscus	11.2%

3.5 Tissue engineering and biologic augmentation strategies for meniscus repair

3.5.1 Scaffolds

Tissue engineering represents an alternative option for creation of soft tissues such as cartilage or meniscus which have a low potential of healing (70). When we compare the meniscus with other musculoskeletal tissues such as bone or cartilage, there is a shortage in the number of studies, methods, and biomaterials for engineering this fibrocartilaginous tissue. This might be related to the complex nature of the tissue and organizational architecture which make it difficult to replicate (71). The ideal scaffold materials for engineering of meniscus should have several requirements: I. Biocompatibility and biodegradability in the long-term allowing ingrowth of new tissue, and remodeling of tissue especially under the load conditions to accelerate cell ingrowth, vasculature, the formation of a new extracellular matrix, and free diffusion of nutrients, II. It could be used as carrier for delivery of GFs either inhibitory or stimulatory, III. It should be strong enough to be able to withstand the load in the joint compartment, maintain balance, and weight distribution, and IV. The graft should be able to reduce degenerative changes as well as pain. It is likely that a combination of scaffolds, cells, and GFs will play a key role for future improvement of meniscus repair approaches. Meniscus scaffolds can be separated into two major categories: synthetic and natural scaffolds. Scaffolds could be seeded with cells or could be acellular. A wide variety of biomaterials have been used to produce meniscus TE-scaffolds in ovine models (14, 71) **..** Different natural scaffolds have been used for TE of the meniscus include protein-based such as fibrin, gelatin, and collagen or polysaccharide-based including alginate, chondroitin sulfate, and chitosan. Other types exist such as small intestine submucosa, perichondral tissue, periosteal tissue, hyaluronan-gelatin hydrogel, and the devitalized meniscus (72-77). Use of autologous perichondral tissue was tested in a complete ovine meniscectomized model by Bruns and colleagues. Their findings demonstrated a new perichondral tissue formed which resembles the healthy tissue regarding size and orientation of collagen fibers after 3 months. However, central calcification, low tensile strength, and stress modulus compared with the native tissue were found (78). Regarding the stability of meniscus prosthesis, collagen-based matrices seem to be one of the best options for meniscus replacement. Martinek and colleagues published the application of collagen meniscus implants (CMI) with or without autologous chondrocytes in an ovine

meniscectomized model after 3 weeks and 3 months. The CMI seeded with fibrochondrocytes reduced AC degeneration compared to the unseeded-scaffold. Histological assessment after 3 months showed a GAG-rich extracellular matrix, scaffold remodeling, and improvement in vascularization. The authors noted that the tissue was biomechanically inferior compared to the normal meniscus tissue (70). Allograft transplantation is an applicable method for substitution following menisci resection. However, this has suboptimal clinical results due to shrinkage of the graft as well as rejection during long-term implantation (79). Several synthetic biomaterials including teflon, carbon fiber, polyurethane (PU), polycaprolacone (PCL), poly-L-lactic acid (PLLA), polyglycolic acid (PGA), polycarbonate-urethane (PCU), and polylactic-co-glycolic acid (PLGA) have been widely used as scaffolds (99)(14, 80). These synthetic scaffolds provide multiple advantages such as satisfactory mechanical properties, tuneability of pore size, fiber size, geometry, and endless supply. Some of the limitations include poor bioactivity, hydrophobic properties, and immune response (81). Combination of both synthetic and natural scaffolds could address some of these limitations. Ibarra and colleagues have reported PGA or PLGA seeded-scaffolds in ovine models of meniscectomy. They aimed to overcome their poor mechanical properties in several pilot studies. Results from 6 weeks implanted in a meniscectomized knee demonstrated the formation of new tissue growth with histologic architecture similar to meniscus with aligned collagen-like fibers. However, no biomechanical studies were completed on the TE-meniscus tissue. Although the number of the animals was small, authors demonstrated a proof-of-principle for this technique (82, 83, 102). A new resorbable biomaterial consisting of derivatives of PCL and HA named HYAFF has been investigated in meniscectomized models. Chiari and colleagues reported on these materials in an ovine total or partial meniscectomized model for 6 weeks. Specimens were assessed by histology and gross inspection. Initial results were promising in terms of the feasibility of the method, tissue formation, cellular infiltration, and vascularization. After these encouraging results, further studies were performed to further test the same scaffold (84). Primarily, in two following studies, Kon and colleagues investigated the same scaffold in total removal of meniscus tissue in 24 sheep with or without autologous chondrocytes seeding after 4 and 12 months. In both studies, scaffolds were seeded with chondrocytes and compared with cell-free scaffold and meniscectomized alone groups. Results after 4 months showed improvement over cell-free scaffolds regarding cell infiltration, vascularization, and cartilage-like formation, however, foreign body reaction and AC degeneration were present. In the second study, they

confirmed the role of cells for increasing the tissue quality and potential of PCL-HA for total meniscus substitution for 12 months (85, 86). Also, Maher and colleagues tested a porous PU scaffold in a partial meniscectomized ovine model at 12 months post-operation. Promotion of tissue ingrowth and chondral protection was noted (87). In another study, Zur and colleagues investigated and tested the use of an artificial meniscus implant composed of Kevlar-reinforced PCU scaffold. Although, the scaffold delays degenerative OA changes after 3- and 6-months post-surgery, there was no significant difference between treated cartilage and control (88). Results of silk fibroin scaffold were reported by Gruchenberg and colleagues with documented evidence of chondroprotective properties and mechanical features comparable to the intact meniscus with less inflammatory response in a sheep model (89). Recently, Patel and colleagues in two different studies reported the effects of a biodegradable fiber-reinforced scaffold in total meniscus replacement model. In the first study, they found that meniscus scaffolds support the formation of neomeniscus tissue and preserve the joint from degeneration after 1-year implantation. In the second study, they reported adverse outcomes of PLLA fiber-reinforced scaffolds in an ovine total meniscus replacement model (90, 91). The same material has been reported by the same group in 11 sheep with the end time point of 2 years. The fiber-reinforced scaffold stimulated the formation of functional neomeniscus tissue that was remodeled into organized circumferential collagen fibers demonstrating its potential to prevent catastrophic joint deterioration associated with meniscectomy (92). Recently, 3-D printed scaffolds in combination with GFs have been gaining attention for meniscus regeneration since they allow replication of meniscus shape and internal fiber architecture to produce patient-specific scaffolds (93).

Table 3.2 List of biomaterials have been used to produce meniscus TE-scaffolds in ovine models.

Author	Polymer type	Fabrication method	Cell seeded	Tissue resected	Additional factors	Study design	Duration	Degree of success
Bruns 1998 (78)	Perichondral tissue	-	No	Meniscectomy	-		12 months	Calcification of central region, low tensile modulus
Martinek 2006 (70)	Collagen meniscus scaffolds (CMI)	-	Yes Precultured autologous chondrocytes	Meniscectomy (total medial)	-	Scaffold autologous chondrocytes, scaffold alone, empty defects.	3 weeks and 3 months	Increased vascularization enhanced scaffold remodeling, high ECM, Biomechanically unstable and shrinkage
Ibarra 1998 (82, 83)	Polylactic-co-glycolic acid (PGLA)	-	Yes Fibrochondrocytes	Meniscectomy (total medial)	-	Cell-seeded scaffolds, cell free scaffolds, empty controls.	6 weeks	Organized collagen matrix, good PG amount Limited analysis, organized collagen structure
Kon 2008 (86)	HYAFF - polycaprolacone (PCL)	Lamination technique	Yes Autologous chondrocytes	Meniscectomy (total medial)	Two fixation techniques, either with or without tibial horn fixation	Cell-seeded scaffolds, cell free scaffolds, empty controls.	4 months	Fibrocartilage formation in the cell seeded group, better integrity with fixation method, incomplete healing, osteochondral degeneration
Kon 2012 (85)	HYAFF-PCL	Lamination technique	Yes Autologous chondrocytes	Meniscectomy (total medial)	-	Cell-seeded scaffolds, cell free scaffolds, empty controls.	12 months	Cell seeded scaffold showed a better regeneration capacity, chondroprotective effect in scaffold group.
Maher 2010 (87)	Poly urethane scaffolds (PU)	-	No	Meniscectomy (partial lateral)	-	Scaffold group, untreated defects.	3, 6, and 12 months	Loss of tissue at inner rim, tissue integration and significant self-healing in partial meniscectomy model
Zur 2011 (88)	Kevlar-reinforced polycarbonate urethane (PCU)	-	No	Meniscectomy (total medial)	-	Scaffold group, unoperated control.	3 and 6 months	Fibrosis of the synovial tissue and osteochondral degeneration, no significant differences found between scaffold and control group

Kelly 2007 (94)	Hydrogel meniscus implant	-	No	Meniscectomy (total lateral)	-	Hydrogel meniscus group, lateral meniscectomy group, meniscus allograft transplant.	2, 4, and 12 months	Promising results for hydrogel meniscus implant at early time point follow up. At 12-months, significant cartilage degeneration and implant failure for hydrogel group compared to allograft transplant.
Gruchenberg 2014 (89)	Silk fibroin scaffolds	-	No	Meniscectomy (total medial)	-	Scaffold group, empty defects.	6 months	No inflammation observed in scaffold group. No significant differences in cartilage degeneration between the scaffold and sham group. Loss of the implant in 3/9 in scaffold group Mechanical properties of the scaffold similar to the native meniscal tissue.
Galley 2011 (95)	Actifit	-	-	Meniscectomy (partial lateral)	-	Scaffold group, intact knee.	12 months	Tissue ingrowth promoted into porous scaffolds
Patel 2016 (90)	Poly desaminotyrosyl-tyrosine dodecyl ester dodecanoate (pDTDDD) fibers	-	No	Meniscectomy (total)	-	Scaffold group, native meniscus.	52 weeks	A resorbable fiber-reinforced meniscus scaffold supports formation of functional neomeniscus tissue with the potential to prevent joint degeneration that typically occurs after total meniscectomy.

3.5.2 Chitosan and its applications

Chitin is a linear, highly crystalline homopolymer of *β*-(1-4) -linked *N*-acetyl glucosamine residues which is a dominant cell wall component and found in fungi and various marine living organisms (20). After cellulose, chitin is the second most plentiful organic compound in nature (96). Materials formed of chitin are usually colorless to white, hard, and inelastic, found in the outer skeletons of crabs and in the internal structures of other invertebrates (20, 96). However, significant sources of chitin are crab and shrimp shells in industry. Chitin has an average molecular weight (MW) ranging from 1.0 to 2.5 million dalton. The variation in the MW is a function of the extent of *N*-acetylation (97). Chitin structures vary in the solid and solution state. Crystallography structure of chitin can be differentiated and characterized by nuclear magnetic resonnace (NMR), spectroscopy, and x-ray diffraction method (96, 97). Depending on its source, the ultrastructure of original chitin is different and needs to be pre-treated and medically graded before it is used in biomedical engineering application (20, 96). Chitin exist under 2 allomorphs termed as *α* and *β*. The crystalline structure of *α* and *β* are organized in piles that hold the lattice by tight hydrogen bond. Chains of *α*-chitin are ampler and found in arthropods, fungi, and the cysts of entamoeba (20, 96). Piles of chains are arranged antiparallel in *α*-chitin (98).

Chitin is systematically formed by recrystallization from solvents, *in vitro* biosynthesis, or enzymatic polymerization. *β*-chitin is rarer and found within squid pens and tubes synthesized by pogonophoran and vestimentiferan worms. *B*-chitin is characterized by a weak intermolecular force and hydrogen bonding by intrasheets. Thermodynamic studies confirmed that *β*-chitin exhibits higher reactivity and affinity for solvents than *α*-chitin (20, 96). The crude chitin is isolated from the outer skeletons of mostly crabs and shrimps. Crustacean shells are composed of 30-40% protein, 30-50% calcium carbonate, 20-30% chitin, and lipidic pigments (97). To obtain pure chitin for biomedical implementation, these components need to be removed by chemical, enzymatic, and biological selected treatments. Depending on the source and objective, the analysis and reagent conditions may differ (20). Isolation of crustacean shell waste consists of three basic steps: I. Protein separation-deproteinization (DP), II. Calcium carbonate-demineralization (DM), and III. Pigment-lipid-decolorization (DC) (20, 99). Exogenous chitin activates macrophages and causes allergic inflammation; therefore, full removal of protein residue by chemical extraction processing is the most important step. Chemical bonds between the chitin and proteins will be disturbed by DP, and the polymer will be depolymerized (20). Several chemicals are adopted as DP reagents

such as sodium hydroxide (NaOH) and potassium hydroxide. Deproteinization is usually accomplished by NaOH (0.125-5.0 Molar) at varying elevated temperature (65-160°C) and treatment duration (few minutes up to several days) at a controlled pH. Enzymatic deproteinization has been done either with the commercial, bacterial, or crude protease to increase purity after or before the DM step. Demineralization is conventionally performed by diluting to mild hydrochloric acid (HCl) (up to 10%) at room temperature to dissolve the minerals such as calcium chloride ($CaCl_2$) with agitation for 2 to 3 hour (20, 99). Treating and bleaching with reagents such as acetone and sodium hypochlorite will also remove pigments, if necessary (99).

To preserve the polymer structure and physicochemical characteristics of chitin, temperature, different incubation time, the concentration of acid, solute/solvent ratio, and particle size should be optimized based on the experimental conditions. Efficacy and quality of deproteinization and DM can be increased either by lactic acid and non-lactic acid fermentation (20). Poor solubility and high hydrophobicity in water and acetylation groups of chitins limit its practical application. Therefore, chitin needs to be modified to one of the most suitable naturally-derived polysaccharide in the biomedical engineering which is chitosan (100).

Chitosan is partially or entirely deacetylated derivative of chitin when average degree of acetylation is lower than 50% (20). Chitosan is a linear cationic polysaccharide (PS) composed of units of D-glucosamine and *N*-acetyl D-glucosamine (101). Chemical and enzymatic deacetylation processing can be used to convert chitin to chitosan. Chitosan is a high MW biopolymer which is soluble in acidic solutions (102). Considering its source and preparation processing, MW of chitosan varies between 300 to 100 kilodalton with the degree of deacetylation (DDA) of 50 to 95% (103). Acid or alkali have been used to deacetylate chitin in a homogeneous or heterogeneous manner (20). Deacetylation of chitin under heterogeneous conditions involves treating chitin with hot concentrated solution of NaOH for few hours generating chitosan with an insoluble residue with 85-99%. Homogeneous deacetylation implies dispersion of chitin in concentrated NaOH, followed by dissolution is crushed ice creating soluble chitosan with a DDA around 45 to 55% (20) (104). Under homogenous conditions physicochemical properties of CS such as solubility and degree of aggregation may differ from the randomly acetylated chitosan. Enzymatic deacetylation of chitin has been performed by using chitin deacetylase which creates chitosan oligomers in most efficient way to prevent energy consumption (20).

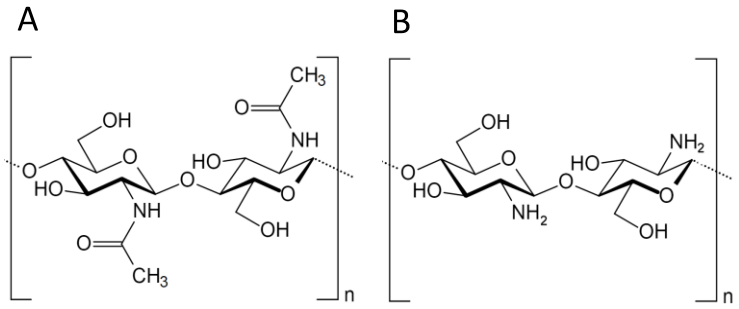

Figure 3.6 Chemical structure of chitin (A) and chitosan (B) (20).

Chitosan-containing composites constitute a most promising multifunctional and versatile biopolymer for orthopedic TE including cartilage, intervertebral disc, ligament, bone, and meniscus (102). Other applications include drug, gene delivery and wound healing management (105). Chitosan presents excellent pharmaceutical properties such as biodegradability, biocompatibility absorbability, non-toxicity, chemical stability, mechanical properties, immunological, antibacterial, anti-cancer, hemostatic, and bioadhesivity (20, 106, 101). Chitosan is a naturally-derived bioactive polymer that has been used as a scaffold in regenerative medicine. Other medical configurations of chitin and chitosan include hydrogels, fibers, films, powder, solutions, gels, sponges, and beads (20, 107, 108). Chitosan can be injected or implanted into soft tissues (20). Both chitin and chitosan are interesting PS due to the presence of amino (NH_3) as well as hydroxyl functional groups, which can be chemically modified to impart desirable properties including solubility (109). The solubility of chitosan depends on DDA, distribution of free amino groups, distribution of *N*-acetyl groups, type of acid for protonation, pH, treatment processing of PS, and concentration of ions. The solubility of CS-based formulations has always been a challenge since it affects its stability (96, 101, 109). Chitosan is a highly reactive PS, and its solubility is facilitated in dilute acidic reagents below pH 6.0 such acetic acid. Chitosan can be considered a strong base as it has free and reactive NH_3 with a pKa value of 6.2. At low pH (PH< 6), these amines get protonated and become positively charged which makes chitosan a water-soluble polyelectrolyte. Once the pH increases above 6, amino groups of chitosan become deprotonated and the polymer loses its charge and becomes insoluble (101, 109).

The degree of acetylation represents the proportion of glucosamine units regarding the total amount of units. Positive charges in chitosan and functional groups which are produced by

deacetylation generate an electrostatic interaction allowing it to interact with negative molecules. (101). During deacetylation and DP reaction process, the molecular weight of chitosan will change. Average characteristic and physicochemical stability of chitosan is influenced by multiple internal and external factors such as MW, deacetylation degree, the pattern of deacetylation, viscosity in solution, moisture content, polydispersity index, purity level, humidity, and temperature (20, 103). Viscosity and molecular weight are related meaning the higher the MW is, the higher the viscosity. DDA and molecular weight are the key features that determine biological characteristics of CS (96, 101). Degree of deacetylation has an effect on both *in vitro* and *in vivo* degradation rate of chitosan. It has been shown that the degradation process is attenuated at higher DDA (80 to 90%). The commercially available preparations often have a DDA between 60 and 90% which will impact on some biological properties of the chitosan such as healing capacity and degradation process by lysozymes (101).

Cytocompatibility and hemocompatibility are the first-line screening tests for CS. Biocompatibility means the ability of the biomaterial to perform with an appropriate host response by emphasizing tissue biomaterial interfaces (101). The process of biodegradation of chitosan can be by either physical and enzymatic degradation. Biodegradation refers to hydrolyzing of glucosamine linkages (20, 101). In human body, eight chitinases have been recognized. Enzymes such as chitinases and lysozyme hydrolyze chitin and acetylated forms of chitosan (101). Lysozyme provides a first-line innate immune defense to pathogens encompassing chitin by generating damage in the cell wall. Therefore, partly acetylated CS (≤85% DDA) are more biodegradable than highly deacetylated chitosan (≥95% DDA) (101). Chitosan has considerable immunomodulatory properties and induces innate immune cells such as macrophages and neutrophils to secrete proinflammatory mediators. The level of DDA and range of MW of chitosan impact biological properties such as cell growth, proliferation, and adhesion. Studies found that low DDA in chitosan decreases cell adhesion to the films. Porosity of CS-based products is important in scaffolds since it provides a platform to facilitate new tissue ingrowth for cells to proliferate, differentiae and interconnect via the pores. Mechanical properties of CS membrane can be improved by incorporation of cross-linked agents (101). Chitosan-based biomaterials have been designed for the following functions: I. Acting as a template to promote cell biomaterial interaction and ECM deposition, II. Cell proliferation and differentiation through the transport of nutrients and gases, III. Degradation at a controllable rate corresponding to the regeneration rate of tissue, IV. Minimal

foreign body reaction, and V. Ability to be molded in the tissue of interest geometries and suitable for cell ingrowth (101, 102).

Chitosan scaffolds can be fabricated by different methods including lyophilization or FD. Freeze-drying is a method that freezes the solution at a certain temperature and then sublime the scaffold at a specific lower temperature (121). This method is widely used for pharmaceuticals to improve the physicochemical stability in aqueous media, long-term storage, provide easy handling for nanoparticle (103, 110). Studies have shown that removal of water by freeze-drying process from chitosan-based products may disturb the polymeric network by imposing stress on both unmodified or modified chitosan (103). Higher viscosity, lengthening of gel strength, decrease of gelation time affect the biological properties of chitosan. To overcome the latter issue, several strategies have been utilized for expanding chitosan maximal stability and shelf-life including: I. Modification of storage conditions such as temperature and humidity, II. Inclusion of a stabilizing agent, III. Association with non-ionic polymers, and IV. Modification of chitosan structure employing small size anionic polymers (103). Freeze-drying is a time-consuming and expensive process that could take days to weeks which needs to be optimized. A typical freeze-drying process consists of three stages; that is, freezing, primary drying, and secondary drying (22).

Chitosan is a positively charged biopolymer that interacts with charged cell membranes, attracts negatively charged platelets to form a loose clot and has a positive effect in engaging hemostasis. Coagulation activity of chitosan varies according to its molecular weight and DDA which dictate final cationic properties of the polymer. Hattori et al., showed that varying DDA and MW of chitosan solutions prior to mixing with blood components and platelets in PRP would change blood activation and aggregation (111, 112). Shen et al., reported that chitosan enhances platelet aggregation and increases release of GFs (113). Microscopic and flow cytometry examinations revealed that platelets adhered on chitosan coated plates leading to activation of platelets, expression of glycoprotein on the platelet surface and release of growth factors. Zhang et al., investigated the effect of chitosan and its derivatives on the function and structure of clot-related proteins including fibrinogen.

Other authors have reported on TE-scaffolds containing chitosan and PRP (113, 114, 115, 116). Shimojo et al., showed the performance of injectable lyophilized porous CS mixed with PRP as a composite scaffold for TE applications (116, 117, 118). Also, Kutlu et al., reported the sustained release of platelet-derived growth factor-BB (PDGF-BB) from CS-PRP scaffolds by either adding

PRP to a chitosan gel before freeze-drying or by delivering PRP to a lyophilized chitosan sponge (119). Similar to the previous studies, Tello et al., found that activated PRP induce nesting and differentiation of human chondrocytes cultured in chitosan scaffold, as shown by high expression type I and II collagen in ECM (120). Due to its hemostatic potential, chitosan can initiate the wound healing process by arresting bleeding, activating, promoting coagulation, and forming an interconnected blood clot. Periayah et al., showed that platelets adhere to chitosan and that platelet number influences the formation of the hemostatic plug (121).

Scanning electron microscopy (SEM) analysis revealed that depending on the type of chitosan, platelets adhered to each other and the surface of chitosan and extended into pseudopodal shape. Similar to that study, Romani et al., confirmed the presence of pseudopodia and expression of human platelet-p-selectin when chitosan film is placed in contact with blood components, although, platelets respond differently to chitosan depending on the molecular weight and DDA. Both chitin and chitosan promote wound healing through cytokine production and fibroblast stimulation. Foreign body giant cell (FBGC) formation depends on the chitosan properties and biodegradation rate. Deacetylated forms of CS are susceptible to degradation by the enzymes existing in body fluids such as lysozyme and *N*-acetylglucosoaminidase creating products called chito-oligomers. These products stimulate macrophages and positively influence collagen deposition, thus accelerating the wound healing process (122). Hydrogel-based biomaterials such as chitosan are gaining high interest for meniscus TE due to its high hydration degree (72, 122). Chitosan hydrogels in animal studies have been shown to stimulated migration, proliferation of fibroblasts, and production of collagen.

To the best of my knowledge, the number of publications assessing the interaction of chitosan with meniscus tissue are limited. In an *in vitro* study, Sarem et al., showed that combination of two biopolymers of gelatin-chitosan scaffolds which are cross-linked with genipin have a highly inter-connected pore architecture and support human-derived meniscus cells (123). Injection of *N*-carboxymethyl CS by itself has been shown to modulate the healing sequence in a rabbit model of meniscus repair (124). In another study, CS-calcium polyphosphate composite scaffolds which were cross-linked with alginate dialdehyde were reported to improve the properties of CS and could be the potential candidate for meniscus tissue engineering (125). Chen et al., reported beneficial effects of a thermo-responsive chitosan-poly injectable hydrogel implant. Results from SEM confirmed these hydrogels could be used as an injectable cell-carrier material for entrapping

chondrocytes, meniscus cells and preserve cell viability, the phenotypic morphology of the trapped cells, and stimulate cell-cell interactions (126).

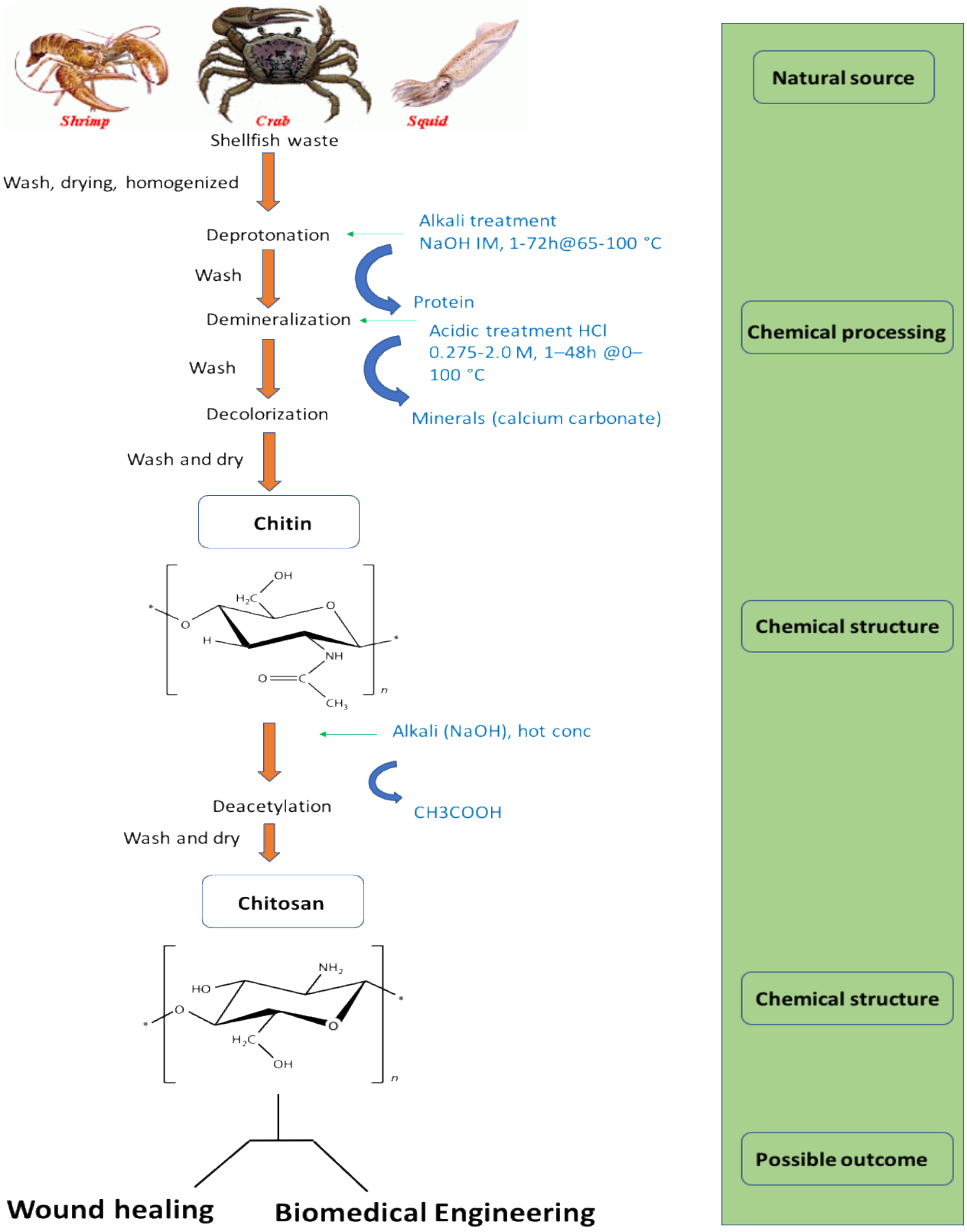

Figure 3.7 Simplified flowchart of preparation of chitosan from chitin (20, 96).

3.6 Cell sources

Studies show that seeding of cells onto the matrix, mesh, or scaffolds enhance healing and regeneration of the meniscus *in* vitro and in animal models (14, 40, 127). Multiple cell sources are available for meniscus regeneration including either mature cells or stem cells. The former include fibrochondrocytes-derived from meniscus, chondrocytes-derived from cartilage and the latter include bone marrow-derived mesenchymal stem cells, synovium-derived mesenchymal stem cells (SMSCs) adipose-derived stem cells, meniscus-derived mesenchymal stem cells, cartilage progenitor cells, myoblasts, and multipotent vascular endothelial cells (15, 73). Depending on the animal model used in the studies, the regenerative capacity of the cells and the efficiency of the delivery method may vary. Cells can be delivered using different techniques such as intraarticular injection, embedded in fibrin clot, tissue engineered construct, pellet, aggregate, or hydrogel (80, 90, 128, 129).

Fibrochondrocytes from the meniscus are the most frequently utilized cell source. Most of the studies demonstrated fibrochondrocytes have the potential to proliferate in 3-D matrix scaffolds *in vitro*. These cells have also been evaluated in animal models. Immunohistological staining of tissues shows cells express their phenotype and synthesize sufficient extracellular matrix *in vitro* (15, 36). From a clinical point of view, biopsies of autologous fibrochondrocytes could be isolated from the contralateral healthy meniscus or the torn meniscus. Baker et al., showed that seeding of meniscal debris-derived cells onto nanofibrous scaffolds results in neotissue with mechanical properties approximating that of the native meniscus (15, 130). In another study, Nakata et al., investigated the potential for meniscus cells isolated from meniscectomised knee. In this study, the authors expanded human meniscus cells and seeded them on a collagen scaffold. They could successfully isolate adequate number of cells from meniscal samples and showed that seeding them on scaffolds is feasible (131).

However, some of the limitations include I. An additional surgery is required to isolate autologous fibrochondrocytes, II. Some concern exists over the functionality of cells harvested from damaged tissue from patients at the time of surgery, and III. The low number of cells and the de-differentiation of these cells in culture (15, 36). The second source of cells for meniscus TE are chondrocytes isolated from articular cartilage. Articular cartilage could also be easily harvested

from non-weight bearing areas. Peretti et al., tested autologous chondrocytes isolated from porcine on allogenic meniscus fragments as the scaffold. These meniscus fragments were implanted in the avascular zones of the meniscus. They found that chondrocytes were able to synthesize meniscal tissue *in vivo* (42). It was reported in multiple studies that AC has the potential to accumulate large quantities of the matrix by secreting more GAGs and type II collagen than synovial membrane cells and fat pad cells. Applying of physical forces and specific regimen could alter gene expression of articular cartilage to secreting the meniscus-like matrix including type II and type I collagen (15, 77, 127, 132). Many studies have focused on the use of MSCs as a potential cell source. Also, SMSCs have been shown as the most promising source for meniscus repair and play an important role in menisci healing and restoration (15, 127, 132). Some of the advantages of synovial cells are: I. Cluster analysis studies have shown these cells have a superior capacity to generate cartilaginous tissues compared with MSCs from other tissues and have a gene expression profile similar to that of the meniscus and II. They are easily harvested during arthroscopic surgery (131). It has been shown that synovial flap or free synovium contributes to the natural course of meniscus healing at the injured site (77). Gene therapy in combination with tissue-engineered approaches has become an attractive strategy as a novel therapy to enhance repair of meniscus lesions. Although there have been several preclinical studies and *in vitro* studies using different cell sources for meniscus repair, up to date, no clinical trial has been initiated in this field (133). The optimal cell source has not yet been determined (77).

3.7 Growth factors and cytokines

Growth factors tested on meniscus cells or explants have been reported to be useful for meniscus healing (134) GFs can be inserted into suitable scaffolds or meshes. Local delivery of GFs boosts repair by producing a favorable environment for tissue growth. Some of the GFs that have been studied for meniscus repair include transforming growth factor beta (TGF-β), PDGF-AB, insulin-like growth factor, connective tissue growth factor, and bone morphogenetic protein-2 (135). Following injection, GFs rapidly disappear within the tissue, however, to achieve controlled release of such cytokines, addition of scaffolds which seeded with growth factors could be a solution (136). GFs are produced by platelets and fibroblasts and are able to control growth, stimulate proliferation, cell migration, and differentiation of different cells (152). Spindler et al., reported on the effect of

PDGF-AB on ovine cells and showed that PDGF-AB only affected the outer zone of the meniscus by increasing the mitogenic response (135). Bhargava and colleagues investigated the effect of PDGF-AB on bovine cells and demonstrated the increased migration of fibrochondrocytes from the inner, middle, and outer thirds of the meniscus as well as the mitogenic response from the peripheral one-third of the meniscus (137). Ionescu et al., assessed the effect of basic fibroblast growth factor (b-FGF) and TGF-β3 on electrospun PCL scaffolds for meniscus repair. They found that meniscus constructs refilled with native tissue when cultured in serum-containing media for 4 and 8 weeks with various growth factor formulations. Short-term delivery of bFGF or sustained delivery of TGF-β3 increased integration strength for both juvenile and adult bovine tissue and increased PG content in the explants to levels similar to that of the native tissue (136). Recently, Tarafder et al., used a novel approach to enhance avascular meniscus healing by recruitment of SMSCs. They created a longitudinal tear in the avascular zone of the bovine meniscus and applied a combination of connective tissue growth factor and TGF-β3, as chemotactic cues for further recruitment of SMSCs into the defect sites. They achieved sustained released of TGF-β3 which resulted in remodeling of the matrix into fibrocartilaginous matrix and fully healed incised meniscal tissues with improved functional properties (138). There is still no clinical study using GFs for meniscus repair.

3.7.1 Platelet-rich plasma and bone marrow aspirate concentrate

Platelet-rich plasma is currently used in the non-surgical management of sports injuries to treat different musculoskeletal conditions particularly those that are difficult to treat such as chronic, degenerative tendinopathy, and OA. Interest in utilizing PRP has skyrocketed over the last decade in the orthopedics field (139). Platelet-rich plasma is made merely by obtaining of the patient's blood and separating elements of blood by centrifuging to concentrate platelets. PRP and its derivatives are used for clinical augmentation of meniscus repair during or after the arthroscopic surgery (15). PRP is an autologous blood-derived product that contains increased concentrations of platelets above physiological levels. Platelets secrete many growth factors and bioactive components either from alpha and dense granules. Different types of growth factors exist in PRP including PDGF, TGF-β, vascular endothelial growth factor, epidermal growth factor, insulin-like growth factor-I, fibroblastic growth factor, and hepatocyte growth factor. Since PRP is a

heterogeneous product, it is important to characterize it before use. Different PRP preparation systems are available, which produce PRPs that contain varying concentrations of platelets, leukocytes, and erythrocytes. Depending on the baseline platelet count, efficiency, and variability of the PRP device, the produced PRP may vary (140, 141). On the basis of the platelet concentration, inclusion or exclusion of leukocytes, and fibrin architecture, Ehrenfest et al., classified 4 families of PRP preparations: I) Leukocyte-rich PRP (L-PRP), II) Leukocyte-poor PRP (P-PRP), both of which are liquid suspensions that form solid clots upon activation of the coagulation cascade; III) Leukocyte-rich platelet-rich fibrin (L-PRF), and IV) Leukocyte-rich platelet-rich fibrin (P-PRF), both of which are in solid format. The systems that produce L-PRP are systems with two-step centrifugations and result in a product that is 5 to 9 above the baseline level of platelets in the blood. Systems that produce P-PRP often use single, slower centrifugation leading to typically providing a platelet count of 1.5-3 above the baseline level of platelets in blood (142, 143).

PRP is thought to modulate the tissue healing process by supplying GFs, cytokines, and other bioactive compounds which play fundamental roles in hemostasis as well as tissue repair and remodeling. PRP safety profile, ease of preparation and application, low potential for disease transmission, and minimal tissue rejection are some advantages (17, 144). Regarding the therapeutic effects of the different types of PRP preparations, platelet content has been a primary focus, since platelet-derived GFs contribute to tissue repair. However, it is well established that the concentration of erythrocytes and leukocytes are also important factors to consider (142, 143). Like PRP, bone marrow aspirate concentrate (BMAC) is another alternative or option as a novel treatment for the management of pathologies of the knee and meniscus. BMAC is obtained by centrifugation of iliac crest aspiration and serves as a source of GFs and anabolic anti-inflammatory factors and stem cells and plays an essential role in treating mild-to-moderate osteoarthritis. The idea of augmentation of meniscus repair with blood-derived components is not new; it dates back to 1988 when Arnoscky et al., reported that use of exogenous fibrin clots augmented the healing response in the avascular areas of the meniscus in the dog model.

Preclinical data that incorporated PRP for meniscus repair is scarce. Most studies used rabbit models in combination with biomaterials, scaffolds, and stem cells. In some of those studies, application of PRP improved *in vivo* defects in the meniscus while others showed no enhancement in repair (145, 146). A comprehensive review of the effects of PRP on meniscus cells *in vitro* has

been performed (13). Few clinical studies have investigated PRP application for treatment of meniscal lesions (147, 148). In a case study for a single patient, Betancourt et al., attempted to treat meniscus rupture in knees with degenerative OA symptoms with P-PRP. After 30 months follow-up, clinical outcomes by the knee injury and osteoarthritis outcome score such as global rating of change core and visual analog scale improved (149). Recently, Kemmochi et al., compared application of autologous PRF and L-PRP in meniscus repair surgeries in 70 patients. They demonstrated the feasibility of the method and showed improvement of clinical scores while there was no significant difference between two groups (150). In another study by Kaminski et al, the safety and efficacy of L-PRP were assessed on 37 patients with vertical meniscus defects in the W-R zone. PRP was injected intraarticular and outcomes were evaluated after 18- and 42-weeks post-injection. Primary and secondary outcomes were assessed by MRI and second look arthroscopy. Although the number of the patients was low, PRP injections improved functional knee outcomes (151). An analysis of current treatment trends in the USA for the utilization of PRP for different musculoskeletal injuries concluded that patients receiving PRP injection for knee meniscus pathologies ranked with the most frequency (152).

Despite numerous investigations on the effect, efficiency, and role of PRP therapy for augmentation of the meniscus repair, this treatment is not widely used in clinical practice (146-148, 150, 152). There is difficulty in interpreting the effects of PRP on tissues owing to the variability of the contents of each specific preparation and non-uniform content of PRP, further highlighting the need for understanding the complex PRP composition (17, 142). Long-term studies with a higher number of patients, quantification of the degree of meniscus restoration with MRI, careful evaluation of clinical outcomes and thorough characterization of PRPs are still needed (145, 153). As of now, it is still unclear what type of PRP preparation should be used to treat specific conditions (142, 144). Longer longitudinal and evidence-based studies with increasing sample size would be recommended in future studies.

3.8 Commercially available products for meniscus replacement

Irreparable meniscal tears are usually treated by partial or total meniscectomy. In some cases, in which the peripheral meniscal rim is still intact, treatment with a meniscal substitute is indicated. Manufactured acellular scaffolds can be used to improve clinical outcomes following meniscus

injuries (154). Three implants are commercially available and have received European Union market approval for use clinically: I. The Menaflex collagen meniscus implant (CMI®; Ivy Sports Medicine GmbH., Gräfelfing, Germany), II. The Actifit® implant (Orteq Ltd., London, UK), and III. The non-biologic NUsurface meniscus implant (The NUsurface®; Active Implants, USA) (155, 156). The first two options are being used for partial meniscectomized knee in the cases when the peripheral meniscus zone is still intact. Menaflex is a xenograft collagen-based scaffold derived from highly purified type I bovine collagen achilles tendon and enriched with GAG. The Actifit is made from biodegradable aliphatic PCL and PU and is highly porous (154). It has been shown that both scaffolds minimize pain and improve knee function demonstrating their safety with no adverse effects. Both products are scaffolds made from degradable porous materials that induce vascular ingrowth (154). Menaflex has been studied widely as it has been available clinically for more than 10 years. In 2010, the FDA revoked their initial approval citing that the product did not meet the requirements for 510(k) approval (137). Actifit has only been in clinical use for the last 3-4 years in non-USA markets. Actifit has a much longer degradation time taking more than 5 years and promotes tissue remodeling better than Menaflex (136, 154). The total failure rate for both meniscal implants is approximately 10% at mid-term and are related to pain, swelling, infection, and mechanical failure of the scaffold (154). The NUsurface meniscus implant is used as medial meniscus replacement for patients with persistent knee pain following meniscectomy.

3.9 Rationale for using chitosan-autologous blood components for meniscus repair

Our laboratory has worked extensively with chitosan for cartilage repair applications for some years. Bone marrow stimulation (BMS) is a cartilage repair technique that initiates repair by drilling or fracturing the bone underneath a cartilage lesion to induce the formation of a blood clot in the lesion and healing by marrow-derived cells. Incomplete tissue regeneration and poor durability are some of the limitations of this procedure. We initially hypothesized that stabilizing the blood clot in cartilage defects would induce cell recruitment and improve neotissue formation. CS, a thrombogenic biomaterial with the ability to modulate several phases of the wound healing cascade, appeared to be a good candidate for this. By adding a buffer comprising glycerol phosphate (GP), solutions of CS having physiological pH and osmolality can be prepared (157).

Near-neutral solutions of CS-GP can be mixed with freshly drawn autologous whole blood to form hybrid clots that significantly resist retraction (158). These CS-GP-blood formulations can be utilized as injectable implants and adhere to cartilage lesions treated with BMS (158-160). Hoemann et al., and Chevrier et al., applied CS-GP-blood implant to microdrilled cartilage defects in rabbit models and assessed healing at day 1 to 56. The histological results showed that application of CS-GP-blood implants led to significant modifications in the healing sequence at early stages. These implants reside into the defect, induce cell recruitment to the holes, increase transient vascularization of the repair tissue, and remodeling of subchondral bone which leads to considerable integration of the repair tissue to a porous subchondral bone plate (23, 160, 161). Hoemann et al., also tested the same CS-GP-blood implants for repair of full thickness chondral defects in a large sheep model. Histology and gross examination of joints demonstrated that implants anchored to the walls of the defects and partly filled the surfaces of the defects. Repair tissue quantity and quality were improved after 6 months (158).

Some of the mechanisms responsible for this improved outcome include polarization of the macrophage phenotype towards the alternatively-activated pro-wound healing lineage and secretion of anabolic wound repair factors (24). Role of macrophages in repair is significant. Once macrophages are activated, they differentiate to specific phenotypes such as macrophage-1 and macrophage-2 and release GFs as well as angiogenic mediators which modulate the healing sequence. Other mechanisms of action of the CS-GP-blood implants include promotion of osteoclasts and remodeling which leads to improved tissue integration (162). Following the initial studies, we showed that implant coagulation could be accelerated by adding external coagulation factors to the mix (162-164). CS-GP-blood implants solidified with thrombin induced structurally integrated hyaline cartilage in a rabbit model at 6 months (162, 163).

Mathieu et al., treated rabbits with CS-GP-blood implants or implant solidified with thrombin, tissue factor with recombinant human factor (rhFVIIa), and rhFVIIa alone. Implants increased bone remodeling and blood vessel immigration to the cartilage lesion zone by suppressing fibrocartilage scar tissue formation (164). A different approach to treat the BMS holes with pre-solidified formulations of chitosan was then devised (165-168). Lafantaisie-Favreau et al., tested different MW of chitosan in a rabbit model. All implants attracted neutrophils, osteoclasts and abundant bone marrow-derived stromal cells, stimulated bone resorption followed by bone remodeling and a good integrated fibrous tissue (165). In a challenging aged rabbit model, subchondral defects

treated by chitosan-blood implant demonstrated bone marrow-derived hyaline cartilage repair by improvement of bone plate resorption after 70-day post-operation when comparing with empty drill holes left to bleed. In other 2 studies, chitosan-blood implants were tested in microdrilled subchondral bone in critical-size sheep cartilage defects after one day, 3 weeks, 3 month, and 6 months. Repair tissues were assessed histologically, biochemically, biomechanically, and by micro-computed tomography and results showed chitosan implant was resident at day 1, variable cartilage repair tissue observed after 3 weeks, angiogenesis and granulation tissue seen after 3 month and finally bone remodeling, and GAG synthesis in the treated defects were found compared with intact tissue (166-168). CS-GP-blood implants (BST-CarGel^{TM}) were tested in a randomized controlled trial for treatment of focal cartilage lesions on femoral condyles in 80 patients. Treatment was either microfracture in combination with CS-GP-blood implants or microfracture alone. Outcomes were assessed after 12 months by MRI and clinical assessment on patients showing that tissue repair quantity and quality was superior for patients treated with BST-CarGel (169). 21 out of 41 BST-CarGel treated patients and 17 of the 39 microfracture patients underwent elective second look arthroscopies during which osteochondral biopsies were collected at an average of 13 months. Polarized light microscopy and histological assessment of osteochondral biopsies from patients treated with BST-CarGel group showed significantly better ICRS scores of tissue organization, collagen alignment, and cell characteristics compared to microfracture (170). At 5 years follow-up, BST-CarGel patients demonstrated greater lesion filling, greater repair tissue, T2 relaxation time, and superior tissue quantity and quality compared to microfracture alone (171). BST-CarGel is currently commercialized in several countries by Smith and Nephew.

More recently, we have developed freeze-dried formulations of chitosan that can be solubilized in PRP to form injectable implants that solidify *in situ* and are used for tissue repair (19). Lyophilization of chitosan is expected to provide long-term stability to the product while PRP constitutes a rich source of platelet-derived GFs that can solubilize lyophilized chitosan for delivery to the wound site to improve repair. In contrast to PRP-only implants which were rapidly cleared *in vivo* and had little bioactivity, these CS-PRP implants were shown to reside for several weeks and induce vascularization and cell recruitment in a subcutaneous implantation model, both of which are desirable in the context of meniscus repair. Chevrier et al., used a systematic approach to adjust chitosan number average molar mass, chitosan concentration, and lyoprotectant concentration to obtain freeze-dried CS formulations that are completely and rapidly solubilized in

PRP and coagulate quickly to form mechanically stable implants (19). Deprés-Tremblay et al., demonstrated that platelet aggregation and clot retraction were suppressed through chitosan covering the blood components. They also showed that CS-PRP implants release more platelet-derived growth factors than PRP alone (172). CS-PRP implants were then used to augment repair of rotator cuff and cartilage in small and large animal models (25). Based on all of the above, it is expected that a combination of chitosan and PRP would be successful in enhancing healing of the meniscus. The work presented in the thesis provides a new approach for the treatment of meniscus tears, bringing us one step closer to a new clinical option for meniscus repair.

CHAPTER 4 STRUCUTRE AND ORGANIZATION OF ARTICLES

The significant contribution in this thesis is reflected and exemplified in the comprehensive literature review on various augmentations techniques recently developed to increase healing of meniscus tears. This review paper is entitled «Augmentation Strategies for Meniscus Repair," and more than 100 peer-review publications were covered. The results were published in the «Journal of knee surgery» which ranks within the top journals regarding both orthopedics and sports medicine and is considered an indispensable source by many knee surgeons.

In this comprehensive publication, I concisely discussed the current clinical management guidelines for primary meniscus repair techniques as well as augmentation strategies to enhance the rate of meniscus healing by using trephination, synovial rasping, abrasion, blood clot placement, platelet-rich plasma (PRP) injections, and wrapping with extracellular matrix materials. Further development of these approaches and bioactive materials may improve repair of currently irreparable meniscus tears. Eventually, we discussed the rationale for using chitosan polymer and autologous blood component implants to improve meniscus repair. To the best of my knowledge, this is the first existing comprehensive manuscript that covered preclinical and clinical studies using the latest augmentation approaches for meniscus repair. Performing such a review covering treatment algorithms of meniscus lesions guided me to better design my experimental research and addressed my research question during my Ph. D.

My second study aimed to assess the feasibility of applying freeze-dried (FD) chitosan (CS) solubilized in PRP implants to improve meniscus repair in large ovine animal models. Lyophilized formulations containing chitosan, trehalose, and calcium chloride were solubilized in autologous PRP and applied to surgically induced meniscus lacerations. I consider this publication to be one of my most significant research contributions to date. The results are presented in the article titled «Freeze-Dried Chitosan-PRP Injectable Surgical Implants for Meniscus Repair: Pilot Feasibility Studies in Ovine Models » The findings were published in the «Journal of Regenerative Medicine and Therapeutics» In these studies, either bilateral or unilateral tears were treated by suturing, trephination, and injecting either CS-PRP or/and wrapping the meniscus with a collagen membrane and injecting CS-PRP in tears and under the wrap. This study explored the cellular repair, integration, and potential application of CS-PRP injectable implants to improve meniscus repair outcomes in preclinical models at 3 different time points. The purpose of conducting sheep studies

of meniscus repair is to approximate as closely as possible the clinical pattern, cartilage pathology, and progression of the regenerative process induced by CS-PRP injectable implants.

My third study aimed to assess the compatibility of freeze-dried CS-PRP with the various types of PRP preparations isolated with commercially available systems and define a range of chitosan with a range of degree of deacetylation and number average molar mass that would yield freeze-dried formulations with favorable performance characteristics for orthopedic conditions. We assessed physiological properties such as solubility, pH and osmolality. Also, clotting properties, runniness, liquid expression, clot mechanical strength, and clot homogeneity for freeze-dried CS-PRP formulations were evaluated. This paper entitled «Multiple platelet-rich plasma preparations can solubilize freeze-dried chitosan formulations to form injectable implants for orthopedic indications» was submitted to «The Journal of Biomedical Material engineering».

The objective of the fourth study was to optimize the freeze-drying cycle of the chitosan formulation to decrease overall freeze-drying time duration from 3 days to 1 day and to assess performance characteristics of the freeze-dried CS with benchtop human PRP and human commercial plasma. Performance characteristics of freeze-dried CS formulations was examined for solubility, pH, and osmolality, as well as clotting properties with TEG, runniness, liquid expression, clot mechanical strength, and histology. Cakes that were non-collapsed following freeze-drying were solubilized either in citrated pooled normal plasma or benchtop human PRP. CS-PRP formulations were less runny and resisted platelet-mediated clot retraction when compared with PRP controls and citrated pooled normal plasma.

CHAPTER 5 ARTICLE 1: AUGMENTATION TECHNIQUES FOR MENISCUS REPAIR

(Journal of Knee Surgery)

Leili Ghazi zadeh MSc [1], Anik Chevrier PhD [2], Jack Farr MD [3], Scott Rodeo MD [4] and Michael D. Buschmann PhD [5]

[1]Biomedical Engineering Institute, Polytechnique Montreal, Montreal, QC, Canada, leili.ghazi-zadeh@polymtl.ca. [2]Chemical Engineering Department, Polytechnique Montreal, Montreal, QC, Canada, anik.chevrier@polymtl.ca. [3]OrthoIndy Knee Care Institute and Cartilage Restoration Center of Indiana, Greenwood, IL, USA, indyknee@hotmail.com. [4]Sports Medicine and Shoulder Service, The Hospital for Special Surgery, New York, NY, USA, rodeos@hss.edu. [5]Biomedical Engineering Institute and Chemical Engineering Department, Polytechnique Montreal, Montreal, QC, Canada, caroline.hoemann@polymtl.ca. [6]Biomedical Engineering Institute and Chemical Engineering Department, Polytechnique Montreal, Montreal, QC, Canada, michael.buschmann@polymtl.ca

Corresponding author: Prof Michael D. Buschmann, Department of Chemical Engineering, Polytechnique Montreal, PO Box 6079 Succ Centre-Ville, Montreal, Quebec, Canada, H3C 3A7, Fax: 514 340 2980 Tel: 514 340 4711 ext. 4931, E-mail: michael.buschmann@polymtl.ca.

Abstract

Menisci display exquisitely complex structure and play an essential weight-bearing role in the knee joint. A torn meniscus is one of the most common knee injuries which can result in pain and mechanical abnormalities. Tear location is one aspect which determines the endogenous healing response; tears that occur in the peripheral densely vascularized zone of the meniscus have the potential to heal while the healing capacity is more limited in the less vascularized inner zones. Meniscectomy was once widely performed but led to poor radiographic and patient-reported mid and long-term outcomes. After the advent of arthroscopy, orthopedic opinion in the 1980s has been swaying towards salvaging or repairing the torn meniscus tissue in order to prevent osteoarthritis rather than performing meniscectomy. Meniscus repair in young active individuals has been shown to be effective, reproducible and reliable if indications are met, however, only a small proportion of all tears are considered repairable with available technologies. Biological augmentation techniques and meniscus tissue engineering strategies are being devised to enhance the likelihood and rate of healing in meniscus repair. Pre-clinical and clinical studies have shown that introduction of cellular elements of the blood, bone marrow and related growth factors have the potential to enhance meniscus repair. This article reviews the current state of clinical management of meniscus tears (primary repair) as well as augmentation techniques to improve healing by meniscus wrapping with extracellular matrix materials, trephination, synovial rasping and abrasion, fibrin/blood clot placement, and platelet-rich plasma injections. In addition, the rationale for using polymer/autologous blood component implants to improve meniscus repair will be discussed.

Keywords: Meniscus repair, Augmentation techniques, Platelet rich plasma, Chitosan

Level of evidence: Review article

Disclaimer: None

5.1 Introduction

Menisci are semilunar shaped fibrocartilaginous structures[1,2] that play central load bearing and load distribution roles in the knee joint[3]. Population-based data suggest that meniscal damage is present in at least one-third of the knees of middle-aged or elderly individuals[4] and meniscus-deficient knees are more likely to develop radiographic evidence of osteoarthritis (OA)[5] and increased degeneration over time[6]. Although there has been a recent increase in the number of meniscus repairs performed yearly in the US[7], only a small portion of all meniscal tears are considered repairable so that current surgical treatment of symptomatic meniscal tears often involves partial removal of torn meniscus, which increases the risk of developing OA[8-10]. Tear properties such as tear pattern, length, depth, size, stability, location (medial vs lateral and where geographically in each), chronic or acute, patient profile (age, health, symptoms) and joint stability are all important factors affecting the rate of healing and should be considered before patients undergo meniscus repair.

One of the major impediments in repairing a damaged meniscus is that only the outer rim of the tissue is vascularized[11-13]. Since wound healing in adult tissues is triggered by the products released with blood clotting, the capacity for natural repair is optimal in the periphery of the meniscus and diminished in the inner margins[14]. Tear location thus becomes critical, and tears occurring in the peripheral vascularized portion of the meniscus are the most amenable to healing and thus, repair. Healing is more difficult in the case of other tear patterns such as radial, horizontal, fragmented, or white-white displaced bucket-handle and in the case of complex, chronic or degenerative tears[15,16]. When meniscal tears occur in the peripheral vascularized area of the meniscus, repair by suturing leads to satisfactory clinical improvement in 70-90% of patients. Nonetheless, the clinical failure rate can be as high as 20-24% depending on, among other factors, the status of the anterior cruciate ligament (ACL)[17], while incomplete healing corresponding to structural failure is yet higher than the clinical failure rate[18]. Although previously considered to be irrepairable, the current trend is to suture tears that occur in the inner non-vascularized margins, with reports of surprising clinical success in up to 68% of patients[19], while here again structural failure can be much higher. There remains a need to develop reproducible and efficient meniscus repair augmentation techniques. The purpose of the current review is to describe the current clinical management of meniscus tears and different repair augmentation techniques that are available including meniscus wrapping with extracellular matrix materials, trephination, synovial rasping

and abrasion as well as application of exogenous fibrin/blood clots and platelet-rich plasma (PRP). Finally, the rationale for using chitosan-PRP implants to improve meniscus repair will be discussed.

5.1.1 Current clinical management of meniscus tears

Meniscus tears are among the most common type of knee injuries[20,21], and treatment of meniscal tears account for half of the arthroscopic procedures performed in the US[22]. Overall, meniscus tears fall into two overlapping categories: either traumatic or degenerative[15]. Age, gender, work-related kneeling, squatting or climbing stairs are among the risk factors for developing degenerative tears, while acute meniscal tears tend to be sports-related[23] understanding that an acute tear can occur in a degenerating meniscus. Meniscus lesions in young children are predominantly due to acute trauma or congenital meniscus variant such as discoid meniscus. In older children, they are a result of accident/sport and in adults, they are more chronic tears that occur because of trauma, degenerative disease or a combination of both. In adults, medial meniscus tears are often associated with cartilage lesions and/or concomitant ligament damage[16]. Medial and lateral meniscus tears are usually categorized based on the anatomic location of the tear, vascularity of the tissue where the tear occurs, and the tear pattern (radial, longitudinal, horizontal, circumferential, root lesions, bucket handle, oblique/flap tears and complex degenerative tears) [16,24]. Meniscal root tears are defined as radial tears or an avulsion of the insertion of the meniscus [25,26]. Due to failure of the meniscus to convert axial loads into hoop stresses, these types of injuries alter load-sharing and the continuity of circumferential fibers leading to progressive arthrosis-like changes in the knee. Initially, a ramp lesion was defined as a longitudinal tear of the peripheral attachment of the posterior horn of the medial meniscus at the meniscocapsular junction of > 2.5 cm in length. Due to different anatomical locations, there is no current agreement regarding the definition of meniscal ramp lesions. Some authors suggest that ramp lesions are associated with injury to the meniscotibial ligament attachment of the posterior horn of the medial meniscus, while others say it is produced by a tear of the peripheral attachment of the posterior horn of the medial meniscus[27,28]. Patient-reported history of recent trauma or prior injury followed by symptoms of meniscal injury (instability, locking, effusion, and tibiofemoral joint line pain) as well as physical

examination of the knee (joint line tenderness, effusion, limitation of range of motion) allow for diagnosis of a meniscal tear[15,29].

Treatment algorithm of meniscus lesions has evolved tremendously in recent years. The decision as to whether conservative nonsurgical treatment should be preferred to surgical treatment is highly dependent on the size, pattern and location of the tear, the patient's age, health status and activity level, and on the surgeon's experience[16]. Although a considerable number of patients having traumatic or degenerative meniscus lesions are treated non-operatively, meniscus lesions that seem to be mechanically unstable, complex tears, and mostly degenerative meniscus lesions that are symptomatic are often removed by meniscectomy[24]. Arthroscopic partial meniscectomy (APM) is still the most frequent orthopedic procedure in orthopedic surgery, although there is evidence that more conservative treatments should be preferred as first-line treatment when not associated with an acute tear, such as with an ACL tear[30-33].

Indications for meniscus repair include symptoms directly attributable to the tear, reducibility of the tear, good tissue integrity and favorable tear characteristics (e.g. single vertical) in one plane in the red-red or red-white zones of the meniscus or when an ACL is reconstructed [15,29,34]. The following tears are generally considered less amenable for repair: chronic tears with plastic deformity, complete tears with oblique, horizontal cleavage, or complex degenerative pattern in the white-white zone of the meniscus[29,34,35]. Longitudinal tears < 10 mm are often stable and are therefore often left untreated. Incomplete radially oriented tears that do not extend into the outer periphery are less likely to heal and are often left untreated or treated by debridement of the unstable edges. Repair of a radial tear to the periphery is usually encouraged to reduce the risk of having a non-functional meniscus. The presence of either untreated instability or OA is also a contraindication for meniscus repair. It has been demonstrated that meniscus repair at the time of anterior cruciate ligament (ACL) reconstruction is highly correlated with superior healing rates over "isolated" meniscus tear repairs[15]. Recently, there has been a shift towards attempting repair of tears previously deemed irrepairable since preservation of the meniscus structure is expected to maintain meniscus function and prevent degenerative changes to the joints[16]. Satisfactory results have been reported for repair of some horizontal cleavage tears[36] and radial tears[37], for tears extending into the avascular portion of the meniscus[38] and for patients[39] 40 years and older at the time of surgery. Rehabilitation after meniscus repair surgery usually begins with early active range of motion and restoration of strength exercises, followed by a return to low-impact daily activity

within one month and return to sports usually at 4-6 months, when appropriate functional goals are reached, and the patient no longer has point tenderness over the repair site[40].

Surgical repair of meniscal tears can be performed with inside-out, outside-in and all-inside techniques. Tears in the anterior or body of the medial or lateral meniscus are easily accessed with the outside-in technique. For far posterior tears, the inside-out or all-inside techniques are preferred. Although inside–out techniques with vertical divergent sutures are still suggested to be the "gold standard" for meniscus repair, all-inside techniques have the advantages of reduced surgical times, ease of use and low risk of damage of neurovascular structures[16,34] and comparable healing rates in several studies[41-45]. Early meniscal repair devices such as the meniscal arrows and meniscal screws have been associated with chondral damage and have been gradually replaced by suture-based devices. More recently, the all-inside circumferential compression stitching technique has been developed for tears that are difficult to treat with traditional all-inside techniques[46]. Level I and Level II studies comparing different meniscus repair techniques report failure rates between 9% and 43% and anatomic healing rates between 65% and 100% (**APPENDIX A:**

Table 1). A systematic review of 13 studies reporting the outcomes of meniscal repair at a minimum of five years reported a pooled failure rate of 23% with no difference between the different techniques (outside-in, inside-out or all-inside with arrows)[17]. Another systematic review of 27 studies also reported no difference in failures, clinical scores or complications between inside-out and all-inside repairs (excluding meniscal arrows and screws)[47]. In a third systematic review of 31 studies, the authors were unable to determine which all-inside device had the lowest failure rate[48]. A meta-analysis of 21 studies reported a higher failure rate of 16% for all-inside meniscal repair versus 10% for inside-out meniscal repair, both performed concurrently with anterior cruciate ligament reconstruction (ACLR)[49]. Nerve injuries are associated with inside-out technique and implant-related problems are the most common complications with all-inside technique[50]. In all of the above-mentioned studies, the authors highlighted the present lack of prospective studies with long-term follow-up and the low level of evidence of available data.

Long-term comparisons of meniscus repair versus meniscectomy are scarce and there remains a lack of high-level evidence to guide the surgical management of meniscal tears[51]. A randomized prospective comparative study showed normal or near-normal findings in 100% of

patients (n=11) treated with arthroscopic partial meniscectomy versus 90% of patients (n=10) treated with arthroscopic suture repair with access channels at 27 months follow-up[52]. In a retrospective study following 41 patients up to 96 months, failure rates were 14% in the repair group and 10% in the partial meniscectomy group[53]. Clinical outcomes were similar for both groups and no OA progression was noted but pre-injury levels were regained only in the repair group. Another retrospective study compared patients treated with inside-out suturing (n=67) or meniscectomy (n=24) and showed more pain in the latter group[54]. In a retrospective study with 10 years follow-up of 32 patients, Lutz et al 2015 showed higher functional and quality of life scores for repaired vertical lesions in stable knees compared to meniscectomized knees[55]. Radiographic scores were improved for the repaired group suggesting a close correlation between functional and radiographic scores and protective effect of meniscus repair against OA. Finally, recent systematic reviews and meta-analyses concluded that, although meniscus repairs were associated with higher reoperation rate, they result in better long-term patient reported outcomes and activity levels compared to meniscectomy[56,57]. The Multicenter Orthopaedic Outcomes Network (MOON) prospective longitudinal cohort study reported that a subset of patients treated with meniscus repair at the time of ACL reconstruction had an overall failure rate of 14% and significant clinical improvement that was sustained for 6 years[58].

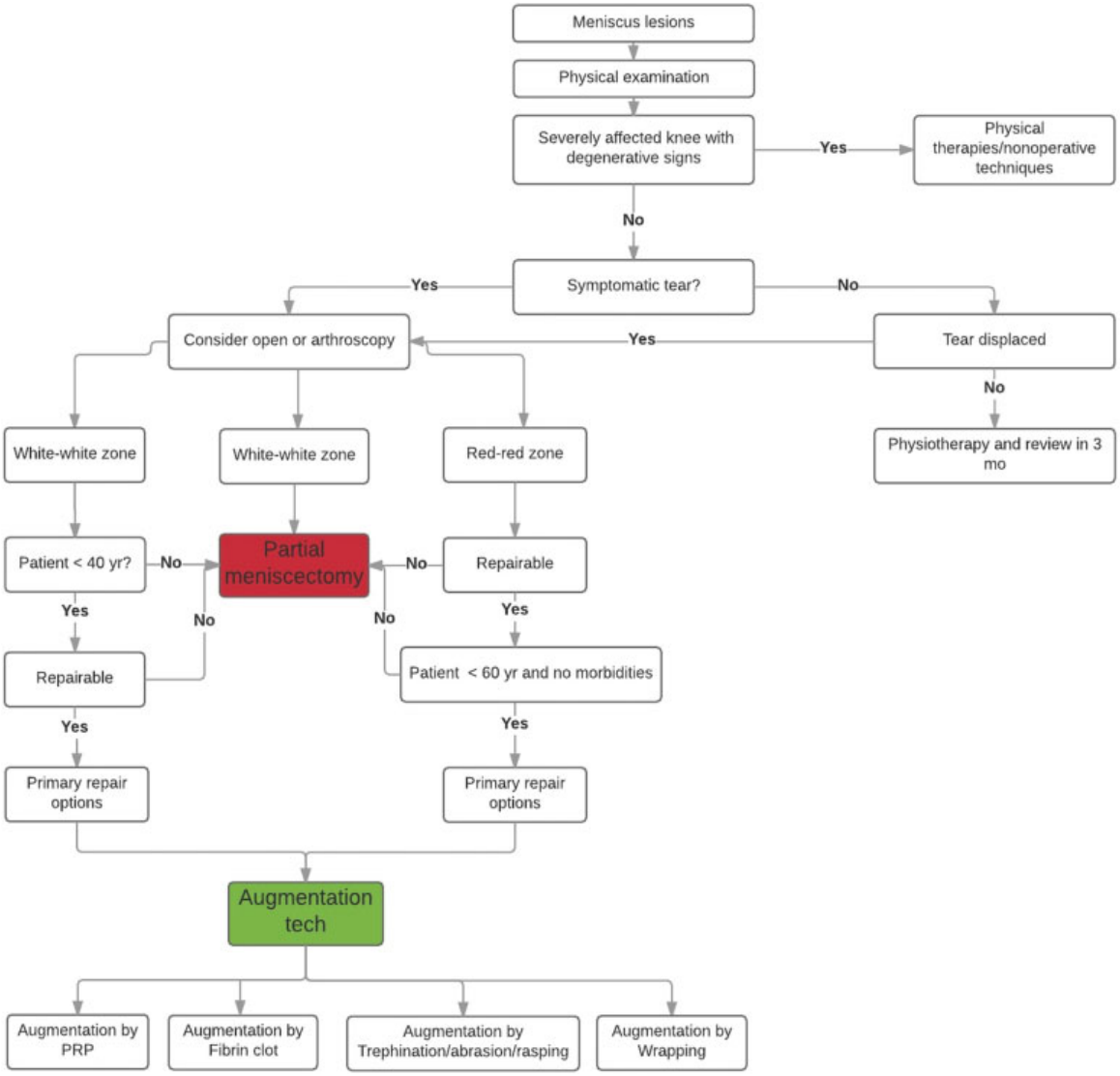

Figure 5.1 Treatment algorithm of meniscus lesions (Adapted from Mordecai et al, 2014).

5.1.2 Augmentation of meniscus repair through trephination, rasping and abrasion

Vascularity of the meniscus is an important determinant for healing[11,12]. The vascular supply of the meniscus is age-dependent, and the adult meniscus receives vascularity from the perimeniscal capillary plexus (PCP), which comes from the superior and inferior branches of the medial and lateral genicular arteries. Multiple preclinical and clinical studies have demonstrated that lesions in the vascular portions of the meniscus with access to the peripheral blood supply have the potential for producing a healing response which is similar to what occurs in other dense fibrous

connective tissues during healing, including hemorrhage, proliferation, differentiation and remodeling. Injuries in the peripheral zones of the meniscus are filled primarily and initially with a highly cellular fibrin clot which acts as a scaffold for repair cells that migrate, proliferate, differentiate, and synthesize repair tissues. Scar tissue remodeling may then take months to mimic the meniscus structure and function. Trephination involves the creation of vascular access channels that run from the vascular portions of the peripheral meniscus toward the more central avascular area to enable bleeding, clot formation, cell migration and repair. Several pre-clinical studies have shown that trephination channels enhance the healing of avascular meniscal tears.

Arnoczky and Warren investigated healing response of the meniscus in a dog model at different time-points post-injury[11]. The creation of vascular access channels resulted in complete healing of avascular lesions by synthesis of fibrovascular scar tissue which was similar to fibrocartilaginous meniscus tissue after 10 weeks. The healing response appeared to originate from the peripheral synovial tissues. Zhang et al used trephination to treat longitudinal incisions in the avascular area of the meniscus in a unilateral model in dogs and investigated the role of synovial tissues during the healing process[59]. Trephined meniscus repaired first by formation of a granulation tissue which gradually matured into scar tissue. Zhang et al repaired longitudinal meniscus tears located at the avascular portion of the meniscus by suturing and trephination in 20 goats[60]. At 25 weeks post-surgery, 4 out of 20 defects were fully repaired and 16 were partially repaired. The amount, distribution and organization of collagen bundles were similar to that of normal meniscus, suggesting that repair tissue has the potential to remodel and mature with time. Cook et al tested poly-L-lactic acid (PLLA) bioabsorbable conduits designed to maintain trephination channels in surgically created longitudinal avascular meniscus tears in 25 dogs[61]. Treatments with the conduits in conjunction with suturing resulted in functional healing with bridging tissue and biomechanical integrity in 71% of avascular meniscal defects while no healing was observed with trephination and suturing. Peripheral displacement of the device was observed although no conduit was completely dislodged into the joint nor articular cartilage damage noted.

Trephination has also shown some benefits in clinical studies (**APPENDIX A:** Table 2). Fox et al repaired symptomatic incomplete meniscus tears (vertical and longitudinal) in 30 patients by using arthroscopic trephination and 90% of patients reported satisfactory to excellent subjective results after 20 months[62]. Zhang and Arnold repaired longitudinal tears by a tooth-like tip trephine device and inside-out arthroscopic horizontal sutures[63]. At an average follow-up of 47 months, 7

patients had symptomatic meniscal re-tear (failure rate of 25%) in the suture group, while 2 patients in the trephination and suture group showed symptomatic meniscal re-tear (failure rate of 6%). Shelbourne and Rask repaired peripheral vertical medial meniscus tears > 1 cm in length (100% with concomitant ACL reconstruction) by using different techniques[64]. Failure rate was 6% for the 233 patients who had undergone abrasion and trephination. Shelbourne and Dersam repaired radial flap tear, posterior horn tear, and peripheral tears in the lateral meniscus using abrasion and trephination or left the tears *in situ* at the time of ACL reconstruction[54]. Overall failure rate was 2.4% at 79 months and clinical outcome was similar for both groups. Shelbourne et al repaired peripheral non-degenerative medial meniscus tears at least 1 cm in length by arthroscopic trephination during ACL reconstruction[65]. Failure rate was 16.3% at 5.6-year follow-up and trephination-treated tears showed 95% normal radiographs. However, none of these studies objectively evaluated anatomic meniscus healing using an imaging study or second-look arthroscopy.

Other augmentation techniques involve rasping the meniscal tear and slightly abrading the synovium. Okuda et al surgically created full-thickness longitudinal lesions in the avascular zone the medial meniscus in a rabbit model and repaired it by rasping on the surface of the meniscus from the parameniscal synovium to the injured portion[66]. Early macroscopic and histological evaluation showed hypertrophic synovial tissue invading the lesion from the parameniscal synovium. Fibrous repair was complete in all layers of the injured portion in the rasped meniscus at 16 weeks. They concluded that rasping of parameniscal synovium without suturing could be an uncomplicated way to augment meniscus healing. Ochi et al created full-thickness longitudinal tears in the avascular zone of the medial menisci in a rabbit model and assessed mechanisms of meniscus healing following rasping of the parameniscal synovium and meniscus surface[67]. Immunohistochemistry showed that the rasped surface stayed highly positive for interleukin-1α (IL-1α), transforming growth factor-β1 (TGF-β1), platelet-derived growth factor (PDGF), and proliferating cell nuclear antigen (PCNA) at 1, 7, 14, and 7 days post-surgery and then gradually declined. They suggested that rasping could stimulate chondrocytes in the meniscus surface area to synthesize specific types of growth factors and cytokines, and such synthesized proteins can stimulate the metabolism of the chondrocytes and attract the synovial tissue with its rich vascularity to the injured site to aid in healing.

Synovial abrasion and rasping have also been applied clinically (**APPENDIX A:** Table 2). Uchio et al treated full-thickness and partial-thickness longitudinal tears in 47 patients by rasping the tear and synovial abrasion[68]. Healing rate was a reported 92%. They found no effect of age, sex, the time between injury and rasping, the time between rasping and second-look arthroscopy and concomitant ACL reconstruction on the healing rate. However, healing was better for partial-thickness tears, shorter tears, tears near the capsule, and tears in stable menisci. Tetik et al reported repairing horizontal tears in the posterior half of the medial meniscus in 25 patients by rasping of the tear and synovial abrasion[69]. After 15 months follow-up, 88% of the patients were classified as excellent (no pain, no subjective symptoms, full return to sports, no objective pathologic findings). Talley et al repaired longitudinal, double longitudinal and radial tears in 40 patients by synovial abrasion at the time of ACL reconstruction[70]. Overall failure rate was 11% (4% for lateral meniscus and 21% for medial meniscus) at 3.3-year follow-up.

All of the above studies indicate that trephination, rasping and abrasion are easy treatment modalities that can contribute to meniscus repair. In fact, these augmentation techniques are often used in conjunction with outside-in, inside-out or all-inside repair (**APPENDIX A:**

Table 1). One potential drawback of trephination is that the trephination channels may damage the peripheral circumferential fibers and have adverse effects on the biomechanical properties of the meniscus. In addition, self-collapse and channel closure could lead to blocked cell migration. Furthermore, it is still not known whether a single large or multiple small channel are more efficient for meniscus healing. One limitation of synovial abrasion and rasping is that they are less efficient in repairing tears that are far from the capsule.

5.1.3 Augmentation of meniscus repair with fibrin/blood clots

Meniscus healing is a complex process that is associated with many cellular and molecular events, including hemorrhage, clot formation, granulation, vascularization, cell ingrowth, cell infiltration, ECM synthesis, scar tissue formation, and scar remodeling. Depending on the lesion location and size, healing processes may differ. The wound hematoma contains a spectrum of platelet-derived growth factors as well as clot components which are chemotactic and are expected to promote proliferation and differentiation of cells. Fibrin glue, exogenous fibrin clots, and in situ forming fibrin clots have all been used in pre-clinical and clinical studies to augment meniscus

repair. Microfracture of the intercondylar notch was also introduced to enhance the repair of isolated meniscus tears by inducing blood and bone marrow elements into the joint[71]. Although the exact mechanisms of action of fibrin clots have not been completely elucidated at this point, they have the potential to accelerate tissue healing in meniscus.

Ishimura et al[72] surgically created full-thickness lesions in avascular areas on the anterior segment of the medial meniscus in a rabbit model. Autologous plasma-derived fibrin glue used in conjunction with bone marrow cells accelerated histological maturation of the repair tissue and improved repair compared to the acellular fibrin glue by itself at 12 weeks. Ishimura et al[73] arthroscopically repaired 40 meniscal tears in 32 patients using purified fibrin glue. At 3 years follow-up, 2 patients had recurrence of meniscal symptoms and underwent partial meniscectomy. Second-look arthroscopic evaluation rated 20 out of 25 repairs as good (80%), 4 as fair, and 1 as poor. In another study, Ishimura et al[74] used purified fibrin glue to repair 61 menisci in 40 patients. The rate of recurrence of tears in the red–red (R-R) zone or red–white (R-W) zone was 10 % at an average follow-up of 8 years, whereas it was 17 % for tears in the white–white (W-W) zone. Second-look arthroscopy in 27 patients revealed that 77% of repairs were considered good, 11.5% fair, and 11.5% poor. In the study of Arnoczky et al[11], implantation/placement of exogenous fibrin clot into stable full-thickness defects in the avascular medial portion of meniscus in dogs improved the healing response via proliferation of fibrous connective tissue, which gradually remodeled into fibrocartilaginous tissue. Filling the lesion area with a fibrin clot provided a scaffold matrix and secretion of mitogenic components to recruit cells that originated from the adjacent meniscal tissue and synovial membrane.

Ritchie et al surgically created unilateral peripheral longitudinal tears in the meniscus in a goat model to assess the effect of two different adjunctive healing techniques[75]. Goats in Group I received inside-out horizontal mattress sutures, goats in Group II received inside-out sutures plus placement of an exogenous fibrin clot inside the defect as a healing enhancer, and goats in Group III received inside-out sutures, rasping and synovium abrasion. Healing rates were 100% in Group I, 17% in Group II and 87.5% in Group III, which suggests that the use of the adjuncts was not necessary. Port et al[76] surgically created a full-thickness lesion in avascular zones of the meniscus in a goat model and assessed application of fibrin clot and autologous cultured adherent-bone marrow cells (BMC) in the site of the defect by histology and mechanical testing. In this case, administration of cultured bone marrow derived-cells in combination with exogenous fibrin clot

failed to improve meniscal healing by 16 weeks. Nakhostine et al[77] created 5-7 mm longitudinal full-thickness incisions in the avascular portion of the meniscus in an ovine model, which were further injected with 3 mL of blood clot through a trephination channel running from the periphery of the meniscus to the mid portion of the lesion. The addition of exogenous blood clot in this model without additional stabilization was not sufficient to promote complete healing of torn menisci.

Fibrin/blood clots have also been used clinically (**APPENDIX A:** Table 3). Van Trommel et el treated 5 patients that had a tear of the posterolateral aspect of the lateral meniscus with suturing and placement of an exogenous fibrin clot in the seam of the tear[78]. Healing was complete for the 3 patients that were available for follow-up. The authors suggested that application of an exogenous fibrin clot might improve healing of tears located in the avascular portion of the meniscus. Biedert et al compared the effect of four different methods, including conservative therapy (n = 12), arthroscopic suture repair with channels (n = 10), arthroscopic central resection and intra-meniscal administration of fibrin clot by suture repair (n = 7), and arthroscopic partial meniscectomy (n = 11), for treatment of isolated and symptomatic painful horizontal grade 2 meniscal lesions (intrasubstance meniscal lesions) on the medial side in forty patients[52]. Only 43% of the patients treated with administration of fibrin clot had normal or near-normal evaluation at follow-up. Jang et al[79] reported a novel method for delivering fibrin clots to the target area of meniscal tear by arthroscopic technique to augment the rate of healing. In this technique, the sutured fibrin clot is passed through a plastic transparent shoulder cannula to the desired location by pulling off the needle. They reported a success rate of 95%. Ra et al[80] used fibrin clot as an alternative effective method for treatment of complete radial tear of meniscus by arthroscopic inside-out repair suturing in 12 patients. They found improved clinical scores and complete healing in most patients on follow-up MRI and second-look arthroscopy. Horizontal cleavage tears with meniscal degeneration indications are difficult to heal[36]. Kamimura et al showed functional joint improvement and meniscal healing in patients with horizontal cleavage tear with meniscal degeneration (difficult-to-treat injuries) treated with FasT-Fix (Smith and Nephew, USA) vertical sutures and placement of exogenous fibrin clots within the cleft[81]. At 12 months follow-up, they[82] showed 70% complete healing rate and improvement of Lysholm, IKDC subjective scores and Tegner activity level. They suggested that this technique could be considered as a treatment option for younger patients with a stable knee with a degenerative horizontal cleavage tear. To biologically augment repair of meniscal tears, Sethi et al developed a simple intra-articular technique to deliver

blood clots by abrading the synovium and allowing the blood to run down the synovial wall and into the meniscal cleft, pooling there and forming a clot adherent to the edges of the separated meniscal tear close to the tear site[83]. The authors claimed that their technique has a few advantages over using the exogenous fibrin clot such as being simple, easy to handle, safe, minimally invasive (does not depend on exogenous preparation), does not require the assistance of operating room staff, and does not add a significant amount of time to the meniscal repair. Although using fibrin/blood clots in the context of meniscal repair has yielded equivocal and conflicting results in pre-clinical and clinical settings, this remains a simple and easy option to potentially augment healing in the setting of meniscus repair. Further high-level evidence is still required.

5.1.4 Augmentation of meniscus repair with platelet-rich plasma

Platelet-rich plasma (PRP) is currently used in the sports medicine and orthopedics fields to treat different conditions such as tendinopathy or osteoarthritis[84,85]. PRP contains various types of growth factors including platelet-derived growth factor (PDGF), transforming growth factor-beta (TGF-β), vascular endothelial growth factor (VEGF), epidermal growth factor (EGF), insulin-like growth factor-I (IGF-I), fibroblastic growth factor (FGF), and hepatocyte growth factor (HGF). In theory, using PRP to augment meniscus repair appears to be reasonable. Although some orthopedic surgeons have incorporated PRP for meniscus repair in their practice, pre-clinical and clinical data are still lacking. In addition, much of the difficulty in interpreting the effects of PRP is the documented variability of the contents of each specific preparation and that PRP is not a uniform product.

In a study by Ishida et al[86], a gelatin hydrogel scaffold was used as a drug delivery system for growth factors secreted by PRP to enhance the healing of meniscal defects in a rabbit model. The combination of gelatin-PRP was compared to two other groups including platelet-poor plasma (PPP) and control for the intervals of 4, 8 and 12 weeks. Their findings suggested that the combination of hydrogel and PRP supports meniscal cell proliferation and the synthesis of an extracellular matrix, which is rich in glycosaminoglycan. In addition, they found greater mRNA expression of biglycan and decorin. Zellner at al[87] created a circular 2 mm punch meniscal defect in the avascular zone of rabbit meniscus which was then either left empty or treated with biodegradable hyaluronan-collagen composite matrices loaded/seeded with PRP, bone marrow

(BM), BM/mesenchymal stem cells (MSC) pre-cultured in chondrogenic medium (CM) for 2 weeks or BM/MSC without any pre-culture. Their findings illustrated that MSCs appear to be necessary for meniscal healing in repair of punch defect model in rabbit. In line with their previous findings, Zellner et al[88] showed that seeding of MSC on biodegradable hyaluronan-collagen composite matrices, which were pre-cultured in CM produced/generated extensive and organized matrix mimicking native meniscus by better biomechanical integration after 12 weeks of histological/mechanical assessment. In both of the above studies, the groups treated with hyaluronan-collagen composite matrices and PRP did not do better than the empty controls. In another study, Shin et al[89] compared the effect of leukocyte-rich PRP (L-PRP) on healing of the horizontal medial meniscus tears in a rabbit model. The horizontal tear (6 mm in width and 1.5 mm in length) were created in the anterior horn of the medial meniscus and were either injected with L-PRP or left untreated. Histological findings revealed there were no significant differences in quantitative histologic scoring between the two groups at 2, 4, and 6 weeks after surgery. Lee et al[90] created 2 mm full-thickness circular defects in the anterior portion of the inner 2/3rd of the avascular zone of the medial meniscus in rabbits which were filled with fibrin glue or 10% PRP. Upon retrieval after eight weeks, the lesions in both the control and PRP groups were filled with fibrous and fibrillated connective tissue and did not show any meniscal cartilage formation. To our knowledge, there are only a few clinical studies that use PRP application for treatment of meniscal lesions (**APPENDIX A:** Table 4). Pujol et al[91] used PRP to augment repair and promote meniscal healing of horizontal cleavage meniscal tears repaired with an open approach. In this case-control study, 34 young patients underwent either a standard open meniscal repair (n = 17) or the same surgical repair with introduction of PRP in the lesion (n=17). They found that clinical outcome was slightly improved in the PRP group. Griffin et al[92] performed 35 isolated arthroscopic meniscus repairs, 15 of which were augmented with PRP. In contrast to the above-mentioned study, they showed that outcome was similar after meniscus repair without and with PRP. The authors stated that an appropriate larger sample size is needed to elucidate the beneficial effect of PRP.

5.1.5 Augmentation of meniscus repair by wrapping

Meniscus wrapping techniques were first described by Henning who used fascial sheath coverage and exogenous fibrin clot to treat meniscal tears[93,94] (**APPENDIX A:** Table 5). The fibrin clot was believed to act as a scaffold and to also provide chemotactic and mitogenic factors and

stimuli to assist the reparative process. The authors' stated opinion was that the fascia sheath worked by partially encapsulating the meniscus and decreasing the effect of early washout of the exogenous clot injection[94]. The surgical technique involved rasping of the parameniscal synovium, peripheral white rim, and tear surface of the fragment. The meniscus itself was sutured using inside-out technique and then a fascia sheath taken from the distal anterolateral thigh was sutured over the meniscus to cover the repair. Finally, an exogenous fibrin clot was injected under the sheath. Complex tears including double flap, double longitudinal and radial tears all showed improved healing with the addition of the sheath and fibrin clot[93]. Complete or partial healing was seen in 26 of the 31 repairs treated with this technique[94]. However, this technique is considered inadequate for radial tears in the middle portion of the middle one-third of the lateral meniscus[94]. This technique also has the disadvantage of being technically demanding and time-consuming. In 1996, Barrett and Treacy reported that Henning's technique had not been widely adopted partly due to the technical difficulty in securing the sheath around the repaired meniscal tear[95]. Then, they described repair of complex tears in the medial and lateral menisci that involved combining T-fix (Acufex, USA) and inside-out approaches as an improvement to the original technique. The technique consisted of rasping the synovium and the tear, inside-out repair of the meniscus, anchoring and suturing of the fascial sheath using T-fix and inside-out sutures as well as injection of a blood clot under the sheath. They concluded that this technique was much easier than that previously described and suggested that it could be used to improve repair of complex tears. Roland Jakob has been advocating for many years for treating complex human meniscal tears, which otherwise would have a poor clinical probability of healing, with a collagen wrap as an adjunct (personal communication). This meniscus wrapping technique was introduced in 2003 and first used to treat thirty patients that had complex tears, delayed traumatic tears with degenerative aspects, or repeat sutured tears, all in the red-white or white-white zone[96]. In this study, 15 complex tears, 11 bucket-handle and 4 horizontal tears were treated with this technique. The tears in the meniscus were first fixed by preliminary inside-out sutures. Chondro-Gide matrix (Geistlich Pharma, Switzerland) was then introduced through an arthroscopic cannula and multiple sutures were added (up to 10), to complete the fixation of the membrane on the meniscus and the meniscus tear. The porous layer was laid down facing the meniscal defect to favor cell invasion and attachment and allow the in-growth of cells and a newly formed tissue. The compact layer acts as occlusive scaffold with smooth surface to prevent cells from diffusing into the synovial fluid. Three

patients had a symptomatic failure (10%) at mean follow-up of 2.5 years, while all other 27 cases (90%) were asymptomatic. It is believed that the membrane acts as an internal bioreactor or scaffold and attracts cells that are released from the synovial fluid by rasping and bleeding inside the joint. Thus, healing becomes possible even in unfavorable conditions with this technique. Similar to the fascial sheath technique, this procedure is technically demanding and time-consuming.

Meniscus wrapping with a cross-linked Chondro-Gide derivative was similarly used in a pre-clinical study in a goat model[96]. Surgically induced 6 mm horizontal tears in the avascular portion of the meniscus were closed with a single suture introduced with the inside-out technique. The menisci were then wrapped with a collagen membrane and fibrin glue was used to seal the membrane (as a tissue adhesive). In some animals, meniscus wrapping was combined with injection of expanded autologous chondrocytes. Meniscus wrapping by itself improved healing at 3 months compared to suturing alone, but this improved outcome was not observed at the 6-month repair period. Combining the meniscus wrapping and autologous chondrocyte injections improved repair at both 3 month and 6-month time-points. In 2012, Piontek et al reported on the development of a fully arthroscopic wrapping technique to treat meniscal lesions[97]. This arthroscopic method combines suturing techniques with the use of a collagen membrane to wrap the meniscus and the optional application of bone marrow aspirate or concentrate deep to the membrane. In this technique, the tears were first sutured with all-inside FasT-Fix sutures (Smith and Nephew, USA). The meniscus was then wrapped with collagen matrix and bone marrow aspirated from the tibial proximal epiphysis was injected under the matrix into the tears. The authors stated that the technique was technically challenging, but they believed that the use of collagen matrix and addition of bone marrow aspirate will create favourable conditions, which may increase the rate of meniscus healing. The 2-year follow-up data of tears treated with this all arthroscopic suturing and wrapping technique was presented in a subsequent paper[99]. Inclusion criteria for this study included full-thickness tears greater than 20 mm in length, horizontal, radial tears and extensive bucket-handle tears, tears located at greater than 6 mm from the capsular junction including the avascular zone, as well as both degenerative and non-degenerative menisci. Of the 48 cases analyzed, only 2 patients underwent subsequent partial meniscectomy and were considered failures. Subjective and clinical assessment scores were improved at 2 years post-operative in the patients. The authors reported 13 severe adverse events but specified that none of the events were related to the procedure

or material used. They concluded that this technique is safe and promising and can be used by surgeons to repair menisci which would otherwise be removed.

5.1.6 Rationale for using polymer stabilized PRP to augment meniscus repair

Chitosan is a positively charged partially acetylated glucosamine-based polysaccharide that can act as a scaffold and adhere to negatively charged tissue surfaces to mediate tissue repair. Near-neutral solutions of chitosan-glycerol phosphate (GP) can be mixed with whole blood to create hybrid clots[100] that significantly resist retraction[101]. We have previously demonstrated that chitosan-GP/blood clots can be injected over marrow stimulated cartilage defects and yield repair tissues with improved biomechanical and biochemical properties compared to microfracture or microdrilling alone[101,102]. Some of the mechanisms responsible for this improved repair are an increase in inflammatory and marrow-derived stromal cell recruitment to the microdrill holes, increased vascularization and subchondral bone remodeling at early post surgical time-points from day 1 and 56 days when compared with micro drilled control holes[103], polarization of macrophage phenotype towards the alternatively-activated pro-wound healing lineage[104], increased bone remodeling and osteoclast activation leading to better repair tissue integration[105], and stimulated secretion of anabolic wound repair factors from M2a macrophages[106]. More recently, we have developed freeze-dried formulations of chitosan that can be solubilized in PRP to form injectable implants that solidify in situ[107]. These freeze-dried formulations contain chitosan, a lyoprotectant and a clot activator. We found that chitosan molecular size, chitosan concentration, and lyoprotectant concentration control the performance characteristics of these implants and have identified formulations that show promise for meniscus repair. In two pilot studies[108,109], meniscus repair in ovine models was improved by application of freeze-dried chitosan-PRP implants. Chitosan-PRP implants induced cell recruitment to the tears, repair tissue synthesis and remodeling at 3 weeks, 6 weeks and 3 months post-surgery leading to the design of an ongoing pivotal animal study. Chitosan-PRP implants may be able to overcome some of the shortcomings of current augmentation techniques to improve restoration of meniscus structure and function.

5.1.7 Conclusions

Meniscus tears are among the most common knee injuries related to trauma or aging. Understanding of the structure, vascularity, biomechanics and pattern of tears is important and could facilitate the orthopedic surgeon's selection of optimal treatment. Current trends are shifting toward salvaging the meniscus tissue and meniscus repair with good to fair satisfactory long-term outcome. Evidence shows that nonsurgical approaches/management can be successful especially in the short term if tears are not symptomatic. Diverse augmentation techniques have been developed to introduce marrow elements and blood components into the joint to increase healing in the avascular zone of the meniscus. Further development of these approaches and bioactive materials may improve repair of currently irrepairable meniscus tears.

Acknowledgments

This work was supported by the following funding sources: Canadian Institutes of Health Research, Canada Foundation for Innovation, Groupe de Recherche en Sciences et Technologies Biomédicales, Natural Sciences and Engineering Research Council of Canada and Ortho Regenerative Technologies Inc.

Conflict of Interest

AC. and MDB. hold shares; MDB. is a Director and JF.and SR. are clinical advisors or Ortho Renegerative Technologies Inc.

Author Contributions

The authors made substantial contributions in designing the study (LG, AC, JF, SR, and MDB), gathering the data (LG, AC, and MDB) and drafting the article (LG, AC, JF, SR, and MDB). All the authors approved the submitted manuscript.

References

1. McDevitt CA, Webber RJ. The ultrastructure and biochemistry of meniscal cartilage. Clin Orthop Rel Res 1990(252):8-18

2. Messner K, Gao JZ. The menisci of the knee joint. Anatomical and functional characteristics, and a rationale for clinical treatment. Journal of anatomy 1998; 193:161-178

3. Fithian DC, Kelly MA, Mow VC. Material properties and structure-function relationships in the menisci. Clinical Orthopaedics and Related Research 1990(252):19-31

4. Englund M, Guermazi A, Gale D, et al. Incidental meniscal findings on knee MRI in middle-aged and elderly persons. New England Journal of Medicine 2008;359(11):1108-1115

5. Englund M, Guermazi A, Roemer FW, et al. Meniscal Tear in Knees Without Surgery and the Development of Radiographic Osteoarthritis Among Middle-Aged and Elderly Persons The Multicenter Osteoarthritis Study. Arthritis and rheumatism 2009;60(3):831-839

6. Zanetti M, Pfirrmann CWA, Schmid MR, et al. Clinical course of knees with asymptomatic meniscal abnormalities: Findings at 2-year follow-up after MR imaging-based diagnosis. Radiology 2005;237(3):993-997

7. Abrams GD, Frank RM, Gupta AK, et al. Trends in Meniscus Repair and Meniscectomy in the United States, 2005-2011. American Journal of Sports Medicine 2013;41(10):2333-2339

8. Fairbanks TJ. Knee joint changes after meniscectomy. J Bone Joint Surg Br 1948;30(164-70)

9. Cicuttini FM, Forbes A, Wang YY, et al. Rate of knee cartilage loss after partial meniscectomy. J Rheumatol 2002;29(9):1954-1956

10. Englund M, Lohmander LS. Risk factors for symptomatic knee osteoarthritis fifteen to twenty-two years after meniscectomy. Arthritis and rheumatism 2004;50(9):2811-2819

11. Arnoczky SP, Warren RF. The microvasculature of the meniscus and its response to injury. An experimental study in the dog. The American journal of sports medicine 1983;11(3):131-141

12. Arnoczky SP, Warren RF. Microvasculature of the human meniscus. The American journal of sports medicine 1982;10(2):90-95

13. Chevrier A, Nelea M, Hurtig MB, et al. Meniscus Structure in Human, Sheep, and Rabbit for Animal Models of Meniscus Repair. Journal of Orthopaedic Research 2009;27(9):1197-1203

14. Cannon WD, Jr., Vittori JM. The incidence of healing in arthroscopic meniscal repairs in anterior cruciate ligament-reconstructed knees versus stable knees. The American journal of sports medicine 1992;20(2):176-181

15. Angel MJ, Kerker J, Sgaglione N. Meniscus repair and future directions. In: McKeon BP, Bono JV, Richmond JC, eds. Knee arthroscopy. New York, NY, USA: Springer Science+Business Media; 2009:25-40

16. Pereira H, Cengiz IF, Correia JS, et al. Meniscal Repair: Indications, Techniques, and Outcome. In: Randelli P, Dejour D, van Dijk CN, Denti M, Seil R, eds. Arthroscopy, Basic to Advanced.Luxembourg: Springer; 2016:125-142

17. Nepple JJ, Dunn WR, Wright RW. Meniscal repair outcomes at greater than five years: a systematic literature review and meta-analysis. The Journal of bone and joint surgery American volume 2012;94(24):2222-2227

18. Pujol N, Panarella L, Selmi TAS, et al. Meniscal healing after meniscal repair - A CT arthrography assessment. American Journal of Sports Medicine 2008;36(8):1489-1495

19. Gallacher PD, Gilbert RE, Kanes G, et al. White on white meniscal tears to fix or not to fix? The Knee 2010;17(4):270-273

20. Clayton RAE, Court-Brown CM. The epidemiology of musculoskeletal tendinous and ligamentous injuries. Injury-International Journal of the Care of the Injured 2008;39(12):1338-1344

21. Widuchowski W, Widuchowski J, Trzaska T. Articular cartilage defects: Study of 25,124 knee arthroscopies. The Knee 2007;14(3):177-182

22. Kim S, Bosque J, Meehan JP, et al. Increase in Outpatient Knee Arthroscopy in the United States: A Comparison of National Surveys of Ambulatory Surgery, 1996 and 2006. Journal of Bone and Joint Surgery-American Volume 2011;93A(11):994-1000

23. Snoeker BA, Bakker EW, Kegel CA, et al. Risk factors for meniscal tears: a systematic review including meta-analysis. The Journal of orthopaedic and sports physical therapy 2013;43(6):352-367

24. Scotti C, Hirschmann MT, Antinolfi P, et al. Meniscus repair and regeneration: Review on current methods and research potential. European cells & materials 2013; 26:150-170

25. Chung KS, Ha JK, Ra HJ, et al. Prognostic Factors in the Midterm Results of Pullout Fixation for Posterior Root Tears of the Medial Meniscus. Arthroscopy: the journal of arthroscopic & related surgery: official publication of the Arthroscopy Association of North America and the International Arthroscopy Association 2016;32(7):1319-1327

26. Moatshe G, Chahla J, Slette E, et al. Posterior meniscal root injuries. Acta orthopaedica 2016;87(5):452-458

27. Chahla J, Dean CS, Moatshe G, et al. Meniscal Ramp Lesions: Anatomy, Incidence, Diagnosis, and Treatment. Orthopaedic journal of sports medicine 2016;4(7):2325967116657815

28. Thaunat M, Fayard JM, Guimaraes TM, et al. Classification and Surgical Repair of Ramp Lesions of the Medial Meniscus. Arthroscopy techniques 2016;5(4): e871-e875

29. Hutchinson ID, Moran CJ, Potter HG, et al. Restoration of the Meniscus Form and Function. American Journal of Sports Medicine 2014;42(4):987-998

30. van de Graaf VA, Wolterbeek N, Mutsaerts EL, et al. Arthroscopic Partial Meniscectomy or Conservative Treatment for Nonobstructive Meniscal Tears: A Systematic Review and Meta-analysis of Randomized Controlled Trials. Arthroscopy: the journal of arthroscopic & related surgery: official publication of the Arthroscopy Association of North America and the International Arthroscopy Association 2016;32(9):1855-1865

31. Khan M, Evaniew N, Bedi A, et al. Arthroscopic surgery for degenerative tears of the meniscus: a systematic review and meta-analysis. Canadian Medical Association Journal 2014;186(14):1057-1064

32. Mezhov V, Teichtahl AJ, Strasser R, et al. Meniscal pathology - the evidence for treatment. Arthritis Research & Therapy 2014;16(2)

33. Monk P, Garfjeld Roberts P, Palmer AJ, et al. The Urgent Need for Evidence in Arthroscopic Meniscal Surgery: A Systematic Review of the Evidence for Operative Management of Meniscal Tears. The American journal of sports medicine 2016

34. Noyes FR, Barber-Westin SD. Meniscus Tears: Diagnosis, Repair Techniques, and Clinical Outcomes In: Noyes FR, ed. Noye's knee disorders: Surgery, rehabilitation, clinical outcomes.USA: Saunders, an imprint of Elsevier Inc.; 2010:733-771

35. Katz LM, Weitzel PP. Partial meniscectomy. In: McKeon BP, Bono JV, Richmond JC, eds. Knee arthroscopy.USA: Springer; 2009:11-23

36. Kurzweil PR, Lynch NM, Coleman S, et al. Repair of Horizontal Meniscus Tears: A Systematic Review. Arthroscopy: the journal of arthroscopic & related surgery : official publication of the Arthroscopy Association of North America and the International Arthroscopy Association 2014;30(11):1513-1519

37. Moulton SG, Bhatia S, Civitarese DM, et al. Surgical Techniques and Outcomes of Repairing Meniscal Radial Tears: A Systematic Review. Arthroscopy: the journal of arthroscopic & related surgery : official publication of the Arthroscopy Association of North America and the International Arthroscopy Association 2016;32(9):1919-1925

38. Rubman MH, Noyes FR, Barber-Westin SD. Arthroscopic repair of meniscal tears that extend into the avascular zone - A review of 198 single and complex tears. American Journal of Sports Medicine 1998;26(1):87-95

39. Steadman JR, Matheny LM, Singleton SB, et al. Meniscus suture repair: minimum 10-year outcomes in patients younger than 40 years compared with patients 40 and older. The American journal of sports medicine 2015;43(9):2222-2227

40. Cavanaugh JT, Killian SE. Rehabilitation following meniscal repair. Current reviews in musculoskeletal medicine 2012;5(1):46-58

41. Bryant D, Dill J, Litchfield R, et al. Effectiveness of bioabsorbable arrows compared with inside-out suturing for vertical, reparable meniscal lesions: a randomized clinical trial. The American journal of sports medicine 2007;35(6):889-896

42. Albrecht-Olsen P, Kristensen G, Burgaard P, et al. The arrow versus horizontal suture in arthroscopic meniscus repair - A prospective randomized study with arthroscopic evaluation. Knee Surgery Sports Traumatology Arthroscopy 1999;7(5):268-273

43. Barber FA, Johnson DH, Halbrecht JL. Arthroscopic meniscal repair using the BioStinger. Arthroscopy: the journal of arthroscopic & related surgery: official publication of the Arthroscopy Association of North America and the International Arthroscopy Association 2005;21(6):744-750

44. Choi NH, Kim TH, Victoroff BN. Comparison of arthroscopic medial meniscal suture repair techniques: inside-out versus all-inside repair. The American journal of sports medicine 2009;37(11):2144-2150

45. Spindler KP, McCarty EC, Warren TA, et al. Prospective comparison of arthroscopic medial meniscal repair technique: inside-out suture versus entirely arthroscopic arrows. The American journal of sports medicine 2003;31(6):929-934

46. Saliman JD. The circumferential compression stitch for meniscus repair. Arthroscopy techniques 2013;2(3): e257-264

47. Fillingham YA, Riboh JC, Erickson BJ, et al. Inside-Out Versus All-Inside Repair of Isolated Meniscal Tears: An Updated Systematic Review. The American journal of sports medicine 2016

48. Lozano J, Ma CB, Cannon WD. All-inside meniscus repair: a systematic review. Clinical Orthopaedics and Related Research 2007; 455:134-141

49. Westermann RW, Duchman KR, Amendola A, et al. All-Inside Versus Inside-Out Meniscal Repair with Concurrent Anterior Cruciate Ligament Reconstruction: A Meta-regression Analysis. The American journal of sports medicine 2016

50. Grant JA, Wilde J, Miller BS, et al. Comparison of Inside-Out and All-Inside Techniques for the Repair of Isolated Meniscal Tears A Systematic Review. American Journal of Sports Medicine 2012;40(2):459-468

51. Mutsaerts EL, van Eck CF, van de Graaf VA, et al. Surgical interventions for meniscal tears: a closer look at the evidence. Archives of orthopaedic and trauma surgery 2016;136(3):361-370

52. Biedert RM. Treatment of intrasubstance meniscal lesions: a randomized prospective study of four different methods. Knee Surgery Sports Traumatology Arthroscopy 2000;8(2):104-108

53. Stein T, Mehling AP, Welsch F, et al. Long-term outcome after arthroscopic meniscal repair versus arthroscopic partial meniscectomy for traumatic meniscal tears. The American journal of sports medicine 2010;38(8):1542-1548

54. Shelbourne KD, Dersam MD. Comparison of partial meniscectomy versus meniscus repair for bucket-handle lateral meniscus tears in anterior cruciate ligament reconstructed knees. Arthroscopy: the journal of arthroscopic & related surgery : official publication of the Arthroscopy Association of North America and the International Arthroscopy Association 2004;20(6):581-585

55. Lutz C, Dalmay F, Ehkirch FP, et al. Meniscectomy versus meniscal repair: 10 years radiological and clinical results in vertical lesions in stable knee. Orthopaedics & traumatology, surgery & research : OTSR 2015;101(8 Suppl):S327-331

56. Xu C, Zhao J. A meta-analysis comparing meniscal repair with meniscectomy in the treatment of meniscal tears: the more meniscus, the better outcome. Knee Surgery Sports Traumatology Arthroscopy 2015;23(1):164-170

57. Paxton ES, Stock MV, Brophy RH. Meniscal Repair Versus Partial Meniscectomy: A Systematic Review Comparing Reoperation Rates and Clinical Outcomes. Arthroscopy-the Journal of Arthroscopic and Related Surgery 2011;27(9):1275-1288

58. Westermann RW, Wright RW, Spindler KP, et al. Meniscal Repair With Concurrent Anterior Cruciate Ligament Reconstruction Operative Success and Patient Outcomes at 6-Year Follow-up. American Journal of Sports Medicine 2014;42(9):2184-2192

59. Zhang ZN, Tu KY, Xu YK, et al. Treatment of longitudinal injuries in avascular area of meniscus in dogs by trephination. Arthroscopy: the journal of arthroscopic & related surgery : official publication of the Arthroscopy Association of North America and the International Arthroscopy Association 1988;4(3):151-159

60. Zhang Z, Arnold JA, Williams T, et al. Repairs by trephination and suturing of longitudinal injuries in the avascular area of the meniscus in goats. The American journal of sports medicine 1995;23(1):35-41

61. Cook JL, Fox DB. A novel bioabsorbable conduit augments healing of avascular meniscal tears in a dog model. American Journal of Sports Medicine 2007;35(11):1877-1887

62. Fox JM, Rintz KG, Ferkel RD. Trephination of incomplete meniscal tears. Arthroscopy : the journal of arthroscopic & related surgery : official publication of the Arthroscopy Association of North America and the International Arthroscopy Association 1993;9(4):451-455

63. Zhang ZN, Arnold JA. Trephination and suturing of avascular meniscal tears: A clinical study of the trephination procedure. Arthroscopy: the journal of arthroscopic & related surgery : official publication of the Arthroscopy Association of North America and the International Arthroscopy Association 1996;12(6):726-731

64. Shelbourne KD, Rask BP. The sequelae of salvaged nondegenerative peripheral vertical medial meniscus tears with anterior cruciate ligament reconstruction. Arthroscopy : the journal of arthroscopic & related surgery : official publication of the Arthroscopy Association of North America and the International Arthroscopy Association 2001;17(3):270-274

65. Shelbourne KD, Benner RW, Nixon RA, et al. Evaluation of Peripheral Vertical Nondegenerative Medial Meniscus Tears Treated with Trephination Alone at the Time of Anterior Cruciate Ligament Reconstruction. Arthroscopy-the Journal of Arthroscopic and Related Surgery 2015;31(12):2411-2416

66. Okuda K, Ochi M, Shu N, et al. Meniscal rasping for repair of meniscal tear in the avascular zone. Arthroscopy : the journal of arthroscopic & related surgery : official publication of the Arthroscopy Association of North America and the International Arthroscopy Association 1999;15(3):281-286

67. Ochi M, Uchio Y, Okuda K, et al. Expression of cytokines after meniscal rasping to promote meniscal healing. Arthroscopy: the journal of arthroscopic & related surgery: official publication of the Arthroscopy Association of North America and the International Arthroscopy Association 2001;17(7):724-731

68. Uchio Y, Ochi M, Adachi N, et al. Results of rasping of meniscal tears with and without anterior cruciate ligament injury as evaluated by second-look arthroscopy. Arthroscopy: the journal of arthroscopic & related surgery : official publication of the Arthroscopy Association of North America and the International Arthroscopy Association 2003;19(5):463-469

69. Tetik O, Kocabey Y, Johnson DL. Synovial abrasion for isolated, partial thickness, undersurface, medial meniscus tears. Orthopedics 2002;25(6):675-678

70. Talley MC, Grana WA. Treatment of partial meniscal tears identified during anterior cruciate ligament reconstruction with limited synovial abrasion. Arthroscopy: the journal of arthroscopic & related surgery: official publication of the Arthroscopy Association of North America and the International Arthroscopy Association 2000;16(1):6-10

71. Freedman KB, Nho SJ, Cole BJ. Marrow stimulating technique to augment meniscus repair. Arthroscopy : the journal of arthroscopic & related surgery : official publication of the Arthroscopy Association of North America and the International Arthroscopy Association 2003;19(7):794-798

72. Ishimura M, Ohgushi H, Habata T, et al. Arthroscopic meniscal repair using fibrin glue. Part I: Experimental study. Arthroscopy: the journal of arthroscopic & related surgery: official publication of the Arthroscopy Association of North America and the International Arthroscopy Association 1997;13(5):551-557

73. Ishimura M, Tamai S, Fujisawa Y. Arthroscopic meniscal repair with fibrin glue. Arthroscopy : the journal of arthroscopic & related surgery : official publication of the Arthroscopy Association of North America and the International Arthroscopy Association 1991;7(2):177-181

74. Ishimura M, Ohgushi H, Habata T, et al. Arthroscopic meniscal repair using fibrin glue. Part II: Clinical applications. Arthroscopy: the journal of arthroscopic & related surgery: official publication of the Arthroscopy Association of North America and the International Arthroscopy Association 1997;13(5):558-563

75. Ritchie JR, Miller MD, Bents RT, et al. Meniscal repair in the goat model. The use of healing adjuncts on central tears and the role of magnetic resonance arthrography in repair evaluation. The American journal of sports medicine 1998;26(2):278-284

76. Port J, Jackson DW, Lee TQ, et al. Meniscal repair supplemented with exogenous fibrin clot and autogenous cultured marrow cells in the goat model. American Journal of Sports Medicine 1996;24(4):547-555

77. Nakhostine M, Gershuni DH, Danzig LA. Effects of an in-substance conduit with injection of a blood clot on tears in the avascular region of the meniscus. Acta orthopaedica Belgica 1991;57(3):242-246

78. van Trommel MF, Simonian PT, Potter HG, et al. Arthroscopic meniscal repair with fibrin clot of complete radial tears of the lateral meniscus in the avascular zone. Arthroscopy: the journal of arthroscopic & related surgery: official publication of the Arthroscopy Association of North America and the International Arthroscopy Association 1998;14(4):360-365

79. Jang SH, Ha JK, Lee DW, et al. Fibrin clot delivery system for meniscal repair. Knee surgery & related research 2011;23(3):180-183

80. Ra HJ, Ha JK, Jang SH, et al. Arthroscopic inside-out repair of complete radial tears of the meniscus with a fibrin clot. Knee Surgery Sports Traumatology Arthroscopy 2013;21(9):2126-2130

81. Kamimura T, Kimura M. Repair of horizontal meniscal cleavage tears with exogenous fibrin clots. Knee Surgery Sports Traumatology Arthroscopy 2011;19(7):1154-1157

82. Kamimura T, Kimura M. Meniscal Repair of Degenerative Horizontal Cleavage Tears Using Fibrin Clots: Clinical and Arthroscopic Outcomes in 10 Cases. Orthopaedic journal of sports medicine 2014;2(11):2325967114555678

83. Sethi PM, Cooper A, Jokl P. Technical tips in orthopaedics: Meniscal repair with use of an in situ fibrin clot. Arthroscopy : the journal of arthroscopic & related surgery : official publication of the Arthroscopy Association of North America and the International Arthroscopy Association 2003;19(5):E44

84. Andia I, Maffulli N. Platelet-rich plasma for managing pain and inflammation in osteoarthritis. Nature Reviews Rheumatology 2013;9(12):721-730

85. Braun HJ, Wasterlain AS, Dragoo JL. The Use of PRP in Ligament and Meniscal Healing. Sports Med Arthr Rev 2013;21(4):206-212

86. Ishida K, Kuroda R, Miwa M, et al. The regenerative effects of platelet-rich plasma on meniscal cells in vitro and its in vivo application with biodegradable gelatin hydrogel. Tissue engineering 2007;13(5):1103-1112

87. Zellner J, Mueller M, Berner A, et al. Role of mesenchymal stem cells in tissue engineering of meniscus. Journal of Biomedical Materials Research Part A 2010;94A (4):1150-1161

88. Zellner J, Hierl K, Mueller M, et al. Stem cell-based tissue-engineering for treatment of meniscal tears in the avascular zone. Journal of Biomedical Materials Research Part B: Applied Biomaterials 2013;101(7):1133-1142

89. Shin KH, Lee H, Kang S, et al. Effect of Leukocyte-Rich and Platelet-Rich Plasma on Healing of a Horizontal Medial Meniscus Tear in a Rabbit Model. BioMed research international 2015;2015:179756

90. Lee HR, Shon OJ, Park SI, et al. Platelet-Rich Plasma Increases the Levels of Catabolic Molecules and Cellular Dedifferentiation in the Meniscus of a Rabbit Model. International journal of molecular sciences 2016;17(1):E120

91. Pujol N, De Chou ES, Boisrenoult P, et al. Platelet-rich plasma for open meniscal repair in young patients: Any benefit? Knee Surgery Sports Traumatology Arthroscopy 2015;23(1):51-58

92. Griffin JW, Hadeed MM, Werner BC, et al. Platelet-rich Plasma in Meniscal Repair: Does Augmentation Improve Surgical Outcomes? Clinical Orthopaedics and Related Research 2015;473(5):1665-1672

93. Henning CE, Lynch MA, Yearout KM, et al. Arthroscopic meniscal repair using an exogenous fibrin clot. Clinical Orthopaedics and Related Research 1990(252):64-72

94. Henning CE, Yearout KM, Vequist SW, et al. Use of the fascia sheath coverage and exogenous fibrin clot in the treatment of complex meniscal tears. American Journal of Sports Medicine 1991;19(6):626-631

95. Barrett GR, Treacy SH. Use of the T-Fix suture anchor in fascial sheath reconstruction of complex meniscal tears. Arthroscopy: the journal of arthroscopic & related surgery: official publication of the Arthroscopy Association of North America and the International Arthroscopy Association 1996;12(2):251-255

96. Jacobi M, Jakob RP. Meniscal Repair: Enhancement of Healing Process. In: Beaufils P, Verdonk R, eds. The Meniscus.London New York: Springer-Verlag Berlin Heidelberg; 2010

97. Julke H, Mainil-Varlet P, Jakob RP, et al. The Role of Cells in Meniscal Guided Tissue Regeneration: A Proof of Concept Study in a Goat Model. Cartilage 2015;6(1):20-29

98. Piontek T, Ciemniewska-Gorzela K, Szulc A, et al. All-arthroscopic technique of biological meniscal tear therapy with collagen matrix. Polish Orthopedics and Traumatology 2012; 77:39-45

99. Piontek T, Ciemniewska-Gorzela K, Naczk J, et al. Complex meniscus tears treated with collagen matrix wrapping and bone marrow blood injection: a 2-year clinical follow-up. Cartilage 2016;7(2):123-139

100. Iliescu M, Hoemann CD, Shive MS, et al. Ultrastructure of hybrid chitosan-glycerol phosphate blood clots by environmental scanning electron Microscopy. Microscopy Research and Technique 2008;71(3):236-247

101. Hoemann CD, Sun J, McKee MD, et al. Chitosan-glycerol phosphate/blood implants elicit hyaline cartilage repair integrated with porous subchondral bone in microdrilled rabbit defects. Osteoarthritis and Cartilage 2007;15(1):78-89

102. Hoemann CD, Hurtig M, Rossomacha E, et al. Chitosan-glycerol phosphate/blood implants improve hyaline cartilage repair in ovine microfracture defects. Journal of Bone and Joint Surgery-American Volume 2005;87A(12):2671-2686

103. Chevrier A, Hoemann CD, Sun J, et al. Chitosan-glycerol phosphate/blood implants increase cell recruitment, transient vascularization and subchondral bone remodeling in drilled cartilage defects. Osteoarthritis and Cartilage 2007;15(3):316-327

104. Hoemann CD, Chen G, Marchand C, et al. Scaffold-Guided Subchondral Bone Repair Implication of Neutrophils and Alternatively Activated Arginase-1+Macrophages. American Journal of Sports Medicine 2010;38(9):1845-1856

105. Chen G, Sun J, Lascau-Coman V, et al. Acute Osteoclast Activity following Subchondral Drilling Is Promoted by Chitosan and Associated with Improved Cartilage Repair Tissue Integration. Cartilage 2011;2(2):173-185

106. Fong D, Ariganello MB, Girard-Lauziere J, et al. Biodegradable chitosan microparticles induce delayed STAT-1 activation and lead to distinct cytokine responses in differentially polarized human macrophages in vitro. Acta biomaterialia 2015; 12:183-194

107. Chevrier A, Darras V, Picard G, et al. Injectable chitosan-platelet-rich plasma (PRP) implants to promote tissue regeneration: In vitro properties, in vivo residence, degradation, cell

recruitment and vascularization. Journal of tissue engineering and regenerative medicine 2017; In press

108. Chevrier A, Deprés-Tremblay G, Hurtig MB, et al. Chitosan-platelet-rich plasma implants can be injected into meniscus defects to improve repair. Paper presented at: Orthopaedic Research Society; March 5th-8th, 2016; Orlando, FL, USA.

109. Ghazi zadeh L, Chevrier A, Hurtig MB, et al. Freeze-dried chitosan-PRP implants improve meniscus repair in an ovine model. Paper presented at: International Cartilage Repair Society; September 24th-27th, 2016; Sorrento, Italy.

110. Mordecai SC, Al-Hadithy N, Ware HE, et al. Treatment of meniscal tears: An evidence based approach. World journal of orthopedics 2014;5(3):233-241

111. Kise NJ, Drogset JO, Ekeland A, et al. All-inside suture device is superior to meniscal arrows in meniscal repair: a prospective randomized multicenter clinical trial with 2-year follow-up. Knee surgery, sports traumatology, arthroscopy: official journal of the ESSKA 2015;23(1):211-218

112. Hantes ME, Zachos VC, Varitimidis SE, et al. Arthroscopic meniscal repair: a comparative study between three different surgical techniques. Knee Surgery Sports Traumatology Arthroscopy 2006;14(12):1232-1237

113. Jarvela S, Sihvonen R, Sirkeoja H, et al. All-Inside Meniscal Repair with Bioabsorbable Meniscal Screws or With Bioabsorbable Meniscus Arrows A Prospective, Randomized Clinical Study With 2-Year Results. American Journal of Sports Medicine 2010;38(11):2211-2217

114. Shelbourne KD, Heinrich J. The long-term evaluation of lateral meniscus tears left in situ at the time of anterior cruciate ligament reconstruction. Arthroscopy: the journal of arthroscopic & related surgery: official publication of the Arthroscopy Association of North America and the International Arthroscopy Association 2004;20(4):346-351

CHAPTER 6 ARTICLE 2: FREEZE-DRIED CHITOSAN-PRP INJECTABLE SURGICAL IMPLANTS FOR MENISCUS REPAIR: PILOT FEASIBILITY STUDIES IN OVINE MODELS

(Journal of Regenerative Medicine and Therapeutics-The Scientific Page)

Ghazi zadeh L[1], Chevrier A[2], Hurtig MB[3], Farr J[4], Rodeo S[5], Hoemann CD[6], and Buschmann MD[7]

[1]Biomedical Engineering Institute, Polytechnique Montreal, Montreal, QC, Canada, leili.ghazi-zadeh@polymtl.ca. [2]Chemical Engineering Department, Polytechnique Montreal, Montreal, QC, Canada, anik.chevrier@polymtl.ca. [3]Department of Clinical Studies, University of Guelph, Guelph, ON, Canada, mark.hurtig@gmail.com. [4]OrthoIndy Knee Care Institute and Cartilage Restoration Center of Indiana, Greenwood, IL, USA, indyknee@hotmail.com. [5]Sports Medicine and Shoulder Service, The Hospital for Special Surgery, New York, NY, USA, rodeos@hss.edu. [6]Biomedical Engineering Institute and Chemical Engineering Department, Polytechnique Montreal, Montreal, QC, Canada, caroline.hoemann@polymtl.ca. [7]Biomedical Engineering Institute and Chemical Engineering Department, Polytechnique Montreal, Montreal, QC, Canada, michael.buschmann@polymtl.ca

Corresponding author: Prof Michael D. Buschmann, Biomedical Engineering Institute and Chemical Engineering Department, Polytechnique Montreal, PO Box 6079 Succ Centre-Ville, Montreal, Quebec, Canada, H3C 3A7, Tel: 514-340-4711 ext. 4931, Fax: 514-340-2980, E-mail: michael.buschmann@polymtl.ca.

Abstract

Clinical management of meniscus tears often involves partial meniscectomy, which can lead to osteoarthritis (OA). Meniscus repair augmentation strategies are being developed to compensate for the tissue's limited healing response. The purpose of the study was to assess the feasibility of using implants composed of freeze-dried chitosan (CS) solubilized in platelet-rich plasma (PRP) to improve meniscus repair in ovine models. Lyophilized formulations containing 1% (w/v) chitosan (degree of deacetylation 82% and number average molar mass 38 kDa), 1% (w/v) trehalose and 42.2 mM calcium chloride were solubilized in autologous PRP and applied to surgically induced meniscus lacerations. In the first study, bilateral tears in 7 ewes were treated by suturing, trephination and injecting either CS-PRP (10 knees) or PRP (4 knees) into the tears. In the second study, unilateral tears in 6 ewes were treated by suturing, trephination and injecting CS-PRP in the tears (2 knees), wrapping the meniscus with a collagen membrane and injecting CS-PRP in the tears and under the wrap (2 knees) or wrapping only (2 knees). CS-PRP implants were partly resident in the tears and trephination channels at 1 day, where they induced cell recruitment from the vascularized periphery of the menisci. Complete repair and seamless repair tissue integration were observed in 1 out of 4 CS-PRP treated defects in the first study after 3 months and in 1 out of 2 CS-PRP treated defects in the second study after 6 weeks, while there was no healing with PRP or wrapping alone. These pilot feasibility studies demonstrated that CS-PRP injectable implants display some potential to improve meniscus repair outcomes in pre-clinical models and could overcome some of the current limitations of meniscus repair by assisting in restoring meniscus structure and function.

Keywords

Meniscus repair, chitosan, platelet-rich plasma, injectable implants, ovine models

Level of evidence: Exprimental work

Disclaimer: None

6.1 Introduction

Menisci play a critical role in shock absorption and joint stability[1]. A meniscal tear is one of the most common orthopaedic diagnoses[2] and treatment for meniscal tears account for nearly half of arthroscopic knee procedures performed in the US[3]. Tear characteristics (e.g., tear pattern, length, depth, size, stability of tear, age of tear, chronicity, and reducibility of tear) and patient-related factors (e.g., general health, age, and compliance) all affect the rate of healing and determine the most appropriate treatment for a given patient[4]. Although there has been a recent slight increase in the number of meniscus repairs performed yearly[5], the percentage of meniscal tears that are considered repairable using existing surgical techniques remains small, and thus the vast majority of tears are excised with partial meniscectomy. Clinical follow-up studies have demonstrated that the risk of developing osteoarthritis (OA) is increased in patients with untreated meniscal damage or meniscectomized knees[6-8].

The outer 10-30% of the adult meniscus is vascularised[9], giving rise to the clinical labeling of different zones. Vascularity of the meniscus is a prime determinant for the endogenous repair response, and longitudinal tears located in the vascularized red/red portion of the meniscus are considered good candidates for repair. Repair potential is more limited in the inner white/white portion due to a decreased vascular network and a low density of meniscal chondrocytes that fail to migrate to induce a repair response. Several repair augmentation approaches have been proposed in order to stimulate the meniscus healing response to facilitate clinical success[10,11]. These include mechanical stimulation techniques such as trephination, insertion of a duct, abrasion and rasping[12-15], use of patch or scaffold materials[16], and application of blood clots or blood-derived components[117-19]. Although some studies have reported promising findings, there remains a lack of high-level evidence to support the use of one augmentation technique over another.

Chitosan is a linear, natural cationic polymer composed of glucosamine and N-acetyl-glucosamine units that has been used for tissue repair and regeneration[20]. Our laboratory has worked extensively with chitosan for cartilage repair applications[21-24]. Chitosan-glycerol phosphate (GP) solutions can be mixed with whole blood and applied to microfractured cartilage defects to augment repair[21-24] and is now approved for clinical use to treat cartilage lesions in several countries (BST-CarGel®, Smith and Nephew, USA). Some of the mechanisms responsible for this improved outcome have been elucidated in laboratory and animal studies and include an

increase in cell recruitment and vascularization, as well as a polarization of the macrophage phenotype towards the alternatively-activated pro-wound healing lineage and stimulated secretion of anabolic wound repair factors[25-27], all of which are also expected to be beneficial in the context of meniscus repair. More recently, we have developed freeze-dried formulations of chitosan (CS) that can be solubilized in platelet-rich plasma (PRP) to form injectable CS-PRP implants for tissue repair[28]. Lyophilization is expected to provide long-term stability to the product, while PRP constitutes an autologous source of platelet-derived factors and can solubilize lyophilized chitosan for delivery to the wound site to improve repair. In contrast to PRP implants which were rapidly cleared *in vivo* and had little bioactivity, these CS-PRP implants were shown to reside for several weeks and induce vascularization and cell recruitment[28] in a subcutaneous implantation model, both of which are desirable in the context of meniscus repair.

Here we describe two sequential pilot feasibility studies, where we tested the effect of CS-PRP implants in ovine meniscus repair models. In the first study, a bilateral longitudinal surgical laceration model was used to test the hypothesis that meniscus repair is improved by the application of CS-PRP to the tears, but not by application of PRP alone, due to the latter's short-term residency that limits its influence on wound repair, that takes place over several weeks. In the second study, we created a unilateral complex laceration model that was treated with one of 3 approaches; the tears were treated with the CS-PRP implant, or the tears were treated with a wrapping technique using a Geistlich collagen membrane, or the tears were treated with both CS-PRP and the wrapping technique. Our original hypothesis for the second pilot study was that repair outcomes would be improved by using CS-PRP implants in conjunction with the wrapping technique over CS-PRP implants injected in the tear site alone or wrapping alone, due to an increased implant retention and resulting bioactivity. Repair was assessed with histological and electromechanical methods at 3 weeks, 6 weeks and 3 months post-surgery.

6.2 Materials and methods

6.2.1 Preparation of freeze-dried chitosan (FD-CS) formulations

Chitosan (Raw material purchased from Marinard) was processed in-house and the medical-grade polymer was characterized for its degree of deacetylation (DDA) and molar mass

by NMR spectroscopy and analytical size exclusion chromatography/multi-angle laser light scattering[29,30], respectively. Chitosans with number average molar mass (M_n) of 38 ± 4 kDa and DDA 82 ± 3 % were dissolved in 29 mM HCl overnight at room temperature. Then, a lyoprotectant and a clot activator were added to obtain formulations with final concentrations of 1% (w/v) chitosan, 1% (w/v) trehalose dihydrate and 42.2 mM calcium chloride. This particular formulation was chosen based on our previous work[28] because it met the following performance criteria: 1) Rapid and complete solubilization in PRP; 2) Paste-like properties of the CS-PRP material and fast coagulation; 3) Production of homogenous CS-PRP implants that resist platelet-mediated clot retraction; 4) Significant bioactivity *in vivo* with associated cell recruitment and pro-angiogenic potential. The solutions were sterilized with a 0.22 µm polyvinylidene difluoride filter and dispensed in individual sterile glass vials (1-mL per vial) for freeze-drying. The freeze-drying process was divided into 3 phases: 1) ramped freezing to -40°C in 1 hour, isothermal for 2 hours at -40°C (without applying vacuum), 2) -40°C for 48 hours, at 100 millitorrs, 3) ramped heating to 30°C in 12 hours, isothermal for 6 hours at 30°C, at 100 millitorrs. Filter-sterile rhodamine-chitosan tracer[31] of M_n 40 kDa was added to the vials that were used for imaging purposes at 1 day post-surgery.

6.2.2 Isolation of platelet-rich plasma (PRP)

On the day of surgery, sodium citrate anti-coagulated whole blood was collected from each sheep and centrifuged with the ACE EZ-PRP system at 160 g for 10 minutes. The supernatant fraction, buffy coat and top ~ 1 mm of the erythrocyte fraction were moved to another tube and then centrifuged again at 400 g for 10 minutes. Following the second centrifugation step, the supernatant fraction was removed and only the bottom ~ 1.5 mL fraction of the tube was kept and resuspended to extract leukocyte-platelet-rich plasma (L-PRP containing leukocytes and a small fraction of erythrocytes). On average, the PRP contained 488±359 X 10E9/L platelets; 1.6±1.2 X 10E12/L erythrocytes; and 5.5±3.4 X 10E9/L leukocytes.

6.2.3 Experimental study design and surgical technique

Institutional animal care committee approvals were obtained for all experiments involving animals, consistent with Canadian Council on Animal Care guidelines. Surgery was conducted under general anesthesia using aseptic technique. Texel-cross ewes aged 2-6-year-old with body weights 55-70 kg were used in the first study (n=7) and in the second study (n=6).

In the first study (**Figure 6.1**), the joints were opened using a ~ 1.5 cm-long anteromedial arthrotomy to allow access to the anterior portion of the medial meniscus. Bilateral 10-mm long full-thickness longitudinal lacerations were created with scalpel blade and rasped with curved Kelly hemostatic forceps. Two trephination channels were created by inserting 18-gauge needles from the meniscocapsular border to the tears. Freeze-dried chitosan cakes (1 mL) were solubilized with 1 mL autologous PRP and 0.5 mL of CS-PRP was injected into the tears through the two 18-gauge needles (**Figure 6.1**). CS-PRP implants have previously been shown to be paste- like and to coagulate within 5 minutes, much more rapidly than recalcified PRP[28]. The tears were secured using two prolene^{TM} sutures in a horizontal mattress pattern 5 minutes after injection. Controls were injected with 0.5 mL of autologous PRP recalcified with 42.2 mM calcium chloride. Acute implant residency was assessed in 1 sheep at 1 day (n=2 CS-PRP treated knees). Repair was assessed at 3 weeks and at 3 months (n=4 CS-PRP treated knees and n=2 PRP treated knees at each time-point).

In the second study (**Figure 6.2**), the joints were opened using a ~ 1.5 cm-long anteromedial arthrotomy and greater exposure of the medial compartment was achieved by releasing the medial collateral ligament (MCL) with an attached bone block[32]. A custom-designed 10-mm titanium tool was used to punch out unilateral 10-mm longitudinal lacerations in the anterior portion of the medial meniscus. A sharp scalpel blade was then used to ensure that the tears were full-thickness and to create a 3-mm horizontal pocket from the tears towards the capsular border to introduce a horizontal component and create a complex T-shaped defect[33]. The tears were then rasped, and two 20-gauge needles were inserted to create trephination channels from the meniscocapsular border to the tear. Freeze-dried chitosan cakes (1 mL) were solubilized with 1 mL autologous PRP and 0.5 mL chitosan-PRP mixture total was injected into the tears through the two 20-gauge needles. Three prolene ^{TM} sutures were placed in a vertical pattern to stabilize the meniscus tears and sutures were tightened immediately after implant injection. A 12.5 X 25 mm piece of collagen

membrane (Chondro-Gide, Geistlich Pharma) was wrapped around the meniscus and sutured first at the meniscus capsular border, and then further secured by introducing two vertical sutures through the membrane and meniscal tissue. 0.5 mL chitosan-PRP mixture was injected under the membrane (**Figure 6.2**) and the bone block was reattached with a screw. The tears were treated by suturing, trephination and either injecting CS-PRP alone (n=2 knees), injecting CS-PRP and wrapping the meniscus (n=2 knees) or wrapping alone (n=2 knees) and healing was assessed at 6 weeks. No post-operative bracing and or knee immobilization was used in both studies.

6.2.4 Evaluation of defect placement

Sheep were sacrificed at 3 weeks, 6 weeks, and 3 months post-surgery using sedation followed by a captive bolt pistol. Photodocumentation of the meniscus lesions was performed using a digital camera. Defect placement was assessed with Image J (NIH, USA) by measuring the width between the meniscus outer border and the tear (A) and the total width of the meniscus (B) and calculating the ratio (A/B) X 100%. Values closer to 0% are therefore near the vascularised periphery and values closer to 100% are near the avascular free border.

6.2.5 Electromechanical mapping of articular surfaces

Streaming potentials of cartilage originate from the displacement of positively charged mobile ions in the fluid phase relative to the fixed negatively charged proteoglycans entrapped within the collagen network during a light compression of the cartilage. It has been long established that streaming potentials are particularly sensitive to the integrity of the collagen network of the extracellular matrix and glycosaminoglycan (GAG) content[34,35]. Several studies have revealed correlations between the electromechanical properties of cartilage and its histological and biochemical properties[36-39]. Electromechanical properties of cartilage are altered by cartilage degeneration and repair[35,38-40]. In the current study, electromechanical properties were mapped manually *ex vivo* across the entire tibial plateau and the distal femurs using the Arthro-BST device (Biomomentum Inc.). This medical device measures streaming potentials generated during a rapid compression of the articular cartilage with an array of microelectrodes lying on a semispherical indenter (effective radius of the tip 3.18 mm, 5 microelectrodes/mm^2)[36]. A positioning software with live video feed was used to overlay a 17 X 13 position grid on the articular surfaces to locate

measurements and create a uniform mapping. The spherical indenter of the Arthro-BST was manually compressed onto the cartilage surface at each point. The device calculates a quantitative parameter (QP, arbitrary units) of cartilage electromechanical activity corresponding to the number of microelectrodes in contact with the cartilage when the sum of their streaming potential reaches 100 mV. A high QP therefore indicates weak electromechanical properties and poor load-bearing capacity and low QP indicates strong electromechanical properties and high load-bearing capacity[36]. Following mapping, osteochondral cores were collected for further processing.

6.2.6 Histoprocessing and microscopic evaluation

Menisci, synovial membrane biopsies and osteochondral cores were fixed in 10% neutral buffered formalin, dehydrated through a graded series of ethanol, cleared in xylene, infiltrated and embedded in paraffin. 5-micrometer-thick sections were collected on slides (Superfrost plus) and stained with iron hematoxylin/safranin-O/fast green (menisci and osteochondral core) or hematoxylin and eosin (synovial membrane biopsies). Stained histological slides were scanned with a Nanozoomer RS (Hamamatsu, Japan) and NDPView (Hamamatsu, Japan) was used to export images for further analysis. Two sections per meniscus were scored by two blinded observers using a scoring system based on Zhang et al[41]. Briefly, scores for the character of the predominant tissue, safranin-O staining, surface, integrity, cellularity, repair tissue quality and adjacent tissue quality were summed to obtain the overall tissue quality score (ranging from 0, normal, to 26 for the worst quality). In addition, scores for tissue morphology in the defect, thickness and bonding to host tissue were summed to obtain the repair tissue quality score (ranging from 0, normal, to 7 for the worst quality). Synovial membrane sections were scored as in Little et al[42], in which scores for intimal hyperplasia, inflammatory cell infiltration, sub-intimal fibrosis and vascularity are summed to obtain a total score ranging from 0, normal, to 12 for severe abnormalities. Osteochondral sections were scored according to Mankin[43], in which scores for structure, cells, safranin-O staining and tidemark integrity are summed to obtain a final score ranging from 0, normal, to 14 for severe abnormalities.

6.2.7 Data compilation

The data were compiled with SAS Enterprise Guide 7.1 and SAS version 9.4 (SAS Institute Inc, Cary, NC, USA). The data in the text are presented as average±SD. For each knee, the average of the scores from the 2 readers was calculated and is presented in dot plots.

6.3 Results

6.3.1 Meniscus repair is improved in some tears treated with chitosan-PRP implants while no improvement was observed for other treatments

Surgical lacerations were created on average midway between the capsular borders and the free borders of the menisci (at average 47%±9% the length of the meniscus in the first study and 48%±6% the length of the meniscus in the second study, (**Erreur ! Source du renvoi i ntrouvable.**). All the tears were located within the anterior half of each meniscus. CS-PRP implants were easily injected into the tears via trephinations channels where they were shown to be partly resident at 1-day post-surgery (**Figure 6.1.E-F**), and induced cell recruitment from the vascularized peripheral red-red zone towards the trephination channels (**Figure 6.1.G-H).** All tears were macroscopically visible at the time of necropsy 3 weeks, 6 weeks and 3 months post-surgery and the edges of the tears were usually well apposed with sutures (**Figure 6.3**). Aside from the surgically induced tears, no other sign of meniscal degeneration such as fibrillation or structure disruption was observed (**Figure 6.3**). Red repair tissue and evidence of neo-vascularization were visible on the tibial and femoral surfaces of the menisci in two CS-PRP only treated tears at 6 weeks in the second study and at 3 months in the first study (**Figure 6.3.B&E**). None of the other menisci displayed macroscopic signs of healing (**Figure 6.3**). Extent of healing did not directly correlate with defect location in both studies (**Erreur ! Source du renvoi introuvable.**). A highly c ellular repair tissue was seen in 1 out of 4 CS-PRP-treated tears at 3 weeks post-surgery in the first study (**Figure 6.4.A&B**). Partial integration between the repair tissue and the original meniscal tissue was achieved in this treated tear (**Figure 6.4.A&B**). Complete healing with a highly-vascularized repair tissue and almost seamless repair tissue integration was seen in 1 out of 4 CS-PRP treated tear at 3 months in the first study (**Figure 6.4.E&F**). No repair tissue synthesis was apparent in any of the PRP control tears at 3 weeks or at 3 months (**Figure 6.4.C-D&G-H),** or in

the other CS-PRP treated tears. Neutrophils were present in the outer vascularized portion of 2 out 4 CS-PRP treated menisci at 3 weeks but were not detected at 3 months, or in any of the PRP treated tears. The overall tissue quality score and repair tissue quality score reflected the histological observations with 1 out of 4 treated defects having lower scores indicative of improved quality at 3 weeks (**Figure 6.4.I&J**) and 3 months (**Figure 6.4.K&L**) post-surgery. Complete healing, seamless integration and a vascularized repair tissue were observed in 1 out of 2 CS-PRP only treated tears after 6 weeks in the second study (**Figure 6.5.A-C**). Partial repair and integration were observed in 1 out of 2 tears treated with CS-PRP and wrapping at 6 weeks in the second study (**Figure 6.5.D-F**). In both cases, structural organization was different in matching areas in intact menisci (**Figure 6.5.J-L**)**.** In contrast, there was no healing in the menisci treated with wrapping alone (**Figure 6.5.G-I**)**.** Significant cell infiltration at the outer meniscus border and variable glycosaminoglycan (GAG) depletion was observed in all experimental menisci compared to contralateral intact menisci (**Figure 6.5**). Suture tracks were abundant in menisci treated with the wrapping technique (**Figure 6.5.D&G**) with sparse foreign body giant cells (FBGCs) accumulating near the outer vascularized red-red region (**Figure 6.5.F&I**). The overall tissue quality score (**Figure 6.5.M**) and repair tissue quality score (**Figure 6.5.N**) reflected the histological observations, with one CS-PRP only treated meniscus having the lowest scores (scored 6 and 1 respectively), indicating the highest quality of repair, followed by one meniscus treated with wrapping + CS-PRP (scored 12 and 3 respectively).

Table 6.1 Placement of meniscal defects. Values closer to 0% were near the vascularised periphery and values closer to 100% were near the avascular free border.

First study			**Second study**		
Sheep # (Time)	**Right leg**	**Left leg**	**Sheep # (Time)**	**Right leg**	**Left leg**
1 (3w)	PRP 33%	CS-PRP 54%	1 (6w)	Wrap only 55%	Intact N/A
2 (3w)	CS-PRP 56%	PRP 56%	2 (6w)	Intact N/A	44% Wrap only
3 (3w)	CS-PRP** 42%	CS-PRP 40%	3 (6w)	CS-PRP only 51%	Intact N/A

4 (1d)	CS-PRP 44%	CS-PRP 33%	4 (6w)	Intact N/A	CS-PRP only* 45%
5 (3m)	PRP 43%	CS-PRP 58%	5 (6w)	CS-PRP + Wrap 53%	Intact N/A
6 (3m)	CS-PRP 44%	PRP 59%	6 (6w)	Intact N/A	CS-PRP + Wrap** 40%
7 (3m)	PRP 51%	CS-PRP* 45%			

* Defects that were completely healed.

** Defects that were partially healed.

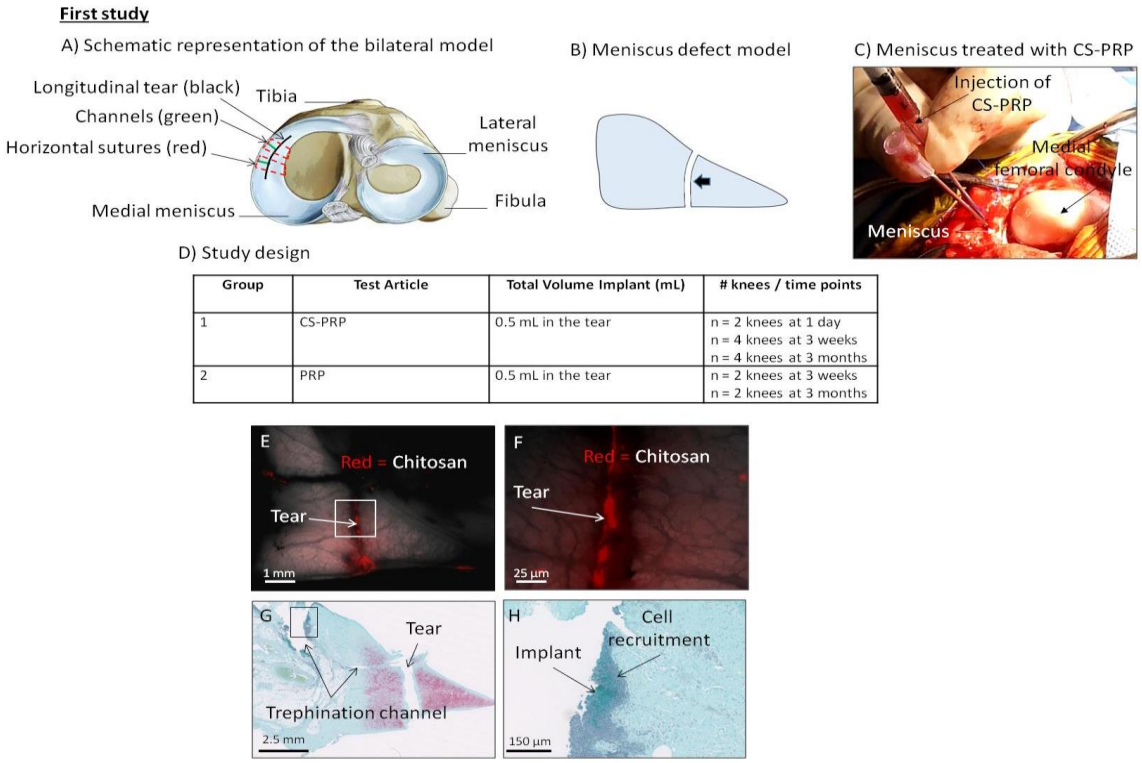

Figure 6.1 A) Schematic representation of the bilateral surgical model. 10-mm long incisions were created bilaterally in the anterior portion of the medial menisci in 7 sheep (black in A). Freeze-dried chitosan formulations were solubilized in autologous PRP and 0.5 mL of chitosan-PRP was injected into the meniscal tear through two trephination channels created with 18-gauge needles (in green in A). The tears were sutured in a horizontal mattress pattern (in red in A). B) Schematic

representation of the surgically induced defect model. C) Picture of a meniscus treated with CS-PRP. D) Seven ewes (2-6 years old) were included in the study and treated with either chitosan-PRP only (n = 2 knees at 1 day, n = 4 knees at 3 weeks & 3 months) or PRP only (n = 2 knees at 3 weeks & 3 months). E&F). A rhodamine-chitosan tracer was added to the freeze-dried formulations to allow detection of the implants with epifluorescent microscopy (E&F). The chitosan-PRP implants were partly resident in the tears and trephination channels at 1-day post-surgery (E&F). Safranin O/fast green stained sections showed that chitosan-PRP implants induced cell recruitment from the vascularized periphery of the menisci towards the trephination channels (G&H). The rectangles in panel E&G indicate the regions where the higher magnification images F&H were acquired.

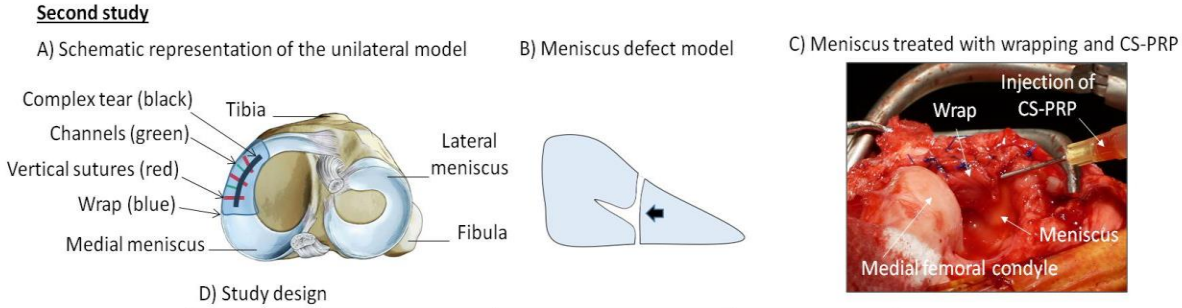

D) Study design

Group	Test Article	Total Volume Implant (mL)	# knees / time points
1	CS-PRP only	0.5 mL in the tear	n = 2 knees at 6 weeks
2	CS-PRP + Wrap	0.5 mL in the tear + 0.5 mL under membrane	n = 2 knees at 6 weeks
3	Wrap only	None	n = 2 knees at 6 weeks

Figure 6.2 A) Schematic representation of the unilateral surgical model. A bone block with medial collateral ligament attached was detached to increase access to the meniscus. A 10-mm longitudinal tear with a horizontal component was created towards the anterior portion of the medial meniscus (in black in A). Two 20-gauge needles were used to create trephination channels from the capsular border of the meniscus to the tear (in green in A). 0.5 mL chitosan-PRP implant was injected into the tear through the trephination channels and the tear was stabilized with three sutures tightened in a vertical pattern (in red in A). A piece of collagen membrane (12.5 mm X 25 mm) was wrapped around the meniscus (in blue in A) and sutured first at the capsular border, and then with two vertical sutures placed through the meniscal tissue. 0.5 mL chitosan-PRP implant was then injected under the membrane. The contralateral knee was left intact. B) Schematic

representation of the surgically induced defect model. C) Picture of a meniscus treated with wrapping + CS-PRP. D) Six ewes (2-6 years old) were included in the study and treated with either chitosan-PRP only (n = 2 knees), chitosan-PRP + wrap (n = 2 knees) or wrap only (n = 2 knees). The contralateral knees were left intact (n = 6 knees).

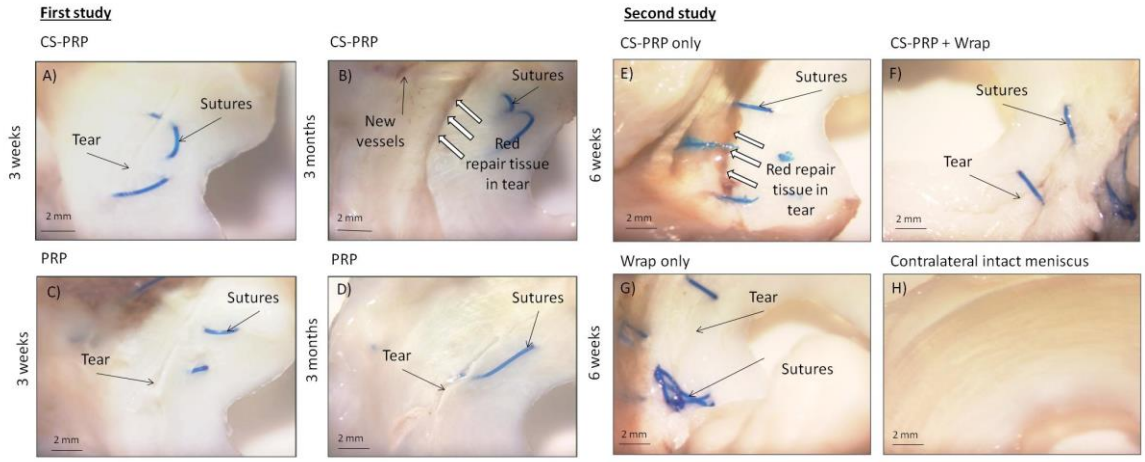

Figure 6.3 The tears were macroscopically visible at the time of necropsy 3 weeks, 6 weeks and 3 months after surgery and the edges of the tears were usually well apposed (A to G). A reddish repair tissue and signs of neo-vascularization were visible in two chitosan-PRP treated tears at 6 weeks (E) and at 3 months (B) post-surgery (white arrowheads). Sutures were apparent in all treatment groups. Aside from the surgically-induced tears, no other sign of macroscopic meniscal degeneration was observed.

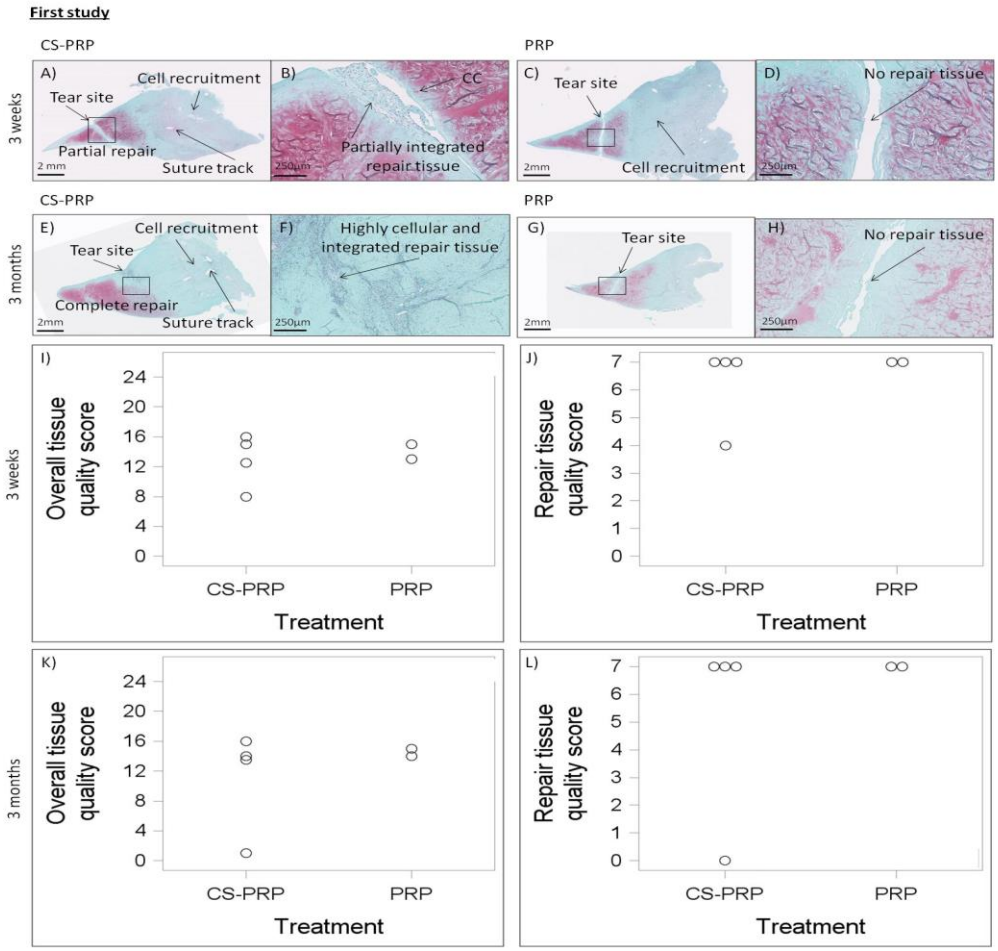

Figure 6.4 Histological sections of the repaired tissue stained with safranin O/fast green were used to evaluate tissue repair in the bilateral model. A highly cellular repair tissue was seen in one chitosan-PRP treated tear at 3 weeks post-surgery (A&B). Partial integration between the repair tissue and the original meniscal tissue was achieved in this treated tear (B). Complete healing with a highly vascularized repair tissues and seamless repair tissue integration were seen in one chitosan-PRP treated tear at 3 months (E&F). There was no repair tissue synthesis in the PRP controls at 3 weeks or at 3 months (C&D and G&H), and in the other CS-PRP treated tears. The surgical approach induced some fibroplasia in the outer portion of the menisci at 3 weeks and 3 months (A, C, E, & G). Rectangles in panels A, C, E, & G indicate regions where the higher magnification images B, D, F, & H were taken. Histological sections were scored based Zhang et al for overall meniscal tissue quality (i, ranging from 0 for the best to 26 for the worst quality) and repair tissue quality (j, ranging from 0 for the best to 7 for the worst quality) and were consistent with the histological observations[41].

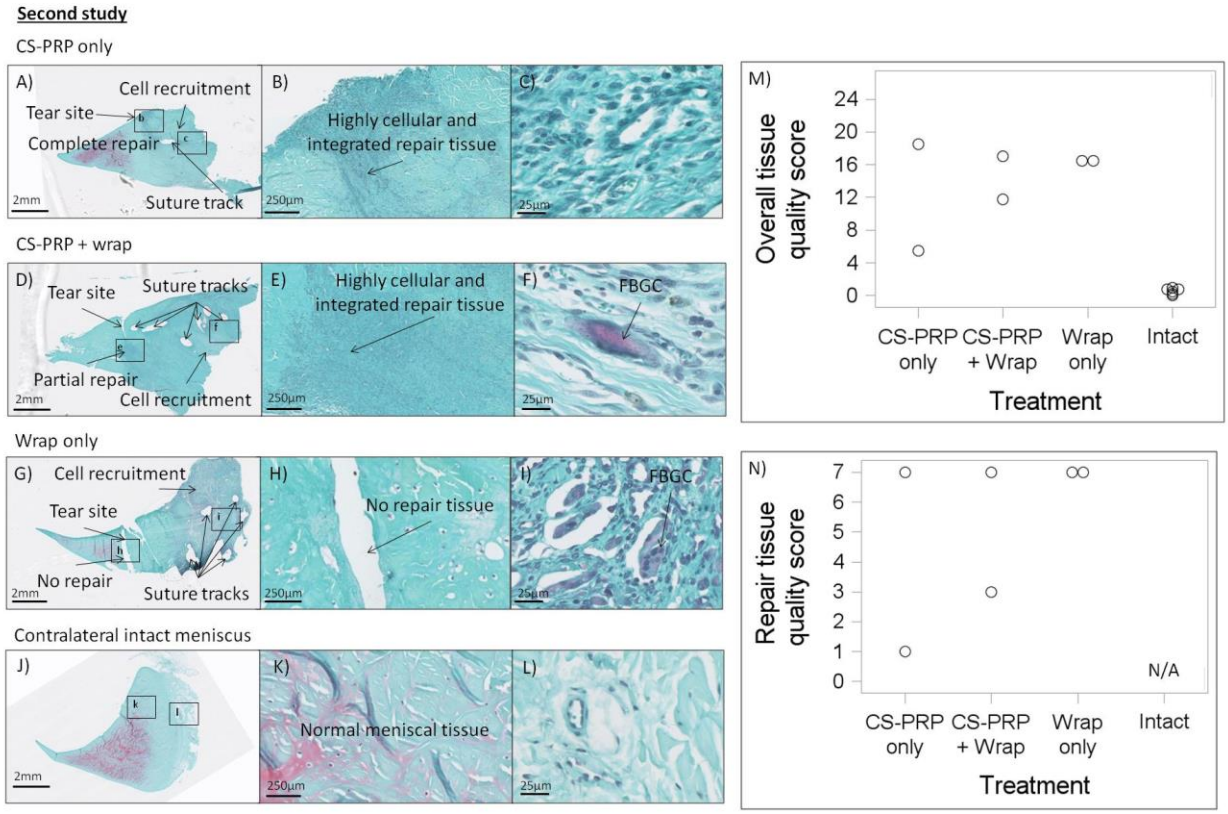

Figure 6.5 Histological sections of the repaired tissue stained with safranin O/fast green were used to evaluate tissue repair in the unilateral model. One tear treated with chitosan-PRP only showed complete repair (A-C), while one tear treated with chitosan-PRP with wrapping was partially healed (D-F). There was no repair tissue in the group treated with wrapping only (G-I). In the two cases where repair was observed, the repair tissue was highly cellular, well integrated to the adjacent meniscal tissue, but structurally different than the contralateral intact menisci (j-L). Significant cell recruitment into the outer portion of all treated menisci was observed compared to contralateral intact menisci. Suture tracks were frequently observed in menisci treated with the wrapping technique, along with sparse foreign body giant cells (FBGCs) in the outer vascularized area (D-I). Rectangles in A, D, G & J demonstrate regions where the higher magnification images B, C, E, F, H, I, K & L were acquired. Histological sections were scored based on Zhang et al for overall meniscal tissue quality (m, ranging from 0 for the best to 26 for the worst quality) and repair tissue quality (n, ranging from 0 for the best to 7 for the worst quality) and were consistent with the histological observations. N/A: Non-applicable.

6.3.2 Mild changes to other joint tissues were observed and were independent of specific treatments

All animals tolerated the operative approach well and no postoperative complications were seen after the surgery. The sheep had some intermittent lameness and effusion for the first few weeks post-surgery but recovered thereafter. Mild to moderate synovitis was present at 3 weeks and at 6 weeks post-surgery (**Figure 6.6.D&F**), but scores were closer to normal at 3 months (**Figure 6.6.E**)**.** Changes included intimal hyperplasia, some subintimal fibrosis, and an increase in vascularization (**Figure 6.6.A-C**) and were not associated with any specific treatment (**Figure 6.6.D-F**)**.** Mild to moderate histological changes were apparent in the articular cartilage surfaces as shown by safranin-O/fast green stained sections of osteochondral cores collected from the medial femoral condyle and medial tibial plateau (**Figure 6.7**). Changes include a loss of glycosaminoglycan and some structural abnormalities (**Figure 6.7.B&C**) and were not specific to any treatment (**Figure 6.7.D-F**)**.** The average quantitative parameter (QP) calculated for the medial femoral condyles and for the medial tibial plateau were similar in all treatment groups at all time-points, with values indicative of good load-bearing capacity (**Figure 6.8**).

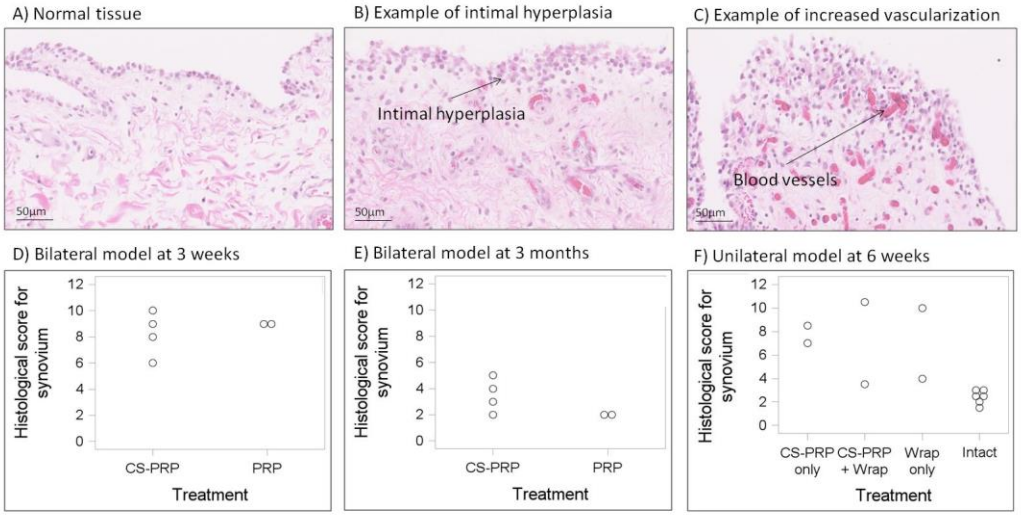

Figure 6.6 Hematoxylin and eosin stained sections of synovial membrane (A to C). There was a mild to moderate transient synovitis in most treated knees. Changes included intimal hyperplasia, inflammatory cell infiltration (B), some sub-intimal fibrosis, and an increase in vascularization (C). Histological sections were scored as in Little et al (D to F, ranging from 0 to 12 for severe abnormalities) and scores reflected those observations.

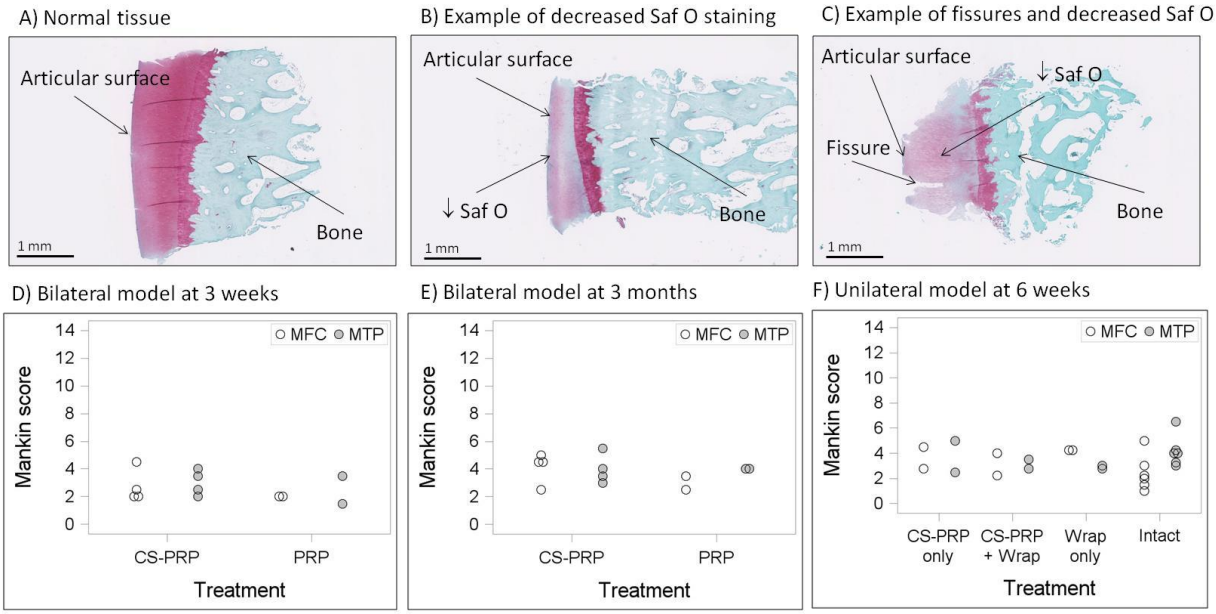

Figure 6.7 There were mild to moderate changes to the articular surfaces as shown by safranin O/fast green stained sections of osteochondral cores collected from the medial femoral condyles (A to C) and from the medial tibial plateau (not shown). Changes included depletion of glycosaminoglycan (B&C) and some structural abnormalities (C). Histological sections were scored according to Mankin (D to F, ranging from 0 to 14 for severe abnormalities) and scores reflected those observations. There was no effect of treatment on the histological scores.

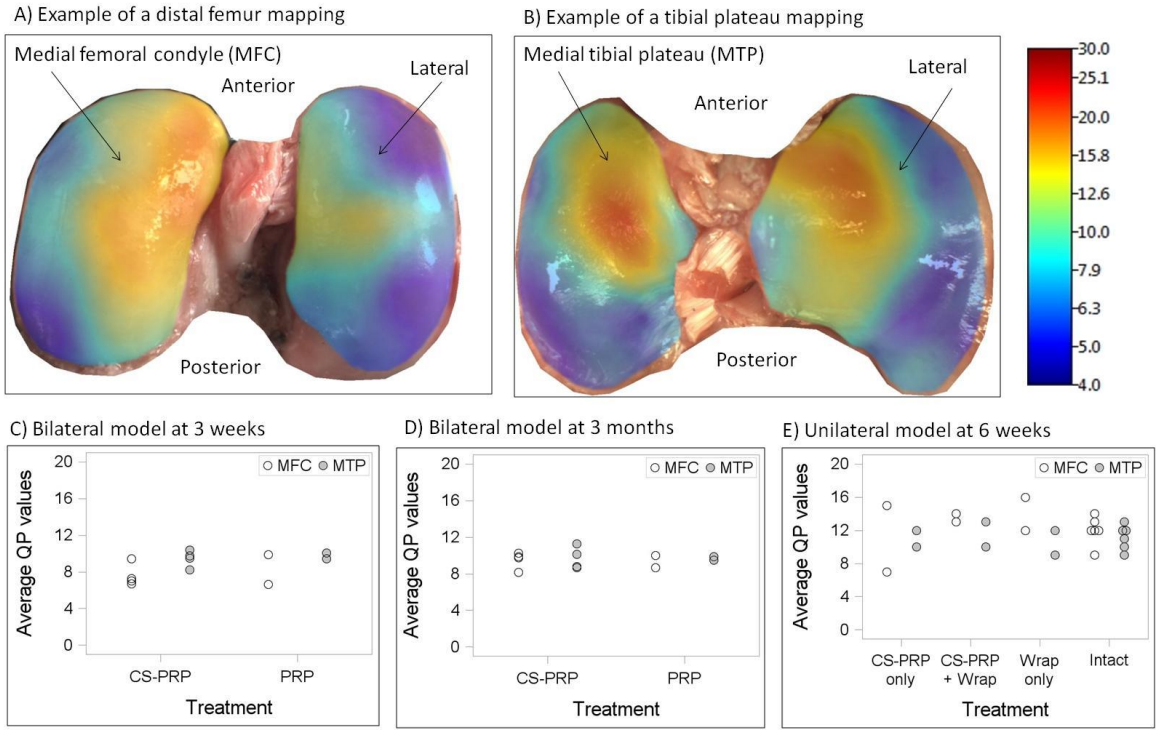

Figure 6.8 Electromechanical properties of the tibial plateau and the distal femurs were mapped across the entire articular surfaces using the hand-held Arthro-BST device (A&B). Panels a and b are representative examples of mapping of distal femurs (A) and tibial plateau (B) with corresponding QP. A high QP (shown in red) indicates weak electromechanical properties and poor load-bearing capacity and a low QP (in blue) shows strong electromechanical properties and high load-bearing capacity. Average QP values for medial femoral condyles and medial tibial plateau are shown in panels C to E and showed that articular surfaces displayed good load-bearing properties. There was no effect of treatment on QP values.

6.4 Discussion

The purpose of these pilot studies was to investigate the feasibility of using CS-PRP implants to improve meniscus repair in ovine models. In the first study, we found that CS-PRP implants stimulated repair tissue synthesis in 1 out of 4 treated tears while PRP alone did not, which supports our starting hypothesis. In the second study, in contrast to our original hypothesis, we found that using the meniscus wrapping technique in conjunction with CS-PRP implants did

not further improve repair, and that CS-PRP implants alone was sufficient to stimulate repair in 1 out of 2 treated tears.

The bilateral model in the first study (**Figure 6.1**) was conceived to control for inter-individual variability and minimize the number of required animals. However, we found that it was challenging since it did not permit the sheep to protect their treated knee from weight-bearing post-operatively, which we believe caused some implant loss and led to only partial retention of the CS-PRP implant in the tears (**Figure 6.1**) and thus a minority of tears that healed (1 out of 4). The unilateral model in the second study (**Figure 6.2**) utilizing a medial collateral bone block approach to the entire meniscus provides increased access to the tear site and allowed us to introduce the meniscus wrapping technique, as well as the T-shaped tears to mimic clinically relevant complex tears. Furthermore, we found that the sheep were protecting the operated knee from weight-bearing post-operatively, which is one potential reason why the success rate was improved to 1 out of 2 treated tears by switching from the bilateral model to the unilateral model. Some form of post-operative immobilization, analogous to the gradual return to weight-bearing protocols used clinically, would be expected to further improve implant retention and the reproducibility of the healing response. Although the tears located closer to the periphery might be expected to heal better, there was no effect of defect placement on healing in our pilot studies (**Erreur ! Source du renvoi introuvable.**). Vascular penetration in sheep is less than in humans a nd is limited to the 11-15% outer region of the meniscus[44], so that all of the tears were in the avascular portion of the meniscus, which may explain why defect placement had no significant effect here.

CS-PRP implants were found to induce cell recruitment as early as one day post-surgery. An immature highly cellular partially integrated tissue filled the tears at 3 weeks (**Figure 6.3Figure 6.4**), which was remodeled into a vascularized integrated repair tissue between 6 weeks and 3 months (**Figure 6.3Figure 6.4Figure 6.5**). The origin of the cells that filled the gap at the defect site was not identified in the current study; however, the cells may originate from extrinsic and/or intrinsic sources. The synovial membrane, the peripheral blood supply, and meniscal fibrochondrocytes themselves have all been suggested to be the source of repair in animal studies of meniscus repair[35,45-47]. Meniscal fibrochondrocytes possess the capability to further differentiate towards chondrogenic, adipogenic, and osteogenic lineages[48] and exogenous synovial-derived mesenchymal cells have the capacity of homing and attaching to meniscus tears to mediate

reparative process[49]. A combination of healing techniques (e.g. trephination, tear rasping, wrapping and application of CS-PRP) were used in our 2 pilot studies. We used trephination channels to deliver our implants efficiently to the tear site and stimulate healing from the meniscus periphery in a fashion similar to what was previously done in pre-clinical models[50-52], and observed cells migrating towards the channels at 1 day post-surgery, although it is uncertain if those channels remained open and if the cells actually entered the channels to migrate to the tears. Our purpose in rasping the tears was to create a rough surface for the implant to adhere to, but others have suggested that tear rasping can induce cytokine release beneficial to healing[53]. Although this was not done here, synovial rasping is often performed clinically to stimulate ingrowth of synovial-derived cells. Further characterization of the type of cells migrating into the defect (for example progenitor cells versus inflammatory cells) and evaluation of cell survival would provide mechanistic information on the repair process, including the origin of the repair cells. Similar to what was observed with CS-GP/blood implants in the context of cartilage repair[26], CS-PRP implants also displayed the potential to induce neovascularisation. Based on the histological appearance of our contralateral intact menisci and on previously published data on vascular penetration in sheep meniscus[44], we can state with some confidence that the blood vessels observed in the vicinity of the tears in CS-PRP treated menisci are in fact new blood vessels, and not pre-existing vessels. A better understanding of the vascular response induced by CS-PRP implants would be of high interest for future studies. Our data are also consistent with the notion that remodeling of the meniscus is essential for good tissue integration[54], and it is interesting to note that CS-PRP implants have previously been shown to promote tissue remodeling in the context of cartilage repair[55].

Most available pre-clinical studies have not shown a beneficial effect of applying leukocyte-rich-PRP to meniscal tears[56-59], and clinical data is lacking. We postulate that one reason for the poor performance of PRP is its poor residency *in vivo*. In line with this, we have previously shown that recalcified PRP degrades in a single day when implanted *in vivo*, while CS-PRP implants reside for several weeks and induce cell recruitment and neo-vascularization[26]. Lyophilized chitosan scaffolds have been proposed as delivery tools for PRP[60-62], and those studies as well as our own preliminary data[63] suggest that chitosan scaffolds can provide sustained release of PRP-derived growth factors, although it is difficult to extrapolate such *in vitro* data regarding platelet derivatives to pre-clinical and clinical settings[64]. Exposure to PDGF-AB has been shown

to induce meniscal fibrochondrocytes to proliferate and synthesize new matrix *in vitro*[65]. It therefore becomes logical to suggest that sustained release of platelet-derived growth factors is one mechanism by which CS-PRP implants improved meniscus repair in the current pilot studies. Of note, the single pre-clinical study that reported improved meniscus repair outcomes in the rabbit used a combination gelatin hydrogel for delivery of PRP[66], another biomaterial-PRP combination. N-carboxymethyl chitosan by itself has been shown to modulate the healing sequence in a rabbit model of meniscus repair[76], and we hypothesize that the sustained presence of chitosan at the tear site was another mechanism by which repair was modulated and ultimately improved in the current pilot studies.

Using the wrap in conjunction with CS-PRP implants did not further improve repair and the additional sutures needed to secure the wrap created significant damage to the meniscus (**Figure 6.5**). In addition, the wrap appeared to stimulate a foreign body giant cells in wrapped meniscal tissues that was not seen with CS-PRP alone (**Figure 6.5**), although foreign body reactions are often observed when very slowly degrading biomaterials are implanted in the body[68]. Although the sheep meniscus is considered an acceptable model[44-69], no animal model is truly like the human, which may account for the poor performance the of the meniscus wrapping technique in the animal model that has uncontrolled post-operative weight bearing compared to humans[16]. The combination of the meniscus wrapping technique with the CS-PRP implants could still prove to be a good option for the clinical treatment of degenerated, complex meniscal tears. CS-PRP implants were well-tolerated and induced only a transient synovitis in the knee **(Figure 6.6**). Meniscal damage can easily induce osteoarthritis in the sheep[70], which was not observed here. The histological changes that were observed on the articular surfaces (**Figure 6.7**) appear to be normal for sheep of that age and weight[71], and electromechanical mappings (**Figure 6.8**) revealed that the articular surfaces had good load-bearing properties[36].

Our study was intended as a pilot feasibility study and had several limitations. The major limitation is the low number of animals used, which precluded statistical analysis, and associated conclusions. Results should therefore be viewed appropriately. Performing these pilot studies allowed us to refine our procedures for design and implantation of the product. We further propose that controlled post-operative weight-bearing would allow for better implant retention and increased reproducibility and efficiency. Clearly, these pilot feasibility studies need to be substantiated in a longer-term follow-up study with a larger number of animals. In light of the

results obtained during the second pilot study, groups of n=25 would be sufficient to allow us to see a statistical difference between the histological quality of the repair tissue elicited by CS-PRP versus wrap treatment (using significance level α of 5% and power 1-β of 80% for calculations). In addition, the mechanical strength of the repair tissue was not assessed, an important factor to prevent recurrent tears. Ideally, functional assessment of the repaired meniscus tissue would be evaluated by biomechanical testing in the future. Another limitation which would be addressed in a subsequent study design would be the addition of sham operated animals and a suture-only group which was absent in the current studies. Finally, sheep are a convenient large-animal model due to availability, geometric similarities between the joints of sheep and humans, ease of handling and housing. Nonetheless, the distribution of forces is quite different in quadruped compared to humans[69].

Meniscus repair remains a significant challenge for orthopaedic surgeons and developing a viable augmentation option is still needed. Freeze-dried chitosan formulations can be rapidly solubilized in autologous PRP to form injectable *in situ* solidifying implants that have tissue regeneration capacity. Even with our pilot studies' limitations, data in this study makes an important advance in showing the importance of using unilateral meniscal repair model, that untreated tears fail to remodel, and that CS-PRP implants displayed some potential to improve repair of meniscal tears, including complex tears. Although further work is required to support these early findings, CS-PRP implants could eventually assist in restoring meniscus structure and function in the future.

Acknowledgements

We thank Geneviève Picard, Gabrielle Deprés-Tremblay, Insaf Hadjab and Sotcheadt Sim for their technical contributions and the funding sources (Ortho Regenerative Technologies Inc, Prima Quebec, Canadian Institutes of Health Research, Canada Foundation for Innovation, Groupe de Recherche en Sciences et Technologies Biomédicales, Natural Sciences and Engineering Research Council of Canada).

Conflict of Interest

A.C. and M.D.B. hold shares; M.D.B. is a Director and J.F.and S.R. are clinical advisors or Ortho Renegerative Technologies Inc.

Author Contributions

The authors made substantial contributions in designing the study (LG, AC, JF, SR, MH, CH, and MDB), gathering the data (LG, MH, and AC) and drafting the article (LG, AC, JF, SR, MH, CH, and MDB). All the authors approved the submitted manuscript. We collaborated with a professional orthopaedic veterinarian (MH) to carry out the surgery, implantation of the CS-PRP formulation and the necropsy.

References

1. Fithian DC, Kelly MA, Mow VC. (1990) Material properties and structure-function relationships in the menisci. Clin Orthop Rel Res. 252, 19-31.

2. Clayton RAE, Court-Brown CM. (2008) The epidemiology of musculoskeletal tendinous and ligamentous injuries. Injury-Int J Care Injured. 39, (12): 1338-1344.

3. Kim S, Bosque J, Meehan JP, et al. (2011) Increase in Outpatient Knee Arthroscopy in the United States: A Comparison of National Surveys of Ambulatory Surgery, 1996 and 2006. J Bone Joint Surg-Am. 93A, (11): 994-1000.

4. Mordecai SC, Al-Hadithy N, Ware HE, et al. (2014) Treatment of meniscal tears: An evidence-based approach. World J Orthop. 5, (3): 233-41.

5. Abrams GD, Frank RM, Gupta AK, et al. (2013) Trends in Meniscus Repair and Meniscectomy in the United States, 2005-2011. Am J Sports Med. 41, (10): 2333-2339.

6. Englund M, Guermazi A, Roemer FW, et al. (2009) Meniscal Tear in Knees Without Surgery and the Development of Radiographic Osteoarthritis Among Middle-Aged and Elderly Persons The Multicenter Osteoarthritis Study. Arthr Rheum. 60, (3): 831-839.

7. Englund M, Roemer FW, Hayashi D, et al. (2012) Meniscus pathology, osteoarthritis and the treatment controversy. Nature reviews. Rheumatology. 8, (7): 412-9.

8. Cicuttini FM, Forbes A, Yuanyuan W, et al. (2002) Rate of knee cartilage loss after partial meniscectomy. J Rheumatolog. 29, (9): 1954-6.

9. Arnoczky SP, Warren RF. (1982) Microvasculature of the human meniscus. Am J Sports Med. 10, (2): 90-95.

10. Taylor SA, Rodeo SA. (2013) Augmentation techniques for isolated meniscal tears. Curr Rev Musculoskelet Med. 6, (2): 95-101.

11. Ghazi zadeh L, Chevrier A, Farr J, et al. (2017) Augmentation techniques for meniscus repair. The journal of knee surgery.

12. Shelbourne KD, Benner RW, Nixon RA, et al. (2015) Evaluation of Peripheral Vertical Nondegenerative Medial Meniscus Tears Treated with Trephination Alone at the Time of Anterior Cruciate Ligament Reconstruction. Arthroscopy. 31, (12): 2411-2416.

13. Shelbourne KD, Dersam MD. (2004) Comparison of partial meniscectomy versus meniscus repair for bucket-handle lateral meniscus tears in anterior cruciate ligament reconstructed knees. Arthroscopy. 20, (6): 581-5.

14. Shelbourne KD, Rask BP. (2001) The sequelae of salvaged nondegenerative peripheral vertical medial meniscus tears with anterior cruciate ligament reconstruction. Arthroscopy. 17, (3): 270-274.

15. Cook JL, Fox DB. (2007) A novel bioabsorbable conduit augments healing of avascular meniscal tears in a dog model. Am J Sports Med. 35, (11): 1877-1887.

16. Piontek T, Ciemniewska-Gorzela K, Naczk J, et al. (2016) Complex meniscus tears treated with collagen matrix wrapping and bone marrow blood injection: a 2-year clinical follow-up. Cartilage. 7, (2): 123-139.

17. Jang SH, Ha JK, Lee DW, et al. (2011) Fibrin clot delivery system for meniscal repair. Knee Surg Rel Res. 23, (3): 180-3.

18. Griffin JW, Hadeed MM, Werner BC, et al. (2015) Platelet-rich Plasma in Meniscal Repair: Does Augmentation Improve Surgical Outcomes? Clin Orthop Rel Res. 473, (5): 1665-1672.

19. Pujol N, De Chou ES, Boisrenoult P, et al. (2015) Platelet-rich plasma for open meniscal repair in young patients: Any benefit? Knee Surg Sports Traumatol Arthrosc. 23, (1): 51-58.

20. Liu X, Ma L, Mao Z, et al. (2011) Chitosan-Based Biomaterials for Tissue Repair and Regeneration. Adv Polym Sci. 244, 81–128.

21. Hoemann CD, Sun J, McKee MD, et al. (2007) Chitosan-glycerol phosphate/blood implants elicit hyaline cartilage repair integrated with porous subchondral bone in microdrilled rabbit defects. Osteoarthr Cart. 15, (1): 78-89.

22. Stanish WD, McCormack RG, Forriol F, et al. (2013) Novel Scaffold-Based BST-CarGel Treatment Results in Superior Cartilage Repair Compared with Microfracture in a Randomized Controlled Trial. J Bone Joint Surg-Am. 95A, (18): 1640-1650.

23. Shive MS, Stanish WD, McCormack R, et al. (2015) BST-CarGel(R) Treatment Maintains Cartilage Repair Superiority over Microfracture at 5 Years in a Multicenter Randomized Controlled Trial. Cartilage. 6, (2): 62-72.

24. Hoemann CD, Hurtig M, Rossomacha E, et al. (2005) Chitosan-glycerol phosphate/blood implants improve hyaline cartilage repair in ovine microfracture defects. J Bone Joint Surg-Am. 87A, (12): 2671-2686.

25. Hoemann CD, Chen G, Marchand C, et al. (2010) Scaffold-Guided Subchondral Bone Repair Implication of Neutrophils and Alternatively Activated Arginase-1+Macrophages. Am J Sports Med. 38, (9): 1845-1856.

26. Chevrier A, Hoemann CD, Sun J, et al. (2007) Chitosan-glycerol phosphate/blood implants increase cell recruitment, transient vascularization and subchondral bone remodeling in drilled cartilage defects. Osteoarthr Cart. 15, (3): 316-327.

27. Fong D, Ariganello MB, Girard-Lauziere J, et al. (2015) Biodegradable chitosan microparticles induce delayed STAT-1 activation and lead to distinct cytokine responses in differentially polarized human macrophages in vitro. Acta Biomaterialia. 12, 183-94.

28. Chevrier A, Darras V, Picard G, et al. (2017) Injectable chitosan-platelet-rich plasma (PRP) implants to promote tissue regeneration: In vitro properties, in vivo residence, degradation, cell recruitment and vascularization. Journal of tissue engineering and regenerative medicine. In Press.

29. Lavertu M, Xia Z, Serreqi AN, et al. (2003) A validated 1H NMR method for the determination of the degree of deacetylation of chitosan. J Pharm Biomed Anal. 32, (6): 1149-58.

30. Nguyen S, Winnik FM, Buschmann MD. (2009) Improved reproducibility in the determination of the molecular weight of chitosan by analytical size exclusion chromatography. Carbohydrate Polymers. 75, (3): 528-533.

31. Ma O, Lavertu M, Sun J, et al. (2008) Precise derivatization of structurally distinct chitosans with rhodamine B isothiocyanate. Carbohydrate Polymers. 72, (4): 616-624.

32. Mora G, Alvarez E, Ripalda P, et al. (2003) Articular cartilage degeneration after frozen meniscus and Achilles tendon allograft transplantation: Experimental study in sheep. Arthroscopy. 19, (8): 833-841.

33. Ghadially FN, Wedge JH, Lalonde JM. (1986) Experimental methods of repairing injured menisci. The Journal of bone and joint surgery. British volume. 68, (1): 106-10.

34. Sim S, Chevrier A, Garon M, et al. (2014) Non-destructive electromechanical assessment (Arthro-BST) of human articular cartilage correlates with histological scores and biomechanical properties. Osteoarthr Cart. 22, (11): 1926-1935.

35. Changoor A, Coutu JP, Garon M, et al. (2011) Streaming potential-based arthroscopic device is sensitive to cartilage changes immediately post-impact in an equine cartilage injury model. J Biomech Eng. 133, (6): 061005.

36. Legare A, Garon M, Guardo R, et al. (2002) Detection and analysis of cartilage degeneration by spatially resolved streaming potentials. J Orthop Res. 20, (4): 819-26.

37. Sim S, Chevrier A, Garon M, et al. (2017) Electromechanical probe and automated indentation maps are sensitive techniques in assessing early degenerated human articular cartilage. J Orthop Res. 35, (4): 858-867.

38. Abedian R, Willbold E, Becher C, et al. (2013) In vitro electro-mechanical characterization of human knee articular cartilage of different degeneration levels: a comparison with ICRS and Mankin scores. J Biomec. 46, (7): 1328-34.

39. Becher C, Ricklefs M, Willbold E, et al. (2016) Electromechanical Assessment of Human Knee Articular Cartilage with Compression-Induced Streaming Potentials. Cartilage. 7, (1): 62-9.

40. Schagemann JC, Rudert N, Taylor ME, et al. (2016) Bilayer Implants: Electromechanical Assessment of Regenerated Articular Cartilage in a Sheep Model. Cartilage. 7, (4): 346-60.

41. Zhang H, Leng P, Zhang J. (2009) Enhanced Meniscal Repair by Overexpression of hIGF-1 in a Full-thickness Model. Clin Orthop Rel Res. 467, (12): 3165-3174.

42. Little CB, Smith MM, Cake MA, et al. (2010) The OARSI histopathology initiative - recommendations for histological assessments of osteoarthritis in sheep and goats. Osteoarth Cart. 18 Suppl 3, S80-92.

43. Mankin HJ, Dorfman H, Lippiello L, et al. (1971) Biochemical and metabolic abnormalities in articular cartilage from osteo-arthritic human hips. II. Correlation of morphology with biochemical and metabolic data. J Bone Joint Surg-Am. 53, (3): 523-37.

44. Chevrier A, Nelea M, Hurtig MB, et al. (2009) Meniscus Structure in Human, Sheep, and Rabbit for Animal Models of Meniscus Repair. J Orthop Res. 27, (9): 1197-1203.

45. Kawai Y, Fukubayashi T, Nishino J. (1989) Meniscal suture. An experimental study in the dog. Clin Orthop Relat Res. 243, 286-93.

46. Arnoczky SP, Warren RF, Kaplan N. (1985) Meniscal remodeling following partial meniscectomy--an experimental study in the dog. Arthroscopy. 1, (4): 247-52.

47. Heatley FW. (1980) The meniscus--can it be repaired? An experimental investigation in rabbits. J Bone Joint Surg-Br. 62, (3): 397-402.

48. Mauck RL, Martinez-Diaz GJ, Yuan X, et al. (2007) Regional multilineage differentiation potential of meniscal fibrochondrocytes: implications for meniscus repair. Anatom Rec. 290, (1): 48-58.

49. Mizuno K, Muneta T, Morito T, et al. (2008) Exogenous synovial stem cells adhere to defect of meniscus and differentiate into cartilage cells. J Med Dent Sci. 55, (1): 101-11.

50. Arnoczky SP, Warren RF, Spivak JM. (1988) Meniscal repair using an exogenous fibrin clot. An experimental study in dogs. J Bone Joint Surg-Am. 70, (8): 1209-17.

51. Zhang ZN, Tu KY, Xu YK, et al. (1988) Treatment of longitudinal injuries in avascular area of meniscus in dogs by trephination. Arthroscopy. 4, (3): 151-9.

52. Zhang ZN, Arnold JA, Williams T, et al. (1995) Repairs by trephination and suturing of longitudinal injuries in the avascular area of the meniscus in goats. Am J Sports Med. 23, (1): 35-41.

53. Ochi M, Uchio Y, Okuda K, et al. (2001) Expression of cytokines after meniscal rasping to promote meniscal healing. Arthroscopy. 17, (7): 724-731.

54. Kambic HE, Futani H, McDevitt CA. (2000) Cell, matrix changes and alpha-smooth muscle actin expression in repair of the canine meniscus. Wound Repair Regen. 8, (6): 554-61.

55. Dwivedi G, Chevrier A, Hoemann CD, et al. (2016) Freeze dried chitosan/platelet-rich-plasma implants improve marrow stimulated cartilage repair in rabbit chronic defect model. Proceedings of International Cartilage Repair Society, Sorrento, Italy (2016).

56. Zellner J, Hierl K, Mueller M, et al. (2013) Stem cell-based tissue-engineering for treatment of meniscal tears in the avascular zone. J Biomed Mat Res B. 101, (7): 1133-42.

57. Zellner J, Mueller M, Berner A, et al. (2010) Role of mesenchymal stem cells in tissue engineering of meniscus. J Biomed Mat Res A. 94A, (4): 1150-1161.

58. Shin KH, Lee H, Kang S, et al. (2015) Effect of Leukocyte-Rich and Platelet-Rich Plasma on Healing of a Horizontal Medial Meniscus Tear in a Rabbit Model. BioMed research international. 2015, 179756.

59. Lee HR, Shon OJ, Park SI, et al. (2016) Platelet-Rich Plasma Increases the Levels of Catabolic Molecules and Cellular Dedifferentiation in the Meniscus of a Rabbit Model. Int J Mol Sci. 17, (1): E120.

60. Kutlu B, Aydin RST, Akman AC, et al. (2013) Platelet-rich plasma-loaded chitosan scaffolds: Preparation and growth factor release kinetics. J Biomed Mat Res B. 101B, (1): 28-35.

61. Shimojo AA, Perez AG, Galdames SE, et al. (2015) Performance of PRP associated with porous chitosan as a composite scaffold for regenerative medicine. TheScientificWorldJournal. 2015, 396131.

62. Shimojo AA, Perez AG, Galdames SE, et al. (2016) Stabilization of porous chitosan improves the performance of its association with platelet-rich plasma as a composite scaffold. Mat Sci Eng C. 60, 538-46.

63. Deprés-Tremblay G, Chevrier A, Tran-Khanh N, et al. (2016) Chitosan-platelet-rich plasma implants for tissue repair - in vitro and in vivo characteristics. Proceedings of World Biomaterials Congress, Montreal, QC, Canada (2016).

64. Borzini P, Mazzucco L. (2005a) Tissue regeneration and in loco administration of platelet derivatives: clinical outcome, heterogeneous products, and heterogeneity of the effector mechanisms. Transfusion. 45, (11): 1759-67.

65. Tumia NS, Johnstone AJ. (2009) Platelet derived growth factor-AB enhances knee meniscal cell activity in vitro. The Knee. 16, (1): 73-6.

66. Ishida K, Kuroda R, Miwa M, et al. (2007) The regenerative effects of platelet-rich plasma on meniscal cells in vitro and its in vivo application with biodegradable gelatin hydrogel. Tiss Eng. 13, (5): 1103-1112.

67. Muzzarelli RA, Bicchiega V, Biagini G, et al. (1992) Role of N-Carboxybutyl Chitosan in the Repair of the Meniscus. J Bioact Compat Polym. 7, (2): 130-148.

68. Anderson JM, Rodriguez A, Chang DT. (2008) Foreign body reaction to biomaterials. Sem Immunol. 20, (2): 86-100.

69. Deponti D, Di Giancamillo A, Scotti C, et al. (2015) Animal models for meniscus repair and regeneration. J Tiss Eng Reg Med. 9, (5): 512-527.

70. Burger C, Mueller M, Wlodarczyk P, et al. (2007) The sheep as a knee osteoarthritis model: early cartilage changes after meniscus injury and repair. Lab Animals. 41, (4): 420-31.

71. Vandeweerd JM, Hontoir F, Kirschvink N, et al. (2013) Prevalence of naturally occurring cartilage defects in the ovine knee. Osteoarthr Cart. 21, (8): 1125-31.

CHAPTER 7 ARTICLE 3: MULTIPLE PLATELET-RICH PLASMA PREPARATIONS CAN SOLUBILIZE FREEZE-DRIED CHITOSAN FORMULATIONS TO FORM INJECTABLE IMPLANTS FOR ORTHOPEDIC INDICATIONS

(Journal of Bio-Medical Materials and Engineering)

Leili Ghazi zadeh[1], Anik Chevrier[2], Martin Lamontagne[3], Michael D Buschmann[4], Caroline D Hoemann[1,2], Marc Lavertu[2]

[1] Biomedical Engineering Institute, Polytechnique Montreal, Montreal, QC, Canada. [2] Department of Chemical Engineering, Polytechnique Montreal, Montreal, QC, Canada. [3] Faculty of Medicine, University of Montreal, Montreal, QC, Canada. [4] Department of Bioengineering, George Mason University, Institute for Advanced Biomedical Research, Manassas, VA 20110, USA

Corresponding author: Dr Marc Lavertu, Chemical Engineering Department, Polytechnique Montreal, PO Box 6079 Succ Centre-Ville, Montreal, Quebec, Canada, H3C 3A7, Fax: 514 340 2980 Tel: 514 340 4711 ext. 3609, E-mail: marc.lavertu@polymtl.ca

Abstract

BACKGROUND: Platelet-rich plasma (PRP) has been used to solubilize freeze-dried chitosan (CS) formulations to form injectable implants for tissue repair.

OBJECTIVE: To determine whether the *in vitro* performance of the formulations depends on the type of PRP preparation used to solubilize CS.

METHODS: Formulations containing 1% (w/v) CS with varying degrees of deacetylation (DDA 80.5-84.8%) and number average molar mass (M_n 32-55 kDa), 1% (w/v) trehalose and 42.2 mM calcium chloride were freeze-dried. Seven different PRP preparations were used to solubilize the formulations. Controls were recalcified PRP.

RESULTS: CS solubilization was achieved with all PRP preparations. CS-PRP formulations were less runny than their corresponding PRP controls. All CS-PRP formulations had a clotting time below 9 minutes, assessed by thromboelastography, while the leukocyte-rich PRP controls took longer to coagulate (> 32 min), and the leukocyte-reduced PRP controls did not coagulate in this dynamic assay. In glass culture tubes, all PRP controls clotted, expressed serum and retracted (43-82 % clot mass lost) significantly more than CS-PRP clots (no mass lost). CS dispersion was homogenous within CS-PRP clots.

CONCLUSIONS: *In vitro* performance of the CS-PRP formulations was comparable for all types of PRPs assessed.

Keywords: Chitosan, Platelet-rich plasma, Injectable implants

Level of evidence: Exprimental work (*in vitro*)

Disclaimer: None

7.1 Introduction

Platelet-rich plasma (PRP) is an autologous blood-derived product that contains platelet concentrations above physiological levels. PRP is thought to modulate the tissue healing process by supplying growth factors, cytokines, and other bioactive compounds which play fundamental roles in hemostasis as well as tissue repair and remodeling. PRP safety profile, ease of preparation and application, low potential for disease transmission and minimal tissue rejection are some advantages. Initially, PRP's first clinical applications were limited to dentistry, oral and maxillofacial surgery to improve bone healing with platelet gels[1], but PRP is now used to treat several musculoskeletal and orthopaedic conditions, including osteoarthritis, meniscus tears, tendinopathy, rotator cuff tears and ligament tears[2].

To date, numerous PRP preparation systems are available, which produce PRP that contain varying concentrations of platelets, leukocytes and erythrocytes. On the basis of the platelet concentration, inclusion or exclusion of leukocytes, and fibrin architecture, Dohan Ehrenfest et al classified 4 families of PRP preparations[3]: 1) Leukocyte-rich PRP; and 2) Leukocyte-poor (or leukocyte-reduced) PRP, both of which are liquid suspensions that form solid clots upon activation of the coagulation cascade; and 3) Leukocyte-rich platelet-rich fibrin (PRF); and 4) Leukocyte-poor (or leukocyte-reduced) PRF, both of which are in solid format. Regarding the therapeutic effects of the different types of PRP preparations, platelet content has been a primary focus, since platelet-derived growth factors contribute to tissue repair, however, it is well established that concentration of erythrocytes and leukocytes are also important factors to consider. The exact role of these cells in the PRP-mediated reparative process has not been completely elucidated yet. Leukocytes are thought to induce a proinflammatory response by releasing some inflammatory mediators and catabolic enzymes such as interleukin (IL-1β), tumor necrosis factor (TNF-α) and IL-6. This has clearly been shown *in vitro*[4-6], which led to the notion that leukocyte-reduced PRP preparations would be superior to leukocyte-rich PRP preparations. However, increased levels of platelet-derived growth factor (PDGF)-ab, PDGF-bb, vascular endothelial growth factor (VEGF) and transforming growth factor (TGF)-β from leukocyte-rich PRP compared to leukocyte-poor PRP have been reported *in vitro*[7,8], which could potentially contribute to the improved tissue repair. In addition, the inflammatory response induced by leukocyte-rich PRP preparations appears to be limited to the early post-treatment period *in vivo*[9]. Furthermore, there is clinical evidence that a

single ultrasound-guided injection of leukocyte-rich PRP is beneficial for treating tendinopathy[10]. As of now, it is still unclear what type of PRP preparation should be used to treat specific conditions.

Chitosan (CS) is a nontoxic, biodegradable and biocompatible polysaccharide composed of glucosamine and *N*-acetyl-glucosamine units, which is derived by alkaline deacetylation of chitin[11]. Our laboratory has developed freeze-dried formulations of CS that can be solubilized in PRP to form injectable CS-PRP implants that coagulate *in situ* and can be used for different tissue repair applications[12]. Previous studies showed that CS-PRP implants resist platelet-mediated retraction post-clotting, release increased amounts of platelet-derived growth factors and have prolonged residency *in vivo* compared to PRP alone[13]. CS-PRP implants have also shown potential to improve repair of rotator cuff, meniscus and cartilage in small and large animal models[14-17].

The goal of the current study was to answer multiple questions regarding this technology. First, in all of our previous studies, we used a leukocyte-rich PRP preparation that was prepared manually by double centrifugation, and not PRP preparations isolated with commercially available kits. Second, acceptable CS specifications for combination with PRP need to be defined. Therefore, the purpose of the current study was to 1) Assess compatibility of this technology with the various types of PRP preparations that can be isolated with commercially available systems and 2) Define a range of CS degree of deacetylation (DDA) and the number average molecular weight (M_n) that would yield freeze-dried formulations with acceptable performance characteristics. Our starting hypothesis was that although the different PRP preparation systems would yield PRPs with varying properties, all PRP preparations would be compatible with this technology.

7.2 Materials and methods

7.2.1 Preparation of freeze-dried chitosan formulations

Five CS (Raw material purchased from Primex) were deacetylated by alkaline treatment, depolymerized with nitrous acid, characterized by NMR spectroscopy[18] and analytical size exclusion chromatography/multi-angle laser light scattering[19]. DDA, M_n and polydispersity index (PDI) of the CS were: 1) 82.5% DDA M_n 45 kDa PDI 1.83, 2) 80.7% DDA M_n 35 kDa PDI 1.81,

3) 80.5% DDA M_n 49 kDa PDI 1.97, 4) 84.8% DDA M_n 32 kDa PDI 1.90 and 5) 84.6% DDA M_n 55 kDa PDI 1.95 (**Table 7.1**). These ranges of CS DDA and M_n were chosen based on the precision with which the deacetylation and depolymerization processes can be controlled. CS were dissolved in nuclease-free water and acid overnight at room temperature with sufficient HCl (Fluka, Product N° 1135328) added to protonate 60% of glucosamine groups. Trehalose (Life Sciences, Product N° TDH033) was added as lyoprotectant and calcium chloride ($CaCl_2$, Spectrum, Product N° CA95032) was added as a clot activator to final concentrations of 1% (w/v) and 42.2 mM respectively. The solutions were sterilized with a 0.22 µm polyvinylidene difluoride filter (Millipore) and dispensed into individual 3 mL sterile glass vials (1-mL per vial) for freeze-drying using a MillRock stoppering freeze-drier (LAB series). The freeze-drying process was divided into 3 phases: 1) ramped freezing to -40°C in 1 hour, isothermal for 2 hours at -40°C (without applying vacuum), 2) -40°C for 48 hours, at 100 millitorrs, 3) ramped heating to 30°C in 12 hours, isothermal for 6 hours at 30°C, at 100 millitorrs.

Table 7.1 Properties of the CS used in the study.

Degree of deacetylation (DDA)	**Number average molar mass (M_n)**	**Polydispersity index (PDI)**
82.5%	45 kDa	1.83
80.7%	35 kDa	1.81
80.5%	49 kDa	1.97
84.8%	32 kDa	1.90
84.6%	55 kDa	1.95

7.2.2 Isolation of platelet-rich plasma preparations

The male subject enrolled in this research responded positively to an Informed Consent Form (Certificate #CÉR-15/16-17 dated Jan 28th, 2016) which was approved by the Polytechnique Montreal institutional committee (Comité d'éthique à la recherche avec des êtres humains). Blood was drawn from the same donor twice; once to isolate PRP using the ACE EZ-PRP system, and once to isolate PRP using the following systems: 1) Arthrex Angel set at 2% hematocrit, 2) Arthrex Angel set at 7% hematocrit, 3) Harvest SmartPrep 2, 4) RegenLab RegenKit-BCT, 5) RegenLab RegenKit-THT, 6) Arthrex ACP double syringe system. Isolation protocols are further described in **Table 7.2**. Complete blood count analysis was performed on whole blood and PRP preparations using the Advia 120 hematology system (Siemens).

Table 7.2 Characteristics of the different PRP preparations used for the study.

Device name	Company	Type of PRP	Hematocrit setting	Blood drawn (mL)	Centrifugal force (rpm) & time (min)	Features and method of preparation	Final volume (mL)
ACE EZ-PRP	ACE Surgical Supply	Leucocyte-rich	Unavailable	10 mL	1. 1300 rpm for 10 min 2. 2000 rpm for 10 min	Manual	1.5 mL per tube; 4 tubes processed
Angel	Arthrex	Leukocyte-reduced	2% hematocrit	120 mL	Centrifugation for 22 min	Automated, Cellular photospectrometry and fractionation	6 mL
Angel	Arthrex	Leucocyte-rich	7% hematocrit	60 mL	Centrifugation for 18 min	Automated, Cellular photospectrometry and fractionation	6 mL
SmartPrep 2	Harvest Technologies	Leucocyte-rich	Unavailable	60 mL	1. 2500 rpm for 4 min 2. 2300 rpm for 10 min	Automated	6 mL
RegenKit-BCT	RegenLab	Leukocyte-reduced	Unavailable	8 mL	3500 rpm for 5 min	Automated, Thixotropic gel	2.5 mL per tube; 3 tubes processed
RegenKit-THT	RegenLab	Leucocyte-rich	Unavailable	8 mL	3500 rpm for 9 min	Automated, Thixotropic gel	4 mL per tube; 2 tubes processed

ACP double-syringe system	Arthrex	Leukocyte-reduced	Unavailable	16 mL	1500 rpm for 5 min	Automated	6 mL

7.2.3 Solubilization of freeze-dried CS formulations

Each 1 mL cake was solubilized with 1 mL PRP, hand-shaken vigorously for 10 seconds and different performance characteristics were immediately assessed (**Figure 7.1**). All five different CS formulations were solubilized with each PRP preparation, producing n=5 CS-PRP samples per PRP preparation. Controls were prepared by recalcifying PRP to a final concentration of 42.2mM $CaCl_2$, yielding n=1 PRP control per PRP preparation.

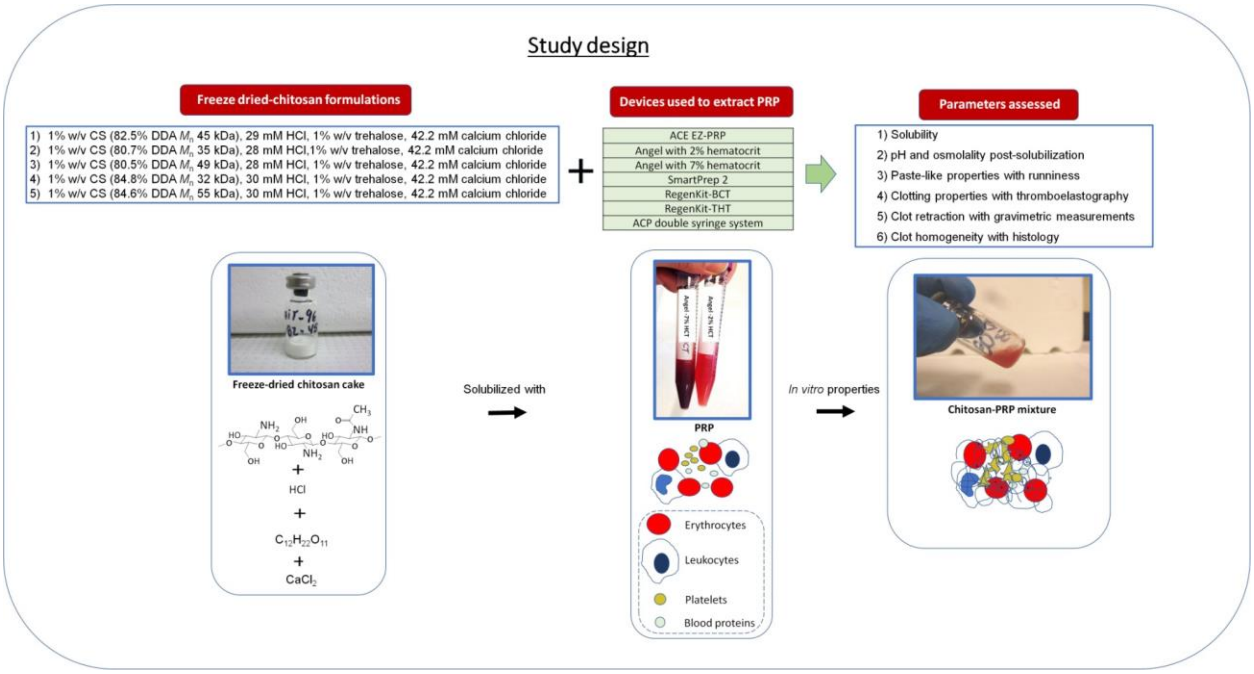

Figure 7.1 Study design. Five different CSs (with Mn ranging from 32 to 55 kDa and DDA ranging from 80.5 to 84.8%) were used to prepare freeze-dried formulations that also contained trehalose as lyoprotectant and calcium chloride as clot activator. Freeze-dried cakes were solubilized with 7 different PRP preparations (Angel with 2% hematocrit and Angel with 7% hematocrit are pictured here). Performance characteristics of the solubilized CS-PRP mixtures were assessed in vitro.

7.2.4 Assessment of formulation paste-like properties

A previously developed runniness test was used to assess paste-like properties[12]. Briefly, a 40 µl drop of each CS-PRP formulation was pipetted onto a rigid piece of plastic fixed at 38 degrees to horizontal, pictures were acquired after 10 minutes and the drop mobility was measured using Image J 1.47v. Note that in this assay water runs off the plate and has a runniness exceeding 310 mm.

7.2.5 Assessment of formulation coagulation

360 µl of each CS-PRP formulation was loaded into a standard specimen thromboelastography (TEG) cup pre-warmed to 37ºC. TEG measurements were carried out for 60 min using a TEG Model 5000 hemostasis analyzer system (Haemoscope Corp).

7.2.6 Assessment of clot retraction

250 µl of each CS-PRP formulation was dispensed into glass tubes and placed in a heat block set at 37°C and left to clot for 60 min. Serum expressed from the clots was removed and % mass lost was measured.

7.2.7 Assessment of clot homogeneity

CS-PRP clots were fixed in 10% neutral buffered formalin (NBF), paraffin-embedded, sectioned at 5 µm using a RM2155 microtome (Leica) and stained with Fast Green/Iron Hematoxylin. Stained slides were scanned at 40X with a Nanozoomer RS scanner NDPView (Hamamatsu, Japan) and NDPView (Hamamatsu) was used to export images.

7.2.8 Statistical analysis

All analyses were performed with SAS Enterprise Guide 7.1 and SAS 9.4. For each PRP preparation, data obtained with the 5 different CS were averaged (n=5) and compared to its

corresponding recalcified PRP control (n=1). Data are presented as either dots (for the PRP controls) or boxes where median (line); Box: 25th and 75th percentile; Whisker: Box to the most extreme point within 1.5 interquartile range. Correlations between the different performance criteria assessed and CS M_n, CS DDA, PRP platelet content, PRP leukocyte content and PRP erythrocyte content were analyzed by calculating the Pearson correlation coefficients. p-values < 0.05 were considered significant.

7.3 Results

7.3.1 There were important differences in the properties of the different PRP preparations

The lowest platelet concentration was obtained with the RegenLab BCT system (207 X 10E9/L, 1.0X that of whole blood), and the highest platelet concentration was obtained with the Harvest SmartPrep 2 system (905 X 10E9/L, 4.3X that of whole blood) (Erreur ! Source du renvoi i ntrouvable. and **Figure 7.2**). Similarly, the lowest leukocyte concentration was obtained with the RegenLab BCT system (0.3 X 10E9/L, 0.1X that of whole blood), and the highest leukocyte concentration was obtained with the Harvest SmartPrep 2 system (11.5 X 10E9/L, 2.4X that of whole blood) (Erreur ! Source du renvoi introuvable. and **Figure 7.2**). Again, the lowest erythrocyte concentration was obtained with the RegenLab BCT system (0.02 X 10E12/L, 0.002X that of whole blood), and the highest erythrocyte concentration was obtained with the Harvest SmartPrep 2 system (2.0 X 10E12/L, 0.4X that of whole blood) (Erreur ! Source du renvoi introuvable. and **Figure 7.2**). Erythrocyte concentration determined the color of the different PRP preparations, ranging from pale yellow to dark red (**Figure 7.2.d**).

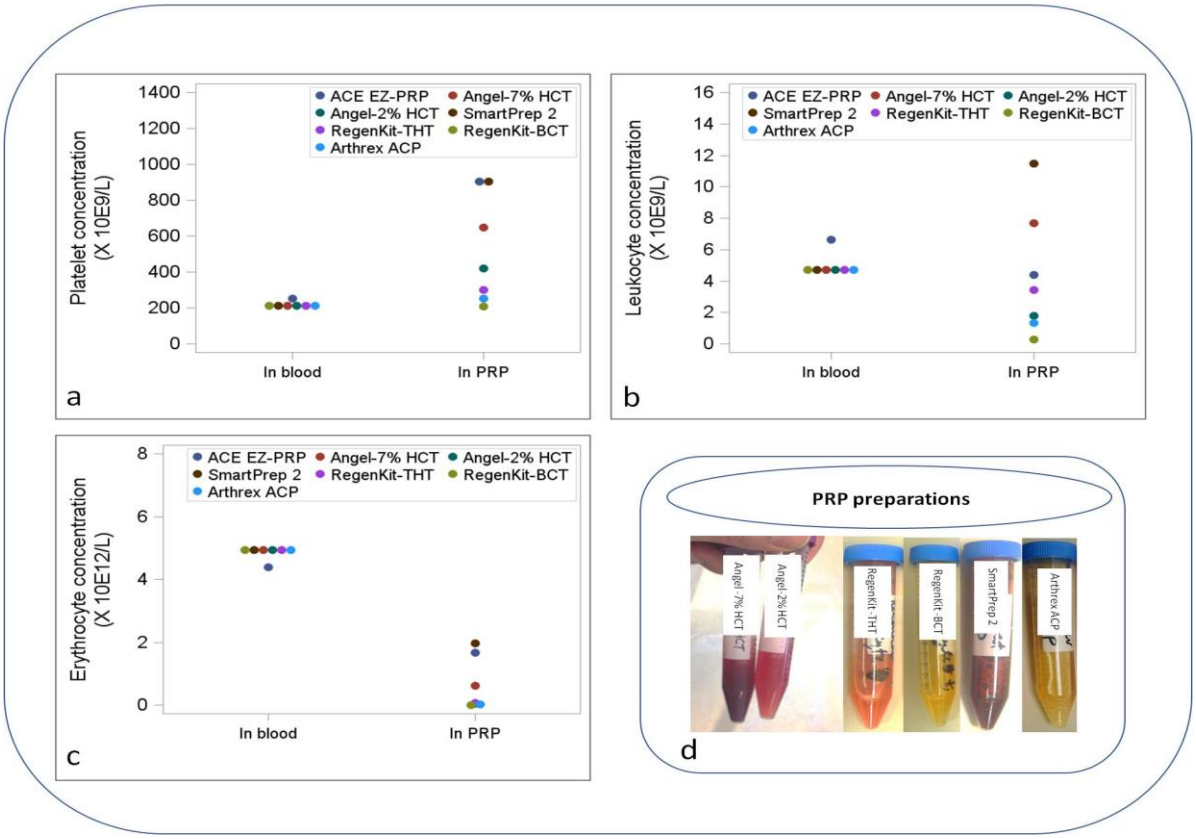

Figure 7.2 Complete blood count (CBC) analysis of whole blood and resultant PRP from each system is shown in panels a (platelet concentration), b (leukocyte concentration) & c (erythrocyte concentration). Macroscopic appearance of different PRP preparations is shown in panel d. Erythrocyte concentration (panel c) influenced the colour of PRP preparations (panel d).

Table 7.3 Complete blood count (CBC) analysis in whole blood and different PRP preparations.

Device name	Platelets (X 10E9/L)			Leukocytes (X 10E9/L)			Erythrocytes (X 10E12/L)		
	Whole blood	PRP	Fold change	Whole blood	PRP	Fold change	Whole blood	PRP	Fold change
ACE EZ-PRP	254	905	3.6	6.7	4.4	0.7	4.4	1.7	0.380
Angel-2% HCT	212	419	2.0	4.7	1.8	0.4	5.0	0.05	0.010
Angel-7% HCT	212	650	3.1	4.7	7.7	1.6	5.0	0.6	0.124
SmartPrep 2	212	903	4.3	4.7	11.5	2.4	5.0	2.0	0.402

RegenKit-BCT	212	207	1.0	4.7	0.3	0.1	5.0	0.01	0.002
RegenKit-THT	212	299	1.4	4.7	3.4	0.7	5.0	0.08	0.016
Arthrex ACP	212	253	1.2	4.7	1.4	0.3	5.0	0.02	0.004

7.3.2 CS cakes were soluble in all PRP preparations tested

Macroscopically, the cakes were white, homogenous and were slightly retracted from the vial walls following lyophilisation. Cake solubility was rated as excellent in most cases, except for the cakes prepared with CS M_n 55 kDa, which had to be shaken for a few extra seconds to become completely homogenous. pH of the CS formulations was between 6.27 and 6.47 before freeze-drying. Osmolality of the CS formulations was between 147 and 192 mOsm prior to freeze-drying. Post-solubilization, pH of the CS-PRP formulations was lower than physiological (from average 6.56 to average 7.12), and always lower than that of the recalcified PRP preparations (from 7.10 to 8.10) (**Figure 7.3.a**). Post-solubilization, osmolality of the CS-PRP formulations was higher than physiological (from average 389 mOsm to average 448 mOsm) and higher than that of the recalcified PRP preparations (from 282 mOsm to 320 mOsm) (**Figure 7.3.b**).

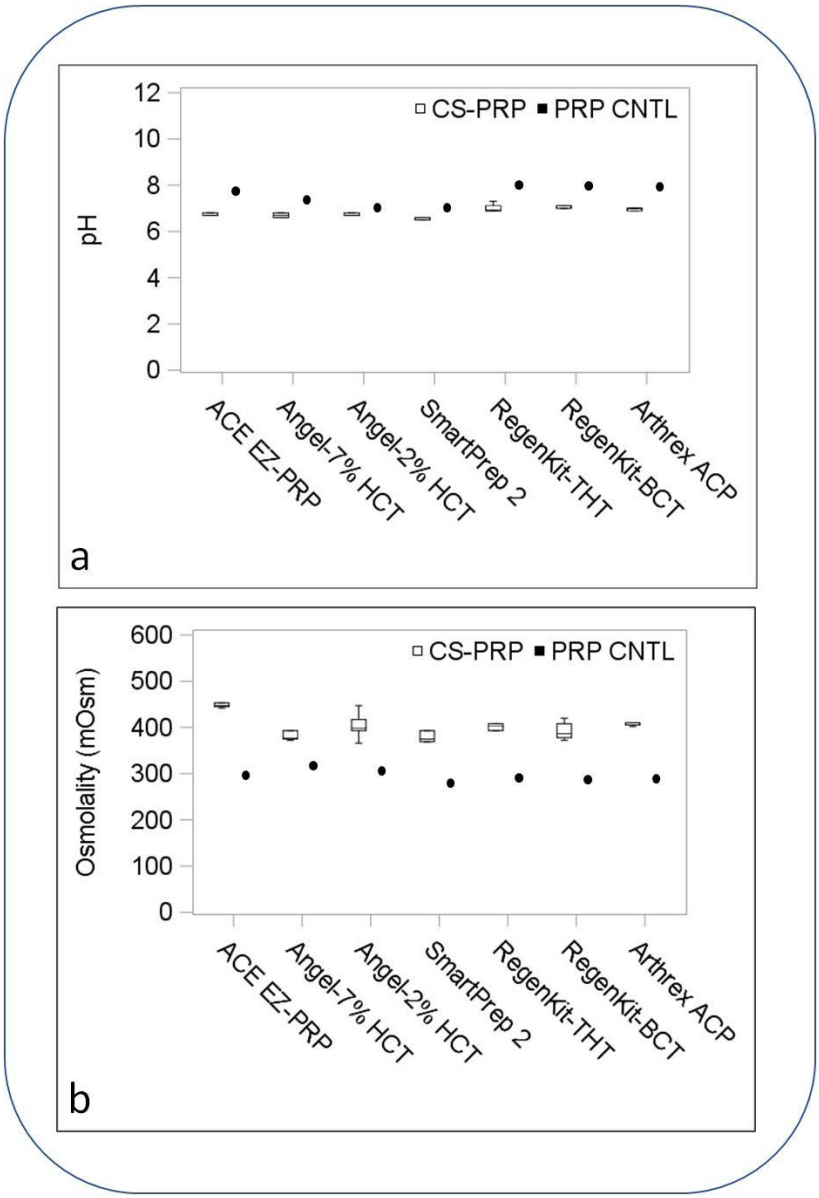

Figure 7.3 pH (panel a) and osmolality (panel b) of formulations post-solubilization with PRPs isolated with the different devices. pH of CS-PRP formulations was lower than recalcified PRP controls (a). Osmolality of CS-PRP formulations was higher than recalcified PRP controls (b). Data are presented as box plots where median box indicates the 25th and 75th percentile; Whisker extends to the most extreme data point within 1.5 times the interquartile range of data. n=5 samples for each type of CS-PRP formulation and n=1 for each recalcified PRP control.

7.3.3 CS-PRP formulations were more paste-like than PRP controls

A representative example illustrating runniness of CS-PRP (prepared with CS 84.6% DDA M_n 55 kDa and ACE EZ-PRP) and its recalcified PRP control is shown in Erreur ! Source du renvoi introuvable.**.a**. Runniness of the CS-PRP formulations (from average 7 mm to average 32 mm) was always lower than that of the recalcified PRP controls (from 25 mm to 86 mm).

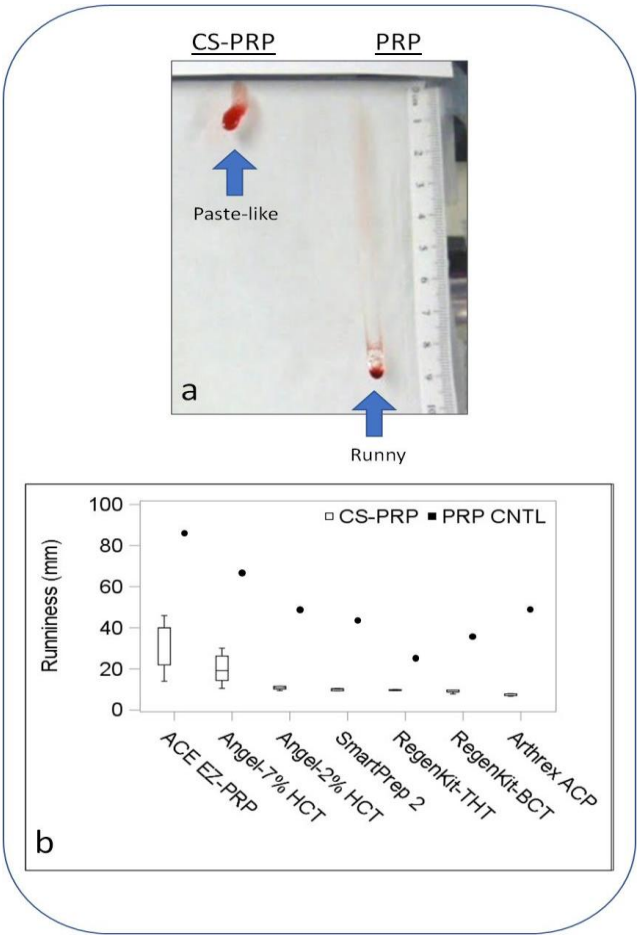

Figure 7.4 Runniness of the CS-PRP and PRP formulations was assessed on an inclined plate. Panel a shows runniness of CS-PRP and a recalcified PRP control prepared with CS 84.6% DDA M_n 55 kDa and ACE EZ-PRP as an example. CS-PRP formulations were paste-like and less runny than the recalcified PRP controls panel b). Note that in this assay water runs off the plate and has a runniness exceeding 310 mm. Data are presented as box plots where median box indicates the 25th and 75th percentile; Whisker extends to the most extreme data point within 1.5 times the interquartile range of data. n=5 samples for each type of CS-PRP formulation and n=1 for each recalcified PRP control.

7.3.4 CS-PRP formulations clotted rapidly with all PRP preparations tested

Representative TEG tracings obtained for formulations prepared with CS 84.6% DDA M_n 55 kDa and RegenLab RegenKit-BCT or RegenKit-THT and their recalcified PRP controls are shown in **Figure 7.5.b**. Clot reaction time of the CS-PRP formulations (from average 2 min to average 9 min) was lower than that of the recalcified PRP preparations (from 32 min to 57 min) (**Figure 7.5.c**). Clot maximal amplitude of the CS-PRP formulations was between 42 mm and 84 mm (Figure 5d). Recalcification of the leukocyte-reduced PRP preparations was insufficient to induce coagulation in this dynamic system, while the leukocyte-rich PRP preparations clotted (**Figure 7.5.c&d).** Of note, the Harvest SmartPrep 2 control had barely started to clot when the assay was terminated so that its clot reaction time was high (57 minutes) (**Figure 7.5.c**) and its clot maximal amplitude was low (11 mm) (**Figure 7.5.d**).

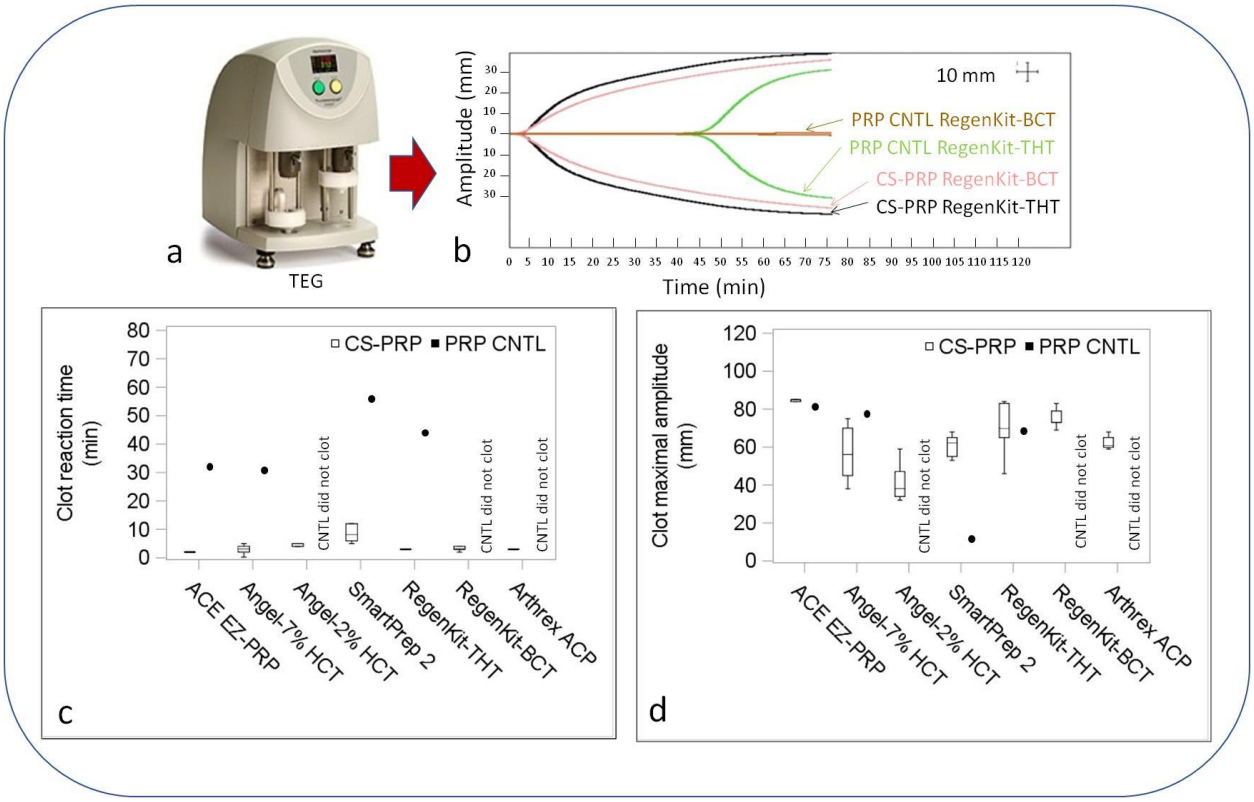

Figure 7.5 A thrombelastograph (panel a) was used to assess clotting properties of formulations *in vitro*. Panel b shows TEG traces obtained for formulations prepared with CS 84.6% DDA M_n 55 kDa and RegenKit-BCT or RegenKit-THT as an example. Clot reaction time (R) is the time in

minutes from initiation of the tracing to the point where branches have diverged by 2 mm. Maximal amplitude (MA) is the maximal distance in mm between the two diverging branches and corresponds to clot strength. All CS-PRP formulations clotted and had average clot reaction times between 2 and 9 minutes (panel c). Clot reaction times of the recalcified leukocyte-rich PRP controls were greater, between 32 and 57 minutes (panel c). CS-PRP formulations had average clot maximal amplitude above 42 mm (d). Recalcification of the leukocyte-reduced PRP controls with 42.2 mM was insufficient to induce clotting in this dynamic system (c & d). Recalcified SmartPrep 2 PRP control had barely started to clot when the assay was terminated so that its clot reaction time was high (57 minutes) (c) and its clot maximal amplitude was low (11 mm) (d). Data are presented as box plots where median box indicates the 25^{th} and 75^{th} percentile; Whisker extends to the most extreme data point within 1.5 times the interquartile range of data. n=5 samples for each type of CS-PRP formulation and n=1 for each recalcified PRP control.

7.3.5 CS-PRP hybrids did not express any serum with all PRP preparations tested

Images of a CS-PRP hybrid clot prepared with CS 84.8% DDA M_n 32 kDa and Harvest SmartPrep 2 and its recalcified PRP control are shown in **Figure 7.6.a**. Images of a CS-PRP hybrid clot prepared with CS 82.5% DDA M_n 45 kDa and Arthrex ACP and its recalcified PRP control are shown in Figures 6b. The absence/presence of erythrocytes in the two PRP preparations is easily observed by the yellow/red hue of the preparation. None of the CS-PRP formulations expressed serum and the hybrid clots remained voluminous after clotting for 1 hour at 37^oC (**Figure 7.6.a, b & c**). Recalcification with 42.2 mM $CaCl_2$ was sufficient to induce coagulation of all PRP preparations in this static assay in glass tubes, and PRP clots lost up to 82% of their original mass through serum exudation upon clotting (**Figure 7.6.a, b & c**).

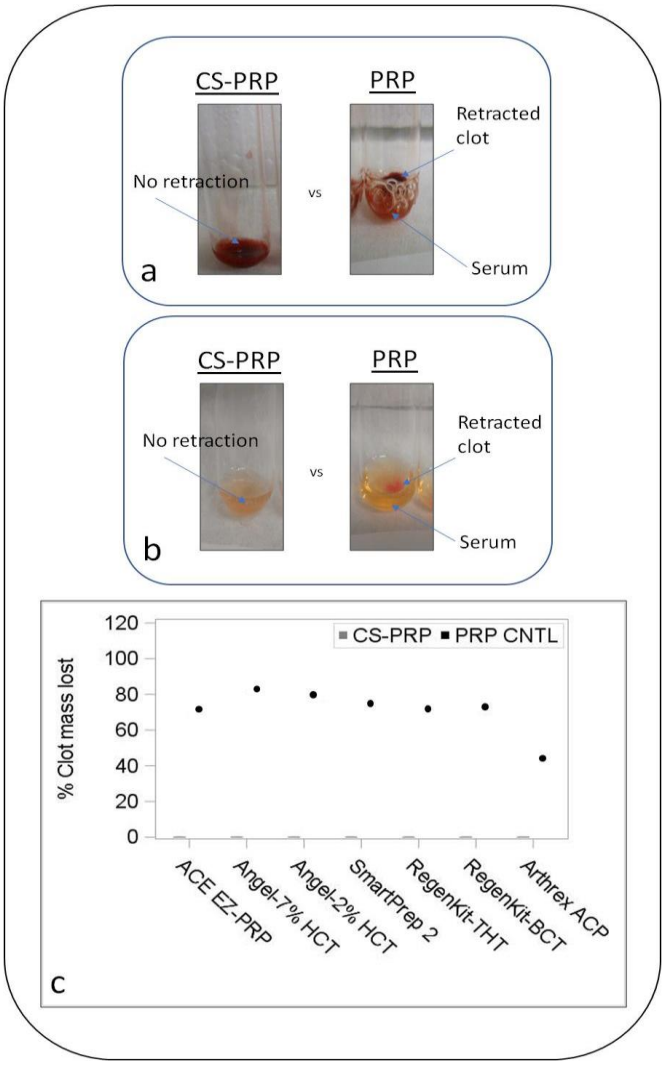

Figure 7.6 Clot retraction was assessed by gravimetric measurement. Panel a show a CS-PRP hybrid clot and a recalcified PRP control prepared with CS 84.8% DDA M_n 32 kDa and SmartPrep 2 as an example. Panel b shows a CS-PRP hybrid clot and a recalcified PRP control prepared with CS 82.5% DDA M_n 45 kDa and Arthrex ACP as an example. All CS-PRP hybrid clots remained voluminous after clotting for 1 h at 37°C and did not express any serum (panel c). Recalcification with 42.2 mM $CaCl_2$ was sufficient to induce coagulation of all PRP controls in this static assay. Recalcified PRP controls expressed a lot of serum upon clotting and lost 43% to 82% of their original mass upon clotting (panel c). n=5 samples for each type of CS-PRP formulation and n=1 for each recalcified PRP control.

7.3.6 Chitosan dispersion was homogenous within all hybrid clots

Histological sections of a CS-PRP hybrid clot prepared with CS 84.8% DDA M_n 32 kDa and Arthrex Angel with 7% hematocrit and its recalcified PRP control are shown in **Figure 7.7a-d.** Histological sections of a CS-PRP hybrid clot prepared with CS 84.8% DDA M_n 32 kDa and Arthrex Angel with 2% hematocrit and its recalcified PRP control are shown in **Figure 7.7e-h**. As expected, erythrocytes were more abundant and densely packed in clots prepared with Arthrex Angel with 7% hematocrit compared to Arthrex Angel with 2% hematocrit. CS dispersion was homogenous within most CS-PRP clots (**Figure 7.7 a, b, e & f),** while a minority of clots contained some larger CS aggregates.

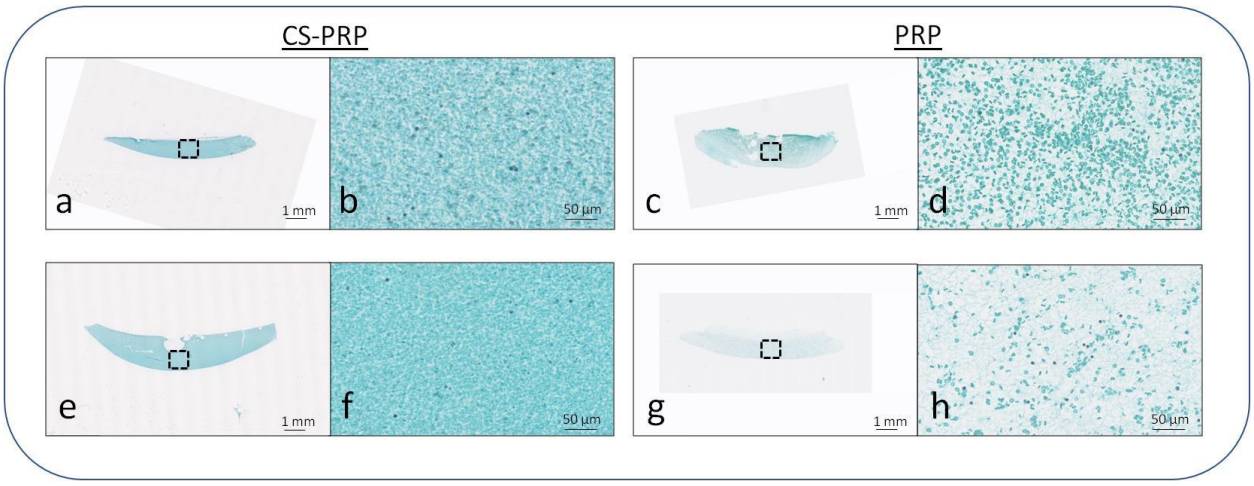

Figure 7.7 Clot homogeneity was assessed with Fast Green and Iron Hematoxylin staining of paraffin sections. Panels a & b show a CS-PRP hybrid clot prepared with CS 84.8% DDA M_n 32 kDa and Angel with 7% hematocrit as an example and panels c & d show the recalcified PRP control. Panels e & f show a CS-PRP hybrid clot prepared with CS 84.8% DDA M_n 32 kDa and Angel with 2% hematocrit as an example and panels g & h show the recalcified PRP control. Dispersion of CS within the hybrid clots was usually homogenous (b & f). Erythrocytes were more abundant in clots prepared with Angel with 7% hematocrit compared to Angel with 2% hematocrit (compare panel d to h). Outlines in panels a, c, e & g show where higher magnification images b, d, f & h were acquired.

7.3.7 Chitosan and platelet-rich plasma properties did not affect the in vitro performance characteristics of the CS-PRP implants

There were no significant correlations between runniness, clot reaction, and clot maximal amplitude of the CS-PRP hybrids and CS M_n, CS DDA, platelet concentration, leukocyte concentration and erythrocyte concentration (**Erreur ! Source du renvoi introuvable.**). In a ddition, there were no significant correlations between runniness, clot reaction, and clot maximal amplitude of the recalcified PRP controls and platelet concentration, leukocyte concentration and erythrocyte concentration (**Erreur ! Source du renvoi introuvable.**).

Table 7.4 Pearson correlation coefficients r and corresponding p values between the performance characteristics of the CS-PRP formulations and the properties of the CS and PRP preparations used to prepare the formulations. * % clot mass lost was 0 for all CS-PRP formulations assessed; N/A = Non -applicable.

Performance characteristic assessed	**Chitosan M_n**	**Chitosan DDA**	**Platelet concentration (X 10E9/L)**	**Leukocyte concentration (X 10E9/L)**	**Erythrocyte concentration (X 10E9/L)**
Runniness (mm)	-0.161 *(0.357)*	-0.138 *(0.430)*	0.354 *(0.059)*	0.330 *(0.070)*	0.139 *(0.457)*
Clot reaction time (min)	-0.173 *(0.319)*	0.235 *(0.174)*	0.008 *(0.965)*	0.218 *(0.230)*	-0.007 *(0.969)*
Clot maximal amplitude (mm)	0.289 *(0.093)*	-0.105 *(0.550)*	0.115 *(0.510)*	-0.095 *(0.586)*	0.240 *(0.165)*
Clot retraction (% clot mass lost) *	N/A	N/A	N/A	N/A	N/A

Table 7.5 Pearson correlation coefficients r and corresponding p values between the performance characteristics of the recalcified PRP controls and the properties of the PRP preparations.

Performance characteristic assessed	Platelet concentration (X 10E9/L)	Leukocyte concentration (X 10E9/L)	Erythrocyte concentration (X 10E9/L)
Runniness (mm)	0.662 *(0.105)*	0.206 *(0.657)*	0.513 *(0.239)*
Clot reaction time (min)	0.048 *(0.952)*	0.567 *(0.433)*	0.315 *(0.685)*
Clot maximal amplitude (mm)	-0.347 *(0.653)*	-0.819 *(0.181)*	-0.547 *(0.453)*
Clot retraction (% clot mass lost)	0.389 *(0.388)*	0.386 *(0.393)*	0.242 *(0.602)*

7.4 Discussion

The main objectives of the current study were to define CS specifications for the previously developed technology[12] and assess its compatibility with the various types of PRPs that can be isolated with commercial systems. We found that *in vitro* performance of CS-PRP implants was similar for all PRP preparations tested, so that our starting hypothesis was supported. We also found that freeze-dried cakes prepared with CS of DDA between 80.5-84.8% and M_n between 32-55 kDa had acceptable performance characteristics when solubilized with PRP. In the current study, two families of PRPs were prepared according to the definition of Dohan Ehrenfest[3]: Leukocyte-rich PRPs (ACE EZ-PRP, Arthrex Angel with 7% hematocrit, Harvest SmartPrep 2 and RegenLab RegenKit-THT) and leukocyte-reduced PRPs (Arthrex Angel with 2% hematocrit, RegenLab RegenKit-BCT and Arthrex ACP). As expected, and earlier shown by others[7,8,20-23], the various PRP preparation devices varied in their abilities to concentrate platelets, leukocytes and erythrocytes (Erreur ! Source du renvoi introuvable. and **Figure 7.2**). This might explain the significant variability in the clinical effectiveness of PRP which has been published in the literature and supports the notion that PRP should always be characterized when used. Variability in donor blood parameters and PRP's poor stability *in vivo*[24] are two other possible reasons why results

have been inconsistent so far. Although some authors have stated that PRP should possess a 3 to 5 -fold increase over baseline in platelet concentration (~1 million platelet/µl) to be effective[25], the optimal PRP recipe has yet to identified, and could very well be different for different indications.

Interestingly, recalcified PRP controls performed differently from one another with respect to runniness, coagulation and clot retraction in the current study, and this could not be attributed to platelet, leukocyte and erythrocyte concentrations individually. Other properties that were not assessed here might control performance characteristics or a combination of several properties. One unexpected finding in this study is that recalcification with 42.2 mM was insufficient to induce clotting of the leukocyte-poor PRP preparations in the dynamic thromboelastography assay, which suggests that leukocytes also contribute to coagulation, possibly through release of coagulation factors or by contributing to platelet activation[26]. In addition, the leukocyte-poor PRP preparations were also the ones that had the lowest concentration of erythrocytes, which are believed to also participate in thrombin generation[27]. We should highlight that this finding was restricted to the thromboeastography assay, that higher concentrations of $CaCl_2$ or the addition of another platelet agonist might have induced coagulation, and that the thromboelastrography assay is not representative of the *in vivo* situation.

Combinations of freeze-dried CS and PRP have been described by other authors[28-30], but, to our knowledge, these have all been solid scaffolds intended to remain solid for implantation. In contrast, our aim here was to solubilize freeze-dried CS formulation with PRP so that they become liquid and coagulate post-injection. As expected, CS-PRP formulations had pH lower than their respective PRP controls and lower than physiological (**Figure 7.3**), due to the presence of acid, but we do not expect that this would negatively affect tissues *in vivo*. In addition, osmolality of CS-PRP formulations was higher than physiological and their respective PRP controls (**Figure 7.3**) since the cakes contained excipients (trehalose and $CaCl_2$), but not enough to impair coagulation and associated events as previously shown[12]. Regardless of the PRP preparation used to solubilize the freeze-dried cakes, CS-PRP formulations were all paste-like due to the presence of the polysaccharide (**Erreur ! Source du renvoi introuvable.**) and clotted rapidly since CS contributes t o platelet activation in this system[13], and possibly through inducing red blood cell agglutination[31,32] (**Figure 7.5).** Resulting CS-PRP clots did not retract post-coagulation (**Figure 7.6**) due to CS ability to physically impair platelet-mediated clot retraction[13] and were for the most part homogenous (**Figure 7.7**), since the CS selected to prepare the cakes had M_n close to 40 kDa, which has been shown to result in homogenous distribution of CS throughout the blood components[12].

Since rather narrow ranges of CS DDA and M_n were selected, it was not surprising to find that all CS-PRP formulations tested behaved similarly *in vitro*. However, although the *in vitro*

performance characteristics assessed were similar for all PRP preparations tested, we expect that other assessments would most likely show differences between the various PRP preparations. For example, release of platelet-derived growth factors and inflammatory factors and cytokines would be expected to depend on the cellular profile of the PRP preparations used to solubilize the formulations[4-8], and this could very well modulate repair events *in vivo*. Further studies are required to determine the bioactivity level of the CS-PRP formulations and how this would influence the repair process. It is possible that some PRP preparations would be preferable for indications, while others should be avoided.

This study had some limitations. First, although a single donor was used to generate all PRP preparations in order to avoid inter-individual variability and allow direct comparisons between the different separation systems, it would be useful to increase sample size and isolate PRP from additional donors. Second, we chose the commercial isolation systems based upon their availability and we are aware that other systems are also widely used in the clinic. Third, the release of platelet-derived growth factors and inflammatory factors and cytokines was not measured in this study. Fourth, the runniness test is insufficient to fully characterize viscoelastic behavior of the CS-PRP formulations. Fifth, the study was limited to an *in vitro* assessment of product performance. The current study allowed us to establish the CS specifications (DDA and M_n) for the product and that it is compatible with different PRP preparations isolated with commercial systems. However, further *in vitro* and *in vivo* studies are necessary to understand how the properties of the PRP preparations used to solubilize the CS will affect bioactivity and healing potential of the implants.

7.5 Conclusion

PRP remains controversial in the orthopaedic field, and inconsistent results in the literature may have resulted from inter-individual variability in blood parameters, the heterogeneity of the PRP preparations used, or its poor stability *in vivo*. Freeze-dried CS formulations containing a lyoprotectant and a clot activator can be solubilized in different types of PRP preparations to yield injectable implants that are paste-like and coagulate rapidly to form homogenous CS-PRP hybrid clots that remain voluminous. These could possibly be used as implants to treat different orthopaedic conditions in the future.

ACKNOWLEDGEMENTS

We acknowledge the technical contributions of Vincent Darras and the funding sources (Canadian Institutes of Health Research, Canada Foundation for Innovation, Groupe de Recherche en Sciences et Technologies Biomédicales, Natural Sciences and Engineering Research Council of Canada and Ortho Regenerative Technologies Inc).

Author Contributions

The authors made substantial contributions in designing the study (LG, AC, ML and MDB), gathering the data (LG, AC, ML, MLN, and MDB) and drafting the article (LG, AC, ML, MLN, CDH and MDB). All the authors approved the submitted manuscript.

Conflict of Interest

AC. ML. CDH. and MDB. hold shares; CDH. and MDB. are Directors of Ortho Renegerative Technologies Inc.

REFERENCES

[1] Marx RE, Carlson ER, Eichstaedt RM, Schimmele SR, Strauss JE, Georgeff KR. Platelet-rich plasma: Growth factor enhancement for bone grafts. Oral surgery, oral medicine, oral pathology, oral radiology, and endodontics 1998; 85(6): 638-46.

[2] Wang D, Rodeo SA. Platelet-Rich Plasma in Orthopaedic Surgery: A Critical Analysis Review. JBJS reviews 2017; 5(9): e7.

[3] Dohan Ehrenfest DM, Rasmusson L, Albrektsson T. Classification of platelet concentrates: from pure platelet-rich plasma (P-PRP) to leucocyte- and platelet-rich fibrin (L-PRF). Trends in biotechnology 2009; 27(3): 158-67.

[4] McCarrel T, Fortier L. Temporal growth factor release from platelet-rich plasma, trehalose lyophilized platelets, and bone marrow aspirate and their effect on tendon and ligament gene

expression. Journal of orthopaedic research : official publication of the Orthopaedic Research Society 2009; 27(8): 1033-42.

[5] McCarrel TM, Minas T, Fortier LA. Optimization of leukocyte concentration in platelet-rich plasma for the treatment of tendinopathy. The Journal of bone and joint surgery American volume 2012; 94(19): e143(1-8).

[6] Braun HJ, Kim HJ, Chu CR, Dragoo JL. The effect of platelet-rich plasma formulations and blood products on human synoviocytes: implications for intra-articular injury and therapy. The American journal of sports medicine 2014; 42(5): 1204-10.

[7] Castillo TN, Pouliot MA, Kim HJ, Dragoo JL. Comparison of Growth Factor and Platelet Concentration From Commercial Platelet-Rich Plasma Separation Systems. American Journal of Sports Medicine 2011; 39(2): 266-71.

[8] Parrish WR, Roides B, Hwang J, Mafilios M, Story B, Bhattacharyya S. Normal platelet function in platelet concentrates requires non-platelet cells: a comparative in vitro evaluation of leucocyte-rich (type 1a) and leucocyte-poor (type 3b) platelet concentrates. BMJ Open Sport & Exercise Medicine 2016; 2(1).

[9] Dragoo JL, Braun HJ, Durham JL, Ridley BA, Odegaard JI, Luong R, et al. Comparison of the acute inflammatory response of two commercial platelet-rich plasma systems in healthy rabbit tendons. The American journal of sports medicine 2012; 40(6): 1274-81.

[10] Fitzpatrick J, Bulsara M, Zheng MH. The Effectiveness of Platelet-Rich Plasma in the Treatment of Tendinopathy: A Meta-analysis of Randomized Controlled Clinical Trials. The American journal of sports medicine 2017; 45(1): 226-33.

[11] Liu X, Ma L, Mao Z, Gao C. Chitosan-Based Biomaterials for Tissue Repair and Regeneration. Adv Polym Sci 2011; 244: 81–128.

[12] Chevrier A, Darras V, Picard G, Nelea M, Veilleux D, Lavertu M, et al. Injectable chitosan-platelet-rich plasma (PRP) implants to promote tissue regeneration: In vitro properties, in vivo residence, degradation, cell recruitment and vascularization. Journal of tissue engineering and regenerative medicine 2017; In Press.

[13] Deprés-Tremblay G, Chevrier A, Tran-Khanh N, Nelea M, Buschmann MD. Chitosan inhibits platelet-mediated clot retraction, increases platelet-derived growth factor release, and

increases residence time and bioactivity of platelet-rich plasma in vivo. Biomedical materials (Bristol, England) 2017; 13(1): 015005.

[14] Deprés-Tremblay G, Chevrier A, Hurtig MB, Snow M, Rodeo S, Buschmann MD. Freeze-dried chitosan-platelet-rich plasma implants for rotator cuff tear repair: Pilot ovine studies. ACS Biomaterials Science & Engineering 2017; In press.

[15] Deprés-Tremblay G, Chevrier A, Buschmann MD, editors. Freeze-dried chitosan-PRP in a rabbit model of rotator cuff repair. Transactions Orthopaedic Research Society; 2017 San Diego, CA, USA.

[16] Ghazi zadeh L, Chevrier A, Hurtig MB, Farr J, Rodeo S, Hoemann CD, et al. Freeze-dried chitosan-PRP injectable surgical implants for meniscus repair: Pilot feasibility studies in ovine models. Regenerative Medicine and Therapeutics 2017; 1(1): 16-29.

[17] Dwivedi G, Chevrier A, Hoemann CD, Buschmann MD. Freeze dried chitosan/platelet-rich-plasma implants improve marrow stimulated cartilage repair in rabbit chronic defect model Transactions Orthopaedic Research Society; San Diego, CA, USA2017.

[18] Lavertu M, Xia Z, Serreqi AN, Berrada M, Rodrigues A, Wang D, et al. A validated 1H NMR method for the determination of the degree of deacetylation of chitosan. J Pharm Biomed Anal 2003; 32(6): 1149-58.

[19] Nguyen S, Winnik FM, Buschmann MD. Improved reproducibility in the determination of the molecular weight of chitosan by analytical size exclusion chromatography. Carbohydrate Polymers 2009; 75(3): 528-33.

[20] Fitzpatrick J, Bulsara MK, McCrory PR, Richardson MD, Zheng MH. Analysis of Platelet-Rich Plasma Extraction. Variations in Platelet and Blood Components Between 4 Common Commercial Kits. The Orthopaedic Journal of Sports Medicine 2017; 5(1): 2325967116675272

[21] Magalon J, Bausset O, Serratrice N, Giraudo L, Aboudou H, Veran J, et al. Characterization and comparison of 5 platelet-rich plasma preparations in a single-donor model. Arthroscopy : the journal of arthroscopic & related surgery : official publication of the Arthroscopy Association of North America and the International Arthroscopy Association 2014; 30(5): 629-38.

[22] Pochini AC, Antonioli E, Bucci DZ, Sardinha LR, Andreoli CV, Ferretti M, et al. Analysis of cytokine profile and growth factors in platelet-rich plasma obtained by open systems and commercial columns. Einstein (Sao Paulo, Brazil) 2016; 14(3): 391-7.

[23] Degen RM, Bernard JA, Oliver KS, Dines JS. Commercial Separation Systems Designed for Preparation of Platelet-Rich Plasma Yield Differences in Cellular Composition. HSS J 2017; 13(1): 75-80.

[24] Chao FC, Shepro D, Tullis JL, Belamarich FA, Curby WA. Similarities between platelet contraction and cellular motility during mitosis: role of platelet microtubules in clot retraction. Journal of cell science 1976; 20(3): 569-88.

[25] Marx RE. Platelet-rich plasma: evidence to support its use. J Oral Maxillofac Surg 2004; 62(4): 489-96.

[26] Swystun LL, Liaw PC. The role of leukocytes in thrombosis. Blood 2016; 128(6): 753-62.

[27] Whelihan MF, Zachary V, Orfeo T, Mann KG. Prothrombin activation in blood coagulation: the erythrocyte contribution to thrombin generation. Blood 2012; 120(18): 3837-45.

[28] Kutlu B, Aydin RST, Akman AC, Gumusderelioglu M, Nohutcu RM. Platelet-rich plasma-loaded chitosan scaffolds: Preparation and growth factor release kinetics. Journal of Biomedical Materials Research Part B-Applied Biomaterials 2013; 101B(1): 28-35.

[29] Shimojo AA, Perez AG, Galdames SE, Brissac IC, Santana MH. Performance of PRP associated with porous chitosan as a composite scaffold for regenerative medicine. TheScientificWorldJournal 2015; 2015: 396131.

[30] Shimojo AA, Perez AG, Galdames SE, Brissac IC, Santana MH. Stabilization of porous chitosan improves the performance of its association with platelet-rich plasma as a composite scaffold. Materials science & engineering C, Materials for biological applications 2016; 60: 538-46.

[31] Rao SB, Sharma CP. Use of chitosan as a biomaterial: Studies on its safety and hemostatic potential. Journal of biomedical materials research 1997; 34(1): 21-8.

[32] Okamoto Y, Yano R, Miyatake K, Tomohiro I, Shigemasa Y, Minami S. Effects of chitin and chitosan on blood coagulation. Carbohydrate Polymers 2003; 53(3): 337-42.

CHAPTER 8 OPTIMIZATION OF FREEZE-DRYING CYCLES OF CHITOSAN-BASED FORMULATIONS

8.1 Introduction

Lyophilization, or freeze-drying (FD), is a cost-effective and low-temperature dehydration process for the preservation of labile materials for long-term storage at room temperature while maintaining physicochemical and biological properties. FD is a process in which bulk water is frozen and involves the direct transition between the solid and the gaseous state without going through the liquid phase, first by sublimation under vacuum which is followed by desorption (22, 174-176). FD overcomes some of the storage limitations for macromolecules such as peptides or nanoparticles which include chemical instability and reactivity during the storage. The process is useful for the pharmaceutical, biotechnology, and the food industry. Stability of pharmaceutical products, storage, choice of excipients and collapse temperature (T_c) of the formulation is of paramount importance for optimization of FD process. The T_c of a formulation corresponds to the temperature above which the frozen product collapses during FD because of a too high molecular mobility. The T_c is equals to the eutectic temperature (T_{eu}) in the case of solutes that are crystallized in the frozen state or is about 2^o C above the glass transition temperature of the maximally cryoconcentrated phase (T_g') in the case of amorphous solutes. In order to avoid product collapse, the product temperature in the course of the sublimation process should always be lower than T_c. FD product should possess specific favorable features such as stability, short reconstitution time, elegant cake appearance, maintenance of the characteristics, and (near) isotonicity upon reconstitution toward clinical uses. Lyophilization remains a slow and energy-intensive process, and it needs to be optimized (22, 177). The lyophilization process consists of three stages: 1. freezing, 2. primary drying, and 3. secondary drying **Figure 8.1** (175).

- **Freezing (solidification):** Freezing is the first step in which the liquid suspension is cooled, and crystals of ice generated. It represents the main dehydration step of a FD process. Typically, this step takes a few hours and is performed at high chamber pressure (P_c) using a moderate cooling rate (~ 1^{o}C/min) with a final shelf temperature (T_s) below T_c. As the freezing process evolves, ice crystals form and exclude solutes which becomes highly concentrated in a phase referred to as the maximally cryoconcentrated (or freeze-concentrated) phase. Typically, at the end of the freezing

process, more than 99% of water is in the ice phase and the cryoconcentrated phase contains about 20% of water (w/w) for an amorphous product (22).

- **The primary drying (ice sublimation):** This stage involves sublimation of ice from the frozen cake which occurs by decreasing the chamber pressure and increasing the shelf temperature. It is the longest stage of the FD process and its duration can be reduced by optimizing the shelf temperature (T_s) and the chamber pressure (P_c). There are several physicochemical events that occur during this stage: i) heat is transferred from the shelf to the frozen solution via the tray to the vial, ii) the ice sublimes and the water vapor passes through the surface of the sample, iii) the water vapor is transferred from the surface of the product via the chamber to the condenser, then condenses and is deposited on the coils which are cooled continuously. The direction of heat and mass transfer from the shelf to the top of the vial is shown in **Figure 8.2** (22, 173, 174, 175). The sublimation process is endothermic and the product temperature during this phase can thus be significantly lower than the shelf temperature. The rate of sublimation is controlled by the difference between the vapor pressure of ice and the chamber pressure. Since the vapour pressure of ice is strongly dependent upon temperature, a slight temperature increase can significantly accelerate sublimation and reduce primary drying duration. This step is optimized by selecting operating conditions for which product temperature is maintained as high as possible, without inducing any collapse.

- **Secondary drying**: This step involves the removal of water that did not freeze (water in the cryoconcentrated phase) from the cake by desorption. This is performed by raising the temperature of the product by increasing the T_s while taking care of not melting the product by never exceeding the glass transition temperature of the dry cake (increases as water content is reduced). For pharmaceuticals, a residual moisture content of 1% or less is more desired as high moisture contents may cause crystallization of the formulation, post-collapse, or degradation during long-term storage. This step typically takes a few hours. At the end of this stage, chamber of the lyophilizer is backfilled with an inert gas, vials are capped, and the process is finished.

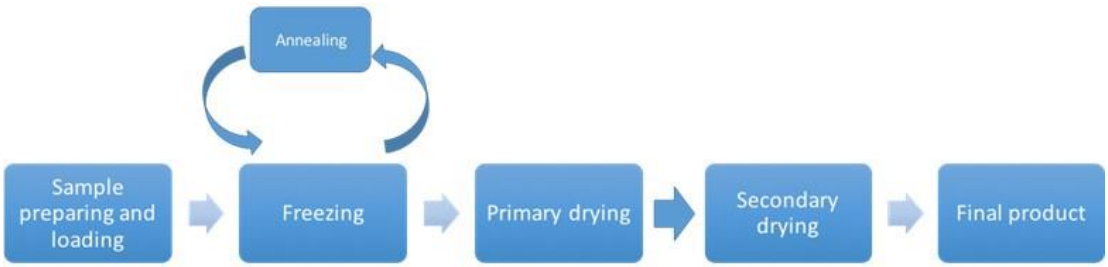

Figure 8.1 Schematic of the freeze-drying process (175).

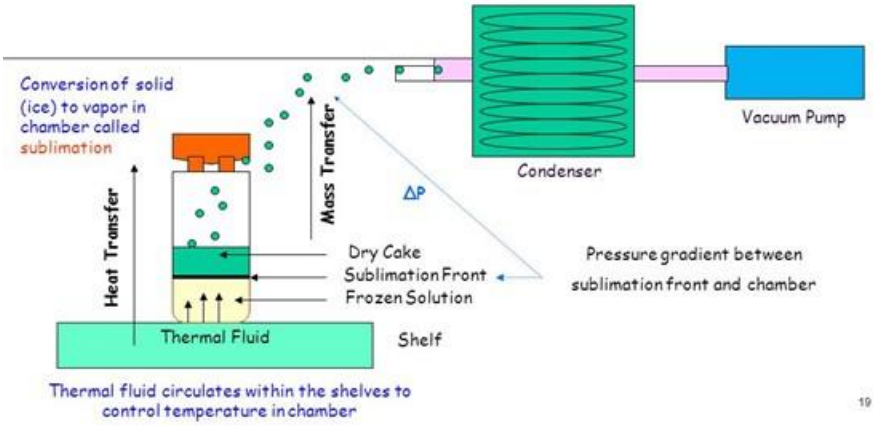

Figure 8.2 The diagram showing the freeze-drying process in a shelf-type instrument (175).

The current freeze-drying cycle duration for chitosan-based formulation is three days and the cycle must be optimized, especially the primary drying step for which the shelf temperature of -40ºC is too low (slow sublimation). The goal of the present study was to optimize and reduce the FD cycle from 3 days to 1 or 2 days and to assess the performance of the product with benchtop human PRP and human commercial plasma. Formulation containing 1% w/v chitosan DDA 82-84% Mn 45-55 kDa with 1% w/v trehalose, and 42.2 mM calcium chloride were prepared for FD. The FD cycles were designed based on recommendations and a theoretical model from the seminal paper of Tang and Pikal (22).

Following FD, the cakes that were non-collapsed were solubilized either in citrated pooled normal plasma or benchtop human PRP to assess different performance characteristics, namely: 1) Solubility, 2) pH and osmolality, 3) Clotting properties with TEG, 4) Clotting properties with a

modified Lee-White method, 5) Runniness, 6) Liquid expression, 7) Clot mechanical strength, 8) Clot homogeneity.

Our starting hypotheses were that:

I. The current FD cycle can be optimized (mostly primary drying) to decrease FD time from 3 days to 1-2 days and produce cakes that are not collapsed.

II. The FD cakes prepared with the shorter cycles will be soluble in benchtop human PRP to yield chitosan-PRP formulations which are paste-like, coagulate rapidly, and produce mechanically robust homogenous hybrid clots.

III. Commercial citrated plasma can be used instead of PRP to assess formulation performance.

8.2 Materials and methods

This study was separated into 2 different phases. In phase I, FD cycles were optimized to identify candidate cycles that produce non-collapsed cakes. In phase II, performance of products obtained using candidate cycles identified in phase I was assessed.

8.2.1 Experimental study design and comparison of theoretical model with experiment for phase I

The goals for phase I of the study were to:

1. Optimize primary drying conditions and set points (T_s, P_c, and duration) to minimize cycle time.

2. Optimize the secondary drying conditions to minimize cycle time and maximize water desorption.

Design of freezing drying cycles:

General guidelines and recommendations for amorphous products from Tang and Pikal were followed to design the freezing and secondary drying stages. The freezing step conditions where

the same for all cycles tested while two different sets of operating conditions were evaluated for the secondary drying step. The theoretical model from Tang and Pikal was used to guide the optimization of the primary drying step. Relying on tabulated thermodynamic quantities such as ice vapour pressure and ice heat of sublimation, vials thermal properties and formulation characteristics, the model allows for the calculation of the shelf temperature (T_s) and chamber pressure (P_c) required to achieve a given product temperature (T_p) during the primary drying phase. Some of the parameters required for calculations are defined and numerical values provided in **Table 8.1** and **Table 8.2**. The thermal properties of the vials reported by Tang and Pikal were used. A key parameter of the model that is determinant for the sublimation rate is the dry layer resistance to vapour flow (R_p). Previous experiments in the laboratory allowed for the estimation of the normalized dry layer resistance ($\hat{R}_P$) of the formulation used in this study. A value of 1.67 $\mathrm{cm^2 \cdot Torr \cdot h/g}$ was found (Note that $R_p = \hat{R}_P / A_p$ where A_p is the sample surface area). In the Phase I of this study, FD cycles for which calculated product temperature during the primary drying step was varied to get progressively closer to the estimated product collapse temperature were tried in sequence. More specifically, theoretical T_p values 2, 3.5 and 5ºC lower than the estimated formulation T_c of -28.5ºC were used (T_p = -30.5, -32 and -33.5 ºC) to determine (calculate) the corresponding set of values of T_s and P_c to use in the primary drying phase (22). Detailed parameters for the freeze-drying cycles used in phase I of the study are shown in **Table 8.3** (22).

Freeze-drying experiments:

For each cycle tested, 3 mL of the CS-based formulation were added into 4 vials of 10 mL (2 vials were tested with thermocouples/2 without). The thermocouple probe was placed carefully at the bottom of the vial and centered for consistency of measurement in different vials. The primary drying step duration was extended to a value larger than the theoretical value (safety factor). Following the end of the FD process, each cake was photodocumented and assessed for collapse and shrinkage. Note that cake shrinkage cannot be avoided with this type of formulation which does not contain any crystalline component (177). The cakes were stored at 4°C, and the data log of the cycle was saved. From the data log file, the curves showing the temperature of the shelf and the temperature readouts from the thermocouples that were placed into the vials were generated. For each sample, the time point at which the primary drying is complete was identified as the time

at which sample temperature reaches that of the shelf (see **Figure 8.3** for an example) (22). Temperature of the product during the sublimation process (primary drying) and the duration of the primary drying step were compared to values predicted from the model.

Table 8.1 Definition of parameters and their values for the freeze-drying cycles used in phase I of this study

Symbol	Description	Value used in this study	Units	Comments
$\mathbf{T_g'}$	Glass transition temperature in the frozen sate	-30.5	°C	See table 7.2
$\mathbf{T_c}$	Collapse temperature (estimated from T_g')	-28.5 (Trehalose)	°C	See table 7.2
$\mathbf{T_{eu}}$	Eutectic temperature (for crystalline solutes)	-	°C	
$\mathbf{T_p}$	Target product temperature during primary drying	Varies with cycle, controlled by T_s, P_c and vial and sample properties	°C	Should be below T_c to avoid product collapse
$\mathbf{R_s}$	Stopper resistance	0	Torr*h/g	Negligible compared to dry layer resistance
$\boldsymbol{\hat{R}_p}$	Normalised dry layer resistance to vapour flow (Normalized product resistance)	1.67	cm^2*Torr*h/g	Value estimated from previous experiments performed on the same formulation
$\boldsymbol{R_p}$	Dry layer resistance to vapour flow	0.439	Torr*h/g	$R_p = \hat{R}_p / A_p$
$\mathbf{P_c}$	Chamber pressure	Calculated from model for a given target T_p	mTorr	
$\mathbf{T_s}$	Temperature of shelf	Calculated from model for a given target T_p	°C	
$\mathbf{A_v}$	Outside cross-sectional area of 10 mL vial	4.71	cm^2	
$\mathbf{A_p}$	Inside cross-sectional area of 10 mL vial	3.8	cm^2	
KC	Sum of the contact and radiative heat transfer parameters of 10 mL vial	$2.64x10^{-4}$	$cal/s \cdot cm^2 \cdot K$	
KD	Parameter that is related to the average distance between shelf and 10 mL vial bottom	3.64	$Torr^{-1}$	

Table 8.2 T_g', T_c, and T_{eu} of the formulation components (22, 176, 177).

Component	% w/v	Conc. mM	T_g' (°C)	T_{eu} (°C)	T_c (°C)	T_g (°C)
Chitosan	1	-	~-17	-	~-15-	-
Trehalose	1	-	-29	-	~-28.5*	118
$CaCl_2$	0.47	42.2	-	-52	-	-

* We estimated the collapse temperature of the chitosan-based formulation tested in this study to that of trehalose.

Table 8.3 Detailed parameters for the freeze-drying cycles used in phase I of the study.

FD cycle	Freezing phase	Primary Drying phase	Secondary Drying phase	FD total duration (h)	Comments
Cycle 1	Step cool to 5 C, then isothermal 30 min, step cool to -5 C, isothermal 30 min, ramp freeze to -40 C in 35 min, isothermal for 2h. Total duration: 2.8h.	Target Tp = -33.5 C Ts = -7 (0.5 C/min). Pc = 67 mTorr. Theoretical duration of primary drying: 11.1 h Total duration: 22.3h	**Conditions 1:** Ts = 30 C (0.1 C/min). Holding time at 30C of 6 h Pc = 67 mTorr.	38.5	-
Cycle 2		Target Tp = -32 C Ts = 0 (0.5 C/min). Pc = 72 mTorr. Theoretical duration of primary drying: 9.1h Total duration: 18.3h	**Conditions 1:** Ts = 30 C (0.1 C/min). Holding time at 30C of 6 h Pc = 72 mTorr.	33.5	-
Cycle 3		Tp = -33.5 C Ts = -7 (0.5 C/min). Pc = 67 mTorr. Theoretical duration of primary drying: 11.1 h Total duration: 18h	**Conditions 2:** Ts = 40 C (0.15 C/min). Holding time at 40C of 6 h Pc = 67 mTorr.	33.2	Based on cycle 1 with reduced primary drying duration and conditions 2 for secondary drying
Cycle 4		Tp = -32 C Ts = 0 (0.5 C/min) Pc = 72 mTorr. Theoretical duration of primary drying: 9.1h Total duration: 13h	**Conditions 2:** Ts = 40 C (0.15 C/min). Holding time at 40C of 6 h Pc = 72 mTorr.	27.7	Based on cycle 2 with reduced primary drying duration and conditions 2 for secondary drying
Cycle 5		Tp = -30.5 C Ts = 8 (0.5 C/min). Pc = 76 mTorr. Theoretical duration of primary drying: 7.4h 780 min 13h	**Conditions 2:** Ts = 40 C (0.15 C/min). Holding time at 40C of 6 h Pc = 76 mTorr.	27	-

8.2.2 Experimental study design and characterization of cakes for phase II

Any cycle tested that didn't lead to product collapse was a potential candidate cycle for phase II of this study. The selection of candidate cycles for phase II was made by considering that cycle duration should be as short as possible and there should be a sufficient difference between product temperature and approximate collapse temperature of the FD-CS. For phase II, 3 mL glass vials were filled with 1 mL of formulation or 10 mL glass vials were filled with 3 mL of formulation. Thermocouple probes were added in selected vials to monitor sample temperature during the FD process. The vials were freeze-dried according to conditions detailed in **Table 8.4** .Cakes from phase II were solubilized in either benchtop human PRP or citrated pooled normal plasma as described below to assess: 1) Solubility, 2) pH and osmolality, 3) Clotting properties with thromboelastography (TEG), 4) Clotting properties with a modified Lee-White method, 5) Runniness, 6) Liquid expression, 7) Clot mechanical strength, 8) Clot homogeneity.

Table 8.4 Detailed parameters for the freeze-drying cycles used in phase II of the study.

FD cycle	Freezing phase	Primary Drying phase	Secondary Drying phase	FD total duration (h)
3-day FD cycle	Step cool to 5 C, then isothermal 30 min, step to -5 C, isothermal 30 min, ramp freeze to -40 C in 35 min, isothermal for 2h. Total duration: 2.8h	Target Ts = -40 C (0.5 C/min). Pc = 100 mTorr. Total duration: 48h	Ts = 30 C Pc = 100 mTorr. Holding time at 40C of 6 h	69
Cycle 1 (Phase II)		Target Tp = -33.5 C Ts = -7 (0.5 C/min). Pc = 67 mTorr. Total duration: 19h	Ts = 40 C (0.15 C/min). Holding time at 40C of 6 h Pc = 67 mTorr	34.4
Cycle 2 (Phase II)		Target Tp = -32 C Ts = 0 (0.5 C/min). Pc = 72 mTorr. Total duration: 13h	Ts = 40 C (0.15 C/min). Holding time at 40C of 6 h Pc = 72 mTorr	27.7
Cycle 3 (Phase II)		Target Tp = -30.5 C Ts = 8 (0.5 C/min). Pc = 76 mTorr. Total duration: 10.8h	Ts = 40 C (0.15 C/min). Holding time at 40C of 6 h Pc = 76 mTorr	24.9

8.2.3 Preparation of CS formulations

Two CSs (82.5% DDA M_n 45 kDa and 84% DDA M_n 55 kDa) were used to prepare formulations containing 1% (w/v) chitosan with 1% (w/v) trehalose and 42.2 mM $CaCl_2$ according to methodoly previously described (19).

8.2.4 Preparations and isolation of PRP

The male subject enrolled in this research responded positively to an Informed Consent Form (Certificate #CÉR-15/16-17) which was approved by the Polytechnique Montreal institutional committee (Comité d'éthique à la recherche avec des êtres humains). Whole blood was extracted and mixed with 3.8% (w/v) trisodium citrate dihydrate solution (9 mL blood to 1 mL sodium citrate). The blood was centrifuged in an ACE E-Z PRP centrifuge at 1300 rpm for 10 minutes at room temperature. The supernatant fractions containing plasma and the buffy coat as well as the first 1-2 mm of the erythrocyte layer was removed and further centrifuged at 2000 rpm for 10 minutes at room temperature to separate platelet-rich plasma (PRP) from platelet poor plasma (PPP). Complete blood count analysis was performed on whole blood and PRP preparations with the Advia 120 hematology system (Siemens).

8.2.5 Properties of human pooled normal plasma

Pooled normal plasma was purchased commercially (Precision Biologic, Product N° CCN-10). Pooled normal plasma is described by the manufacturer as consisting of platelet-poor plasma from 20 or more carefully screened male and female donors aged 18 to 66. Each lot number is verified to be normal for factors II, V, VII, VIII, IX, X, XI, and XII (factor assay value sheet available upon request) as well as fibrinogen.

8.2.6 Solubilization of FD chitosan with pooled plasma hybrids and benchtop PRP

For each freeze-dried formulation (1 or 3-mL per vials), 1 or 3 mL of pooled normal plasma or benchtop PRP was pipetted into the vial. The vial was shaken vigorously for 10 secs to mix. The

assays described below were run immediately. PRP-only controls were prepared by recalcifying 1 mL PRP with 200 µL 3% (w/v) $CaCl_2$ solution. These controls contain 42.2 mM calcium chloride, the same concentration as the solubilized chitosan formulations. Testing solubility of clots with pooled normal plasma and PRP, paste-like properties of formulations, coagulation, clot retraction, clot homogeneity was processed according to methodology previously described (19).

8.2.7 Assessment of clot mechanical strength

The clot was placed in the left gloved hand and the right index finger was used to put pressure on the clot in one smooth motion.

8.3 Results

8.3.1 Freeze-drying cycle adjustments

For all cycles tested, the sample temperature (T_p) during the primary drying step and the theoretical T_p value were compared. Predicted and measured primary drying durations were also compared (see **Table 8.5**). A representative graph of product and shelf temperatures vs time is shown in (**Figure 8.**3). From the experimentally measured primary drying duration (from the thermocouples), the FD cycles where no collapse was observed were repeated with the following adjustment: 1) The primary drying duration was adjusted to the experimentally measured primary drying duration with a safety factor of 20%. 2) The secondary drying step ramp rate was increased from 0.1 to 0.15°C/min, and the final temperature was increased from 30 to 40°C. The changes to the secondary drying described above were made to reduce the duration of this step and to ensure maximum water desorption. These changes were made according to the recommendations for the secondary drying of an amorphous product (the case for the tested formulations): Ramp rate between 0.1 and 0.15°C/min and final temperature between 40 and 50°C held for 3 to 6 hours (22). By optimizing the primary and secondary drying steps, the duration of the cycle was reduced from 3 days to about 1 day. The 3-day and 1-day cycle are compared in **Table 8.6.**

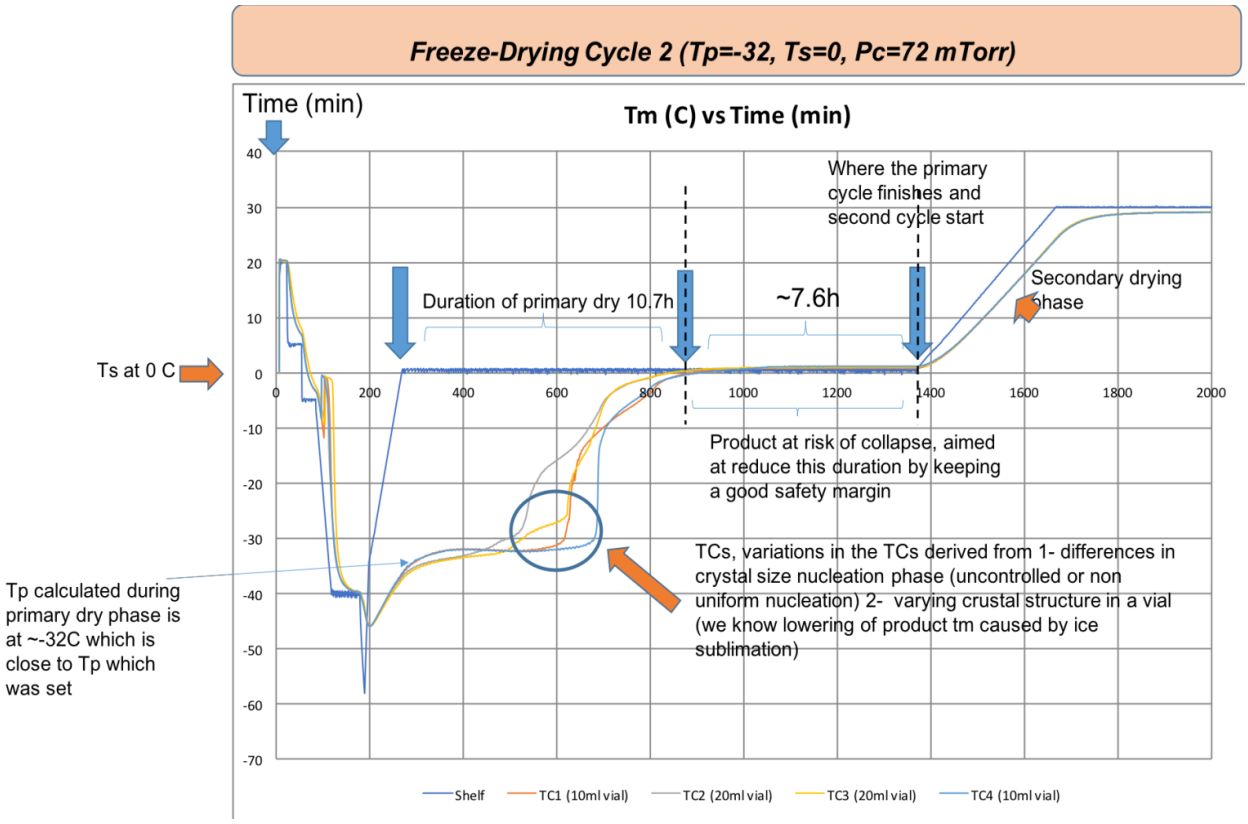

Figure 8.3 Example graph of product and shelf temperature vs time from a cycle (cycle 2) tested in phase I.

Table 8.5 Comparison of measured and theoretical values of product temperature (Tp) and primary drying duration for 5 selected cycles.

FD Cycle	Theoretical T_p	Measured T_p	Theoretical duration time (h)	Estimated duration time (h)
1	-33.5	-32.9	11.1	15.6
2	-32	-31.8	9.1	10.7
3	-33.5	-32.6	11.1	16.3
4	-32	-31.9	9.1	10.8

5	-30.5	-31	7.5	10.0

Table 8.6 A summary of all optimization of cycles from 3 day to 1-day cycle.

Cycles	**3-day cycle**	**1-day cycle**	**Percentage of total reduction time**
Freezing **Duration time**	Step cool to 5°C, isothermal 30 min, step cool to -5°C, isothermal to 30 min, ramp freeze to -40°C in 35 min, isothermal for 2h Total: 2.8 h	Step cool to 5°C, isothermal 30 min, step cool to -5°C, isothermal to 30 min, ramp freeze to -40°C in 35 min, isothermal for 2h Total: 2.8 h	-
Primary drying • **Pc** • **Ts** • **Tp** • **Duration time**	100 mTorr -40 C -40 C 48 h	76 mTorr 8 C -30.5 10.8 h	-
Secondary drying • **Pc** • **Ts** • **Duration time**	100 mTorr 30 C 18.2 h	76 mTorr 40 C 9.5 h	-
Total duration time	**69h**	**23.1h**	**64%**

8.3.2 Preparation of FD-chitosan formulation and cake appearance for phase II

Chitosan (82.5% DDA M_n 45 kDa) was used for phase I of the study. pH of the formulations was between 6.0 and 6.2 before FD. The osmolality of the formulations was between 135 and 160 mOsm before FD (**Table 8.**& **Table 8.**). Shrinkage was observed in most of the vials which cannot be avoided with the current formulation. Cakes produced with 4 different FD cycles are shown with sample ID A to D in **Figure 8.**. Cake shrinkage was observed during the lyophilization process were reported.

Table 8.7 Osmolality and pH of test article prior to FD for vials to be later reconstituted in PRP. Vial A indicates 3-day FD cycle the duration at 69.9h (3-day cycle). B. FD cycle with the duration of 34.5h. C. FD cycle with the duration of 27.7h. D. FD cycle with the duration of 24.4h.

#	Sample name	Test article formulation	Osmolality mOsm	pH
1	A1-3ml vial	82.5%DDA, 45 kDa	154	6.2
2	A3-3ml vial	82.5%DDA, 45 kDa	154	6.2
3	B1-3ml vial	82.5%DDA, 45 kDa	160	6.2
4	B3-10ml vial	82.5%DDA, 45 kDa	160	6.2
5	C1-3ml vial	82.5%DDA, 45 kDa	150	6.0
6	C3-10ml vial	82.5%DDA, 45 kDa	150	6.0
7	D1-3ml vial	82.5%DDA, 45 kDa	146	6.2
8	D3-10ml vial	82.5%DDA, 45 kDa	146	6.2
9	Recalcified PRP	-	280	7.7

Table 8.8 Osmolality and pH of test article prior to FD for vials to be reconstituted in pooled normal plasma. Vial A indicates 3-day FD cycle the duration at 69.9h (3-day cycle). B. FD cycle with the duration of 34.5h. C. FD cycle with the duration of 27.7h. D. FD cycle with the duration of 24.4h.

#	Sample name	Test article formulation	Osmolality mOsm	pH
1	A2-3ml vial	82.5%DDA, 45 kDa	154	6.2
2	A4-3ml vial	82.5%DDA, 45 kDa	154	6.2
3	B2-3ml vial	82.5%DDA, 45 kDa	160	6.2
4	B4-10ml vial	82.5%DDA, 45 kDa	160	6.2
5	C2-3ml vial	82.5%DDA, 45 kDa	150	6.0
6	C4-10ml vial	82.5%DDA, 45 kDa	150	6.0
7	D2-3ml vial	82.5%DDA, 45 kDa	146	6.2
8	D4-10ml vial	82.5%DDA, 45 kDa	146	6.2
9	Plasma	-	350	8.4

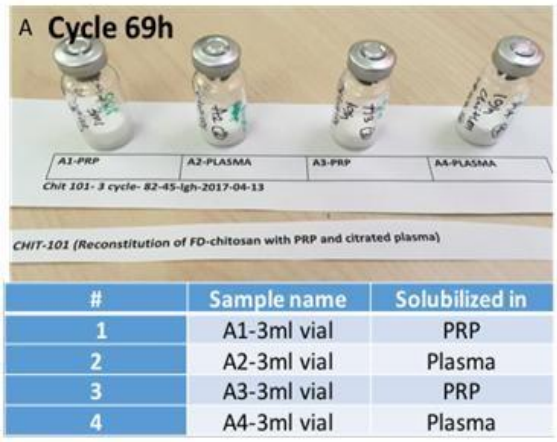

#	Sample name	Solubilized in
1	A1-3ml vial	PRP
2	A2-3ml vial	Plasma
3	A3-3ml vial	PRP
4	A4-3ml vial	Plasma

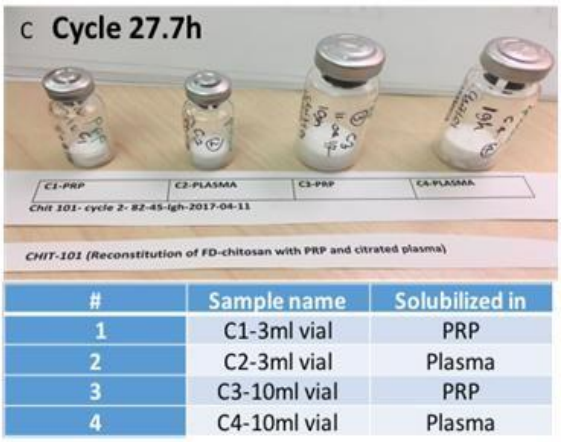

#	Sample name	Solubilized in
1	C1-3ml vial	PRP
2	C2-3ml vial	Plasma
3	C3-10ml vial	PRP
4	C4-10ml vial	Plasma

#	Sample name	Solubilized in
1	B1-3ml vial	PRP
2	B2-3ml vial	Plasma
3	B3-10ml vial	PRP
4	B4-10 ml vial	Plasma

#	Sample name	Solubilized in
1	D1-3ml vial	PRP
2	D2-3ml vial	Plasma
3	D3-10ml vial	PRP
4	D4-10ml vial	Plasma

Figure 8.4 Cake appearance for each FD cycle and its sample IDs which is solubilized either in PRP or pooled normal plasma in 10 mL and 3 mL vials for phase II. Vial A indicates 3-day FD cycle the duration at 69.9h (3-day cycle). B. FD cycle with the duration of 34.5h. C. FD cycle with the duration of 27.7h. D. FD cycle with the duration of 24.4h.

8.3.3 Result of blood analysis

The PRP which was used for the *in vitro* assays, contained 368 X 10^9/L platelets (2X the concentration of whole blood), 0.7 X 10^{12}/L erythrocytes (0.2X the concentration of whole blood) and 3.2 X 10^9/L leukocytes (0.7 X the density of whole blood). The FDA definition of PRP is a blood-derived suspension that contains a platelet concentration ≥ 250 X 10^9/L platelets.

8.3.4 Cake solubility and chitosan-PRP handling properties

All formulations reconstituted with PRP or plasma had acceptable solubility and handling properties. C1 (PRP, 3 mL vial, Cycle 27.7h) and D4 (Plasma, 10 mL vial, Cycle 24.9h) vials appeared to be slightly less soluble than other formulations right when PRP or plasma was pipetted in but were soluble after shaking for 10 seconds.

8.3.5 pH and osmolality of the solubilized chitosan mixtures

pH of the formulations was between 6.7 and 7.2 after reconstitution with PRP (**Table 8.**). pH of the formulations was between 6.8 and 7.2 after reconstitution with plasma (**Table 8.**). pH of recalcified PRP control was at 7.7, and pooled normal plasma was at 8.4. The osmolality of the formulations was between 388 and 432 after reconstitution with PRP (**Table 8.**). The osmolality of the formulations was slightly higher, and it was between 464 and 660 after reconstitution of with plasma (**Table 8.**). The osmolality of recalcified PRP control was at 280 mOsm and pooled normal plasma was at 350 mOsm.

Table 8.9 Osmolality and pH of chitosan formulations for cakes reconstituted in PRP. Vial A indicates 3-day FD cycle the duration at 69.9h (3-day cycle which has been used so far in our lab). B. FD cycle with the duration of 34.5h. C. FD cycle the duration of 27.7h. D. FD cycle the duration of 24.4h.

#	Sample name	Test article formulation	Solubility in PRP	Osmolality mOsm	pH
1	A1-3ml vial	82.5%DDA, 45 kDa	4+	432	7.0
2	A3-3ml vial	82.5%DDA, 45 kDa	4+	408	7.1
3	B1-3ml vial	82.5%DDA, 45 kDa	4+	404	7.1
4	B3-10ml vial	82.5%DDA, 45 kDa	4+	388	6.9
5	C1-3ml vial	82.5%DDA, 45 kDa	3+	400	7.2
6	C3-10ml vial	82.5%DDA, 45 kDa	4+	740	6.7
7	D1-3ml vial	82.5%DDA, 45 kDa	4+	412	7.0
8	D3-10ml vial	82.5%DDA, 45 kDa	4+	384	6.8
9	Recalcified PRP	-	4+	280	7.7

Table 8.10 Osmolality and pH of chitosan formulations for cakes reconstituted in plasma. Vial A indicates 3-day FD cycle the duration at 69.9h (3-day cycle). B. FD cycle with the duration of 34.5h. C. FD cycle the duration of 27.7h. D. FD cycle the duration of 24.4h.

#	Sample name	Test article formulation	Solubility in Plasma	Osmolality mOsm	pH
1	A2-3ml vial	82.5%DDA, 45 kDa	4+	472	7.0
2	A4-3ml vial	82.5%DDA, 45 kDa	4+	492	7.1
3	B2-3ml vial	82.5%DDA, 45 kDa	4+	464	7.1
4	B4-10ml vial	82.5%DDA, 45 kDa	4+	616	6.8
5	C2-3ml vial	82.5%DDA, 45 kDa	4+	744	7.1
6	C4-10ml vial	82.5%DDA, 45 kDa	4+	616	6.8
7	D2-3ml vial	82.5%DDA, 45 kDa	4+	660	7.2
8	D4-10ml vial	82.5%DDA, 45 kDa	3+	652	6.8
9	Plasma	-	4+	350	8.4

8.3.6 Chitosan-PRP formulations have higher paste-like properties than PRP control

Chitosan-PRP formulations were more viscous, less runny, and were more paste-like than the recalcified PRP control (**Figure 8.**). Chitosan-Plasma formulations were also less runny than plasma alone (**Figure 8.**).

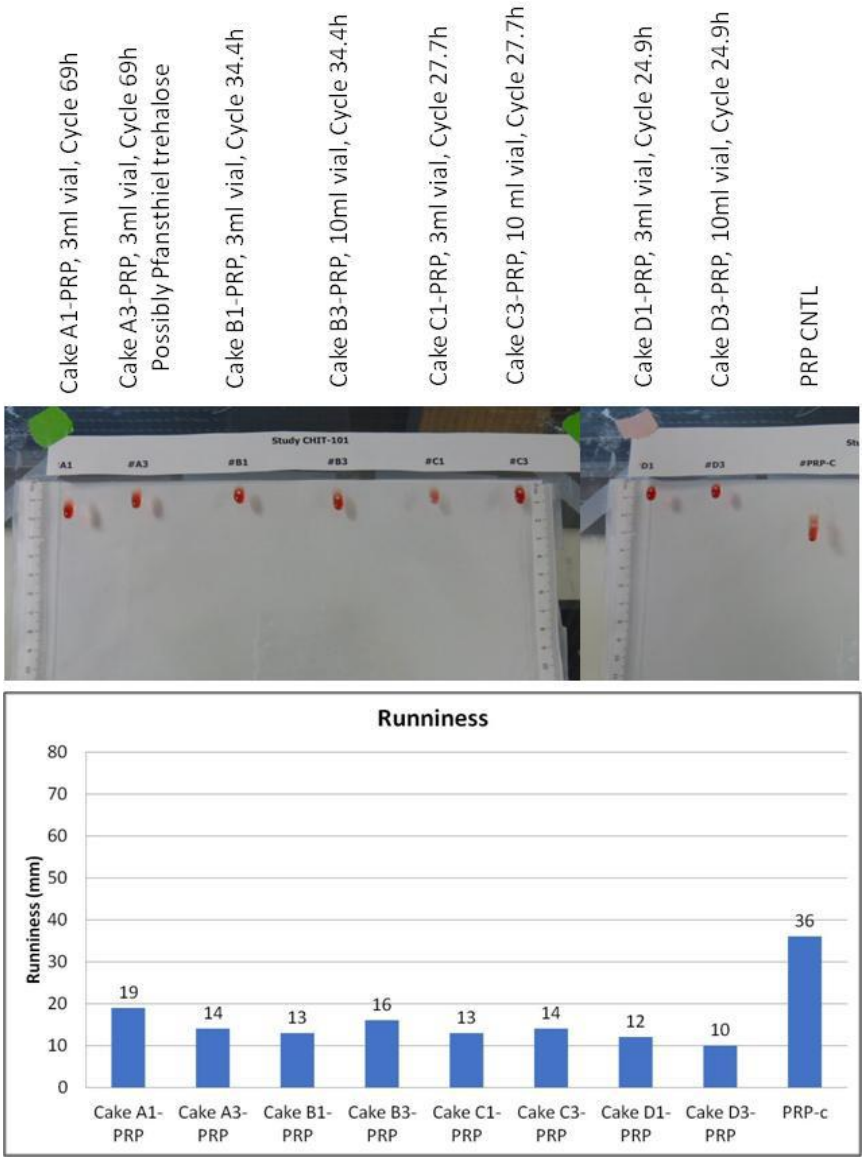

Figure 8.5 Runniness of the chitosan-PRP mixtures (top panel). The bottom panel shows runniness in mm of n = 1 chitosan-PRP mixtures. Clot A indicates 3-day FD cycle the duration at 69.9h (3-day cycle). B. FD cycle with the duration of 34.5h. C. FD cycle the duration of 27.7h. D. FD cycle the duration of 24.4h.

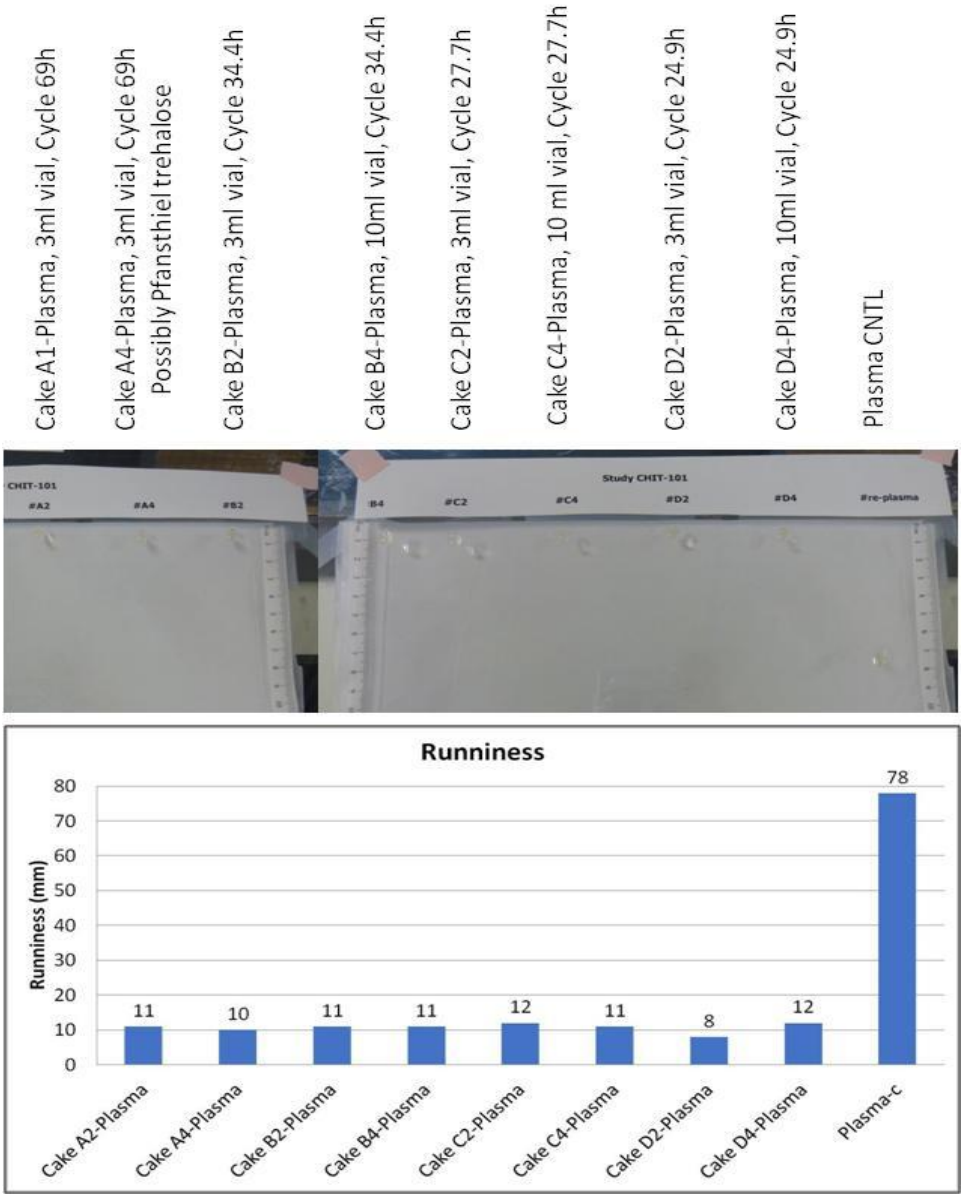

Figure 8.6 Runniness of the chitosan-plasma mixtures (top panel). The bottom panel shows runniness in mm of n = 1 chitosan-plasma mixtures. Clot A indicates 3-day FD cycle the duration at 69.9h (3-day cycle). B. FD cycle with the duration of 34.5h. C. FD cycle the duration of 27.7h. D. FD cycle the duration of 24.4h.

8.3.7 Thromboelastography

The PRP control was recalcified with 42.2 mM calcium chloride prior to TEG, which is the concentration used in the chitosan cakes in our lab. PRP control clotted in the TEG machine, but

much slower than chitosan-PRP formulations so that its clot reaction time was the highest at 28 min compared to less than 4 min for CS-PRP formulations (**Figure 8.**). Clot maximal amplitude was above 78 mm for all formulations solubilized in PRP (**Figure 8.**). Clot maximal amplitude was usually lower when formulations were solubilized in plasma, most were below 60 mm, with B2 being an outlier (**Figure 8.**). Clot reaction time of formulations solubilized in plasma were all 5 min or below (**Figure 8.**). Note that recalcifying commercial plasma with 42.2 mM $CaCl_2$ is not sufficient to induce coagulation.

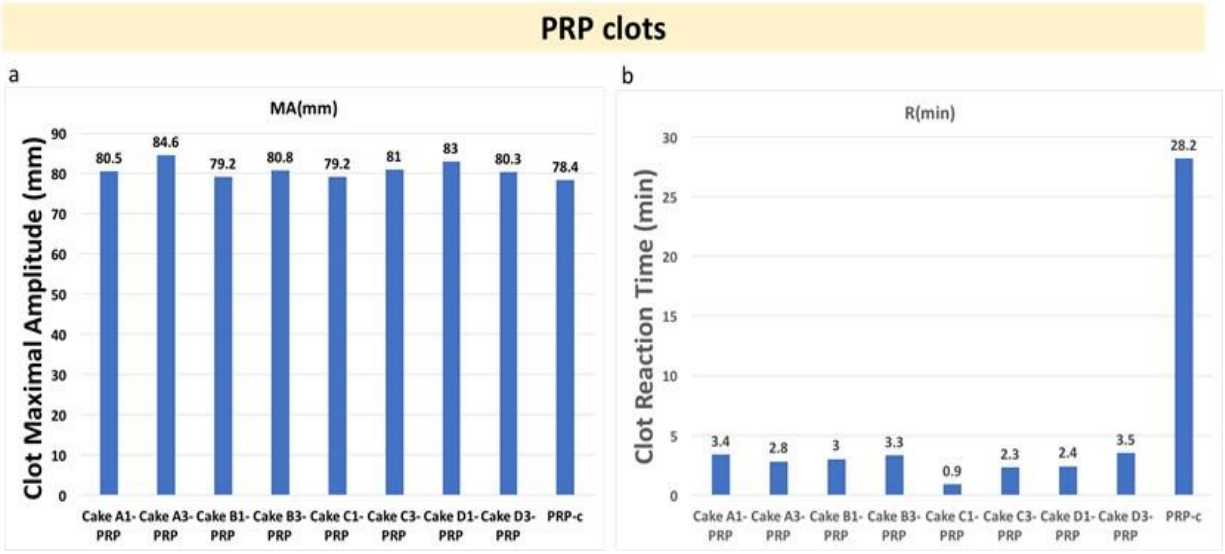

Figure 8.7 Clot maximal amplitude (MA) and clot reaction time R of the chitosan-PRP mixtures (panels a and b). Clot reaction time was higher for recalcified PRP (28 min) compared to CS-PRP formulations (all below 4 min). Clot maximal amplitude was all above 78 mm. Clot A indicates 3-day FD cycle the duration at 69.9h (3-day cycle). B. FD cycle with the duration of 34.5h. C. FD cycle the duration of 27.7h. D. FD cycle the duration of 24.4h.

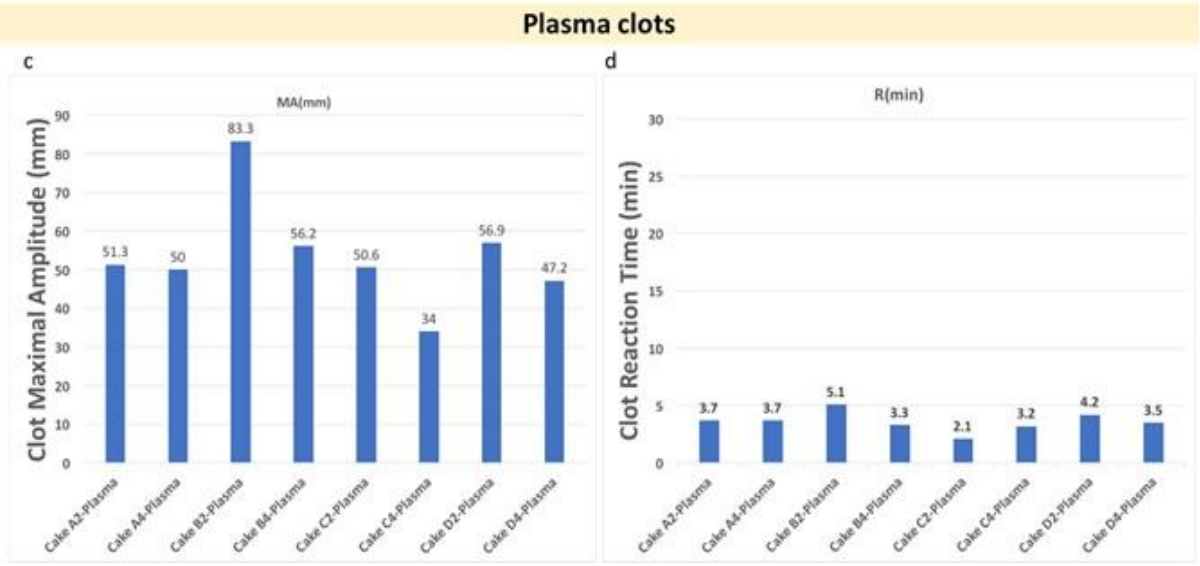

Figure 8.8 Clot maximal amplitude (MA) and clot reaction time R of the chitosan-plasma mixtures (panel c and d). Clot maximal amplitude was usually below 60 mm, with B2 being an outlier. Clot reaction time was all 5 min and below. Clot A indicates 3-day FD cycle the duration at 69.9h (3-day cycle). B. FD cycle with the duration of 34.5h. C. FD cycle the duration of 27.7h. D. FD cycle the duration of 24.4h.

8.3.8 Liquid expression

None of the chitosan-PRP hybrids expressed any serum upon clotting for 1 hour at 37^{o}C (**Figure 8. & Figure 8.**). The recalcified PRP controls clotted in glass tubes placed at 37^{o}C for 1 hour and expressed some serum upon clotting (**Figure 8.**). None of the chitosan-plasma hybrids expressed any serum upon clotting for 1 hour at 37^{o}C (**Figure 8.**).

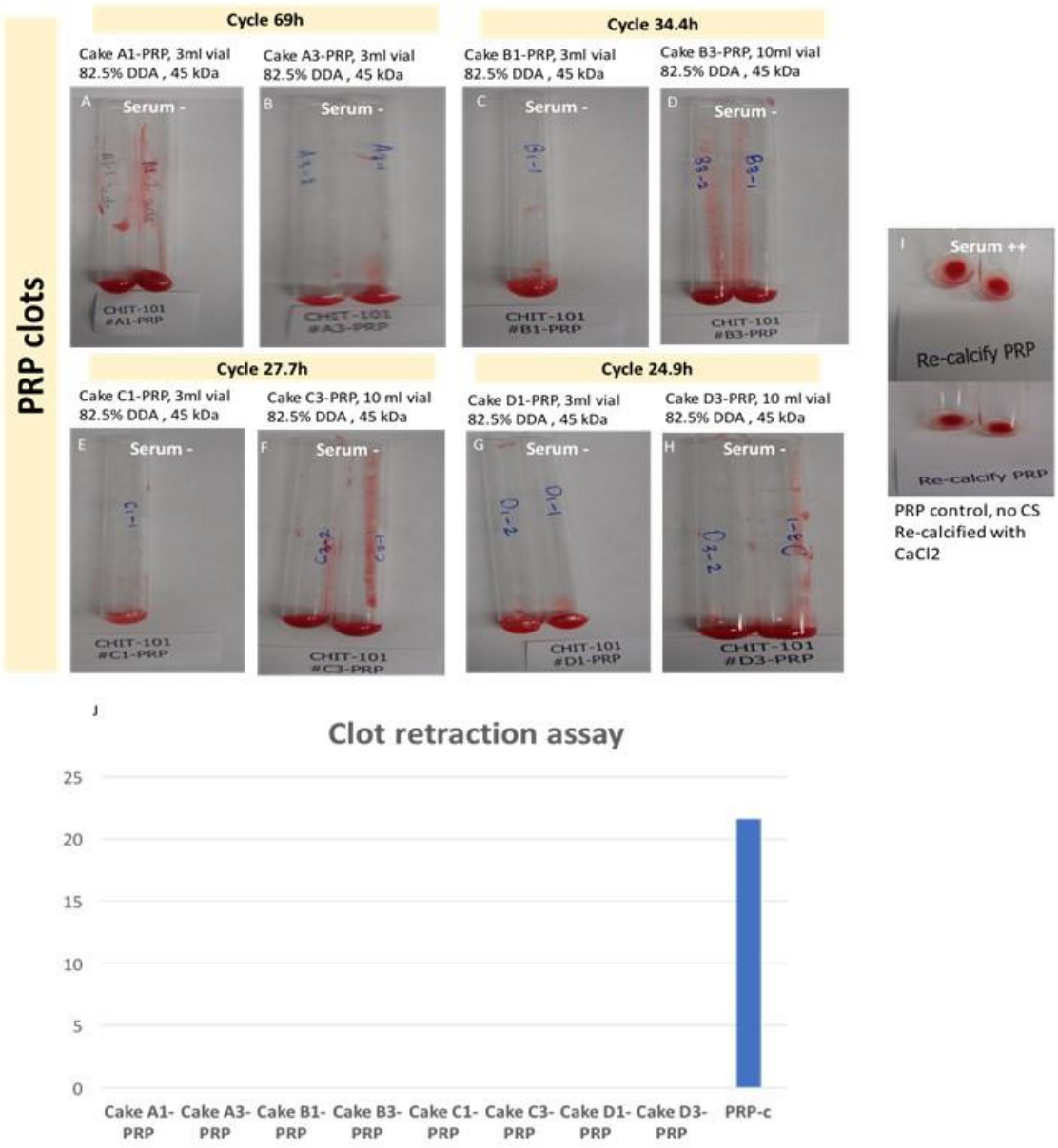

Figure 8.9 Liquid expressed by chitosan-PRP hybrid clots solubilized with PRP left to clot for 1 hour (panels A to H) and from recalcified PRP control (panel I). Panel J shows % Clot mass loss of n = 1 or n = 2 clots of chitosan-PRP clots and recalcified PRP only controls. None of the CS-PRP clots expressed serum upon clotting. Clot A indicates 3-day FD cycle the duration at 69.9h (3-day cycle). B. FD cycle with the duration of 34.5h. C. FD cycle the duration of 27.7h. D. FD cycle the duration of 24.4h.

Figure 8.10 Liquid expressed by chitosan-plasma hybrid clots solubilized with plasma left to clot for 1 hour (panels A to H). None of the CS-plasma clots expressed serum upon clotting. Clot A indicates 3-day FD cycle the duration at 69.9h (3-day cycle). B. FD cycle with the duration of 34.5h. C. FD cycle the duration of 27.7h. D. FD cycle the duration of 24.4h.

8.3.9 Crush test

All chitosan-PRP clots were firm with a 3+ or 4+ clot strength (**Figure 8.**). All chitosan-plasma clots were too fragile, soft, and delicate to handle to do the crush test.

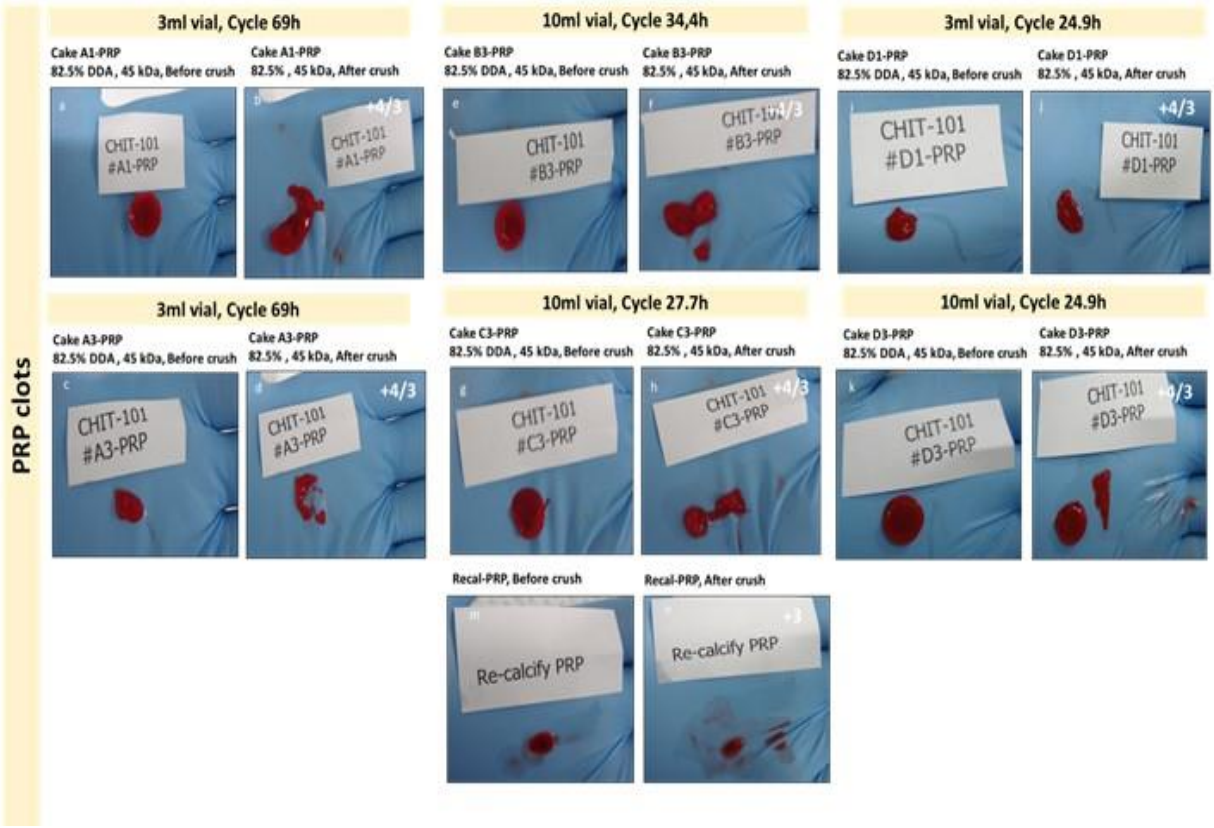

Figure 8.11 Chitosan-PRP clots before (panels a, e, i, c, g, & k) and after (panels b, f, j, d, h, & i) the crush test. Recalcified PRP controls before (panels m) and after (panels n) the crush test. Clot A indicates 3-day FD cycle the duration at 69.9h (3-day cycle). B. FD cycle with the duration of 34.5h. C. FD cycle the duration of 27.7h. D. FD cycle the duration of 24.4h.

8.3.10 Histology result

Fast-Green/Iron hematoxylin stained sections of chitosan-PRP clots and chitosan-plasma clots showed that chitosan distribution was mostly homogeneous (**Figure 8.Figure 8.**). Most samples received a score of + and the remaining a score of +/- for homogeneity.

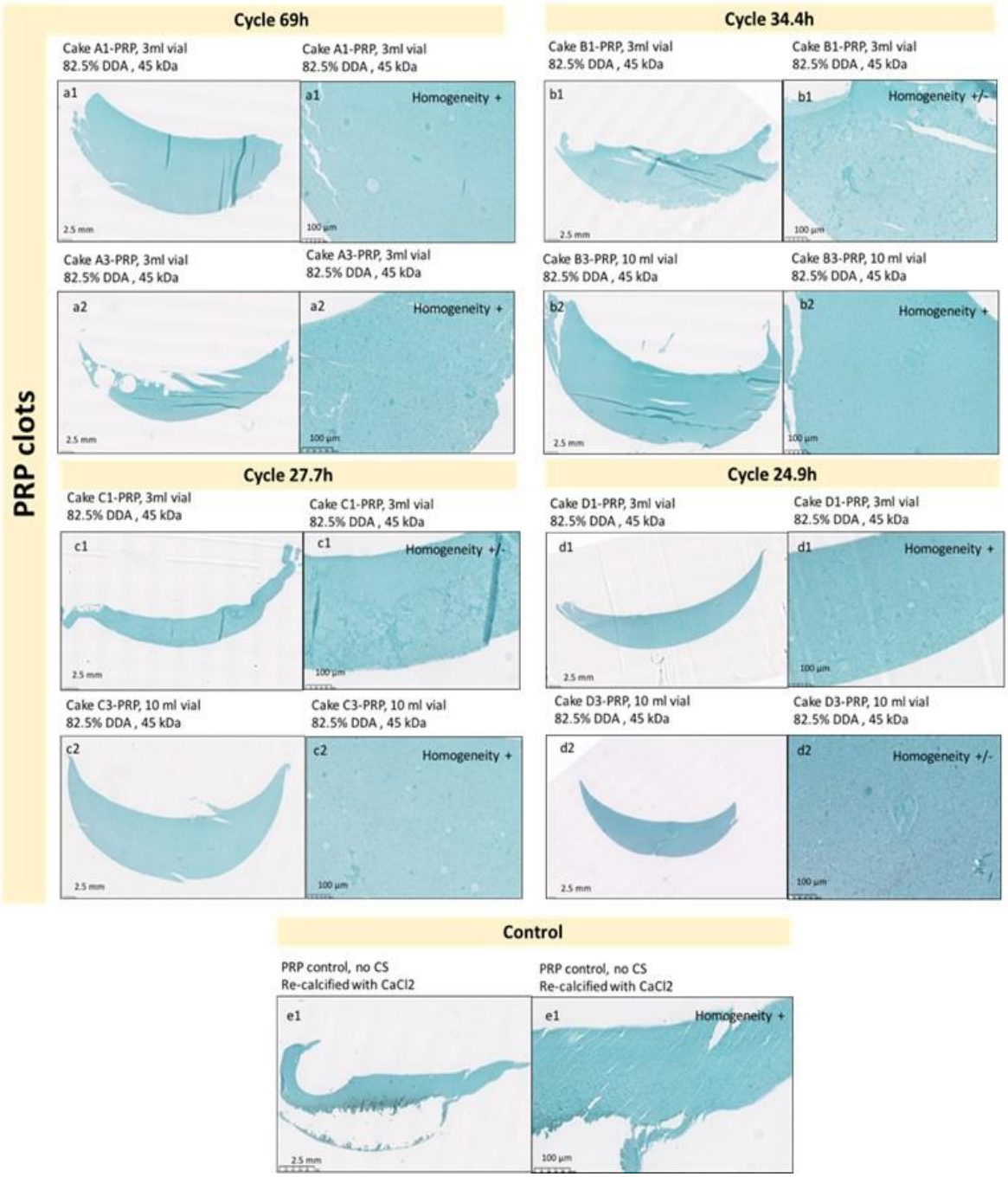

Figure 8.12 Fast-Green/Iron hematoxylin stained sections of chitosan-PRP clots and recalcified PRP control. Clot A indicates 3-day FD cycle the duration at 69.9h (3-day cycle). B. FD cycle with the duration of 34.5h. C. FD cycle the duration of 27.7h. D. FD cycle the duration of 24.4h.

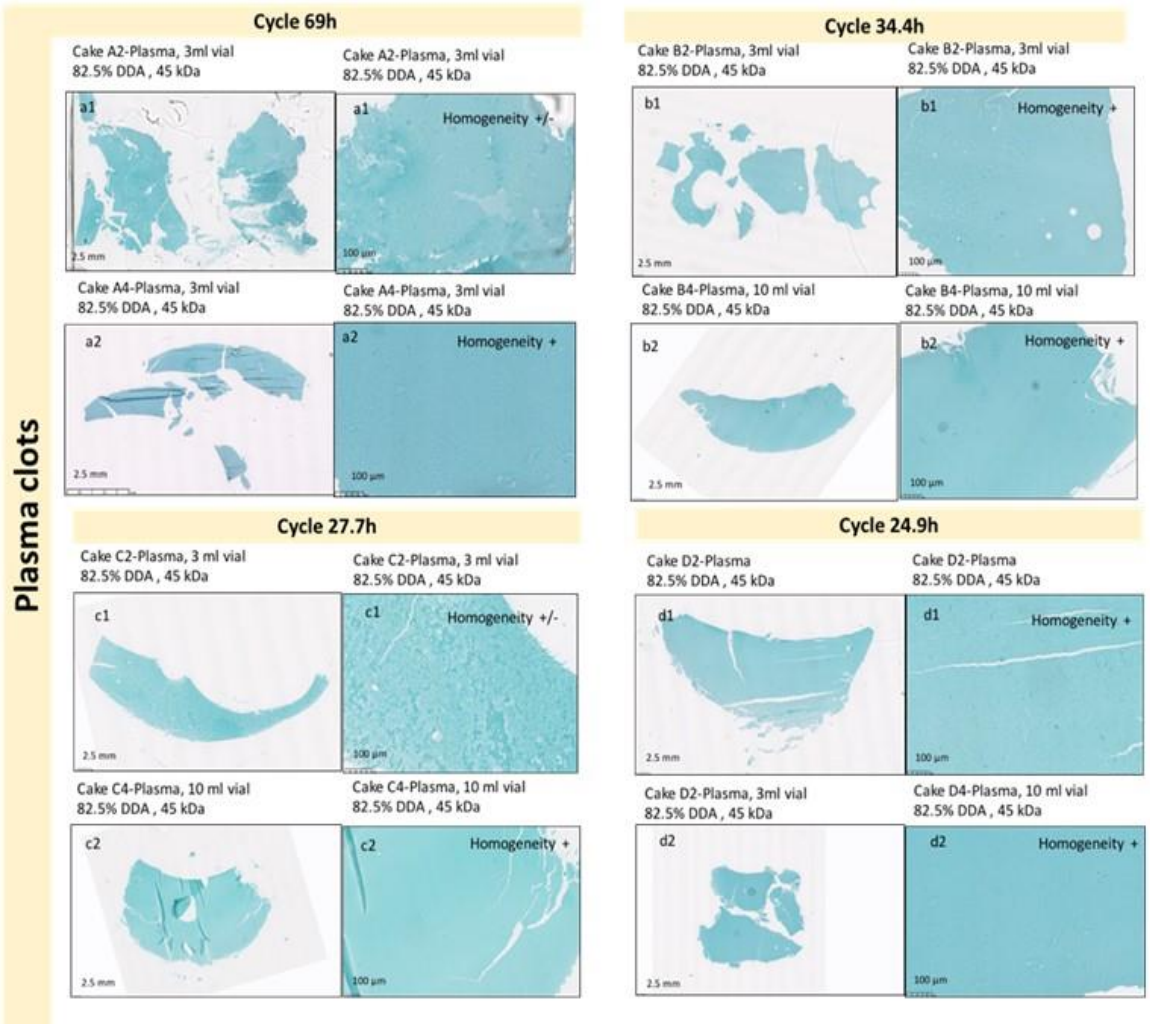

Figure 8.13 Fast-Green/Iron hematoxylin stained sections of chitosan-plasma clots. Clot A indicates 3-day FD cycle the duration at 69.9h (3-day cycle). B. FD cycle with the duration of 34.5h. C. FD cycle the duration of 27.7h. D. FD cycle the duration of 24.4h.

8.3.11 Summary of performance characteristics

Performance characteristics of the FD-chitosan-PRP and FD-chitosan-plasma formulations for different freeze-dried cycles are summarized in **Table 8.11 Table 8.11.**

Table 8.11 Summary of the performance characteristics of chitosan-PRP.

Property assessed	**96h cycle A1-3ml vial-PRP**	**96h cycle A3-3ml vial-PRP**	**34.4h cycle B1-3ml vial- PRP**	**34.4h cycle B3-10ml vial- PRP**	**27.7h cycle C1-3ml vial-PRP**	**27.7h cycle C3-10ml vial-PRP**	**24.9h cycle D1-3ml vial-PRP**	**24.9h cycle D3-10ml vial-PRP**	**PRP control**
Excellent solubility and handling properties	+	+	+	+	±	+	+	+	Not relevant
Close to physiological pH upon solubilisation	+	+	+	+	+	+	+	+	Not relevant
Close to physiological osmol upon solubilisation	+	+	+	+	+	+	+	+	Not relevant
Viscous and paste-like	+	+	+	+	+	+	+	+	-
Timely coagulation	+	+	+	+	+	+	+	+	-
Fully resists clot retraction	+	+	+	+	+	+	+	+	-
Mechanically strong clot	+	+	+	+	+	+	+	+	+
CS dispersion in clot	+	+	±	+	±	+	+	±	Not relevant

Table 8.12 Summary of the performance characteristics of chitosan-plasma.

Property assessed	**96h cycle A2-3ml vial-plasma**	**96h cycle A4-3ml vial-plasma**	**34.4h cycle B2-3ml vial-plasma**	**34.4h cycle B4-10ml vial-plasma**	**27.7h cycle C2-3ml vial-plasma**	**27.7h cycle C4-10ml vial-plasma**	**24.9h cycle D2-3ml vial-plasma**	**24.9h cycle D4-10ml vial-plasma**	**Control**
Excellent solubility and handling properties	+	+	+	+	+	+	+	±	Not relevant
Close to physiological pH upon solubilization	+	+	+	+	+	+	+	+	Not relevant
Close to physiological osmol upon solubilization	+	±	+	±	+	+	±	+	Not relevant
Viscous and paste-like	+	+	+	+	+	+	+	+	-
Timely coagulation	+	+	+	+	+	+	+	+	Not assessed
Fully resists clot retraction	+	+	+	+	+	+	+	+	Not assessed
Mechanically strong clot	Not assessed	Not assessed	Not assessed	Not assessed	Not assessed	Not assessed	Not assessed	Not assessed	Not assessed
CS dispersion in clot	±	+	+	+	±	+	+	+	Not assessed

8.4 Discussion

The objective of this study was to optimize the freeze-drying cycle of the CS formulation and to assess the performance characteristics of the non-collapsed and acceptable cakes upon reconstitution in benchtop human PRP and human commercial plasma. Guided by a theoretical model, we optimized the primary drying step by successfully predicting the product temperature (T_p) for a set of shelf temperature (T_p) and chamber pressure (P_c) values. Interestingly, the model underestimated the primary drying duration for all cycles tested. This could be due to the fact that the dry layer resistance to vapour flow increases during the sublimation process, while we used a constant value in our calculations. All FD cycles tested produced cakes with acceptable macroscopic appearance. Visual assessment of cakes suggests that there is no correlation/relation between the changes in the different FD cycle paremeters, including temperature of shelf, temperature of product, and percentage of shrinkage in the vials. The second and third hypotheses were also supported in that all cakes were soluble in benchtop human PRP and that commercial plasma was successfully used to test performance characteristics. Resulting formulations were paste-like, coagulated rapidly, and produced mechanically robust homogenous hybrid clots that resisted platelet-mediated clot retraction. Preventing hyper-osmolarity is an important element for formulation development since high osmolality will prevent coagulation. We observed a large variation of osmolality upon reconstitution of chitosan with commercial plasma. We expected the osmolality of the CS-plasma formulation to be higher than for the CS-PRP formulations, since commercial plasma has higher osmolality. The 600 mOsm measurements were higher than what we expected, but, fortunately, were not high enough to prevent the formulations from clotting. We speculated that this large variability may come from interaction of large proteins such as albumin or globulins which in plasma with trehalose of the formulation may alter freezing-point (180). Another reason would be due to heterogeneity in the reconstituted product. In this framework, we would suggest repeating the phase II to assess reproducibility. Addition of mannitol could also minimize the shrinkage of the cakes, although it will change the final formulations which might affect the performance for *in vitro* and *in vivo* studies. In summary, guided by the recommendations and theoretical model from Tang and Pikal, we optimized the freeze-drying process by significantly reducing the duration of the primary drying phase. We found that there was no difference in performance characteristics of formulations freeze-dried using the shorter and optimized FD

cycles. Shorter FD cycles will allow for faster preparation of chitosan-based formulations and will also significantly reduces the production cost at the commercial scale.

CHAPTER 9 GENERAL DISCUSSION

Knee meniscal pathologies are a common problem for which current treatment options are limited. Existing surgical treatment options for menisci are meniscectomy and repair. Arthroscopic partial meniscectomy (PM) remains the treatment of choice for meniscal lesions to restore function and minimize pain with more than 465,000 people undergoing the procedure annually only in the USA. Meniscus tears can be of traumatic or degenerative origin. In the case of traumatic tears, which are mostly seen in young and active athletes, first-line choice for treatment is repair. These types of lesions mostly affect the vascularized segments of menisci. However, degenerative meniscal lesions with significant mechanical retardation symptoms in middle to aged patients are predominantly indicated for resection (52, 56). Degenerative complex tears which occur in the avascular zones of meniscus have a limited healing potential and options are less. This could be due to the pattern of these tears, quality of tissue, and old patient profile (181). For example, vertical longitudinal tears in the peripheral zones have good indications for effective meniscal repair while horizonal degenerative component tears in inner avascular are usually resected. Further, menisci tears are associated with several macroscopic and histopathologic structural and functional changes such as attachment at tibial, femoral, and inner borders, tissue fraying, partial tears or complete tears, loss of tissue, calcium deposition, tissue alterations in surface characteristics, cellularity, collagen fiber organization, and Safranin-O matrix staining intensity (182). Although both PM and repair have been reported to minimize morbidity and faster clinical recovery, they are associated with complications during surgery, poor clinical outcome, and OA changes in the long-term. More than 30% failure rates are observed for tears which are considered ideal for repair. Current therapeutic options for meniscus deficiency are allograft and meniscus substitutes. Also, there are increased data support that application of allograft, substitutes and other replacement grafts lack universal efficacy and availability.

For all these reasons, biological approaches and tissue engineering strategies for meniscus repair are becoming important for orthopedic surgeons as alternatives. The histopathologic and imaging of different *in vivo* and preclinical studies have demonstrated the importance of new alternative approaches of treatment modalities. Biologic augmentation techniques have been attempted to promote the healing of torn meniscus to overcome some of the inherent limitations such as lack of cell proliferation, poor vascularity, limited chemotactic responses, and heterogeneous microstructure at the repair site. Nevertheless, the literature suggests that mechanical stimulation

of the adjacent synovium or the meniscus by rasping and trephination, augmentation with fibrin clots and platelet-rich plasma (PRP), stem cell therapy, and biomaterial augmentation via wrapping the meniscal tear (e.g., collagen membrane scaffold) in combination with sutures improve the meniscal healing rate and enhance meniscus repair (183). Also, the aim of the tissue engineering approaches is to enhance host target tissue regeneration by the employment of cells, scaffolds, and growth factors to improve damaged tissue. The ultimate goal of meniscus repair is to restore patients knee function to back to normal. However, there is still no consensus regarding the best cell resource for meniscal regeneration due to the lack of comparative studies (13, 181, 184).

It is worth noting that limited blood supply and cell density pose challenges for meniscus repair. Preclinical studies have shown that abrasion therapies such as trephination and rasping encourage vascular and cell migration from the reduced vascularized zone of the meniscus to the defect site to improve repair. Applicability, the cost-effectiveness, as well as damage to the menisci collagen organization resulting in poor menisci function needs to be further validated with clinical studies. Meniscus and synovial rasping have also been shown to augment healing through cytokine expression. However, the location of the tear from the capsule and the type of defect will affect the healing. Moreover, the addition of collagen membrane and wrapping technique is still at the initial stage for clinical use and is known to be technically demanding and time-consuming. Complete meniscus regeneration remains a challenge because of the difficulty in reproducing the complex meniscal collagen fiber arrangements and biochemical composition which limits treatment options (13, 185).

Chitosan (CS), a naturally derived polysaccharide has shown promise for soft and hard tissue healing. Molar mass (M_n) and degree of deacetylation (DDA) of chitosan are key structural features which influence *in vivo* biodegradation rate, healing capacity, and its performance for polymer-tissue interactions (186). Freeze-drying (FD) has been considered as good technique to improve the long-term stability of chitosan-based products for manufacturing. Recently, *in vitro* studies demonstrated CS could induce extracellular matrix expression in cartilage and reduce catabolic mediators which are generated by chondrocytes. Several studies have also shown that chitosan-based scaffolds could promote chondrogenic differentiation of mesenchymal stem cells. Also, *in vivo* studies suggested that chitosan prevented cartilage degradation and severity of synovial membrane inflammation in surgically-induced rabbit model of osteoarthritis. Chitosan possesses superior properties such as biocompatibility, biodegradability, low immunogenicity, and the

chemical structure of chitosan is similar to glycosaminoglycan (GAGs) in cartilage (186). Therefore, chitosan is an exciting candidate for cartilage lesion repair and intraarticular sustained drug release.

The idea of using blood products for augmentation of menisci repair was first proposed by Arnoscky et al., who implanted fibrin clots. Factors within the blood clot promote healing in a fashion similar to what happens during the healing process. Clots act as a scaffold that bridge the defect between menisci tear fragments, thus allowing cells from synovium and meniscus to repair torn tissue. Following these principles, application of PRP as a biologic was proposed. PRP is a heterogenous blood-derived product with a higher concentration of platelets and growth factors. It has been employed in the clinic for promoting of soft tissue healing such as rotator cuff, cartilage, and meniscus. More clinical trials are required to find out what is the optimal treatment for meniscus tears. Growth and clotting factors derived from centrifugation of blood stimulate menisci fibrochondrocytes, increase cell proliferation and extracellular matrix synthesis and repair process in the context of meniscus repair. Despite the theoretical advantages of PRP, its injection alone is not sufficient to promote meniscus repair. One of the potential reasons for this is that PRP seems to be quickly dissolved from the tissue while combination of a natural biomaterial such as chitosan and PRP enhances its retention *in vivo*. Several research groups investigated the conjunction of chitosan scaffolds and PRP. They found promotion of platelet activation and increases platelet-derived growth factor release from PRP (19, 116).

Our laboratory has been working with chitosan for cartilage repair applications since several years ago. Bone marrow stimulation (BMS) is a cartilage repair technique that initiates repair by drilling into subchondral bone and is considered as the first-line operative treatment for osteochondral lesions. This technique stimulates mesenchymal stem cells and the formation of a blood clot in the lesion to promote cartilage tissue healing. We initially hypothesized that stabilizing the blood clot in cartilage defects would induce cell recruitment and improve neotissue formation. CS, a thrombogenic biomaterial with the ability to modulate several phases of the wound healing cascade, appeared to be an ideal candidate for this. Near-neutral solutions of chitosan-glycerol phosphate (GP) can be mixed with autologous whole blood to form hybrid clots that significantly resist retraction (157, 158). These CS-GP-blood formulations can be utilized as injectable implants and adhere to cartilage lesions treated with BMS (158-160). Some of the mechanisms responsible for this improved repair are an increase in inflammatory and marrow-

derived stromal cell recruitment to the microdrill holes, increased vascularization and subchondral bone remodeling at early post-surgical time-points (187), as well as a polarization of macrophage phenotype towards the alternatively-activated pro-wound healing lineage (188) and increased bone remodeling and osteoclast activation leading to better repair tissue integration (189). CS-GP-blood implants (BST-CarGel^{TM}) were tested in a a randomized controlled trial for the treatment of focal cartilage. BST-CarGel is currently commercialized in several countries by Smith and Nephew.

More recently, we have developed freeze-dried formulations of chitosan that can be solubilized in PRP to form injectable implants that solidify *in situ* and are used for tissue repair. These CS-PRP implants were shown to reside for several weeks and induce vascularization and cell recruitment in a subcutaneous implantation model, both of which are desirable in the context of meniscus repair. Chevrier et al., used a systematic approach to adjust chitosan number average molar mass, chitosan concentration, and lyoprotectant concentration to obtain freeze-dried CS formulations that are completely and rapidly solubilized in PRP and coagulate quickly to form mechanically stable implants (19). Deprés-Tremblay et al., demonstrated that platelet aggregation and clot retraction were suppressed through chitosan covering the blood components. They also showed that CS-PRP implants release more platelet-derived growth factors than PRP alone. CS-PRP implants were then used to augment repair of rotator cuff and cartilage in small and large animal models. Based on all of the above, it is expected that a combination of chitosan and PRP would be successful in improving the healing of the meniscus (21, 25, 190).

The effect of CS-PRP implants was tested in ovine meniscus surgical repair models in two sequential pilot feasibility studies. One of our findings for the first study was that CS-PRP hybrid implants enhanced repair tissue synthesis, induced complete healing, and seamless repair tissue integration in 1 out of 4 treated defects after 3 months post-surgery, while injection of PRP alone did not. One of the possible reasons for the low success rate was that a bilateral longitudinal surgical laceration model was used and did not allow the sheep to protect their treated knee from weight-bearing post-operatively which posed some complications such as minimal implant retention and reproducibility of the model. Developing the unilateral complex laceration model for the second study allowed us to overcome some of these limitations. To achieve full access to the medial compartment of the knee, a displacement of the extensor mechanism was performed, and the medial collateral ligament was detached from its femoral insertion with a bone block. The human meniscus is structurally and functionally heterogeneous. Sheep is a well-established and preferred large

animal model for meniscus tissue repair and replacement technique. The ovine meniscus represents a scaled-down version of the human meniscus due to anatomical and compositional. It should be noted that no animal model is known to totally mimics the human joint (63, 138). The human meniscus experiences 3 histological phases after rupture: a reactive phase, a perimeniscal proliferation phase, and a remodeling phase. Previous investigations indicated that there are some differences and similarities between the response to injury in animal models of meniscus injury and human one (190, 191). In human, the tissue bridging is poor at the rupture site and the presence of a perimeniscal proliferation phase lasts between 12 to 36 weeks.

The current findings indicate that in animal studies both the perimeniscal proliferation phase and synovial ingrowth were found to be critical for repair and the proliferation phase takes longer. Poor intrinsic cell density and revascularization has been reported in both human and animal studies. In addition, our histological results showed there was a broad strip of reparative tissue which was invaded by cells in CS-PRP treated tears after 6 weeks and 3 months, respectively. Although the repair tissue was still not organized, and Safranin-O matrix staining intensity was negative in the gap meaning that meniscus is still in the reactive phase or beginning at the stage of proliferation. Further, our studies indicated that repair reactive phase started as partially integrated after 3 weeks of implantation of CS-PRP and progressed to a full repair after 6 weeks and 3 months. The origin of the cells filling the defect in the meniscus is, to a great extent, uncertain. Source and type of cells that fill the gap in meniscus in sheep in the current study needs to be further examined. There is a possibility that synovial cells (synovium-derived mesenchymal stem cells) and surrounding meniscal cells play a part in the process of meniscal repair (191). The factors that influence meniscal cell migration are not well-understood, nevertheless outer surface meniscus cells migrate quickly and exhibit lower adhesion. There is possibility that healing of the superficial layers is a consequence of the arrival of cellular elements from the synovial fluid and the fibrochondrocytes. Healing of the deeper area could be as a result of the synovial autograft. However, the trigger factor of the healing process remains unknown and the synovium could be a source of repair contributing to healing (54). The cell source for meniscus repair is yet to be fully analyzed. In a recent study, the controlled applications of connective tissue growth factor and transforming growth factor beta-3 have been shown to induce seamless healing of avascular meniscus tears by inducing recruitment and differentiation of synovial mesenchymal stem progenitor cells into the incision site to form an integrated fibrocartilaginous matrix (138).

Generally speaking, the repair response is dependent on the synovial cell ingrowth, the response of fibroblasts, and the vasculature supply. Addition of trephination channels, rasping, and CS-PRP not only allowed us to deliver the implant to the defect site but also stimulated the tear site for further cytokine production which induced regeneration process. Chitosan-PRP demonstrated potential of neovascular formation and tissue remodeling in the context of cartilage repair which was in line with what we found in the meniscus repair process. In addition, the formation of new blood vessels at the proximity of tears treated with chitosan-PRP, cell recruitment, migration of cells through suture channels, presence of immature highly cellular tissue from 6 weeks as early phases of study to 3 month are consistent with the previous publications in goat and sheep models (85, 86, 192).

Chondro-Gide is the bilayer natural collagen matrix membrane widely employed for autologous chondrocytes implantation for cartilage regeneration. Currently, it is the most promising approach to cell-based cartilage repair treatments. Given the similarities between articular cartilage and menisci microstructures, we hypothesized that use of the Chondro-Gide membrane might be beneficial and favorable for the treatments of complex tears in the avascular zones of menisci, allowing prevention of meniscus degeneration or delaying early stages of ostheoarthtics. This biopolymer in combination with sutures was tested clinically for treating complex human meniscal tears with or without bone marrow aspirate deep to the membrane wrap with 2.5 years follow-up. These collagen scaffold membranes could serve a similar purpose to that of fibrin clot by allowing menisci fibrochondocyte cells to migrate to the defect area and become involved in the healing process. Consistent with our result and as was shown previously, introducing of wrapping technique at the same time with implantation of surgical complex defect was technically challenging. One important finding from our study was the difficulties we faced in implementation of the complex defect and the wrapping technique during surgery (185). Addition of Chondro-Gide demands more sutures which disturb meniscus collagen tissues and stimulates formation of foreign body giant cells which were not observed in the other groups. The healing was not achieved with PRP or wrapping alone in this study though some authors have reported good result with the addition of PRP, bone marrow aspirate, and expanded autologous chondrocytes in sheep and goat models (85, 86, 192).

Creation of complex tear with horizontal component in the medial meniscus was more in line with the type of lesions found in clinical setting. Therefore, the animal model used in the present

study was relevant to the pathological joint disease condition discovered in human and results of this study suggest that CS-PRP implants are a promising approach for the treatment of menisci injuries with the potential to prevent degeneration in early stages. To properly consider what are the biological processes during menisci repair, we also should consider the whole joint, which is why we examined the synovial membrane and articular cartilage. CS-PRP hybrids were well-tolerated in the joint environment with minimal effect on the adjacent joint (193). Transient synovitis was only observed at the initial stages of the study, demonstrated by an increase of vascularization and a probable subset population of macrophages in the synovial membrane tissue which is responsible for inflammatory phenotype but decreased after 3 months. In other words, degradation of CS-PRP under physiological loading and integration after 3 months did not induce the inflammatory response in joints with a minimal cartilage degradation and with no adverse effect. CS-PRP implants exhibited good biocompatibility.

It is crucial to keep in mind that both the humoral immunity and the cellular immunity play a role in the early stages of healing after implantation. Although PRP-derived growth factors showed positive effects on meniscus cell proliferation and differentiation, the impact of PRP on enhancing healing of the degenerative meniscus tears is still uncertain (151, 194). The most appropriate type of PRP needs to be determined to treat meniscus injuries. All these signs of regenerative tissue process could be derived by application of CS-PRP since this implant has been shown to modulate macrophage phenotype and tissue remodeling in the context of cartilage repair with evidence of a pro-angiogenesis process. To observe the proliferation ingrowth phase for meniscus repair, we need to expand the time and number of animals. However, it is difficult to draw a definitive conclusion based on the small number of animals in these two pilot studies. In another *in vitro* study we conducted, the freeze-dried cakes of chitosan with a specific and narrow range of DDA between 80.5-84.8% and M_n between 32-55 kDa were tested with various types of PRPs that can be isolated with different commercial systems. Our data showed that the performance of CS-PRP formulations was comparable for all PRP systems.

Obviously, there were differences between the concentration of the blood components including platelets, leukocytes, erythrocytes, and presumably growth factors from each PRP preparation systems. The concentration of platelets is of great importance since cytokines and growth factors released from alpha-granule are partly responsible for the mechanisms of action of PPR and contribute to the healing process. Our results with the combination of chitosan formulations with

leukocyte-poor PRP demonstrated that presence of leukocytes and erythrocytes play a role in platelet activation and thrombin generation. In the current study, two types of PRPs were tested with biopolymer of chitosan which is the leukocyte-poor or rich PRP. Leukocyte-poor PRP encompasses a lower concentration of leukocytes and erythrocytes. All this heterogeneity in the blood-derived devices might explain conflicting therapeutic results since the effect of leukocytes on the repair process is not yet fully understood (172).

Therefore, depending on the targeted tissue, the inclusion or exclusion of leukocytes in PRP preparations is gaining more attention in recent years. In the treatment of ostheoarthritis of the knee, leukocyte-poor PRP seems to be superior to leukocyte-rich PRP because it does not introduce inflammatory factors in the joint, while in chronic tendinopathy, use of leukocyte-rich PRP has been shown to be superior. Not many studies have evaluated the effect of PRP for degenerative menisci tears. On the one hand, the presence of leukocytes in leukocyte-rich PRP is associated with the increase of the concentration of growth factors such as vascular endothelial growth factor. On the other hand, leukocytes increase apoptosis and decrease cell proliferation by the release of inflammatory and catabolic factors (195). Freeze-dried chitosan cakes were easily solubilized in PRP to form CS-PRP formulations that had paste-like properties to adhere to the defect site and modulate the healing tissue process (19). The chitosan biopolymer in CS-PRP formulations coats platelet and blood cells and prevents clot retraction and platelet aggregation (172). In addition, platelets are activated, and growth factors released from granules due to the presence of chitosan. Delivery of PRP alone to the defect site is challenging due to the PRP low residency time and physical stability. Donor-to-donor variations in growth factor content is also a significant concern which could be mitigated by pooling of PRP from different donors as a strategy.

Subsequently, freeze-dried cycle for CS was optimized. Performance characteristics of cakes upon reconstitution in benchtop human PRP and human commercial plasma were evaluated. Our findings showed that a one-day FD cycle produced cakes that were non-collapsed, had acceptable macroscopic appearance, and were soluble in benchtop human PRP and commercial plasma. This provided an optimized freeze-drying process with significantly reduced duration that preserves the quality of the final lyophilized product. In our lab, with the modifications implemented, decreased the freeze-drying process duration was reduced by 44 hours (64%).

In every experimental work there are a number of possible errors, including equipment errors, data analysis, and human errors. We have done our best to minimize these errors and eliminate

them as far (much?) as possible. For instance, in the animal studies, the animals were randomly allocated to the different treatment groups and histological assessment was performed in a double blinded fashion.

In summary, in study 1, we carried out 2 pilot feasibility studies in ovine models by injecting freeze-dried chitosan-PRP surgical implants to improve meniscus repair. In study 2, we showed that multiple PRP preparations can solubilize freeze-dried chitosan formulations to form injectable implants for orthopedic indications and evaluated compatibility of this freeze-dried technology with various types of PRP preparations. In study 3, we optimized the freeze-drying cycle of FD-CS for orthopedic conditions and assessed performance with human platelet rich plasma (PRP) and human commercial plasma. Subsequently we drew the following conclusions based on the understanding gained from the three studies: CS-PRP implants showed the potential to augment meniscus repair through tissue integration, cell infiltration and vascularization in large animal models. CS PRP hybrids was compatible not only with benchtop PRP but also with other commercial PRP preparation devices suggesting its broad application for orthopedic indications. We successfully reduced duration of the FD cycle of chitosan formulations from 3-days to one-day producing cakes had an acceptable macroscopic appearance and were non-collapsed before reconstitution in benchtop human PRP and human commercial plasma and met critical quality attributes. Shorter FD cycles will allow for faster preparation of chitosan-based formulations and will also significantly reduce the production cost at the commercial scale. We believe that these integrated approaches will improve healthcare by reducing the socio-economic burden of menisci injuries.

CHAPTER 10 CONCLUSION AND RECOMMENDATIONS

Repair of degenerative meniscus lesions is a significant challenge in the clinic. The poor intrinsic meniscus healing response and technical difficulties are associated with the high failure rate of repair and meniscectomy outcome. Progression of meniscus tear pathologies is dependent on many factors such as the size of the defect, patient age, and joint stability. Inferior mechanical properties result in removal of the tissue, increasing the likelihood of developing progressive joint degeneration and ostheoarthtics. Recently, there has been a significant shift toward meniscus preservation and repair rather than resection. Current therapeutic approaches either don't regenerate the native tissue or outcomes are not certain in the long-term. There is a great deal of debate about what is the optimal treatment for meniscus injuries in the field of musculoskeletal tissue repair. Although various new repair strategies are available, additional clinical trials are needed to find the optimal therapy for meniscus repair. Application of augmentation strategies may be an effective way to enhance the slow physiologic meniscal healing response for patients who have high demand and elderly individuals. A successful meniscus repair requires synthesis of new tissue containing viable meniscal cells to bridge the defect, differentiation into the proper phenotype, remodeling into the native tissue, and creation of fibrocartilage tissue.

The primary objective of the current thesis was to improve knee meniscus repair by application of freeze-dried (FD)-chitosan (CS) platelet-rich plasma (PRP) implants in ovine models. We tested the feasibility of using FD-CS PRP hybrids, which are a combination of natural biopolymer of chitosan and PRP, in large animal models of meniscus repair and followed-up outcomes at different short and mid-term time-points. Injectable chitosan-PRP implants were shown to induce cell infiltration to the defect, vascularization, integration, and promote repair tissue synthesis.

Our data from first to the second pilot study in sheep meniscus provided support that addition of a horizontal component to the tear likely contributed to implant retention and reproducibility of the meniscus healing response from 25% to 50% success rate. The unilateral model also allowed the sheep to protect their knees from post-operative weight-bearing. Freeze-dried chitosan formulations can be rapidly and wholly solubilized in autologous PRP to form injectable *in situ* solidifying implants that have tissue regeneration capacity. Chitosan-PRP implants showed a superior regenerative effect over wrapping the meniscus with a collagen membrane or injecting PRP alone. Using the wrap in conjunction with chitosan-PRP implants did not further improve repair and the additional sutures needed to secure the wrap created significant damage to the

menisci. The latter suggested that chitosan-PRP implants by themselves could be safe in overcoming the current inherent limitations of meniscus repair. One important finding was the different treatments did not induce any lasting adverse effect on the other joint components aside from transient mild-to-moderate synovitis at 6 weeks' post-surgery. Restoration and healing of meniscus tears are expected to have a chondroprotective effect at longer repair time-points. Chitosan-PRP implants have several features revealing a higher potential than PRP alone to improve repair outcomes and restore meniscus function.

In the next study, we tested the compatibility of different PRPs with a rather narrow range of chitosan formulations. All CS cakes were soluble in different PRP preparations. Although the commercial PRP preparations are vastly heterogenous, the CS-PRP technology was found to be compatible with all of them. In this study 6 different commercially available separation systems were used: 1) Arthrex Angel set at 2% hematocrit, 2) Arthrex Angel set at 7% hematocrit, 3) Harvest SmartPrep 2, 4) RegenLab RegenKit-BCT, 5) RegenLab RegenKit-THT, 6) Arthrex ACP double syringe system. All these systems were either plasma-based or buffy coat-based in terms of PRP production. We found that all these technologies differ regarding the type of PRPs, hematocrit setting, initial blood volume, number of centrifuges, centrifugal force and time, the type of anticoagulant, the method of preparation, and even final volume of PRP. Majority of these systems have a single spin centrifugation method. Both the force and total centrifugation time differ between systems. Also, there is a wide variation in the prices between the systems.

There was a slight variation in pH and osmolality of CS-PRP formulations; however, it is expected that they would be cytocompatible. The concentration of platelets and other blood components differ compared to whole blood. Formulations prepared with the low, mid, and high range of chitosan M_n and DDA performed equally well. CS-PRP cakes were white, and homogenous and contained chitosan, trehalose as lyoprotectant, and calcium chloride as clot activator. CS-PRP formulations were less runny and were more paste-like than PRP controls due to the presence of the chitosan polymer. The platelet, leukocyte and erythrocyte concentration of the PRPs used to solubilize the cakes did not appear to affect the *in vitro* performance of the CS-PRP hybrids. CS-PRP formulations coagulated rapidly to form homogenous hybrid clots that resisted platelet-mediated clot retraction. We would expect properties of PRP such as leukocyte content, activation of platelet, fibrin, and other proteins in plasma to affect the outcome. The proposed specifications for the product of chitosan M_n 35-50 kDa and DDA 80-84% are adequate

for use with different commercial PRP systems. There are still little regulation and evidence for PRP and other blood-derived formulations for soft tissue injuries. Biological activity level of various PRP formulations needs to be rigorously defined. To date, not all the studies provide detailed data regarding the platelets, leucocytes content, and platelet enrichment factors. Therefore, next-generation approaches should concentrate more on a universal formulation with a defined growth factor content.

In the last study, we successfully optimized and reduced duration of the FD cycle of chitosan fromulations from 3-days to one-day. The produced cakes had an acceptable macroscopic appearance and were non-collapsed before reconstitution in benchtop human PRP and human commercial plasma and met critical quality attributes.

The following suggestions are worth considering for future research direction within the theme of my work:

1. *Biomechanical testing of (suture) repair for menisci*: In this dissertation, we did not directly consider the contribution of biomechanical stimuli to meniscal repair. However, in general a tensile testing machine could be used to determine the failure rate. In this case, the anterior and posterior portions of the menisci would be trimmed and prepared for clamping for the device. Menisci would clamp in a machine, preload, and then load up to failure at the same rate. Ultimate load, ultimate elongation, and stiffness would be determined from the load-to-failure for repair stability. All tests could be performed at room temperature, and the menisci would continuously be kept moist with saline solutions.

2. *Additional animals and more end time-point of meniscus repair in ovine*: Investigation is somewhat limited on meniscus implants in large animal models while there are significant publications on cartilage repair by using biomaterials or biologics. Based on the literature review which was performed at the beginning of my study we selected 3-time points for meniscus repair. Although our time points were selected based on our published work and the existing papers, further time-points must be added to evaluate the long-term meniscus repair outcome, as well as the interaction of biomaterial and tissue in the future.

To follow up process of meniscus repair by implants and and mimic degenartion of OA which happens in human, a long-term study will be proposed. Conducting a statistically powered pivotal study in 16 sheep for repairing of meniscus tears with surgical suturing and applying chitosan solubilized in PRP in the tear for 6-months would be suggested. Meniscal tissues should be analyzed by optical microscopy for tissue composition and integrity. Safranin-O staining, collagen type II and I expression, blood vessel density, and cell recruitment would be quantified using histology. We would propose to add polarized light microscopy and scanning environmental electron microscopy for collagen fiber organization assessment. Tissue biopsies would be collected from adjacent to the tear in the meniscus to quantify meniscal biochemical content (GAG, collagen, and DNA content). Global indicators of joint function would be assessed through a lameness test, a macroscopic scoring system, analysis of adjacent tissues including medial condyle and tibial plateau cartilage via electromechanical mapping, biochemistry and histology, and joint inflammation as will judged by macroscopic assessment and synovial tissue histology.

3. *Investigate the biological effects of CS PRP on meniscus tissue and synovial membrane cells and explants in vitro:* To identify the most appropriate cell source for meniscus repair and understand potential anabolic and catabolic influence of implants, we would suggest isolating ovine cells and explants from the outer meniscus, inner meniscus, and synovial membrane and culture them in the presence of CS-PRP for 7 and 14 days. The outcome measures could be analyzed by: gene expression, DNA, collagen, and GAG content, the release of anabolic/catabolic factors in the culture medium, histostaining, immunostaining, and cell migration. Synovium has been shown to play a key role in the natural course of the meniscal healing process. It is demonstrated that synovial stem cells adhered to the injured site, differentiated into cartilage cells, and participated in joint intraarticular tissue injuries with improved functional properties.

4. *Application of bone marrow aspirate concentrate (BMAC):* BMAC is a great source of progenitor cells, MSCs, and associated growth factors which are obtained by iliac crest aspiration. Recent reports showed good to excellent outcomes and pain relief regarding the application of BMAC for treatment of focal chondral lesions and OA. CS-PRP has been

shown to improve and stimulate repair in the rotator cuff, cartilage lesions, and meniscus in preclinical animal models. Both PRP and BMAC have been used for treatment of knee pathologies. Until now there was no document or protocol confirming what is the optimal method for preparing of PRP and BMAC. To identify and compare the therapeutic effect of chitosan-PRP with chitosan-BMAC, I would suggest performing another *in vitro* study. Blood would be extracted from ovine, BMAC and PRP would be isolated, and used to solubilize a range of CS formulations. *In vitro* performance could be assessed for paste-like properties, coagulation, clot retraction, and clot homogeneity.

Altogether, CS-PRP implants showed the potential to augment meniscus repair by tissue integration and vascularization in large animal models. Histological assessment, electromechanical potential, macroscopic, and microscopic analysis of repaired meniscus demonstrated that implants were resident in the tears and trephination channels and induced cell recruitment from the vascularized periphery of the menisci which led to complete or partial repair and seamless repair tissue integration in contrast to PRP or wrapping. CS-PRP implants may have chondroprotective effect on articular surfaces.

CS PRP hybrids was compatible not only with benchtop PRP but also with other commercial PRP preparation devices suggesting its broad application for orthopedic indications. The collection of work described in the current thesis presented several novel findings in the area of orthopedics meniscus repair, by development and validation of a surgical technique which has set the groundwork for future evaluation of the menisci and other connective tissues with the possibility of translation to clinical trials in the future. Augmentation of complex defects in the avascular zones of menisci would be a way for avoiding of meniscectomy and restore meniscus function. Techniques are now focusing to be minimally invasive. We believe that these integrated approaches improve healthcare by reducing of the socio-economic burden of menisci injuries.

BIBLIOGRAPHY

1. Evans CH. Advances in regenerative orthopedics. Mayo Clin Proc. 2013;88(11):1323-39.

2. Englund M, Roemer FW, Hayashi D, Crema MD, Guermazi A. Meniscus pathology, osteoarthritis and the treatment controversy. Nat Rev Rheumatol. 2012;8(7):412-9.

3. Englund M, Guermazi A, Lohmander LS. The meniscus in knee osteoarthritis. Rheum Dis Clin North Am. 2009;35(3):579-90.

4. Chirichella PS, Jow S, Iacono S, Wey HE, Malanga GA. Treatment of Knee Meniscus Pathology: Rehabilitation, Surgery, and Orthobiologics. PM R. 2018.

5. Englund M, Niu J, Guermazi A, Roemer FW, Hunter DJ, Lynch JA, et al. Effect of meniscal damage on the development of frequent knee pain, aching, or stiffness. Arthritis & Rheumatism. 2007;56(12):4048-54.

6. Englund M, Guermazi A, Roemer FW, Aliabadi P, Yang M, Lewis CE, et al. Meniscal tear in knees without surgery and the development of radiographic osteoarthritis among middle-aged and elderly persons: The Multicenter Osteoarthritis Study. Arthritis Rheum. 2009;60(3):831-9.

7. Doral MN, Bilge O, Huri G, Turhan E, Verdonk R. Modern treatment of meniscal tears. EFORT Open Rev. 2018;3(5):260-8.

8. Woodmass JM, LaPrade RF, Sgaglione NA, Nakamura N, Krych AJ. Meniscal Repair: Reconsidering Indications, Techniques, and Biologic Augmentation. J Bone Joint Surg Am. 2017;99(14):1222-31.

9. Nepple JJ, Dunn WR, Wright RW. Meniscal repair outcomes at greater than five years: a systematic literature review and meta-analysis. J Bone Joint Surg Am. 2012;94(24):2222-7.

10. Englund M. Meniscal tear-a feature of osteoarthritis. Acta Orthopaedica Scandinavica. 2004;75(sup312):1-45.

11. Gwathmey FW, Jr., Golish SR, Diduch DR. Complications in brief: meniscus repair. Clin Orthop Relat Res. 2012;470(7):2059-66.

12. Howell R, Kumar NS, Patel N, Tom J. Degenerative meniscus: Pathogenesis, diagnosis, and treatment options. World J Orthop. 2014;5(5):597-602.

13. Ghazi Zadeh L, Chevrier A, Farr J, Rodeo SA, Buschmann MD. Augmentation Techniques for Meniscus Repair. Knee Surg. 2018;31(1):99-116.

14. Buma P, Ramrattan NN, van Tienen TG, Veth RPH. Tissue engineering of the meniscus. Biomaterials. 2004;25(9):1523-32.

15. Bilgen B, Jayasuriya CT, Owens BD. Current Concepts in Meniscus Tissue Engineering and Repair. Adv Healthc Mater. 2018;7(11):e1701407.

16. Ahmad Z, Howard D, Brooks RA, Wardale J, Henson FM, Getgood A, et al. The role of platelet rich plasma in musculoskeletal science. JRSM Short Rep. 2012;3(6):40.

17. Andia I, Maffulli N. Platelet-rich plasma for managing pain and inflammation in osteoarthritis. Nat Rev Rheumatol. 2013;9(12):721-30.

18. Bielecki T, Ehrenfest DMD. Platelet-Rich Plasma (PRP) and Platelet-Rich Fibrin (PRF): Surgical Adjuvants, Preparations for In Situ Regenerative Medicine and Tools for Tissue Engineering. Current Pharmaceutical Biotechnology. 2012;13(7):1121-30.

19. Chevrier A, Darras V, Picard G, Nelea M, Veilleux D, Lavertu M, et al. Injectable chitosan-platelet-rich plasma implants to promote tissue regeneration: in vitro properties, in vivo residence, degradation, cell recruitment and vascularization. Tissue Eng Regen Med. 2018;12(1):217-28.

20. Younes I, Rinaudo M. Chitin and chitosan preparation from marine sources. Structure, properties and applications. Mar Drugs. 2015;13(3):1133-74.

21. Fong D, Hoemann CD. Chitosan immunomodulatory properties: perspectives on the impact of structural properties and dosage. Future Science; 2017.

22. Tang XC, Pikal MJ. Design of freeze-drying processes for pharmaceuticals: practical advice. Pharmaceutical research. 2004;21(2):191-200.

23. Hoemann CD, Sun J, McKee MD, Chevrier A, Rossomacha E, Rivard GE, et al. Chitosan-glycerol phosphate/blood implants elicit hyaline cartilage repair integrated with porous subchondral bone in microdrilled rabbit defects. Osteoarthritis Cartilage. 2007;15(1):78-89.

24. Hoemann CD, Chen G, Marchand C, Tran-Khanh N, Thibault M, Chevrier A, et al. Scaffold-guided subchondral bone repair: implication of neutrophils and alternatively activated arginase-1+ macrophages. Am J Sports Med. 2010;38(9):1845-56.

25. Dwivedi G, Chevrier A, Hoemann CD, Buschmann MD. Bone Marrow Progenitor Cells Isolated from Young Rabbit Trochlea Are More Numerous and Exhibit Greater Clonogenic, Chondrogenic, and Osteogenic Potential than Cells Isolated from Condyles. Cartilage. 2018;9(4):378-90.

26. Fox AJ, Bedi A, Rodeo SA. The basic science of human knee menisci: structure, composition, and function. Sports Health. 2012;4(4):340-51.

27. Fox AJ, Wanivenhaus F, Burge AJ, Warren RF, Rodeo SA. The human meniscus: a review of anatomy, function, injury, and advances in treatment. Clin Anat. 2015;28(2):269-87.

28. Makris EA, Hadidi P, Athanasiou KA. The knee meniscus: structure-function, pathophysiology, current repair techniques, and prospects for regeneration. Biomaterials. 2011;32(30):7411-31.

29. Arnoczky SP, Warren RF. The microvasculature of the meniscus and its response to injury: an experimental study in the dog. The American journal of sports medicine. 1983;11(3):131-41.

30. Gray JC. Neural and vascular anatomy of the menisci of the human knee. Journal of Orthopaedic & Sports Physical Therapy. 1999;29(1):23-30.

31. Pereira H, Cengiz IF, Silva-Correia J, Oliveira JM, Reis RL, Espregueira-Mendes J. Human Meniscus: From Biology to Tissue Engineering Strategies. Sports Injuries2013. p. 1-16.

32. Cheung HS. Distribution of type I, II, III and V in the pepsin solubilized collagens in bovine menisci. Connective tissue research. 1987;16(4):343-56.

33. Nishiumi T, Fukuda T, Nishimura T. Isolation and characterization of a small proteoglycan associated with porcine intramuscular connective tissue. Journal of agricultural and food chemistry. 1997;45(8):2978-83.

34. Ghadially F, Thomas I, Yong N, Lalonde J. Ultrastructure of rabbit semilunar cartilages. Journal of anatomy. 1978;125(Pt 3):499.

35. Sanchez-Adams J, Athanasiou KA. The Knee Meniscus: A Complex Tissue of Diverse Cells. Cellular and Molecular Bioengineering. 2009;2(3):332-40.

36. VAN DER BRACHT H, Verdonk R, Verbruggen A, Elewaut D, Verdonk P. Cell-based meniscus tissue engineering. Topics in tissue engineering. 3: Biomaterials and Tissue Engineering Group (BTE); 2007. p. ch2-1-ch2-13.

37. Melrose J, Smith S, Cake M, Read R, Whitelock J. Comparative spatial and temporal localisation of perlecan, aggrecan and type I, II and IV collagen in the ovine meniscus: an ageing study. Histochem Cell Biol. 2005;124(3-4):225-35.

38. Verdonk PC, Forsyth RG, Wang J, Almqvist KF, Verdonk R, Veys EM, et al. Characterisation of human knee meniscus cell phenotype. Osteoarthritis Cartilage. 2005;13(7):548-60.

39. Gunja NJ, Dujari D, Chen A, Luengo A, Fong JV, Hung CT. Migration responses of outer and inner meniscus cells to applied direct current electric fields. J Orthop Res. 2012;30(1):103-11.

40. Niu W, Guo W, Han S, Zhu Y, Liu S, Guo Q. Cell-Based Strategies for Meniscus Tissue Engineering. Stem Cells Int. 2016;2016:4717184.

41. McDermott ID, Masouros SD, Amis AA. Biomechanics of the menisci of the knee. Current Orthopaedics. 2008;22(3):193-201.

42. Kawamura S, Lotito K, Rodeo SA. Biomechanics and healing response of the meniscus. Operative Techniques in Sports Medicine. 2003;11(2):68-76.

43. AufderHeide AC, Athanasiou KA. Mechanical stimulation toward tissue engineering of the knee meniscus. Annals of biomedical engineering. 2004;32(8):1163-76.

44. Rath E, Richmond JC. The menisci: basic science and advances in treatment. British journal of sports medicine. 2000;34(4):252-7.

45. Loeser RF, Goldring SR, Scanzello CR, Goldring MB. Osteoarthritis: a disease of the joint as an organ. Arthritis Rheum. 2012;64(6):1697-707.

46. Mathiessen A, Conaghan PG. Synovitis in osteoarthritis: current understanding with therapeutic implications. Arthritis Res Ther. 2017;19(1):18.

47. Smith MD. The Normal Synovium. The open rheumatology journal. 2011;5:100.

48. IWANAGA T, Shikichi M, KITAMURA H, YANASE H, NOZAWA-INOUE K. Morphology and functional roles of synoviocytes in the joint. Archives of histology and cytology. 2000;63(1):17-31.

49. Bonnet CS, Walsh DA. Osteoarthritis, angiogenesis and inflammation. Rheumatology (Oxford). 2005;44(1):7-16.

50. Baker BE, Peckham AC, Pupparo F, Sanborn JC. Review of meniscal injury and associated sports. The American journal of sports medicine. 1985;13(1):1-4.

51. Mow VC, Ratcliffe A, Woo SL. Biomechanics of diarthrodial joints: Springer Science & Business Media; 2012.

52. Mordecai SC, Al-Hadithy N, Ware HE, Gupte CM. Treatment of meniscal tears: An evidence based approach. World J Orthop. 2014;5(3):233-41.

53. A. Viidik (auth.) AR, Savio L-Y. Woo, Van C. Biomechanics of Diarthrodial Joints.pdf.

54. de Albornoz PM, Forriol F. The meniscal healing process. Muscles, ligaments and tendons journal. 2012;2(1):10.

55. Tršek D, Hašpl M, Starčević D, Tabak T. Current concept of the meniscal repair. medicina. 2015;51(1):154-74.

56. Beaufils P, Becker R, Kopf S, Matthieu O, Pujol N. The knee meniscus: management of traumatic tears and degenerative lesions. EFORT Open Rev. 2017;2(5):195-203.

57. Forman SK, Oz MC, Lontz JF, Treat MR, Forman TA, Kiernan HA. Laser-assisted fibrin clot soldering of human menisci. Clinical orthopaedics and related research. 1995(310):37-41.

58. Brindle T, Nyland J, Johnson DL. The meniscus: review of basic principles with application to surgery and rehabilitation. Journal of athletic training. 2001;36(2):160.

59. Turman KA, Diduch DR, Miller MD. All-inside meniscal repair. Sports Health. 2009;1(5):438-44.

60. Nelson CG, Bonner KF. Inside-out meniscus repair. Arthrosc Tech. 2013;2(4):e453-60.

61. Hurtig MB, Buschmann MD, Fortier LA, Hoemann CD, Hunziker EB, Jurvelin JS, et al. Preclinical Studies for Cartilage Repair: Recommendations from the International Cartilage Repair Society. Cartilage. 2011;2(2):137-52.

62. Deponti D, Di Giancamillo A, Scotti C, Peretti GM, Martin I. Animal models for meniscus repair and regeneration. J Tissue Eng Regen Med. 2015;9(5):512-27.

63. Brzezinski A, Ghodbane SA, Patel JM, Perry BA, Gatt CJ, Dunn MG. The Ovine Model for Meniscus Tissue Engineering: Considerations of Anatomy, Function, Implantation, and Evaluation. Tissue Eng Part C Methods. 2017;23(12):829-41.

64. Potes JC, Reis J, Capela e Silva F, Relvas C, Cabrita AS, Simões JA. The sheep as an animal model in orthopaedic research. 2008.

65. Martini L, Fini M, Giavaresi G, Giardino R. Sheep model in orthopedic research: a literature review. Comparative medicine. 2001;51(4):292-9.

66. Bansal S, Keah NM, Neuwirth AL, O'Reilly O, Qu F, Seiber BN, et al. Large Animal Models of Meniscus Repair and Regeneration: A Systematic Review of the State of the Field. Tissue Eng Part C Methods. 2017;23(11):661-72.

67. ALLEN MJ, HOULTON JE, ADAMS SB, RUSHTON N. The surgical anatomy of the stifle joint in sheep. Veterinary surgery. 1998;27(6):596-605.

68. Chevrier A, Kouao AS, Picard G, Hurtig MB, Buschmann MD. Interspecies comparison of subchondral bone properties important for cartilage repair. J Orthop Res. 2015;33(1):63-70.

69. Wu C-L, Little D. Animal Models of Meniscal Injury in Post-Traumatic Arthritis. Post-Traumatic Arthritis2015. p. 41-62.

70. Martinek V, Ueblacker P, Braun K, Nitschke S, Mannhardt R, Specht K, et al. Second generation of meniscus transplantation: in-vivo study with tissue engineered meniscus replacement. Arch Orthop Trauma Surg. 2006;126(4):228-34.

71. Sweigart MA, Athanasiou KA. Toward tissue engineering of the knee meniscus. Tissue engineering. 2001;7(2):111-29.

72. Rey-Rico A, Cucchiarini M, Madry H. Hydrogels for precision meniscus tissue engineering: a comprehensive review. Connect Tissue Res. 2017;58(3-4):317-28.

73. Liu C, Toma IC, Mastrogiacomo M, Krettek C, von Lewinski G, Jagodzinski M. Meniscus reconstruction: today's achievements and premises for the future. Arch Orthop Trauma Surg. 2013;133(1):95-109.

74. Schwartz JA, Wang W, Goldstein T, Grande DA. Tissue Engineered Meniscus Repair: Influence of Cell Passage Number, Tissue Origin, and Biomaterial Carrier. Cartilage. 2014;5(3):165-71.

75. Tissue engineering of the meniscus: Scaffolds for meniscus repair and replacement. Musculoskeletal Regeneration. 2015.

76. Zhang Z-Z, Jiang D, Wang S-J, Qi Y-S, Ding J-X, Yu J-K, et al. Scaffolds drive meniscus tissue engineering. RSC Advances. 2015;5(95):77851-9.

77. Zhang Z, Guo W, Gao S, Chen M, Li X, Zhang X, et al. Native tissue-based strategies for meniscus repair and regeneration. Cell Tissue Res. 2018;373(2):337-50.

78. Bruns J, Kahrs J, Kampen J, Behrens P, Plitz W. Autologous perichondral tissue for meniscal replacement. The Journal of bone and joint surgery British volume. 1998;80(5):918-23.

79. Lee AS, Kang RW, Kroin E, Verma NN, Cole BJ. Allograft meniscus transplantation. Sports medicine and arthroscopy review. 2012;20(2):106-14.

80. Chambers MC, El-Amin S. Tissue engineering of the meniscus: scaffolds for meniscus repair and replacement. Musculoskelet Regen. 2015;1:e998.

81. Guo W, Liu S, Zhu Y, Yu C, Lu S, Yuan M, et al. Advances and Prospects in Tissue-Engineered Meniscal Scaffolds for Meniscus Regeneration. Stem Cells Int. 2015;2015:517520.

82. Ibarra C, Jannetta C, Vacanti C, Cao Y, Kim T, Upton J, et al., editors. Tissue engineered meniscus: a potential new alternative to allogeneic meniscus transplantation. Transplantation proceedings; 1997.

83. Ibarra C, Koski JA, Warren RF. Tissue engineering meniscus: cells and matrix. The Orthopedic clinics of North America. 2000;31(3):411-8.

84. Chiari C, Koller U, Dorotka R, Eder C, Plasenzotti R, Lang S, et al. A tissue engineering approach to meniscus regeneration in a sheep model. Osteoarthritis Cartilage. 2006;14(10):1056-65.

85. Kon E, Filardo G, Tschon M, Fini M, Giavaresi G, Marchesini Reggiani L, et al. Tissue engineering for total meniscal substitution: animal study in sheep model-results at 12 months. Tissue Eng Part A. 2012;18(15-16):1573-82.

86. Kon E, Chiari C, Marcacci M, Delcogliano M, Salter DM, Martin I, et al. Tissue Engineering for Total Meniscal Substitution: Animal Study in Sheep Model. Tissue Engineering Part A. 2008;14(6):1067-80.

87. Maher SA, Rodeo SA, Doty SB, Brophy R, Potter H, Foo LF, et al. Evaluation of a porous polyurethane scaffold in a partial meniscal defect ovine model. Arthroscopy. 2010;26(11):1510-9.

88. Zur G, Linder-Ganz E, Elsner JJ, Shani J, Brenner O, Agar G, et al. Chondroprotective effects of a polycarbonate-urethane meniscal implant: histopathological results in a sheep model. Knee Surg Sports Traumatol Arthrosc. 2011;19(2):255-63.

89. Gruchenberg K, Ignatius A, Friemert B, von Lubken F, Skaer N, Gellynck K, et al. In vivo performance of a novel silk fibroin scaffold for partial meniscal replacement in a sheep model. Knee Surg Sports Traumatol Arthrosc. 2015;23(8):2218-29.

90. Patel JM, Merriam AR, Culp BM, Gatt CJ, Jr., Dunn MG. One-Year Outcomes of Total Meniscus Reconstruction Using a Novel Fiber-Reinforced Scaffold in an Ovine Model. Am J Sports Med. 2016;44(4):898-907.

91. Patel JM, Merriam AR, Kohn J, Gatt CJ, Jr., Dunn MG. Negative Outcomes of Poly(l-Lactic Acid) Fiber-Reinforced Scaffolds in an Ovine Total Meniscus Replacement Model. Tissue Eng Part A. 2016;22(17-18):1116-25.

92. Merriam AR, Patel JM, Culp BM, Gatt CJ, Jr., Dunn MG. Successful Total Meniscus Reconstruction Using a Novel Fiber-Reinforced Scaffold: A 16- and 32-Week Study in an Ovine Model. Am J Sports Med. 2015;43(10):2528-37.

93. Szojka A, Lalh K, Andrews SHJ, Jomha NM, Osswald M, Adesida AB. Biomimetic 3D printed scaffolds for meniscus tissue engineering. Bioprinting. 2017;8:1-7.

94. Kelly BT, Robertson W, Potter HG, Deng XH, Turner AS, Lyman S, et al. Hydrogel meniscal replacement in the sheep knee: preliminary evaluation of chondroprotective effects. Am J Sports Med. 2007;35(1):43-52.

95. Galley NK, Gleghorn JP, Rodeo S, Warren RF, Maher SA, Bonassar LJ. Frictional properties of the meniscus improve after scaffold-augmented repair of partial meniscectomy: a pilot study. Clin Orthop Relat Res. 2011;469(10):2817-23.

96. Rinaudo M. Chitin and chitosan: Properties and applications. Progress in Polymer Science. 2006;31(7):603-32.

97. Daraghmeh NH, Chowdhry BZ, Leharne SA, Al Omari MM, Badwan AA. Chitin. Profiles Drug Subst Excip Relat Methodol. 2011;36:35-102.

98. Jang M-K, Kong B-G, Jeong Y-I, Lee CH, Nah J-W. Physicochemical characterization of chitin separated from natural resources. Journal of Polymer Science Part A: Polymer Chemistry. 2004;42(14):3423-32.

99. No HK, Meyers SP. Preparation and Characterization of Chitin and Chitosan-A Review. Journal of Aquatic Food Product Technology. 1995;4(2):27-52.

100. Croisier F, Jérôme C. Chitosan-based biomaterials for tissue engineering. European Polymer Journal. 2013;49(4):780-92.

101. Rodriguez-Vazquez M, Vega-Ruiz B, Ramos-Zuniga R, Saldana-Koppel DA, Quinones-Olvera LF. Chitosan and Its Potential Use as a Scaffold for Tissue Engineering in Regenerative Medicine. Biomed Res Int. 2015;2015:821279.

102. Di Martino A, Sittinger M, Risbud MV. Chitosan: a versatile biopolymer for orthopaedic tissue-engineering. Biomaterials. 2005;26(30):5983-90.

103. Szymanska E, Winnicka K. Stability of chitosan-a challenge for pharmaceutical and biomedical applications. Mar Drugs. 2015;13(4):1819-46.

104. TE-007. 1116502982. In: 09-10-01, editor. TE-006 "B". p. Lab responsibility: J. Tremblay.

105. Singh DK, Ray AR. Biomedical Applications of Chitin, Chitosan, and Their Derivatives. Journal of Macromolecular Science, Part C: Polymer Reviews. 2000;40(1):69-83.

106. Zargar V, Asghari M, Dashti A. A Review on Chitin and Chitosan Polymers: Structure, Chemistry, Solubility, Derivatives, and Applications. ChemBioEng Reviews. 2015;2(3):204-26.

107. TE-054. 12784. Manual TE-054. p. Lab responsibility: Nick or C. Hoemann.

108. Tan H, Marra KG. Injectable, Biodegradable Hydrogels for Tissue Engineering Applications. Materials. 2010;3(3):1746-67.

109. Pillai CKS, Paul W, Sharma CP. Chitin and chitosan polymers: Chemistry, solubility and fiber formation. Progress in Polymer Science. 2009;34(7):641-78.

110. TE-017. 981257. p. Lab responsibility: Marc Lavertu.

111. Hattori H, Ishihara M. Feasibility of improving platelet-rich plasma therapy by using chitosan with high platelet activation ability. Exp Ther Med. 2017;13(3):1176-80.

112. Hattori H, Ishihara M. Changes in blood aggregation with differences in molecular weight and degree of deacetylation of chitosan. Biomedical Materials. 2015;10(1).

113. Shen EC, Chou TC, Gau CH, Tu HP, Chen YT, Fu E. Releasing growth factors from activated human platelets after chitosan stimulation: a possible bio-material for platelet-rich plasma preparation. Clin Oral Impl Res. 2006;17:572-8.

114. Zhang W, Zhong D, Liu Q, Zhang Y, Li N, Wang Q, et al. Effect of chitosan and carboxymethyl chitosan on fibrinogen structure and blood coagulation. Journal of Biomaterials Science-Polymer Edition. 2013;24(13):1549-63.

115. Mohammadi R, Mehrtash M, Mehrtash M, Hassani N, Hassanpour A. Effect of Platelet Rich Plasma Combined with Chitosan Biodegradable Film on Full-Thickness Wound Healing in Rat Model. Bulletin of emergency and trauma. 2016;4(1):29-37.

116. Shimojo AA, Perez AG, Galdames SE, Brissac IC, Santana MH. Performance of PRP associated with porous chitosan as a composite scaffold for regenerative medicine. ScientificWorldJournal. 2015;2015:396131.

117. Shimojo AA, Perez AG, Galdames SE, Brissac IC, Santana MH. Stabilization of porous chitosan improves the performance of its association with platelet-rich plasma as a composite scaffold. Materials science & engineering C, Materials for biological applications. 2016;60:538-46.

118. Shimojo AAM, Galdames SEM, Perez AGM, Ito TH, Luzo ÂCM, Santana MHA. In vitro performance of injectable chitosan-tripolyphosphate scaffolds combined with platelet-rich plasma. Tissue Engineering and Regenerative Medicine. 2016;13(1):21-30.

119. Kutlu B, Aydin RST, Akman AC, Gumusderelioglu M, Nohutcu RM. Platelet-rich plasma-loaded chitosan scaffolds: Preparation and growth factor release kinetics. Journal of Biomedical Materials Research Part B-Applied Biomaterials. 2013;101B(1):28-35.

120. Sancho-Tello M, Martorell S, Mata Roig M, Milián L, Gámiz-González M, Gomez Ribelles JL, et al. Human platelet-rich plasma improves the nesting and differentiation of human chondrocytes cultured in stabilized porous chitosan scaffolds. Journal of tissue engineering. 2017;8:2041731417697545.

121. Periayah MH, Halim AS, Saad AZM, Yaacob NS, Hussein AR, Rashid AHA, et al. Hemostatic Evaluation of Chitosan Derivatives: Effects on Platelets In Vitro. Int Wound J. 2017;14(6):1276-89.

122. Singh R, Shitiz K, Singh A. Chitin and chitosan: biopolymers for wound management. Int Wound J. 2017;14(6):1276-89.

123. Sarem M, Moztarzadeh F, Mozafari M, Shastri VP. Optimization strategies on the structural modeling of gelatin/chitosan scaffolds to mimic human meniscus tissue. Mater Sci Eng C Mater Biol Appl. 2013;33(8):4777-85.

124. Muzzarelli R, Bicchiega V, Biagini G, Pugnaloni A, Rizzoli R. Role of N-carboxybutyl chitosan in the repair of the meniscus. Journal of bioactive and compatible polymers. 1992;7(2):130-48.

125. Wang J, Fu W, Zhang D, Yu X, Li J, Wan C. Evaluation of novel alginate dialdehyde cross-linked chitosan/calcium polyphosphate composite scaffolds for meniscus tissue engineering. Carbohydrate Polymers. 2010;79(3):705-10.

126. Chen JP, Cheng TH. Thermo-responsive chitosan-graft-poly(N-isopropylacrylamide) injectable hydrogel for cultivation of chondrocytes and meniscus cells. Macromol Biosci. 2006;6(12):1026-39.

127. Angele P, Kujat R, Koch M, Zellner J. Role of mesenchymal stem cells in meniscal repair. J Exp Orthop. 2014;1(1):12.

128. Yu H, Adesida AB, Jomha NM. Meniscus repair using mesenchymal stem cells - a comprehensive review. Stem Cell Res Ther. 2015;6:86.

129. Shen W, Chen J, Zhu T, Chen L, Zhang W, Fang Z, et al. Intra-articular injection of human meniscus stem/progenitor cells promotes meniscus regeneration and ameliorates osteoarthritis through stromal cell-derived factor-1/CXCR4-mediated homing. Stem Cells Transl Med. 2014;3(3):387-94.

130. Baker BM, Nathan AS, Huffman GR, Mauck RL. Tissue engineering with meniscus cells derived from surgical debris. Osteoarthritis Cartilage. 2009;17(3):336-45.

131. Scotti C, Hirschmann M, Antinolfi P, Martin I, Peretti G. Meniscus repair and regeneration: review on current methods and research potential. European cells & materials. 2013;26:150-70.

132. Angele P, Johnstone B, Kujat R, Zellner J, Nerlich M, Goldberg V, et al. Stem cell based tissue engineering for meniscus repair. J Biomed Mater Res A. 2008;85(2):445-55.

133. Cucchiarini M, McNulty AL, Mauck RL, Setton LA, Guilak F, Madry H. Advances in combining gene therapy with cell and tissue engineering-based approaches to enhance healing of the meniscus. Osteoarthritis Cartilage. 2016;24(8):1330-9.

134. Forriol F. Growth factors in cartilage and meniscus repair. Injury. 2009;40:S12-S6.

135. Spindler K, Mayes C, Miller R, Imro A, Davidson J. Regional mitogenic response of the meniscus to platelet-derived growth factor (PDGF-AB). Journal of orthopaedic research. 1995;13(2):201-7.

136. Ionescu LC, Lee GC, Huang KL, Mauck RL. Growth factor supplementation improves native and engineered meniscus repair in vitro. Acta Biomater. 2012;8(10):3687-94.

137. Bhargava MM, Attia ET, Murrell GA, Dolan MM, Warren RF, Hannafin JA. The effect of cytokines on the proliferation and migration of bovine meniscal cells. The American journal of sports medicine. 1999;27(5):636-43.

138. Tarafder S, Gulko J, Sim KH, Yang J, Cook JL, Lee CH. Engineered Healing of Avascular Meniscus Tears by Stem Cell Recruitment. Sci Rep. 2018;8(1):8150.

139. Braun HJ, Wasterlain AS, Dragoo JL. The use of PRP in ligament and meniscal healing. Sports Medicine and Arthroscopy Review. 2013;21(4):206-12.

140. Kushida S, Kakudo N, Morimoto N, Hara T, Ogawa T, Mitsui T, et al. Platelet and growth factor concentrations in activated platelet-rich plasma: a comparison of seven commercial separation systems. Journal of Artificial Organs. 2014;17(2):186-92.

141. Castillo TN, Pouliot MA, Kim HJ, Dragoo JL. Comparison of Growth Factor and Platelet Concentration From Commercial Platelet-Rich Plasma Separation Systems. The American Journal of Sports Medicine. 2010;39(2):266-71.

142. Dohan Ehrenfest DM, Rasmusson L, Albrektsson T. Classification of platelet concentrates: from pure platelet-rich plasma (P-PRP) to leucocyte- and platelet-rich fibrin (L-PRF). Trends Biotechnol. 2009;27(3):158-67.

143. Wang D, Rodeo SA. Platelet-Rich Plasma in Orthopaedic Surgery: A Critical Analysis Review. JBJS Rev. 2017;5(9):e7.

144. Alves R, Grimalt R. A Review of Platelet-Rich Plasma: History, Biology, Mechanism of Action, and Classification. Skin Appendage Disord. 2018;4(1):18-24.

145. Freymann U, Degrassi L, Kruger JP, Metzlaff S, Endres M, Petersen W. Effect of serum and platelet-rich plasma on human early or advanced degenerative meniscus cells. Connect Tissue Res. 2017;58(6):509-19.

146. Freymann U, Metzlaff S, Kruger JP, Hirsh G, Endres M, Petersen W, et al. Effect of Human Serum and 2 Different Types of Platelet Concentrates on Human Meniscus Cell Migration, Proliferation, and Matrix Formation. Arthroscopy. 2016;32(6):1106-16.

147. Pujol N, Salle De Chou E, Boisrenoult P, Beaufils P. Platelet-rich plasma for open meniscal repair in young patients: any benefit? Knee Surg Sports Traumatol Arthrosc. 2015;23(1):51-8.

148. Griffin JW, Hadeed MM, Werner BC, Diduch DR, Carson EW, Miller MD. Platelet-rich plasma in meniscal repair: does augmentation improve surgical outcomes? Clin Orthop Relat Res. 2015;473(5):1665-72.

149. Betancourt JP, Murrell WD. Leukocyte-poor platelet-rich plasma to treat degenerative meniscal tear: A case report. J Clin Orthop Trauma. 2016;7(Suppl 1):106-9.

150. Kemmochi M, Sasaki S, Takahashi M, Nishimura T, Aizawa C, Kikuchi J. The use of platelet-rich fibrin with platelet-rich plasma support meniscal repair surgery. J Orthop. 2018;15(2):711-20.

151. Kaminski R, Kulinski K, Kozar-Kaminska K, Wielgus M, Langner M, Wasko MK, et al. A Prospective, Randomized, Double-Blind, Parallel-Group, Placebo-Controlled Study Evaluating Meniscal Healing, Clinical Outcomes, and Safety in Patients Undergoing Meniscal Repair of Unstable, Complete Vertical Meniscal Tears (Bucket Handle) Augmented with Platelet-Rich Plasma. Biomed Res Int. 2018;2018:9315815.

152. Zhang H, Chen S, Qiu M, Zhou A, Yan W, Zhang J. Lateral meniscus allograft transplantation with platelet-rich plasma injections: A minimum two-year follow-up study. Knee. 2018;25(4):568-76.

153. Hutchinson ID, Rodeo SA, Perrone GS, Murray MM. Can platelet-rich plasma enhance anterior cruciate ligament and meniscal repair? J Knee Surg. 2015;28(1):19-28.

154. Zaffagnini S, Fink C, Grassi A, Marcheggiani Muccioli GM, Marcacci M. Menisku simplantate. Arthroskopie. 2015;28(1):38-42.

155. Ndreu Halili A, Karahan S, Kurum B, Hasirci V. Collagen Based Multilayer Scaffolds for Meniscus Tissue Engineering: In Vivo Test Results. Biomaterials and Medical Applications. 2018;02(01).

156. Smith BD, Grande DA. The current state of scaffolds for musculoskeletal regenerative applications. Nat Rev Rheumatol. 2015;11(4):213-22.

157. Chenite A, Chaput C, Wang D, Combes C, Buschmann M, Hoemann C, et al. Novel injectable neutral solutions of chitosan form biodegradable gels in situ. Biomaterials. 2000;21(21):2155-61.

158. Hoemann CD, Hurtig M, Rossomacha E, Sun J, Chevrier A, Shive MS, et al. Chitosan-glycerol phosphate/blood implants improve hyaline cartilage repair in ovine microfracture defects. J Bone Joint Surg Am. 2005;87(12):2671-86.

159. Ahmed S, Ikram S. Chitosan Based Scaffolds and Their Applications in Wound Healing. Achievements in the Life Sciences. 2016;10(1):27-37.

160. Chevrier A, Hoemann CD, Sun J, Buschmann MD. Chitosan-glycerol phosphate/blood implants increase cell recruitment, transient vascularization and subchondral bone remodeling in drilled cartilage defects. Osteoarthritis Cartilage. 2007;15(3):316-27.

161. Chevrier A, Hoemann CD, Sun J, Buschmann MD. Temporal and spatial modulation of chondrogenic foci in subchondral microdrill holes by chitosan-glycerol phosphate/blood implants. Osteoarthritis Cartilage. 2011;19(1):136-44.

162. Marchand C, Chen G, Tran-Khanh N, Sun J, Chen H, Buschmann MD, et al. Microdrilled cartilage defects treated with thrombin-solidified chitosan/blood implant regenerate a more hyaline, stable, and structurally integrated osteochondral unit compared to drilled controls. Tissue Eng Part A. 2012;18(5-6):508-19.

163. Marchand C, Rivard GE, Sun J, Hoemann CD. Solidification mechanisms of chitosan–glycerol phosphate/blood implant for articular cartilage repair. Osteoarthritis and Cartilage. 2009;17(7):953-60.

164. Mathieu C, Chevrier A, Lascau-Coman V, Rivard GE, Hoemann CD. Stereological analysis of subchondral angiogenesis induced by chitosan and coagulation factors in microdrilled articular cartilage defects. Osteoarthritis and Cartilage. 2013;21(6):849-59.

165. Lafantaisie-Favreau CH, Guzman-Morales J, Sun J, Chen G, Harris A, Smith TD, et al. Subchondral pre-solidified chitosan/blood implants elicit reproducible early osteochondral wound-

repair responses including neutrophil and stromal cell chemotaxis, bone resorption and repair, enhanced repair tissue integration and delayed matrix deposition. BMC Musculoskelet Disord. 2013;14:27.

166. Guzman-Morales J, Lafantaisie-Favreau CH, Chen G, Hoemann CD. Subchondral chitosan/blood implant-guided bone plate resorption and woven bone repair is coupled to hyaline cartilage regeneration from microdrill holes in aged rabbit knees. Osteoarthritis Cartilage. 2014;22(2):323-33.

167. Bell AD, Hurtig MB, Quenneville E, Rivard GE, Hoemann CD. Effect of a Rapidly Degrading Presolidified 10 kDa Chitosan/Blood Implant and Subchondral Marrow Stimulation Surgical Approach on Cartilage Resurfacing in a Sheep Model. Cartilage. 2017;8(4):417-31.

168. Bell AD, Lascau-Coman V, Sun J, Chen G, Lowerison MW, Hurtig MB, et al. Bone-Induced Chondroinduction in Sheep Jamshidi Biopsy Defects with and without Treatment by Subchondral Chitosan-Blood Implant: 1-Day, 3-Week, and 3-Month Repair. Cartilage. 2013;4(2):131-43.

169. Stanish WD, McCormack R, Forriol F, Mohtadi N, Pelet S, Desnoyers J, et al. Novel scaffold-based BST-CarGel treatment results in superior cartilage repair compared with microfracture in a randomized controlled trial. J Bone Joint Surg Am. 2013;95(18):1640-50.

170. Methot S, Changoor A, Tran-Khanh N, Hoemann CD, Stanish WD, Restrepo A, et al. Osteochondral Biopsy Analysis Demonstrates That BST-CarGel Treatment Improves Structural and Cellular Characteristics of Cartilage Repair Tissue Compared With Microfracture. Cartilage. 2016;7(1):16-28.

171. Shive MS, Stanish WD, McCormack R, Forriol F, Mohtadi N, Pelet S, et al. BST-CarGel(R) Treatment Maintains Cartilage Repair Superiority over Microfracture at 5 Years in a Multicenter Randomized Controlled Trial. Cartilage. 2015;6(2):62-72.

172. Depres-Tremblay G, Chevrier A, Tran-Khanh N, Nelea M, Buschmann MD. Chitosan inhibits platelet-mediated clot retraction, increases platelet-derived growth factor release, and increases residence time and bioactivity of platelet-rich plasma in vivo. Biomed Mater. 2017;13(1):015005.

173. Veilleux D, Gopalakrishna Panicker RK, Chevrier A, Biniecki K, Lavertu M, Buschmann MD. Lyophilisation and concentration of chitosan/siRNA polyplexes: Influence of buffer

composition, oligonucleotide sequence, and hyaluronic acid coating. J Colloid Interface Sci. 2018;512:335-45.

174. Abdelwahed W, Degobert G, Stainmesse S, Fessi H. Freeze-drying of nanoparticles: formulation, process and storage considerations. Advanced drug delivery reviews. 2006;58(15):1688-713.

175. Khairnar S, Kini R, Harwalkar M, Chaudhari S. A Review on Freeze Drying Process of Pharmaceuticals. International Journal of Research in Pharmacy & Science. 2014;4(1).

176. Taylor LS, Zografi G. Sugar–polymer hydrogen bond interactions in lyophilized amorphous mixtures. Journal of pharmaceutical sciences. 1998;87(12):1615-21.

177. Liu J. Physical characterization of pharmaceutical formulations in frozen and freeze-dried solid states: techniques and applications in freeze-drying development. Pharmaceutical development and technology. 2006;11(1):3-28.

178. Tsinontides SC, Rajniak P, Pham D, Hunke WA, Placek J, Reynolds SD. Freeze drying--principles and practice for successful scale-up to manufacturing. Int J Pharm. 2004;280(1-2):1-16.

179. Ullrich S, Seyferth S, Lee G. Measurement of Shrinkage and Cracking in Lyophilized Amorphous Cakes. Part I: Final-Product Assessment. Journal of pharmaceutical sciences. 2015;104(1):155-64.

180. Veilleux D, Nelea M, Biniecki K, Lavertu M, Buschmann MD. Preparation of Concentrated Chitosan/DNA Nanoparticle Formulations by Lyophilization for Gene Delivery at Clinically Relevant Dosages. J Pharm Sci. 2016;105(1):88-96.

181. Shimomura K, Hamamoto S, Hart DA, Yoshikawa H, Nakamura N. Meniscal repair and regeneration: Current strategies and future perspectives. J Clin Orthop Trauma. 2018;9(3):247-53.

182. Pauli C, Grogan SP, Patil S, Otsuki S, Hasegawa A, Koziol J, et al. Macroscopic and histopathologic analysis of human knee menisci in aging and osteoarthritis. Osteoarthritis Cartilage. 2011;19(9):1132-41.

183. Moran CJ, Busilacchi A, Lee CA, Athanasiou KA, Verdonk PC. Biological augmentation and tissue engineering approaches in meniscus surgery. Arthroscopy. 2015;31(5):944-55.

184. Longo UG, Campi S, Romeo G, Spiezia F, Maffulli N, Denaro V. Biological strategies to enhance healing of the avascular area of the meniscus. Stem Cells Int. 2012;2012:528359.

185. Piontek T, Ciemniewska-Gorzela K, Naczk J, Jakob R, Szulc A, Grygorowicz M, et al. Complex Meniscus Tears Treated with Collagen Matrix Wrapping and Bone Marrow Blood Injection: A 2-Year Clinical Follow-Up. Cartilage. 2016;7(2):123-39.

186. Comblain F, Rocasalbas G, Gauthier S, Henrotin Y. Chitosan: A promising polymer for cartilage repair and viscosupplementation. Biomed Mater Eng. 2017;28(s1):S209-S15.

187. Chevrier A, Hoemann CD, Sun J, Buschmann MD. Chitosan-glycerol phosphate/blood implants increase cell recruitment, transient vascularization and subchondral bone remodeling in drilled cartilage defects. Osteoarthritis Cartilage. 2007;15(3):316-27.

188. Hoemann CD, Chen G, Marchand C, Tran-Khanh N, Thibault M, Chevrier A, et al. Scaffold-Guided Subchondral Bone Repair Implication of Neutrophils and Alternatively Activated Arginase-1+Macrophages. American Journal of Sports Medicine. 2010;38(9):1845-56.

189. Chen G, Sun J, Lascau-Coman V, Chevrier A, Marchand C, Hoemann CD. Acute Osteoclast Activity following Subchondral Drilling Is Promoted by Chitosan and Associated with Improved Cartilage Repair Tissue Integration. Cartilage. 2011;2(2):173-85.

190. Mesiha M, Zurakowski D, Soriano J, Nielson JH, Zarins B, Murray MM. Pathologic characteristics of the torn human meniscus. Am J Sports Med. 2007;35(1):103-12.

191. Ishida K, Kuroda R, Miwa M, Tabata Y, Hokugo A, Kawamoto T, et al. The regenerative effects of platelet-rich plasma on meniscal cells in vitro and its in vivo application with biodegradable gelatin hydrogel. Tissue Eng. 2007;13(5):1103-12.

192. Julke H, Mainil-Varlet P, Jakob RP, Brehm W, Schafer B, Nesic D. The Role of Cells in Meniscal Guided Tissue Regeneration: A Proof of Concept Study in a Goat Model. Cartilage. 2015;6(1):20-9.

193. Shive MS, Hoemann CD, Restrepo A, Hurtig MB, Duval N, Ranger P, et al. BST-CarGel: In Situ ChondroInduction for Cartilage Repair. Operative Techniques in Orthopaedics. 2006;16(4):271-8.

194. Shin KH, Lee H, Kang S, Ko YJ, Lee SY, Park JH, et al. Effect of Leukocyte-Rich and Platelet-Rich Plasma on Healing of a Horizontal Medial Meniscus Tear in a Rabbit Model. Biomed Res Int. 2015;2015:179756.

195. Lee KI, Olmer M, Baek J, D'Lima DD, Lotz MK. Platelet-derived growth factor-coated decellularized meniscus scaffold for integrative healing of meniscus tears. Acta Biomaterals. 2018;76:126-34.

APPENDIX

APPENDIX A – CLINICAL STUDIES OF MENISCUS REPAIR

Table 1 Level I and Level II clinical studies of meniscus repair.

Study	**Design**	**Inclusion criteria**	**Type of tear treated**	**Surgical approach**	**Sample size (% males)**	**Mean age (years)**	**FU rate (%)**	**Mean FU times (months)**	**Outcome measures**	**Definition of failure**	**Results**
Bryant et al., 2007[41]	Level I Randomized controlled trial	Patients with a reducible vertical meniscal tear > 10 mm in length and not > 3 mm displaced into the joint in the R/R, or R/Wzones, that was amenable to repair using sutures or arrows	Vertical tears in the R/R or R/Wzones	1) All-Inside with meniscus arrows (n = 51) 2) Inside-out (n = 49) Synovial abrasion 65% with concomitant ACL reconstruction	100 (62)	25	86	28	Retear rate WOMET ACL QofL RofM	Retear was determined by repeat arthroscopic evaluation of patients with follow-up for symptoms of persistent or new pain, catching, or locking that was possibly related to the meniscal repair	Retear rates were 22% for both groups Clinical outcome similar for both groups OR time longer in Group 2

Kise et al., 2015[111]	Level I Randomized controlled trial	Patients aged 18-40 years with an MRI-verified vertical, longitudinal meniscal tear, 10-40 mm long, located in the peripheral or the middle third of the meniscus, with a preserved central bucket handle eligible for reduction and repair with all-inside technique	Vertical longitudinal tears in the R/R or R/Wzones	1) All-inside with meniscal arrows (n = 21) 2) All-inside with FasT-Fix (n = 25) Rasping of tears 22% with concomitant or earlier ACL reconstruction	46 (57)	26	100 for re-operation 61 for clinical	24	Reoperation rate KOOS Tegner	Reoperation within 2 years as a consequence of complaints due to rerupture or impaired primary healing	Reoperation rates were 43% for Group 1 and 12% for Group 2 (significant) Clinical outcome similar for both groups
Albrecht et al., 1999[42]	Level II Randomized controlled trial	Between 18 and 40 years Reliable patients (no abuse) Full-thickness	Longitudinal vertical, bucket-handle tears (displaced or in situ) in the R/R or R/Wzones	1) All-inside with meniscus arrows (n = 34) 2) Inside-out (n = 34) Rasping of tears	68 (81)	26	96	3-4	Second-look arthroscopy Clinical examination	Menisci were defined as healed if there was no residual tear left and as partially healed if	91% of patients had healed or partially healed in Group 1 compared to 75% in Group 2 (non-significant)

		rupture > 10 mm in length Less than 6 mm from the capsule No former ipsilateral meniscus surgery No complex ruptures No arthroscopic arthritis Informed consent prior to surgery		27% with concomitant ACL reconstruction						there was a residual cleft less than 10 mm and the meniscus was otherwise stable to probing All other arthroscopic cases were defined as non-healed	OR time longer in Group 2
Hantes et al., 2006[112]	Level II Randomized controlled trial	Longitudinal full-thickness tear greater than 10 mm in length Location of the tear less than 6 mm from the meniscocapsular junction	Longitudinal full-thickness tears in the R/R or R/Wzones	1) Outside-in (n = 17) 2) Inside-out (n = 20) 3) All-inside with RapidLoc (n = 20) Rasping of tears	57 (77)	27	100	22	Clinical examination IKDC	Using Barrett's criteria, a repaired meniscus was considered healed if there was no joint line tenderness, effusion, and a negative	Healing rates were 100% for Group 1, 95% for Group 2 and 65% for Group 3 (significant) Clinical outcome worst for Group 3 OR time longer for Group 1

		No former Meniscus surgery No evidence of arthritis during arthroscopy Fixation of the meniscus using only one technique (no hybrid fixation)		51% with concomitant ACL reconstruction						McMurray's test If one or more of these parameters was present, the result was classified as a failure	
Jarvela et al., 2010[113]	Level II Randomized controlled trial	Traumatic longitudinal unstable meniscal tear in the R/R or R/W zones Less than 6 months' time delay between the injury and the operation Absence of degenerative meniscal tear	Traumatic longitudinal unstable tears in the R/R or R/W zones	1) All-inside with meniscal screws (n = 21) 2) All-inside with meniscus arrows (n = 21) Rasping of tears 33% with concomitant ACL reconstruction	42 (69)	31	100	27	Clinical examination Lysholm IKDC MRA	Partial meniscal resection at second-look arthroscopy because of persistent knee pain or mechanical symptoms of catching of the knee	Failure rates were 17% for Group 1 and 30% for Group 2 (non-significant) Clinical outcome similar for both groups More chondral damage for Group 1

		or OA of the knee No previous surgery of the knee									
Bryant et al., 2005[43]	Level II Nonrandomized prospective cohort study	Patients with longitudinal meniscal tears in the R/R or R/W zones of the meniscus	Longitudinal tears in the R/R zone (< 3 mm from the synovial meniscal junction) or in the R/W zone (3 to 5 mm from the synovial meniscal junction)	1) All-inside with BioStinger (n=47) 2) Inside-out (n=29) 3) Hybrid of both (n=13) Rasping of tear Trephination 82% with concomitant ACL reconstruction	85 (64)	27	84	27	Lysholm Tegner Cincinnati IKDC Clinical examination	Identified during second-look arthroscopy due to persistent symptoms	Failure rates were 9% for Group 1, 0% for Group 2 and 15% for Group 3 Clinical outcome similar for all groups No chondral damage due to device
Choi et al., 2009[44]	Level II Nonrandomized prospective cohort study	Patients that underwent ACL reconstructions using hamstring tendon autograft combined with repairs of the medial	Longitudinal tears of the posterior horn of the medial meniscus in the R/R or R/W zones with or without additional posterior horn tears of the lateral meniscus	1) All-inside with sutures (n=14) 2) Inside-out (n=34) Rasping of tear 100% with concomitant	48 (92)	28	100	36	Lysholm Tegner Lachman Pivot-shift Arthrometer	The meniscus was considered healed if there was no fluid signal within the meniscus on MRI	71.4% of menisci were healed in Group 1 and 70.6% in Group 2 as per MRI Clinical outcome similar for both groups

		meniscus in a single center by a single surgeon		ACL reconstruction					Clinical examination MRI		
Spindler et al., 2003[45]	Level II Nonrandomized prospective cohort study	Medial meniscal repairs of the peripheral third or junction of the peripheral third with the middle third performed by the senior surgeon with patellar tendon ACL reconstruction during a certain time period	Longitudinal, bucket-handle and degenerative tears	1) Inside-out (n=47) 2) All-inside with meniscus arrows (n=98) 100% with concomitant ACL reconstruction	145 (55)	24	86	Median 48	KOOS WOMAC SF-36 Lysholm IKDC	Clinical success was defined as no reoperation for failed medial meniscal repair	Failure rates were 18% for Group 1 and 8% for Group 1 (non-significant) Clinical outcome similar for both groups Three-year success rates (proportions with no reoperations) were 88% for Group 1 versus 89% for Group 2
Biedert et al., 2000[52]	Level II Randomized prospective cohort study	Patients with an isolated and painful medial intrasubstance meniscal lesion, with clinical symptoms of	Isolated and painful medial intrasubstance meniscal lesions	1) Conservative therapy (n=12) 2) Arthroscopic suture repair with access channels (n=10)	40 (53)	30	100	27	Clinical examination IKDC Radiographs MRI	Not defined	Near-normal or normal findings for 75% patients in Group 1, 90% in Group 2, 43% in Group 3 and 100% in Group 4 (significant)

		a meniscal tear and a MRI linear high grade 2 signal intensity in the medial meniscus		3) Arthroscopic minimal central resection, intrameniscal fibrin clot and suture repair (n=7) 4) Arthroscopic partial meniscectomy (n=11)							

Table 2 Clinical studies of meniscus repair augmentation by trephination, rasping and abrasion.

Study	**Design**	**Inclusion criteria**	**Type of tear treated**	**Surgical approach**	**Sample size (% males)**	**Mean age (years)**	**FU rate (%)**	**Mean FU times (months)**	**Outcome measures**	**Definition of failure**	**Results**
Zhang &Arnold et al., 1996[63]	Level III	Patients with longitudinal tears of the white zone at mid-third area from peripheral rim to inner rim of meniscus	Longitudinal tears	1) Inside-out and trephination (n=36) 2) Inside-out (n=28) 95% with concomitant ACL	64 (N/S)	22	100	47	Clinical examination	Patients complaining of recurrence of knee swelling and episodes of locking or catching with sign of joint line tenderness, pain with	Failure rates were 6% in Group 1 and 28% in Group 2 (significant)

				reconstruction						squatting, or positive McMurray test were considered to possibly have a retear of the meniscus	
Shelbourne & Rask et al., 2001[64]	Level III	Patients with nondegenerative peripheral vertical medial meniscus tears that were deemed salvageable	Peripheral vertical medial meniscus tears > 1 cm in length	1) Abrasion and trephination (n=233) 2) Left in situ (n=139) 3) Inside-out (n=176) 4) No tear (n=526) 100% with concomitant ACL reconstruction	548	23	79	Objective 58 Subjective 88	Clinical examination Noyes	Clinical failure of meniscal treatment was described as any patient who required subsequent arthroscopy for meniscal symptoms that required removal or further repair	Failure rates were 6% in Group 1, 10.8% in Group 2, 13.6% in Group 3 and 2.9% in Group 4 (non-significant) Group 3 reported more pain and lower activity levels
Shelbourne & Heinrich et al., 2004[114]	Level III	Patients that had lateral meniscus tears that were left in	Posterior horn, radial flap, peripheral or posterior tears	1) Abrasion and trephination (n=43)	332 (57)	23	72	79	Noyes IKDC Radiographs	Subsequent surgery for the lateral meniscus	Failure rate was 2.4%

		situ or that underwent abrasion and trephination		2) Left in situ (n=289) 100% with concomitant ACL reconstruction							Clinical outcome similar for both groups
Shelbourne et al., 2015[65]	Level III	Patients that had an isolated ACL tear, peripheral vertical nondegenerative medial meniscus tear treated with trephination alone, no lateral meniscus tears, normal radiographs before surgery, and no bilateral knee involvement	Peripheral nondegenerative medial meniscus tears at least 1 cm in length	1) Trephination (n=419) 2) No tear (n=462) 100% with concomitant ACL reconstruction	881	22	69 Objective 85 Subjective	69 Objective 85 Subjective	IKDC Cincinnati	Patients were considered to have a symptomatic medial meniscus tear after surgery when they sought treatment for subsequent injury or disabling symptoms that resulted in a subsequentoperation for partial medial meniscectomy	Failure rates were 16.3% in Group 1 and 5.8% in Group 2 (significant) Clinical outcome similar for both groups

Fox et al., 1994[62]	Level IV	Patients that had preoperative subjective and objective findings of a meniscal tear, coinciding with the compartment of the knee with an incomplete meniscal tear, at the time of arthroscopy	Vertical, longitudinal tears that were incomplete	Trephination 17% with concomitant ACL reconstruction	30 (83)	33	97	20	Clinical examination Lysholm	N/S	90% patients reported good to excellent subjective results
Talley & Grana et al., 2000[70]	Level IV	Patients with partial stable meniscal tears who were treated with parameniscal synovial abrasion at the time of ACL reconstruction	Longitudinal, double longitunidal and radial	Synovial abrasion 100% with concomitant ACL reconstruction	40 (50)	22	100	40	Clinical examination Arthrometer Tegner Modified AAOS	Failure was defined as a symptomatic meniscal tear requiring subsequent surgery	Failure rate was 11% More failures on the medial side (non-significant)

Tetik et al., 2002[69]	Level IV	Patients that had medial joint line pain that interfered with daily living activies	Horizontal tears in the posterior half of the medial meniscus	Rasping of tear Synovial abrasion 0% with concomitant ACL reconstructio n	25 (68)	23	100	15	UK-ACL	Excellent result was no pain, no subjective symptoms, full return to sports, no objective pathologic findings	88% patients classified as excellent
Uchio et al., 2003[68]	Level IV	Patients treated by rasping at a particular center during a certain time period	Full-thickness and partial-thickness longitudinal tears	Rasping of tear Synovial abrasion 67% with concomitant ACL reconstructio n	47 (42)	24	100	21	Second-look arthroscop y Arthromet er	"No healing" indicated that the tear length had not shortened at the repaired site or a new tear had developed	8% did not heal No effect of age, sex, the time between injury and rasping, the time between rasping and second-look arthroscopy and concomitant ACL reconstruction on healing Healing better for partial-thickness tears, shorter tears, tears near the capsule, tears in stable menisci

Table 3 Clinical studies of meniscus repair augmentation by fibrin/blood clots.

Study	Design	Inclusion criteria	Type of tear treated	Surgical approach	Sample size (% males)	Mean age (years)	FU rate (%)	Mean FU times (months)	Outcome measures	Definition of failure	Results
Biedert et al., 2000[52]	Level II Randomized prospective cohort study	Patients with an isolated and painful medial intrasubstance meniscal lesion, with clinical symptoms of a meniscal tear and a MRI linear high grade 2 signal intensity in the medial meniscus	Isolated and painful medial intrasubstance meniscal lesions	1) Conservative therapy (n=12) 2) Arthroscopic suture repair with access channels (n=10) 3) Arthroscopic minimal central resection, intrameniscal fibrin clot and suture repair (n=7) 4) Arthroscopic partial meniscectomy	40 (53)	30	100	27	Clinical examination IKDC Radiographs MRI	Not defined	Near-normal or normal findings for 75% patients in Group 1, 90% in Group 2, 43% in Group 3 and 100% in Group 4 (significant)

				(n=11)							
Ishimura et al., 1991[73]	Level IV	Patients who had arthroscopic meniscal repair using fibrin glue	Longitudinal and bucket-handle tears	Fibrin glue Reduction with suturing in unstable tears	32 (25)	18	63 for second-look arthroscopy	46 6 for second-look arthrocopy	Second-look arthroscopy	Patients complained of meniscal symptoms	Failure rate was 6% Twenty repairs rated as good, four as fair, and one as poor by arthroscopic evaluation criteria
Ishimura et al., 1997[74]	Level IV	Patients who had arthroscopic meniscal repair using fibrin glue	Longitudinal and bucket-handle tears in all zones	Fibrin glue Reduction with suturing in the case of unstable tears Rasping of tear 84% with concomitant ACL reconstruction	40 (33)	20	68 for second-look arthroscopy	96 10for second-look arthroscopy	Second-look arthroscopy	Patients complained of meniscal symptoms and received partial meniscectomy	Failure rate was 15% 77% repairs rated as good, 11.5% fair and 11.5% poor by arthroscopic evaluation criteria Recurrence of meniscal symptoms correlated with insufficiency of the reconstructedACL, repair of fresh tears, and repairs requiring

											supplementary meniscal sutures
Van trommel et al., 1998[78]	Level IV	Patients that had complete radial split at the level of the popliteus fossa extending from the periphery to the central part of the lateral meniscus	Radial tears	Outside-in Exogenous fibrin clot Rasping of tear 20% with concomitant ACL reconstruction	5 (N/S)	20	60	71	Second-look arthroscopy MRI	Meniscus was deemed to be healed if there was no fluid imbibition into the substance of the fibrocartilage on MRI	All cases healed
Kamimur &Kimura et al., 2001[81]	Level IV	Patients that had horizontal cleavage tears with meniscal degeneration	Horizontal cleavage tears	All-inside with FasT-Fix Exogenous fibrin clot	9 (N/S)	N/S	100	12	Second-look arthroscopy	N/S	Cleft had closed and had healed with a layer of vascular synovial tissue extending over the proximal surface of the lateral meniscus
Kamimur &Kimura et al., 2014[82]	Level IV	Patients that had a horizontal cleavage tear associated with degeneration	Horizontal cleavage tears	All-inside with FasT-Fix Exogenous fibrin clot	18 (60 for second-look arthroscopy)	36	56	41 7 for second-look arthroscopy	Lysholm IKDC Tegner Second-look	N/S	Complete healing in 70% of patients as assessed by arthroscopy

		identified using MRI and arthroscopy Clinical findings limited to a positive McMurray test or pain during movement, especially in full flexion Tenderness of the femorotibial joint line No limitation of range of motion		17% with concomitant ACL reconstruction					arthroscopy		
Jang & Ra et al., 2011[79]	Level IV	Patients that had a radial tear that was deemed repairable	Radial, longitudinal in R/Wzone, transverse and oblique tears	Suturing Exogenous fibrin clot Rasping of tear Synovial abrasion	41 (N/S)	N/S	100	8	Second-look arthroscopy MRI	N/S	Failure rate was 5%

Ra et al., 2013[80]	Level IV	Patients that had complete radial tears of the meniscus	Radial tears	Inside-out Exogenous fibrin clot Rasping of tear Synovial abrasion 17% with concomitant ACL reconstruction	12 (92)	N/S	100	30 11 for MRI	IKDC Lysholm MRI Second-look arthroscopy	N/S	Complete healing in 92% patients on MRI

Table 4 Clinical studies of meniscus repair augmentation by platelet-rich plasma.

Study	**Design**	**Inclusion criteria**	**Type of tear treated**	**Surgical approach**	**Sample size (% males)**	**Mean age (years)**	**FU rate (%)**	**Mean FU times (months)**	**Outcome measures**	**Definition of failure**	**Results**
Griffin et al., 2015[92]	Level III	Patients who underwent arthroscopic meniscus repair during a particular period at one center and	Bucket handle and horizontal, peripheral horizontal, peripheral longitudinal, horizontal, longitudinal at R/W junction,	Inside-out All-inside Outside-in Application of Cascade PRF delivered arthroscopica	35 (80) 15 with PRP	31	100	48	IKDC Tegner-Lysholm Return to sport Return to work	Known recurrence of reoperation	Failure rates were 27% in PRP+ group and 25% in PRP- group Clinical outcome similar for both groups

		were over 18 years	longitudinal, bucket-handle, vertical and undersurface tears	lly and sutured into the repair site using a PDS suture 0% with concomitant ACL reconstruction	20 without PRP				RofM		
Pujol et al., 2015[91]	Level III	Patients younger than 40 years with a symptomatic horizontal cleavage (Grade II or III) of the meniscus and persisting pain after complete medical treatment (rest, physiotherapy, intraarticular injections of corticosteroids) for at	Horizontal cleavage tears extending into the avascular zone	Open suturing Injection of GPSIII PRP directly into the repair lesion prior to closure Rasping of tear 0% with concomitant ACL reconstruction	34 (71) 17 with PRP 17 without PRP	30	100	32	KOOS IKDC MRI	Failure was defined as a reoperation on the same knee for a meniscectomy or an iterative repair of the same meniscus	Failure rates were 5.8% in PRP+ group and 11.8% in PRP- group Clinical outcomes were slightly improved by the addition of PRP (pain and sports activity subcategories)

		least 6 months									

Table 5 Clinical studies of meniscus repair augmentation by wrapping.

Study	**Design**	**Inclusion criteria**	**Type of tear treated**	**Surgical approach**	**Sample size (% males)**	**Mean age (years)**	**FU rate (%)**	**Mean FU times (months)**	**Outcome measures**	**Definition of failure**	**Results**
Henning et al., 1990[93]	Level IV	Patients aged 14 to 45 years with unstable torn meniscus that underwent repair during a particular period	Single longitudinal, double longitudinal, triple longitudinal, radial, flap, horizontal split and bucket-handle tears	Rasping of tear Suturing Wrapping with fascial sheath Exogenous fibrin clot 92% with concomitant ACL reconstruction	153 (N/S)	23	100	4	Arthrogram Second-look arthroscopy	Healing over less than 50% of the vertical height was considered a failure	Failure rate was 12% Failure rate greater for complex tears Exogenous blood clots decreased failure rate in isolated tears (41% to 8%) Exogenous blood clots with fascial sheath decreased failure rate in

											complex tears (22% to 11%)
Henning et al., 1991[94]	Level IV	Patients with unstable complex tears that underwent repair during a particular period	Double longitudinal, double flap and radial tears	Rasping of tear Suturing Wrapping with fascial sheath Exogenous fibrin clot 81% with concomitant ACL reconstruction	31 with sheath (N/S) 58 without sheath in previous series (N/S)	N/S	100	6 to 9	Arthrogram Second-look arthroscopy	Healing over less than 50% of the vertical height was considered a failure	Failure rates were 8% with sheath and 24% without sheath
Jacobi & Jacob et al., 2010[96]	Level IV	Patients with tears in the R/R or R/W zones, complex tears, delayed traumatic tears with degenerativeas pects, or repeat sutures	Complex, bucket-handle and longitudinal tears	Inside-out Wrapping with collagen matrix 33% with concomitant ACL reconstruction	30 (63)	N/S	100	30	Clinical examinatio n	Persistence of symptoms	Failure rate was 10%
Piontek et al., 2016[99]	Level IV	Full-thickness, combined meniscal tear greater than 20 mm in length Horizontal and radial tear	Combined (horizontal and radial or longitudinal component) and complex meniscal tears (tear extended	All-inside with FasT-Fix Wrapping with collagen matrix 40% with concomitant ACL reconstruction	53 (75)	37	94	24	IKDC Lysholm Barret MRI WORMS	Failure if at the follow-up process patient underwent partial/comple te meniscectomy	Failure rate was 4% Clinical outcome improved in 86.8% of the

		Tear location reaching more than 6 mm from the meniscocapsular junction including the avascular zone Both degenerative and non-degenerative meniscus (i.e., horizontal and radial tears, involving the W/W and R/W zones, as well as extensive tears of the bucket-handle type)	through avascular zones or/and composed with two or more morphological tear pattern)							or knee replacement	intended to treat cases Non-homogeneous signal without meniscal tear in 76% of cases on MRI (WORMS Grade 1)

FU: Follow-Up; N/S: Not Specified; R/R: Red-Red; R/W: Red-White; W/W: White-White; ACL: Anterior Cruciate Ligament; WOMET: Western Ontario Meniscal Evaluation Tool; QofL: Quality of Life; RofM: Range of Motion; KOOS: Knee Injury and Osteoarthritis Score; IKDC: International Knee Documentation Committee; MRA: Magnetic Resonance Arthrography; MRI: Magnetic Resonance Imaging; WOMAC: Western Ontario and McMaster Universities Osteoarthritis Index; SF-36: Short-Form 36; WORMS: Whole Organ MRI Score; AAOS: American Association of Orthopaedic Surgeons; UK-ACL: University of Kentucky Anterior Cruciate Ligament Test.